The role of the ERK1: STAT1 serine 727 phosphorylation axis on key atherosclerosis associated cellular processes and the anti-atherogenic actions of hydroxytyrosol

Wajdan A. Alahmadi

Supervisor: Professor Dipak P. Ramji

A Thesis Presented for the Degree of Doctor of Philosophy
2019

Cardiff School of Biosciences

Cardiff University

Museum Avenue

Cardiff CF10 3AX

Acknowledgement

There are more people to thank than I can remember; as so many have been instrumental in the accomplishment of this thesis, either directly or indirectly.

My gratitude first goes to my supervisor, professor Dipak Ramji, who gave me the opportunity to start this research project and complete it. His patient guidance, advice and understanding through my long time as his student was fundamental to my completion of this project, and whose meticulous comments on my work and on this thesis contributed to its outcome. He has been a teacher, a mentor, and a sharp and fair critic from whom I have learned so much, not only for my PhD project but also for my life. It was indeed a great privilege and honour to work and study under him and will always be indebted to him. And of course, I bear full responsibility for what I have finally presented in my thesis.

I would also like to express my heartfelt thanks to Dr. Timothy Hughes for all his help and guidance, and to my friends and research colleagues who have supported me to complete the research work directly or indirectly. I learnt so much from them, and my thesis depended on their generosity in sharing their time, knowledge and expertise with me.

I wish to thank the members of staff at Cardiff University, most of whom I never met in person, yet without whom I would not have been able to manage the administrative requirements of a PhD.

I cannot express enough thanks and gratitude to my parents, my sisters and brothers for their support and valuable prayers and for providing me with unfailing support and continuous encouragement throughout my years of study. This accomplishment would not have been possible without them.

Most of all I thank my caring, loving and supportive husband for his love, encouragement and sacrifice during this long period of research.

Declaration

This work has not been submitted in substance for any other degree or award at this or any other university or place of learning, nor is being submitted concurrently in candidature for any degree or other award.

Signed …… (candidate) Date ……

Statement 1

This thesis is being submitted in partial fulfilment of the requirements for the degree of Doctor of philosophy.

Signed …… (candidate) Date ……

Statement 2

This thesis is the result of my own independent work/investigation, except where otherwise stated. Other sources are acknowledged by explicit references.

Signed …… (candidate) Date ……

Statement 3

I hereby give consent for my thesis, if accepted, to be available for photocopying and for inter-library loan, and for the title and summary to be made available to outside organisations.

Signed …… (candidate) Date ……

Statement 4:

I hereby give consent for my thesis, if accepted, to be available for photocopying and for inter-library loans

Signed …… (candidate) Date ……

Table of contents

List of tables

List of figures

Abstract

Atherosclerosis, a chronic inflammatory disease of the vasculature that is associated with the build-up of fatty deposits within the walls of arteries, is the underlying cause of cardiovascular diseases (CVD) such as myocardial infarction and stroke. CVD represents a major cause of deaths worldwide and represents a major economic burden. Macrophages play a pivotal role in the pathogenesis of atherosclerosis and represent a promising therapeutic target. The macrophage inflammatory response is regulated by cytokines such as interferon-γ (IFN-γ) via key signalling pathways, such as extracellular-signal regulated kinases (ERKs), and transcription factors such as signal transducer and activator of transcription-1 (STAT1) that is activated by changes in phosphorylation at specific residues. Previous studies in the laboratory had shown that the ERK1:STAT1 serine 727 phosphorylation axis was integral to the IFN-γ-mediated regulation of macrophage gene expression and the uptake of modified lipoproteins. As part of another project in the laboratory, ERK1 ($ERK1^{-/-}$) mice and STAT1 knock-in mice ($STAT1^{S727A}$) in which the serine 727 phosphorylation site, a target for ERKs action, had been mutated to alanine were obtained for studies on atherosclerosis *in vivo*. The availability of these mice provided an excellent opportunity to use bone marrow-derived macrophages (BMDM) from them together with control C57BL/6J mice to probe the role of the ERK1:STAT1 serine 727 phosphorylation axis on key atherosclerosis-associated processes *in vitro*, which therefore formed the first aim of the project.

Current therapies against atherosclerosis are not fully effective and many promising pharmaceutical agents identified from various drug discovery programs have failed at the clinical level. This has generated substantial interest on nutraceuticals, such as hydroxytyrosol (HT) found in olives, but requires an in-depth understanding of their actions *in vitro* and *in vivo* together with the underlying molecular mechanisms. Previous studies had shown that HT specifically attenuated the IFN-γ-induced STAT1 serine 727 phosphorylation. The next aim of the studies was to investigate the role of the ERK1:STAT1 serine 727 phosphorylation axis on key atherosclerosis-associated processes in BMDM regulated by HT *in vitro*. Subsequent studies then probed the effects of HT *in vivo* in wild type C57BL/6J mice fed a high fat diet (HFD) for 3 weeks and in male and female LDL receptor deficient mice ($LDLR^{-/-}$) fed a HFD for 12 weeks.

Results

Use of Atherosclerosis arrays showed that the expression of a large numbers of genes was affected in BMDM of ERK1$^{-/-}$ and STAT1^{S727A} mice when compared to the control with 17 genes in common. In addition, these two genetic modifications had a differential effect on key macrophage processes associated with atherosclerosis and the actions of HT. In C57BL/6J mice fed a HFD for 3 weeks, HT produced several favourable changes [e.g. reduction in plasma levels of reactive oxygen species (ROS) and total cholesterol levels] together with changes in the expression of key atherosclerosis-associated genes in the liver. Some of these beneficial actions (e.g. plasma cholesterol levels) also extended to LDLR$^{-/-}$ mice, which also informed on gender-specific effects (e.g. HT reduced plasma ROS levels in male mice).

Conclusions

The findings of this study show an important role for ERK1 and STAT1 serine 727 phosphorylation on the expression of a large number of atherosclerosis-associated genes and some key cellular processes. In addition, HT produced several anti-atherogenic effects *in vivo*. Reasons for these beneficial effects have been proposed in this thesis and future studies outlined.

Abbreviations

Abbreviation	Full term
ABCA1	ATP-binding cassette transporter A1
ACAT1	Acyl coenzyme A acyl transferase 1
APOB	Apolipoprotein B
BHF	British Heart Foundation
BMDM	Bone marrow-derived macrophages
BSA	Bovine serum albumin
CANTOS	Canakinumab Anti-inflammatory Thrombosis Outcomes Study
CCR2	C-C chemokine receptor 2
CE	Cholesteryl esters
CETP	Cholesterol ester transfer protein
CLP	Common lymphoid progenitor
CMP	Common myeloid progenitor
CRP	C-reactive protein
CSF	Colony stimulating factor
CV	Crystal violet
CVD	Cardiovascular disease
CXCL1	Chemokine (C-X-C motif) ligand 1
DC	Dendritic cells
DCFDA	Dichlorofluorescein diacetate

DPPH	Diphenyl-2- picrylhydrazyl
EC	Endothelial cells
ECM	Extracellular matrix
EFSA	European Food Safety Authority
ER	Endoplasmic reticulum
ERK	Extracellular signal-regulated kinase
FA	Fatty acids
FC	Free cholesterol
FFA	Free fatty acids
FGF	Fibroblast growth factor
GAS	Gamma activated sequence
GF	Growth factor
GMCSF	Granulocyte-macrophage-colony stimulating factor
GMP	Granulocyte macrophage progenitor
GRB2	Growth factor receptor-bound protein 2
GSB	Gel sample buffer
H_2O_2	Hydrogen peroxide
HAOP	Hydrolysed aqueous olive pulp extract
HDL	High density lipoprotein
HFD	High fat diet
HI-FCS	Heat inactivated fetal calf serum

HIV	Human immunodeficiency virus
HL	Hepatic lipase
HMGCOA	3-hydroxymethyl-3-glutaryl-CoA-synthase
HRP	Horseradish peroxidase
HSC's	Haematopoietic stem cells
HT	Hydroxytyrosol
ICAM	Intercellular adhesion molecule-1
IFN	Interferon
IL	Interleukin
IL1R	Interleukin 1 receptor
IRG	IFN-γ responsive genes
JAK	Janus kinase
JNK	c-Jun N-terminal kinase
LCAT	Lecithin cholesterol acyltransferase
LDL	Low density lipoprotein
LDLR	Low density lipoprotein receptor
LOX	Lipoxygenases
LP's	Lipoprotein
LPS	Lipopolysaccharide
LY	Lucifer yellow
MAPK	Mitogen activated protein kinase
MCP-1	Macrophage chemoattractant protein-1

MCSF	Macrophage-colony stimulating factor
MDP	Macrophage-dendritic cells progenitor
MDSC	Myeloid-derived suppressor cell
MEP	Megakaryocyte-erythroid progenitor
MI	Myocardial infraction
MPO	Myeloperoxidase
MSR-1	Macrophages scavenger receptor 1
NADH	Nicotinamide adenine dinucleotide
NFκβ	Nuclear factor kappa-light-chain-enhancer of activated B cells
nHDL	Nascent HDL
NO	Nitric oxide
NPLC1L1	Niemann-Pick C1-like protein
OCT	Optimum cutting temperature formulation
OLE	Olive leaf extract
oxLDL	Oxidised LDL
PBS	Phosphate buffer saline
PCSK9	Proprotein convertase subtilisin/kexin type 9
PF4	Platelet factor 4
PI3K	Phosphatidylinositol 3-kinase
PKC	Protein kinase C
PL	Phospholipids

PLTP	Phospholipid transfer protein
PRR	Pattern recognition receptor
RCT	Reverse cholesterol transport
RNS	Reactive nitrogen species
ROS	Reactive oxygen species
RT-qPCR	Quantitative polymerase chain reaction
SDS-PAGE	Sodium dodecyl sulphate polyacrylamide gel electrophoresis
SH2	Src homology 2
SLAM	Signalling lymphocyte activation molecule
SMC	Smooth muscles cells
SOCS	Suppressor of cytokines signalling
SOS	Son of sevenless
SR	Scavenger receptor
SR-PSOX	Scavenger receptor for phosphatidylserine and oxidised lipoprotein
STAT	Signal transducer and activator of transcription
TG	Triglyceride
TGF	Transforming growth factor
TH-1	T-helper-1
TLR4	Toll like receptor 4
TNF	Tumour necrosis factor

TNFR1	Tumour necrosis factor receptor 1
VCAM-1	Vascular cell adhesion molecule-1
VEC	Vascular endothelial cells
VSMC	Vascular smooth muscles cells
WBC	White blood cells
WHO	World Health Organisation

Chapter 1

1.1 General introduction of cardiovascular disorders

Cardiovascular diseases (CVD), which include diseases of the heart, vascular diseases of the brain and diseases of blood vessels, are the number one cause of death globally. Examples of CVD include coronary artery disease (e.g. myocardial infarction (MI)), cerebrovascular disease (e.g. stroke), diseases of the aorta and arteries, hypertension, peripheral vascular disease, congenital heart disease, rheumatic heart disease, cardiomyopathies and cardiac arrhythmias (Mendis *et al.*, 2011).

According to the World Health Organisation (WHO), more people die annually from CVD than from any other cause (WHO- CVDs, 2018). CVD takes the lives of 17.7 million people every year and accounts for 31% of all global deaths (WHO- CVD, 2018). With increasing global adaptation of westernised life style, lack of balanced diet and elevated stress, heart diseases are increasing even at a young age. Indeed, by 2020, CVD are predicted to be the major cause of morbidity and mortality in most developing nations around the world (Celermajer *et al.*, 2012). In 2011, the United Nations formally recognised non-communicable diseases, including CVD, as a major concern for global health and set out an ambitious plan to dramatically reduce the effect of these diseases in all regions (Roth *et al.*, 2017). Goals to increase awareness of these global non-communicable diseases have expanded national efforts at reducing CVD and other non-communicable diseases (Bonita *et al.*, 2013).

Over 75% of CVD deaths take place in low- and middle-income countries (WHO-CVD, 2018). This leads to difficulties in them accessing an effective health care service that can respond to their needs. In addition, such countries lack the benefits of an integrated primary health care program for early detection and treatment of people with risk factors, compared to people in high-income countries. As a result, the disease in many people in low- and middle- income countries is detected much later and many die younger from CVDs and other non-communicable diseases, often in their most productive years (Bloom *et al.*, 2012).

1.2 Risk factors

According to the British Heart Foundation (BHF), a risk factor is something that increases the chances of getting a disease. Understanding of the risk factors for CVD may yield important insights into the prevention and treatment of this major public health concern. The more risk factors a person has, the higher the chance of developing CVD. Although it is not possible to change all the risk factors, there is plenty that can be done to prevent CVD and reduce its burden (WHO, 2011). Table 1.1 summarises the various risk factors for CVD.

Table 1.1 Risk factors and avenues for the prevention of CVD

(Adapted from World Heart Federation-Fact Sheet, 2017)

Risk factor	Prevention
Smoking	Smoking increases the risk of heart diseases. The risk of having a heart attack and coronary heart disease falls to about half of that of a smoker after one year of quitting smoking.
High blood pressure	High blood pressure is harmful to the arteries and increases the risk of heart attack, heart failure and stroke. Controlling blood pressure will reduce the incidence of CVD.
High blood cholesterol	High cholesterol can become deposited in the walls of arteries, causing damage and blocking the blood flow leading to a MI, stroke or peripheral vascular disease. Adopting healthy habits, such as eating a healthy, balanced diet and keeping active, can help prevent increases in blood cholesterol levels.
Being overweight or obese and physically inactive	Overweight people are more likely to have high blood pressure, diabetes and high levels of detrimental plasma lipid such a low-density lipoproteins (LDL) and triglyceride (TG), all of which increase their chance of having CVD. Regular physical activity helps in reducing these risks.
Diabetes	People with diabetes are at a much higher risk of CVD. This increased risk is associated with high blood sugar levels, high

	blood pressure and raised blood lipids.
A family history of heart disease	The risk for CVD may increase if close blood relatives have experienced early heart diseases. This is a non-modifiable risk but can be controlled by other risk factors (e.g. not smoking and eating a healthy diet) and regular doctor check-up.
Gender	Men are more likely to develop CVD at an earlier age than women.
Age	CVD is more likely to develop with age.
Excessive stress	The increased stress levels, especially if prolonged, can be harmful to health, especially in people with pre-existing heart disease, and can contribute to high blood pressure.
Excessive alcohol	Consuming too much alcohol is harmful to the heart and other organs. It can directly damage the heart's muscle and cause irregular beating of the heart, weight gain, high TG levels, high blood pressure and stroke.

1.3 Inflammation and atherosclerosis

The principal cause of MI and stroke is atherosclerosis, a chronic inflammatory disease characterised by lipid and cholesterol accumulation within the walls of large and medium arteries (Lusis, 2000). The disease is initiated by the sub-endothelial retention of apo-lipoprotein B (ApoB)–containing lipoproteins (LPs) such as LDL in focal areas of arteries, particularly regions in which blood flow is disturbed by bends or branch points in the arteries (Williams and Tabas, 1995). ApoB-LP are made by the liver and intestinal cells and consist of a core of neutral lipids, notably cholesteryl esters (CE) and TG, surrounded by a monolayer of phospholipids (PL) and proteins (Moore and Tabas, 2011). Various modifications of the retained LP likely mimic pathogen and thereby trigger a low-grade inflammatory responses (Williams and Tabas, 1995).

Inflammation is central to all stages of atherosclerosis. For example, it is involved in the formation of early fatty streaks when the endothelium is activated and

expresses chemokines and adhesion molecules, leading to monocyte/lymphocyte recruitment and their infiltration into the sub-endothelium (Tedgui and Mallat, 2006). In addition, activated cells within the plaque secrete proteases under conditions of chronic inflammation that degrade extracellular matrix (ECM) proteins and weaken the fibrous cap, leading to their rupture and subsequent thrombus formation (Tedgui and Mallat, 2006).

The different stages in the pathogenesis of atherosclerosis development that occurs during the lifespan of an individual are summarised in Figure 1.1 and they include:

1.3.1 Lesion initiation

Primary initiating events in atherosclerosis are the physiological and pathophysiological changes that occur to the arterial endothelium leading to an increase in the permeability of the endothelial cell (EC) layer to large biomolecules such as LDL. LDL particles containing ApoB diffuse between EC junctions and accumulate within the sub-endothelial space (Insull, 2009). The trapped LDL becomes susceptible to a range of enzymatic and non-enzymatic chemical modifications (e.g. oxidation). Oxidation is the most significant modification for an early lesion formation and is mediated through the activities of several "oxidative enzymes" such as myeloperoxidases and lipoxygenases (LOX) together with reactive oxygen species (ROS), peroxynitrite and nitric oxide (NO) (Wen and Leake, 2007). Modified LDL particles are immunogenic as the peroxidation of PLs, CEs and TG creates reactive species capable of stimulating inflammatory processes (Frostegård, 2013). As a result, ECs, intimal macrophages and smooth muscles cells (SMCs), secrete chemokines, such as macrophage chemoattractant protein-1 (MCP-1, also known as CCL2), and express several adhesion proteins, including intercellular adhesion molecule-1 (ICAM-1/CD54), vascular cell adhesion molecule-1 (VCAM-1/CD106) as well as P- and E-selectins (CD62).

The chemokines and the adhesion proteins mediate the recruitment and transmigration of immune cells, including monocytes, neutrophils, T cells, B cells, dendritic cells (DCs) and mast cells across the endothelium (Reape and Groot, 1999; Moss and Ramji, 2015). Following the transmigration of monocytes into the intima,

they differentiate into macrophages under the influence of macrophage-colony stimulating factor (M-CSF) or granulocyte-macrophage-CSF (GM- CSF) (Figure 1.1) (Moore *et al.,* 2013).

1.3.2 Foam cell formation

LP uptake by monocyte-derived macrophages (MDM) is thought to be one of the earliest pathogenic events in the nascent plaque and results in the development of foam cells. Although macrophages can clear ApoB-containing LP through the LDL receptor (LDLR), the expression of this receptor is down regulated early during foam cell formation by the increased intracellular cholesterol levels (i.e. negative feedback inhibition). These observations led to the early hypothesis that LPs must become modified in the artery wall and that they must be taken up by other mechanisms (Moore *et al.*, 2013).

As detailed above, the increased oxidative stress in the artery wall promotes modifications of LDL to oxidised LDL (oxLDL), which contains 'damage' signals that are recognised by pattern recognition receptors (PRRs) on the cells of the innate immune system (Moore *et al*. 2013). Scavenger receptors (SRs), which are a type of PRRs expressed by macrophages, have an important role in atherosclerosis and were originally characterised by their ability to recognise and process oxLDL (Moore and Freeman, 2006). Macrophages express numerous SRs that can bind to oxLDL and promote foam cell formation. SRs internalise the LPs and their associated lipids that are then subjected to enzymatic actions in the endolysosomal compartment. This results in the release of free cholesterol (FC) and free fatty acids (FFAs) that can move to the plasma membrane and be effluxed out from the cells or to the endoplasmic reticulum (ER) where they undergo re-esterification by acyl-coenzyme A cholesterol acyltransferase 1 (ACAT1) to CE that are ultimately stored in this form as cytosolic lipid droplets (Moore *et al*, 2013).

This unrestricted uptake of oxLDL by SRs, which is not subject to negative feedback regulation by intracellular cholesterol levels, eventually leads to the formation of lipid-filled foam cells, the initial step in atherogenesis (Figure 1.1) (de Winther *et al.*, 2000; Moore *et al*., 2013).

1.3.3 Advanced plaque formation and rupture

Continued inflammation ultimately causes the cholesterol homeostatic mechanisms to become overwhelmed during atherosclerosis. This leads to ER stress in macrophages and, together with other insults, results in cell death by apoptosis and necrosis (Ramji and Davies, 2015). Mature atherosclerotic plaques are made up of vascular smooth muscle cells (VSMCs) and ECM, as well as accumulated oxLDL, cholesterol and apoptotic cells, which form a lipid-rich necrotic core (Moss and Ramji, 2015).

Efferocytosis (clearance of apoptotic cells) is key to the removal of cell debris and apoptotic cells (Kojima *et al.*, 2017). However, as the disease progresses, the rate of apoptosis within the necrotic core likely overwhelms the phagocytic capabilities of residing phagocytes (Kojima *et al.*, 2017). Defective efferocytosis continues to result in lipid accumulation in the atherosclerotic lesions (Tabas, 2010). Small, asymptomatic lesions referred to as fatty streaks form due to a high concentration of foam cells. The fatty streak may progress into a clinically relevant plaque (Insull Jr., 2009; McLaren *et al.*, 2011; Buckley and Ramji, 2015).

The formation of an intermediate lesion arises due to enhanced migration and proliferation of VSMCs from the tunica media into the inflamed area in response to platelet-derived growth factors (PDGFs) released from plaque-resident cells (Tedgui *et al.*, 2006). The SMCs proliferate and release ECM proteins contributing towards the production of a fibrotic cap (Tedgui *et al.*, 2006). As the fibrous cap continues to develop, it forms a stable lesion by covering the large lipid-rich necrotic core, therefore the balance of ECM production and degradation can affect the stability of the lesion (Tedgui *et al.*, 2006; Moss and Ramji, 2015).

As the disease progresses, the artery is capable of re-modelling itself via gradual dilation. Once the lesion occupies approximately 40% of the internal elastic lamina region, the artery is incapable of maintaining its integrity through dilation and protrudes into the lumen; the growing plaque will lead to restriction of blood flow to the surrounding tissues (Buckley and Ramji, 2015). Towards the later stages of the disease, the atherosclerotic lesion is characterised by disorganised cells, lipids, matrix components and minerals (McLaren *et al.*, 2011). Clinical symptoms may occur during

this phase of the disease as the intimal region is thickened and the area of the arterial lumen may be reduced in size (Tabas, 2010; McLaren *et al.*, 2011). However, as the disease continues, the plaque becomes increasingly unstable and vulnerable as a result of reduced efferocytosis, chronic inflammation, increased expression of proteases such as matrix metalloproteinases (MMPs) and ineffective egress of immune cells (Kojima *et al.*, 2017).

If the plaque ruptures, it triggers a thrombotic reaction and in turn platelet aggregation, which can quickly impede or obstruct blood flow through the artery (Lusis, 2000). Depending on the location of the rupture, it can potentially cause a MI or stroke (Figure 1.1) (Lusis, 2000). Therefore, acute CVD events may be manageable by affecting plaque stability and preventing them from rupturing (Buckley and Ramji, 2015). In terms of inflammation, it is important to understand the roles of key cytokines and their signalling pathways on gene expression and cellular processes associated with the disease. These aspects are addressed in the next section.

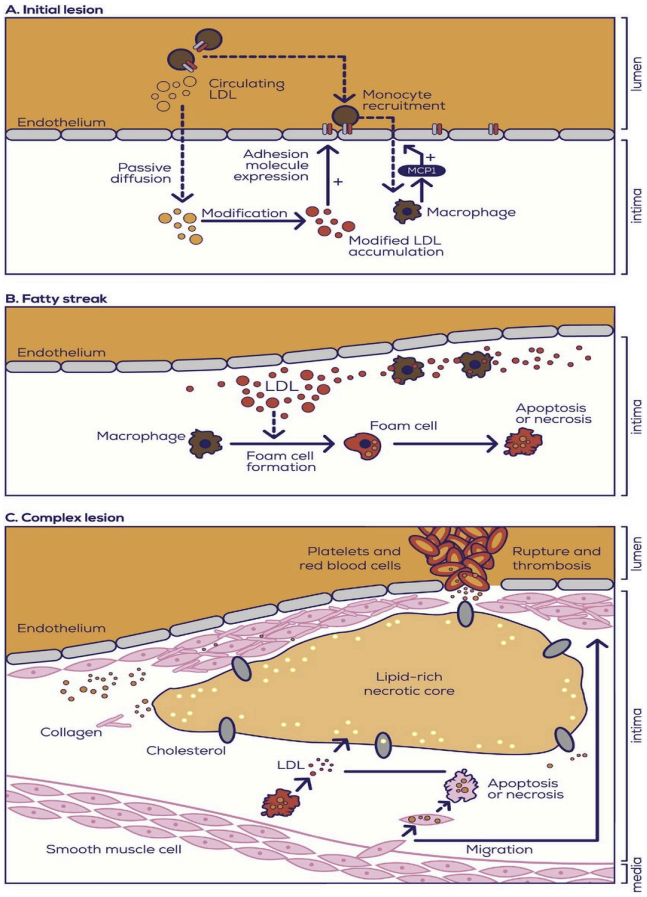

Figure 1.1 Formation of an atherosclerotic plaque

During the development of the initial lesion (A), circulating monocytes are recruited and migrate to the site of inflammation as a result of stimulation of MCP-1 and ICAM-1 expression by ECs. Once in the walls of the artery, monocytes differentiate into macrophages, which are able to take up the oxLDL and become lipid-laden foam cells that soon accumulate and form a fatty streak (B). During complex lesion formation (C), foam cell lysis by apoptosis and necrosis leads to the formation of a necrotic core, and together with defective efferocytosis, leads to the amplification of the inflammatory response. SMCs begin to migrate from the media to the intima and the ECM produced by them forms a fibrous cap that stabilises the plaque. SMCs also transform to foam cells. During later stages of the complex lesion, the plaque can become unstable due to inhibition of ECM formation and/or its excessive degradation. ECM can then start to be degraded by proteases released by macrophages, resulting in an unstable lesion that can rupture and lead to thrombosis, resulting in MI or stroke, depending on the location of plaque formation (Taken from Santhakumar et al., 2018).

1.4 Cytokines and their signalling pathways in CVD

The cardiovascular system is a highly complex and well-organised system in which signal transduction pathways play critical physiological and pathophysiological roles (Prashar *et al.*, 2017). The cellular elements of the heart and vascular wall are equipped with an array of specific receptors and complex intracellular machinery that facilitates and drives appropriate responses to extracellular stimuli (Wheeler-Jones, 2005). The analysis of the function of specific signalling proteins in atherosclerosis pathophysiology is a major goal for biomedical researchers (Prashar *et al.*, 2017).

Previous studies reported that dysregulation of key signalling pathways during atherosclerosis leads to alteration of gene expression that facilitates the disease processes (Muslin, 2008). Several signalling pathways have been implicated within the atherosclerotic state and some of the key ones are associated with the inflammatory response such as mitogen-activated protein kinase (MAPKs) and Janus kinase-Signal transducer and activator of transcription (JAK-STAT) pathway (Muslin, 2008). Previous research on the identification and characterisation of the components of the MAPK cascades has led to an explosion in translational research attempting to link these signalling pathways to CVD (Muslin, 2008).

Important recent advances in the understanding of the mechanisms of atherosclerosis have provided evidence that cytokines play a major role at all stages of the disease process, from the early events whereby leukocytes are recruited at sites of sub-endothelial LDL cholesterol accumulation to the late events, when plaque rupture occurs, leading to thrombus formation and adverse clinical outcomes (Ait-Oufella *et al.*, 2011). Cytokines are low-molecular-weight protein mediators that usually act in a short range between neighbouring cells in lymphoid organs or in inflamed tissues (Tedgui *et al.*, 2006). They are very diverse and consist of more than 100 secreted factors clustered into several classes, including interleukins (IL), tumor necrosis factors (TNF), interferons (IFN), CSF, transforming growth factors (TGF) and chemokines. All cells involved in atherogenesis are capable of producing and responding to cytokines (Ait-Oufella *et al.*, 2011). Table 1.2 summaries the role of some of the interleukins, cytokines, chemokines and their receptors in atherosclerosis.

Table 1.2 The role of cytokines in atherogenesis

Cytokine	Role in atherogenesis	References
IL-1α/ β	Pro-atherogenic cytokines that induce vascular inflammation as a result of cholesterol and fatty acids (FA) accumulation. Studies using ApoE$^{-/-}$ mice showed a 60% reduction in plaque burden following deficiency of IL-1α and 30% decrease following deficiency of IL-1β.	(Kamari *et al.*, 2011; Ridker *et al.*, 2011; Freigang *et al.*, 2013)
IL-2	Can exert both pro- or anti-atherogenic effects depending on the experimental conditions. A study using ApoE deficient mice (ApoE$^{-/-}$) fed a high fat diet (HFD) with an intraperitoneal injection of IL-2 or IL-2 antibody twice a week for a period of 6 weeks, showed that IL-2 is an atherogenic cytokine and anti-IL-2 is protective against atherosclerosis. In another study using the same animal model, intravenous injection of a fusion antibody specific to extra-domain B of fibronectin containing active human IL-2 (L19-IL-2) significantly reduced the size of pre-established atherosclerotic plaques at the thoracic aorta and in the aortic root area.	(Upadhya *et* 2004; Dietrich *al.*, 2012)
IL-4	Produced by activated T-lymphocytes and mast cells. It can exert both pro- and anti-atherogenic effects depending on the mouse model, gender, disease stage analysed and dietary regime.	(Jacob *et al.*, 2000; Kleemann *et al.*, 2008)
IL-5	Atheroprotective cytokine produced by T-lymphocytes and mast cells. In a bone marrow transplant model, IL-5 deficiency led to accelerated atherosclerosis.	(Binder *et* 2004)
IL-6	Pro- and anti-atherogenic cytokine. The pro-atherogenic effects include: activation of ECs, pro-thrombotic effects on platelets and promotion of SMC proliferation and	(Hartman and Frishman, 2014; Reiss *et*

	foam cell formation. The anti-atherogenic properties include: upregulation of expression of "cholesterol efflux" protein [e.g. ATP binding cassette transporter (ABC) A1], inhibition of other inflammatory cytokines like IL-1 and TNF-α. Previous studies using IL-6 receptor blocker that impairs classical IL-6 signalling showed decreased risk of coronary heart disease.	*al.*, 2017)
IL-10	Atheroprotective cytokine. IL-10-transgenic C57/BL6-mice fed a HFD showed reduction in atherosclerotic lesions. In contrast, IL-10-deficient C57/BL6 mice and ApoE$^{-/-}$/IL-10$^{-/-}$ mice exhibited increased early formation of atherosclerotic lesions.	(Pinderski Oslund Laura *et al.*, 1999; Caligiuri *et al.*, 2003)
IL-12	Pro-atherogenic cytokine produced by various inflammatory cell types. IL-12 p40$^{-/-}$/ApoE$^{-/-}$ mice show markedly less atherogenic events than ApoE$^{-/-}$ controls. Inhibition of endogenous IL-12 production by vaccination resulted in a significant 69% reduction of atherogenesis in LDLR$^{-/-}$ mice and improved parameters for plaque stability.	(Davenport and Tipping, 2003; Trinchieri, 2003; Hauer *et al.*, 2005)
IL-33	Atheroprotective cytokine. IL-33 can reduce atherosclerosis development in ApoE$^{-/-}$ mice fed HFD accompanied with reduced serum level of IFN-γ and increased levels of IL-5 and anti-oxLDL antibodies.	(Miller *et al.*, 2008)
IFN-γ	Pro-inflammatory cytokine. A significant 2-fold increase in lesion size was observed in ApoE$^{-/-}$ mice that were injected daily with recombinant IFN-γ. Administration of IFN-γ also significantly increased the number of T-cells within the lesions. IFN-γ$^{-/-}$/ApoE$^{-/-}$ mice fed a HFD showed a decrease in atherosclerosis development.	(Whitman *et al.*, 2000; C Whitman *et al.*, 2002; Moss and Ramji, 2015)
TGF-β	Atheroprotective cytokine. A recent study showed that activation of TGF-β signalling in SMC due to suppression of fibroblast growth factor (FGF) signalling dramatically reduces atherosclerotic plaque size. In ApoE$^{-/-}$/FGF	(Chen *et al.*, 2016)

	receptor$^{-/-}$ mice fed a HFD, an inhibition of atherosclerotic plaque growth was observed when compared to ApoE$^{-/-}$ control mice.	
TNF-α	Pro-atherogenic cytokine produced in high levels by monocytes and macrophages. Increased serum TNF-α levels are associated with increased risk of recurrent MI, atherosclerotic thickening of carotid intima-media and disturbances in TG and glucose homeostasis. TNF receptor1 (TNFR1)/ApoE deficient mice showed that TNFR1 deficiency results in 12% less thoracic atherosclerosis compared to control ApoE$^{-/-}$ mice. Administration of a TNF-α inhibitor to female ApoE$^{-/-}$ mice fed a HFD demonstrated significantly smaller lesion size compared to the control.	(Schreyer *et al.,* 1996; Chew *et al.*, 2003; Kleemann *et al.*, 2008)
CCL2/CCR-2	Pro-atherogeneic chemokine and chemokine receptor expressed mainly by inflammatory cells and ECs. Plays a critical role in early stages of atherosclerosis development such as the recruitment of monocyte to the sites of inflammation. Previous study using CCR2$^{-/-}$/ApoE$^{-/-}$ mice showed significant decrease in lesion size compared to ApoE$^{-/-}$ controls. Similar results have been reported using CCL2$^{-/-}$/LDLR$^{-/-}$ mice. In addition, treatment with 15a, a CCR2 antagonist that was administrated daily with HFD to ApoE$^{-/-}$ mice, showed a reduction in the amount of circulating monocytes and the size of the atherosclerotic plaques in both the carotid artery and the aortic root.	(Gu *et al.*, 1998; Jian *et al.*, 2003; Bot *et al.*, 2017)
CXCL1/CXC2R	Pro-atherogenic chemokine and chemokine receptor involved in the mobilisation of monocytes and neutrophils to the site of inflammation. In ApoE$^{-/-}$ mice fed a HFD, the levels of CXCL1/CXCR2 were induced in the inflammatory monocytes. Inhibition of monocytosis by CXCL1-neutralisation indicates a role for the CXCL1/CXCR2 axis in mobilising inflammatory	(Soehnlein *et al.*, 2013)

	monocytes during hypercholesterolaemia.	
IL-1αR	Pro-atherogenic cytokines receptor. IL-1R-deficient C57BL/6J mice (IL1R1$^{-/-}$) mice fed HFD for 3 months, and ApoE$^{-/-}$ /IL1R1$^{-/-}$ mice fed HFD for 8 weeks exhibit less atherosclerosis, and overexpression of the IL-1R antagonist (IL-1Ra) in LDLR$^{-/-}$ mice reduces the disease.	(Devlin *et al.*, 2002; Chamberlain *et al.*, 2009)

It has been reported that blockade of pro-inflammatory cytokines results in the limitation of plaque development and progression (Tedgui and Mallat, 2006; Ramji and Davies, 2015). Understanding of the roles of cytokines has recently advanced considerably mainly via studies using mouse model systems. Major targets for cytokine actions in atherosclerosis are macrophages, which are dealt with detail in a later section (Section 1.7).

1.5 Major signalling pathways associated with the pathogenesis of atherosclerosis

As mentioned earlier, atherosclerotic lesions develop as a result of an inflammatory process initiated by ECs damage or activation (Lusis, 2000). Several inflammatory mediators (e.g. cytokines, chemokines) have been shown to orchestrate common intracellular signal transduction pathways to regulate both plaque vulnerability and myocardial injury (Montecucco *et al.*, 2012). As mentioned above, two of the major pathways associated with the pathogenesis of atherosclerosis and the actions of pro-inflammatory factors are the MAPKs pathway and the JAK-STAT pathway (Muslin, 2008). Evidence from *in vivo* and *in vitro* studies have shown a crucial role of these pathways in inflammatory diseases and are hence addressed below in more detail (Ren *et al.*, 2005; Muslin, 2008; Valledor *et al.*, 2008; Buckley and Ramji, 2015).

1.5.1 The role of MAPKs pathway in atherogenesis

MAPK pathways include extracellular signal-regulated kinases (ERK1/2), p38 kinase and c-Jun N-terminal kinase (JNK), that all play a role in different cellular

processes such as cell proliferation, growth, apoptosis, inflammation and differentiation (Figure 1.2)(Muslin, 2008).

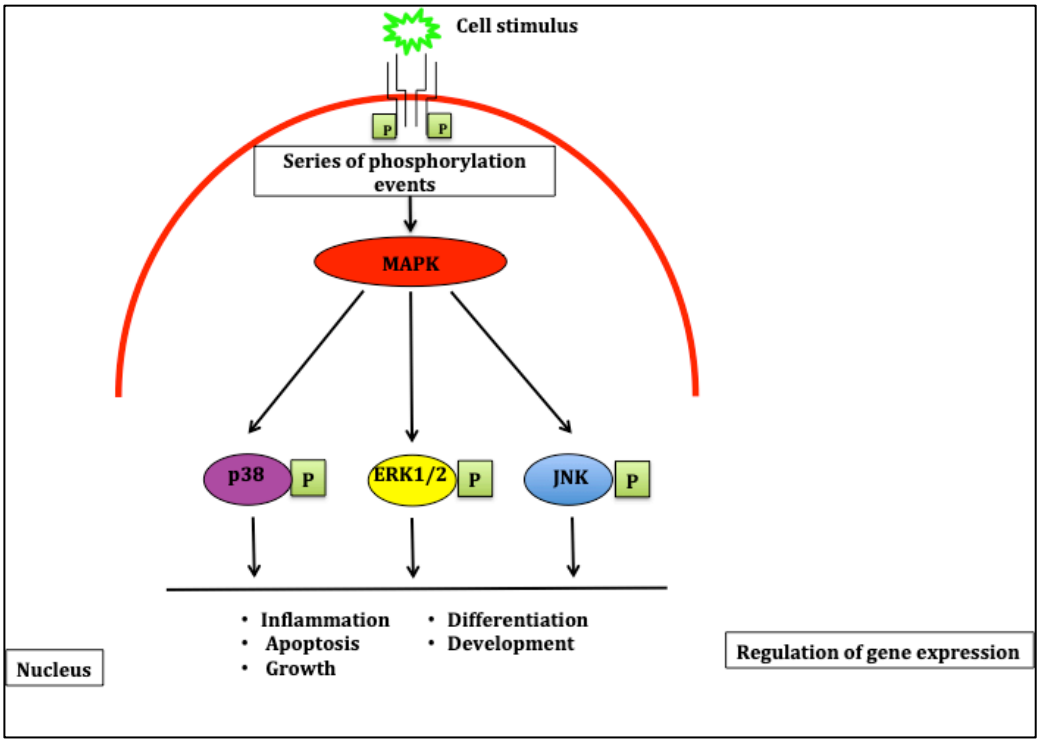

Figure 1.2 Activation of the MAPK family of cell signalling molecules

The MAPK family consists of three main members: p38, JNK and ERK1/2 of which each has important roles in the response of a cell to a stimulus. Upon receiving a cell stimulus (e.g. pathogen or inflammatory cytokines), the activation of the MAPK pathways results in inflammation, cell growth, differentiation or apoptosis.

The ERK1/2 pathway, which plays a key role in the control of cell proliferation and differentiation during the development of atherosclerosis (Hu *et al.*, 2000), is described in more detail here because of direct relevance to the project.

ERK-mediated signalling pathway is a multistep phosphorylation cascade that transmits signals from the cell surface to nuclear targets (Figure 1.3). They are responsible for the activation and phosphorylation of a number of regulatory proteins and transcription factors needed for the expression of genes involved in cell proliferation and inflammation (Hu *et al.*, 2000). Activation of ERK-mediated pathways starts by the binding of specific ligands to their cognate receptors [many are involved including the IFN-γ receptor (IFN-γR)], which then usually gets phosphorylated on

specific tyrosine residues. These phosphorylated intracellular tyrosine residues, in turn, represent docking sites for proteins that are able to bind to phosphorylated motifs, such as the Src homology 2(SH2)-domain containing protein growth factor receptor-bound protein 2 (Grb2) (Muslin, 2008). Grb2 is constitutively bound to the guanine nucleotide-exchange factor Son of sevenless (SOS) When Grb2 binds to the phosphotyrosine motifs on the intracellular portion of the activated receptors, it brings SOS in close proximity to the plasma membrane-tethered small GTPase, Ras, and facilitates Ras activation (Muslin, 2008).

Ras is a master regulator of intracellular signalling cascades and it promotes the activation of ERK cascades as well as other signalling pathways (Muslin, 2008). Activated Ras recruits Raf to the plasma membrane in order to induce its phosphorylation and activation. Thereafter, the signal is transmitted to the MAPK/ERK kinase1 and 2 (MEK1/2) (Plotnikov *et al.*, 2011). Activated MEK1/2 transmits its signal to ERK1/2 by inducing its phosphorylation, and thereby translocation to the nucleus and activation of specific transcription factors (Plotnikov *et al.*, 2011).

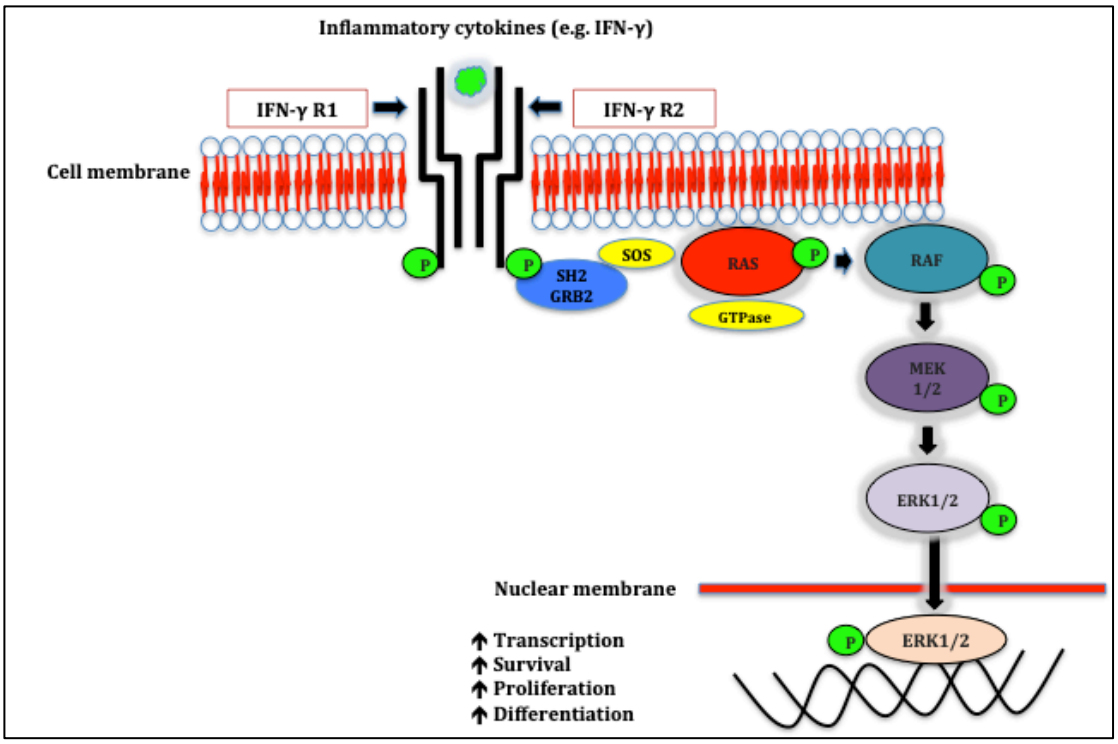

Abbreviations: Interferon gamma (IFN-γ); interferon gamma receptor (IFN-γ R); Src homology 2 (SH2); growth factor receptor-bound protein 2(Grb2); son of sevenless (SOS); guanosine triphosphate enzyme (GTPase); MAPK/ERK kinase (MEK); rapidly accelerated fibrosarcoma (RAF); extracellular regulated kinase (ERK); phosphate (P).

Figure 1.3 Simplified MAPK pathway

The classical activation of ERK1 and ERK2 isoforms is initiated by the binding of a ligand (e.g. IFN-γ) to an extracellular receptor at the plasma membrane (IFN-γR). This is followed by the activation of a small G-protein, which will stimulate the guanine nucleotide exchange factor to convert GDP to GTP, and thereby activate Ras. In turn, Ras recruits and activates the serine/threonine protein kinase, Raf, which activates the MEK. This, in turn, phosphorylates ERK1/2. These events thereby regulate various cellular activities, such as gene expression, differentiation, proliferation and cell survival.

Previous studies that were performed on HFD fed rabbits provided the first evidence of ERK overexpression and activation in atherosclerotic lesions (Hu *et al.*, 2000). Moreover, they demonstrated that the increased migratory and proliferative ability of SMCs derived from the lesions correlates with ERK1/2 activities, which were induced by oxLDL (Hu *et al.*, 2000). Additionally, another study showed that ERK1/2 is integral to the IFN-γ-mediated activation of STAT1; a key regulator of expression of many genes implicated in atherosclerosis such as ICAM-1 and MCP-1 together with the uptake of oxLDL by macrophages (Li *et al.*, 2010). The role of the ERK1:STAT1 axis in

athersosclerosis has not been investigated and hence formed the focus of part of the studies in the project (see Chapter 3-4).

1.5.2 JAK-STAT pathway in atherosclerosis

JAK/STAT is an important signalling pathway regulating the initiation/progression of atherosclerosis (Guadalupe *et al.*, 2009). It is an essential intracellular mechanism for the action of cytokines and other stimuli that regulate gene expression and cellular activation, proliferation and differentiation (Yoshimura *et al.*, 2007). Previous *in vivo* and *in vitro* studies reported activation of the JAK/STAT pathway in atherosclerotic lesions and in vascular cells incubated with cytokines, angiotensin II and lipids (Gharavi *et al.*, 2007; Recinos *et al.*, 2007; Sudesh *et al.*, 2007). STAT1 plays a major role in mediating immune and pro-inflammatory responses such as activation of cellular apoptosis and foam cell formation in atherosclerotic lesion (Lim *et al.*, 2008). Previous study showed that STAT1 deficiency in $ApoE^{-/-}$ mice blocks foam cell formation and early lesion development (Agrawal *et al.*, 2007).

IFN-γ is a major cytokine involved in the initiation of the inflammatory process and in the progression of atherosclerosis. Previous *in vivo* studies pointed to a pro-atherogenic role of this cytokine (Table 1.2)(McLaren and Ramji, 2015). It has been shown to influence many features of atherosclerosis such as the recruitment of monocytes from the blood to the activated arterial endothelium, foam cell formation, adaptive T-helper-1 (Th-1) specific immune responses, plaque development and the expression of pro-inflammatory genes (Ehrt *et al.*, 2001; Ramji and Davies, 2015).

The major signalling pathway that IFN-γ acts through is the JAK-STAT pathway. Activation of this pathway is schematically shown in Figure 1.4. It involves the binding of IFN- γ to two IFN-γR subunits (IFN-γ R1: IFN-γ R2) on the cell surface. These dimers form IFN-γR complex upon binding to the cytokine. The tyrosine residues on the two JAKs (JAK1/2) present on the IFN-γR subunits become phosphorylated leading to the subsequent phosphorylation of the IFN-γR tails. This signals the recruitment of latent STAT1 monomers, which dock to the phosphorylated receptor via their SH2-domains (Kishore and Verma, 2012). Each STAT1 monomer becomes phosphorylated on tyrosine 701 by the JAKs. This is followed by the dissociation of STAT1 from the receptor to form a STAT1: STAT1 homodimer, which translocate to the nucleus to bind

to gamma activated sequence (GAS) elements in the promoters of IFN-γ responsive genes (IRG). IFN-γ stimulated STAT1 homodimers can also be phosphorylated on serine 727, which enhances their transcriptional activity (Kishore and Verma, 2012). Many serine kinases, like ERKs, p38 MAPKs and phosphatidylinositol 3-kinase (PI3K), have been implicated in catalysing this phosphorylation and it's highly likely that this STAT1 modification is both cell- and stimulus-type specific (McLaren and Ramji, 2009).

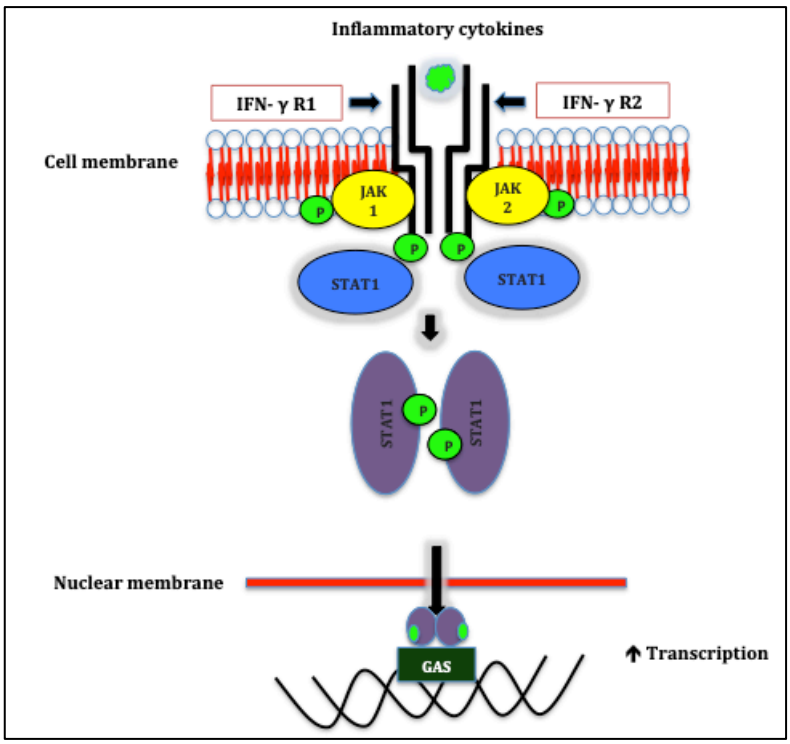

Figure 1.4 IFN-γ signalling pathway

The binding of IFN-γ to its cognate, cell surface receptor involves dimerisation of the two IFN-γ R subunits, made up of IFN-γR1:IFN-γR2 pairs, and results in the activation of two bound tyrosine kinases, JAK1 and JAK2, by tyrosine phosphorylation. Once the JAKs become activated or tyrosine phosphorylated, they mediate tyrosine phosphorylation of the IFN-γR tails through their catalytic, C-terminal kinase domain. Latent STAT1 monomers are then recruited and phosphorylated on tyrosine 701. The tyrosine phosphorylated STAT1 monomers dimerise forming a STAT1:STAT1 homodimer, which can translocate to the nucleus and bind to specific sequence in the promoters of target genes and activate gene transcription.

Previous studies in our laboratory have shown that ERKs are of key importance in macrophages (Li *et al.*, 2010). Whilst IFN-γ is known to primarily activate the JAK-STAT1 signalling pathway, the uptake can also stimulate STAT1- independent

pathways in STAT1$^{-/-}$ mice (Ramana *et al.*, 2002; van Boxel-Dezaire and Stark, 2007). Such signalling pathways include ERKs, protein kinase C (PKC) and PI3K dependent pathways. Some of these pathways can interact with the JAK-STAT1 pathway, and induce STAT1 serine 727 phosphorylation (van Boxel-Dezaire and Stark, 2007; Li *et al.*, 2010). On the other hand, some pathways have been shown to be JAK1-dependent but STAT1- independent, indicating that IFN-γR function is still critical. In addition, other STATs like STAT3 and STAT5b can be activated by IFN-γ, which suggests that the action of IFN-γ stimulated STAT signalling is not necessarily through STAT1 (Ramana *et al.*, 2002).

IFN-γ enhanced the expression of both SR-A and SR for phosphatidyl-serine and oxidised LP (SR-PSOX) in differentiated THP-1 macrophages (a widely employed cell culture system for the study of macrophages in relation to atherosclerosis) and VSMCs, and increased the uptake of oxLDL and acetylated LDL (acLDL) by these receptors in atherosclerotic plaques (Wuttge *et al.*, 2004). Another study showed that IFN-γ promotes the imbalance in cholesterol homeostasis by inducing cholesterol uptake and reducing cholesterol efflux by inhibiting ABCA1 expression in a STAT1-dependent manner and by suppressing the expression of mitochondrial enzymes, such as P450 enzyme cholesterol 27-hydroxylase, which promotes cholesterol removal from the cell (Reiss *et al.*, 2001; McLaren and Ramji, 2009). IFN-γ also increases the expression of ACAT1, which promotes intracellular cholesterol storage and found to be associated with macrophage foam cells in atherosclerotic plaques (Panousis and Zuckerman, 2000).

ApoE deficient mice, which also lack IFN-γR (ApoE$^{-/-}$ / IFN-γR$^{-/-}$), are associated with a reduction in atherosclerosis development as well as a 60% decrease in lipid build up in the lesions when fed a HFD (Buckley and Ramji, 2015). Additionally, IFN-γ can influence the recruitment of immune cells by inducing the expression of MCP-1, ICAM-1 and VCAM-1 on ECs during the early stages of atherosclerosis development (Boisvert, 2004; Charo and Taubman, 2004; Moss and Ramji, 2015).

IFN-γ also regulates the expression of apoptotic genes and therefore induces apoptosis of foam cells (Moss and Ramji, 2015). In addition, IFN-γ enhances the weakening of the fibrous cap around atherosclerotic plaques by inducing the

expression and activities of proteases, such as MMPs, and inhibiting collagen synthesis by SMCs resulting in unstable plaques (Moss and Ramji, 2015). All these events cause rupture of the plaques and stimulate thrombus formation. In the light of these observations, it is clear that IFN-γ can promote disease progression even at an advanced stage when plaque rupture is imminent.

All the evidences detailed above together with other lines of evidence support a role for IFN-γ and its mediated pathways in the promotion rather than prevention of atherosclerosis, which makes it a promising therapeutic target (Whitman *et al.*, 2000; Moss and Ramji, 2015). In addition, suppressor of cytokine signalling (SOCS) proteins are critical modulators of inflammatory processes within the atherosclerotic vascular wall and essential for the negative regulation of the JAK-STAT pathway (Wormald and Hilton, 2004). Activation of such endogenous anti-inflammatory pathways might also be a therapeutic strategy for treating CVD (Rakesh and Agrawal, 2005).

1.6 Gene expression and atherosclerosis

New developments in molecular biology have directed the research of human disease etiology towards its genetic basis. The understanding of the genetic basis, or the molecular origin, of a disorder and the insight into the way genetic information is expressed or modulated by the environment, will have a major impact on protection and treatment of diseases (Doevendans *et al.*, 2001).

The role of only a minority of genes involved in the atherosclerotic process is known and the genetics-based treatment or elimination of the genetic risk factors require a complete understanding of the molecular basis of the disease. Recent studies suggest that treatment of atherosclerosis should be personalised and genotype specific, as the genetic makeup can determine the outcome of a pharmacological intervention (pharmacogenetics) (Funk *et al.*, 1993). Every stage of lesion development depends on a different gene expression program. Once the trigger for atherosclerosis has initiated disease development, the expression of various genes is activated or silenced and contributes to lesion progression (Doevendans *et al.*, 2001).

It is estimated that more than 400 genes are involved in the regulation of processes such as EC dysfunction, coagulation, inflammation, lipid metabolism and

apoptosis (Funke and Assmann, 1999). Many genes involved in LPs metabolism, cholesterol hemostasis and cellular migration have been identified, some of which are strongly related to atherosclerosis or CVD. Table 1.3 lists some of these genes and their roles in atherosclerosis (Funk *et al.*, 1993; Gosling *et al.*, 1999; Kitagawa *et al.*, 2002; Oram and Vaughan, 2006).

Table 1.3 Key genes associated with the development of atherosclerosis

Gene	Role in atherosclerosis	Reference
ICAM-1	An immunoglobulin (Ig)-like cell adhesion molecule that is highly expressed in atherosclerotic lesions as a result of activation of ECs by inflammatory stimulators such as TNF-α, IFN-γ, IL-1 and lipopolysaccharide (LPS), which facilitates the transmigration of leukocytes. Previous study on human coronary and carotid arteries showed that ICAM-1 expression is correlated to vascular lesions. Other studies on mice, rabbits and humans fed a HFD, reported an increase in the expression of various chemo-attracting molecules (CAMs), such as ICAM-1. Knocking out of ICAM-1 in wild-type animals ($ICAM^{-/-}$) showed a 75% reduction in HFD induced atherosclerosis burden when compared with wild-type animals. It is most likely that an absence of ICAM-1 greatly reduces the influx of monocytes to sites of lesions and therefore reduces the associated atherosclerotic events. Monoclonal antibodies directed to ICAM-1 in $ApoE^{-/-}$ animals fed a chow diet significantly reduced the homing of macrophages to atherosclerotic plaques by 65%. In addition, anti-ICAM-1 significantly reduced the homing of macrophages to the intima by 42% in hypercholesterolemic rats.	(Nageh *et al.*, 1997; Patel *et al.*, 1998; Bourdillon *et al.*, 2000; Collins *et al.*, 2000; Wolf and Lawson, 2012)
MCP-1	Also known as CCL2. See Table 1.2	

SR-A1	Member of the PRRs that mediates the innate immune host response through recognition of highly conserved pathogen-associated molecular patterns. It is expressed on the cell surface of macrophages, aortic ECs and VSMCs within atherosclerotic plaques. SRs on macrophages and SMC are not regulated by the intracellular cholesterol content; therefore, the unregulated uptake of modified LDL via SRs is responsible for cholesterol accumulation and foam cell formation. Previous study using SR-A1$^{-/-}$/ApoE$^{-/-}$ mice exhibited increased plasma cholesterol but a reduced atherosclerotic plaque area, compared with ApoE$^{-/-}$ mice. Loss of function of SR-A1 may prevent or decrease the development of atherosclerosis by inhibiting the accumulation of lipids in macrophages.	(Brown and Goldstein, 1986; Suzuki *et al.*, 1997; Moore and Freeman, 2006b; Ben *et al.*, 2015)
ABCA1/ ABCG1	ATP binding cassette transporters that mediate cholesterol homeostasis in macrophages by regulation of the balance between lipid influx and efflux. Therefore, they have a major influence on the progression of atherosclerotic plaques. Previous studies using ApoE$^{-/-}$ mice showed that increased ABCA1 or ABCG1 activity is associated with markedly reduced atherosclerosis. Not only were a decrease in lesion size evident, but also associated with the appearance of less-complex lesions with no fibrous caps and reduced foam cells. Another study where the bone marrow from ABCA1$^{-/-}$ or ABCG1$^{-/-}$ mice was transplanted into hypercholesterolemic LDLR$^{-/-}$ recipients showed a moderate increase in atherosclerosis indicating that ABCA1/ABCG1 deficiency accelerates atherosclerosis.	(van Eck *et al.*, 2002; Barter, 2005; Oram and Heinecke, 2005; Ángel *et al.*, 2006; Mollie *et al.*, 2006; Oram and Vaughan, 2006; Westerterp *et al.*, 2013)
ApoE	Apolipoprotein present on most plasma LP that carries	(Curtiss, 2000;

	dietary and liver-derived cholesterol through blood circulation, and so plays a key role in the maintenance of plasma cholesterol levels and regulation of chronic inflammatory responses. In previous studies, development of complex atherosclerotic lesions were observed in ApoE$^{-/-}$ mice as a result of impaired clearance of cholesterol-enriched particles, which led to the accumulation of cholesterol-rich LP in the plasma compared with wild-type mice.	Buckley and Ramji, 2015)

1.7 Monocytes and macrophages in atherosclerosis

Monocytes and macrophages have crucial and distinct roles in tissue homeostasis and immunity. They contribute to a broad spectrum of pathologies and are therefore considered as attractive therapeutic targets (Moor *et al.*, 2013). Monocytes are key players during inflammation; they are highly heterogeneous cells, which arise from myeloid precursor cells in primary lymphoid organs, including the liver, spleen and bone marrow, during both embryonic and adult haematopoiesis (Dutta *et al.*, 2012; Robbins *et al.*, 2012). They express various receptors, which sense environmental changes that drive them to change their functional phenotype in response to stimulation into inflammatory or anti-inflammatory subsets (Yang *et al.*, 2014).

Monocytes originate and develop from haematopoietic stem cells (HSCs) in the bone marrow via several differentiation steps and intermediate progenitor stages that involve transition from the common myeloid progenitor (CMP) to the granulocyte/macrophage progenitor (GMP), and then to the macrophage/dendritic cells (DC) progenitor (MDP) stages (Figure 1.5). The MDP gives rise to monocytes, which are released into blood circulation (Ginhoux and Jung, 2014). Circulating monocytes are recruited to tissues during the inflammatory response via the influence of cytokines and chemokines, such as CCL2 and IFN-γ, where they can differentiate into tissue macrophages by M-CSF that is highly expressed at the site of inflammation (Ginhoux and Jung, 2014).

As mentioned earlier (Section 1.3.1), during inflammation and following chemokinesis, monocytes migrate to the site of inflammation and firmly adhere to lesion ECs and differentiate to macrophages under the influence of M-CSF. Macrophages actively take part in the immune response by engulfing pathogens and damaged cells via phagocytosis and releasing proinflammatory factors (Klaus Ley *et al.,* 2011).

There has been great interest in macrophage heterogeneity in atherosclerotic lesions, particularly regarding macrophages involved in pro-inflammatory processes (M1) versus those involved in resolution and repair (M2)(Johnson and Newby, 2009). The dynamic roles that macrophages play in early and advanced atherosclerotic plaques make macrophage phenotype modulation an attractive therapeutic target and potent biomarker for the prevention and treatment of CVD (Mclaren *et al.*, 2011; Zhang *et al.*, 2012; Moore, *et al.*, 2013; Wang *et al.* , 2014).

Macrophages play key roles during all stages of atherosclerosis such as foam cell formation, amplification of the inflammatory response and control of plaque stability (Moore *et al.*, 2013). During atherogenesis, oxLDL and cytokines such as IFN-γ, TNF-α, TGF-β and IL-10 can trigger the phenotypic modulation of macrophages (Ley and Miller, 2011). *In vitro*, human monocytes can differentiate into various macrophage subsets. Unpolarised (M0) macrophages are generated after M-CSF treatment, and if these macrophages are treated with IFN-γ and LPS, they polarise to an M1 phenotype with characteristic expression of TNF-α and IL-12 (Jablonski *et al.*, 2015). M2 macrophages were originally described as human blood MDM (HMDM) differentiated in the presence of IL-4 and IL-13. They produce anti-inflammatory signals by secreting cytokines such as IL-10 and TGF-β1, which can switch the proinflammatory M1 macrophages into M2 macrophages and enhance efferocytosis. These macrophages are associated with wound healing and tissue repair (Martinez *et al.*, 2009; Tabas, 2010; Ley *et al.*, 2011). M4 macrophages are a hallmark in human atherosclerotic coronary arteries and can be produced *in vitro* by treatment of bone marrow-derived macrophages (BMDM) with platelet factor 4(PF4). M4 macrophages have a unique transcriptome that is closer to M2 than M1 subtype (Ley *et al.*, 2011).

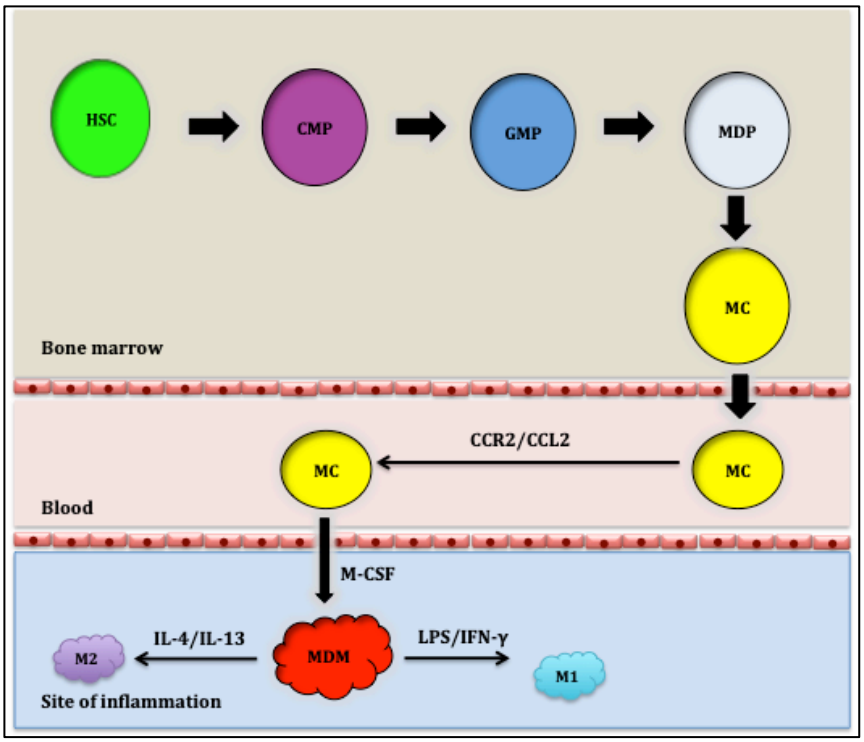

Abbreviations: (HSC) haematopoietic stem cell; (CMP) common myeloid progenitor; (GMP) granulocyte/macrophage progenitor; (MDP) macrophage/dendritic cells progenitor; (MC) monocyte; (MDM) monocyte-derived macrophage; (CCR) chemokine receptor; (IL-4) interleukin-4; (IL-13) interleukin-13; (IFN-γ) interferon gamma); (LPS) lipopolysaccharide; (M-CSF) macrophage colony stimulation factor.

Figure 1.5 Monocyte and macrophage development

Monocytes originate in the bone marrow where they develop from HSCs via several differentiation steps and intermediate progenitor stages that pass-through CMP, GMP and MDP stages. The MDP gives rise to monocytes, which are released in blood circulation. Circulating monocytes are recruited to tissues where they can differentiate into tissue macrophages under the influence of M-CSF. Additional heterogeneity also exists between macrophages, with two major classes being identified: the classically activated (M1) and the alternatively activated (M2) macrophages. M2 macrophages can develop in response to IL-4 and IL-13 whereas M1 can develop in response to IFN-γ and LPS.

1.8 Cellular processes implicated in atherosclerosis

Understanding the cellular biology of atherosclerosis is essential. Recent advances in the cellular pathobiology of atherosclerosis highlight important cellular atherogenic processes, including mechano-transduction and inflammatory processes in ECs, macrophages and SMCs (Tabas *et al.*, 2015). Understanding the molecular-cellular mechanisms of processes involved in plaque development and advanced plaque progression can lead to new avenues for therapies. Some of the steps described

below from the basis of assays used in this project and hence discussed in detail.

1.8.1 Cholesterol homeostasis

1.8.1.1 Foam cell formation

Macrophage foam cells play a critical role in the development of atherosclerosis. The generation of these cells is associated with an imbalance of cholesterol influx, esterification and efflux (Yu *et al.*, 2013). Formation of macrophage foam cells in the intima is a major hallmark of early stage atherosclerotic lesions as described earlier (Section 1.3.2). As macrophage pathways for metabolising LP-derived cholesterol become impaired, cholesterol uptake results in the accumulation of CE as cytoplasmic lipid droplets and subsequently triggers the formation of foam cells (Yu *et al.*, 2013).

Cholesterol uptake via receptor-mediated endocytosis through SRs such as SR-A and CD36 have been implicated in this process. *In vitro* studies have shown that CD36 and SR-A account for 75% to 90% of oxLDL internalisation by macrophages, whereas other SRs cannot compensate for their absence (Kunjathoor *et al.*, 2002). Thus, CD36 and SR-A are the most important receptors responsible for the uptake of modified LPs by macrophages (Moore and Freeman, 2006b; Ben *et al.*, 2015).

Potent inhibitors of ACAT1 have been shown to inhibit macrophage foam cell formation and retard atherosclerosis in $ApoE^{-/-}$ mice (Yoshinaka *et al.*, 2010). Although a role for native LDL in foam cell formation was initially discounted, researchers have shown that in the arterial intima, in addition to receptor-mediated endocytosis, LDL undergoes macropinocytosis by macrophages when it is at concentrations similar to those that occur in hyperlipidemic conditions. This results in foam cell formation (Kruth *et al.*, 2005). This receptor-independent endocytic pathway is also involved in the uptake of modified LPs, and delivers cholesterol to the endolysosomal compartment and stimulates cholesterol esterification (Moore *et al.*, 2013). It is probable that multiple, simultaneous pathways contribute to foam cell formation *in vivo* (Kruth, 2011).

1.8.1.1.1 Macropinocytosis

Macropinocytosis is a highly regulated form of endocytosis that was first described morphologically by Warren Lewis in 1931 (Lewis, 1931) He named this activity pinocytosis that was later renamed macropinocytosis to differentiate the pathway from processes involving smaller vesicles (Lim and Gleeson, 2011). Macropinocytosis is an actin-dependent process that consists of a series of co-ordinated signalling events involving remodelling of the cytoskeleton, which is initiated from the surface membrane ruffles that mediates the non-selective uptake of solute molecules, nutrients and antigens. The process gives rise to large endocytic vacuoles called macropinosomes, which are distinct from other forms of endocytic vesicles (Figure 1.6) (Hewlett *et al.*, 1994; Lim and Gleeson, 2011). It is a signal-dependent process that normally occurs in response to growth factor (GF) stimulation, such as M-CSF, epidermal GF (EGF), PDGFs or tumour-promoting factors (Lim and Gleeson, 2011).

Macropinocytic vesicles have no apparent coat structures and although heterogeneous in size, they are generally considered to be >0.2 μm in diameter (Hewlett *et al.*, 1994). Thus, in addition to its size, macropinosomes can also be easily identified *in vitro* through the use of fluid phase markers such as Lucifer Yellow (LY), horseradish peroxidase (HRP) and dextran (Swanson and Watts, 1995), or *in vivo* by confocal microscopy and live imaging after injection of fluorescence-labelled dextran particles (Chen *et al.*, 2018). The macropinosomes can subsequently either be sent back to the plasma membrane, thus recycling its content back to the cell surface, or the components can be transported to the late endosomes/lysosomes for degradation (Lim and Gleeson, 2011).

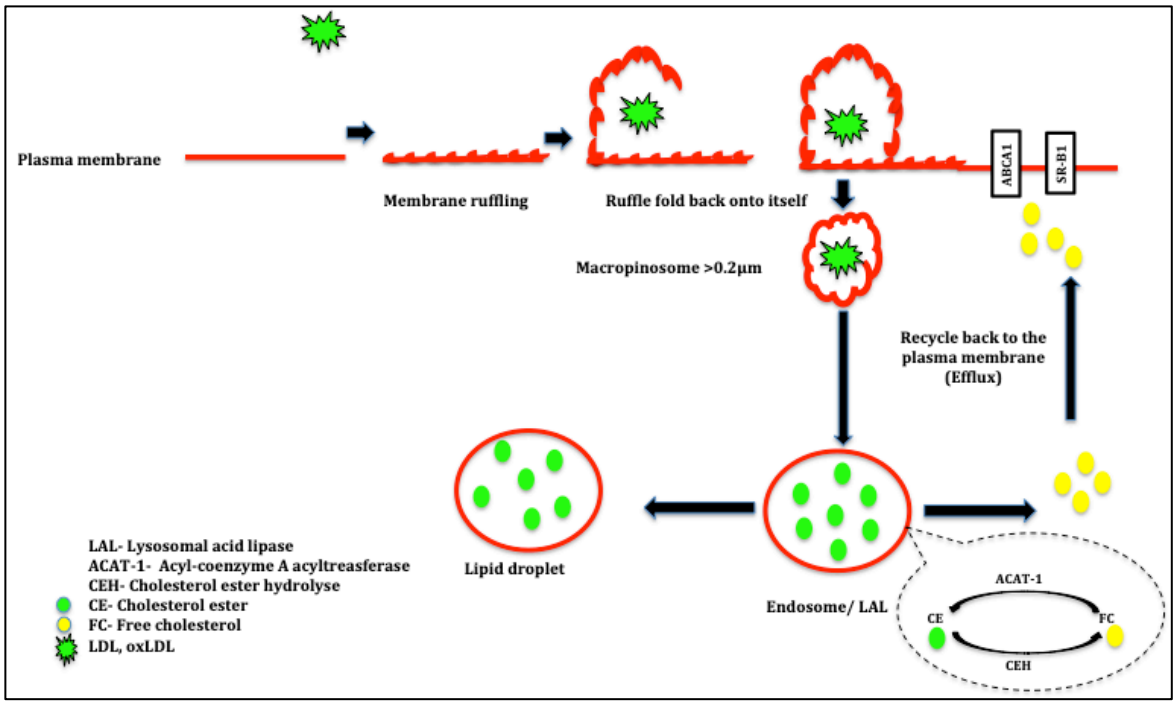

Figure 1.6 Macropinocytosis

Macropinocytosis involves actin cytoskeleton rearrangement at the plasma membrane leading to the formation of membrane ruffles. Ruffles may fold back onto themselves and fuse at the base of the plasma membrane, trapping solute and soluble substances in macropinosomes. The LDL or oxLDL content of the macropinosomes is then metabolised to CE and FC at the late endosome/lysosome. FC is recycled back to the plasma membrane where it can be effluxed through ABCA1 or SR-B1 to ApoA1. Whereas CE will be stored in the cytoplasm in the form of lipid droplets, resulting in foam cells formation.

As mentioned earlier, engorgement of macrophages with cholesterol is the defining pathological characteristic of atherosclerotic plaques. Previous studies demonstrated the importance of macrophage fluid phase endocytosis as a relevant pathway to target in modulating macrophage cholesterol accumulation in atherosclerosis (Kruth *et al.*, 2002). It showed a key role of macropinocytosis as the pathway of LDL uptake by macrophages (e.g. PMA-stimulated uptake of LDL taken up as part of the bulk phase fluid endocytosis) and determined signalling and cytoskeletal components involved in the process (Kruth *et al.*, 2002).

Previous *in vitro* studies reported the effect of cytochalasin-D (cell-permeable and potent inhibitor of actin polymerisation) on macropinocytosis-mediated foam cell formation using THP-1 macrophages and HMDM (Racoosin and Swanson, 1989). It

showed that the uptake of DiI- acetylated LDL (Dil-acLDL) (a form of LDL used in *in vitro* foam cell formation assays) was significantly inhibited in association with a reduction of intracellular cholesterol content (Michael *et al.*, 2013). In addition, an *in vitro* study using LY reported an atheroprotective effect of TGF-β and IL-33 in reducing LY uptake by THP-1 macrophages (Michael *et al.*, 2013). Furthermore, treating cells with IFN-γ also showed a reduction in the uptake levels through macropinocytosis though its effects at stimulating modified LDL uptake through receptor-mediated pathway has been reported in numerous studies (Michael *et al.*, 2013). Overall, all these studies demonstrate the importance of macropinocytosis during foam cell formation and highlight it as a potential target for therapeutic intervention.

1.8.1.1.2 Cholesterol efflux and reverse cholesterol transport (RCT)

Efflux of cholesterol is critical for maintaining homeostasis because most cells in the periphery of the body do not express pathways for catabolising cholesterol (Phillips, 2014). The efflux process is very significant because cholesterol overloading, such as in macrophage foam cells in the arterial wall, leads to the development of atherosclerotic plaques (Phillips, 2014). RCT is a pathway that transports cholesterol from extra hepatic-cells and tissues to the liver and intestine for excretion via the bile system. Major constituents of RCT include acceptors such as HDL and ApoA-I together with enzymes such as lecithin:cholesterol acyltransferase (LCAT), phospholipid transfer protein (PLTP), hepatic lipase (HL) and cholesterol ester transfer protein (CETP), which regulate cholesterol transport (Ohashi *et al.*, 2005). Eventually, cholesterol in the HDL particles is delivered to the liver via SR-B1, converted to bile salts and excreted in part through the gastrointestinal tract (Ohashi *et al.*, 2005).

Cholesterol efflux, part of the RCT process, is a major process by which macrophages within the vessel wall "secrete" cholesterol outside the cells when the extracellular acceptors, like ApoA-I and HDL, approach macrophages in the subintimal space and stimulate intracellular cholesterol to be released outside the cells for excretion (Ohashi *et al.*, 2005). Overall, macrophages possess four pathways for exporting free (unesterified) cholesterol to extracellular HDL:

1. Passive processes that include simple diffusion via the aqueous phase;

2. Facilitated diffusion mediated by SR-BI;
3. Active pathways mediated by the ABC transporters ABCA1 and ABCG1, which are membrane lipid translocases (Phillips, 2014); and
4. The efflux of cellular PL and free cholesterol to ApoA-I promoted by ABCA1 that is essential for HDL biogenesis.

Previous studies showed that HDL apolipoproteins promote efflux of cholesterol, PL and other lipophilic molecules from the cells by an active process mediated by ABCA1 (Oram, 2003). ABCA1, either directly or indirectly, translocates PLs and cholesterol to the cell surface, where they appear to form lipid domains that interact with amphipathic α-helixes in apolipoproteins. This interaction solubilises these lipids and generates nascent HDL (nHDL) particles that dissociate from the cell. Binding of apolipoproteins to ABCA1 may also enhance the activity of this lipid-transport pathway. Thus, the apolipoprotein/ABCA1 pathway efficiently clears cells of excess cholesterol that would otherwise accumulate as intracellular lipid droplets leading to foam cell formation and accelerate atherosclerosis (Figure 1.7) (Oram, 2003).

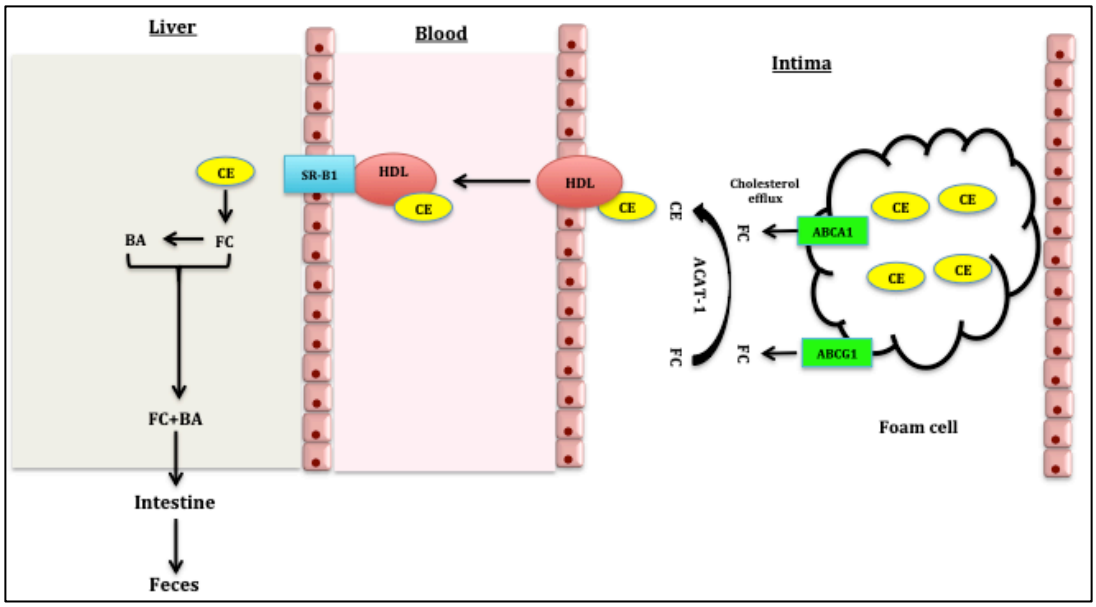

Abbreviations: (CE) cholesterol ester; (FC) free cholesterol; (SR-B1) scavenger receptor-b1; (HDL) high density lipoproteins; (BA) bile acids.

Figure 1.7 Reverse cholesterol transport

CE stored in lipid droplets of macrophage foam cells is hydrolysed by neutral CE hydrolases. Lipid-poor nascent preβ-migrating HDL particles acquire free cholesterol (FC) from macrophage foam cells via ABCA1, whereas the ABCG1 transporter facilitates cholesterol efflux from macrophages to α-HDL particles. FC is esterified to CE within nascent HDL particles by LCAT, thereby generating mature α-HDL. The liver selectively takes up HDL-associated CE via SR-BI and excretes HDL-derived cholesterol into the bile as FC or as bile acids (BA) after conversion (taken from Escolà-Gil *et al.*, 2015).

1.8.2 Reactive oxygen species production

Free radicals/ROS and reactive nitrogen species (RNS) production occurs continuously in all cells as part of a normal cellular function (Emerit *et al.*, 2004). However, excess production originating from endogenous or exogenous sources play a key role in many diseases (Young and Woodside, 2001; Bulotta *et al.*, 2014). Several lines of evidence show that oxidative damage to LPs is an important step in the early event leading to the development of atherosclerosis (Pham-Huy and He, 2008). An excess production of ROS has also been implicated in the pathogenesis of other diseases such as diabetes, cancer, neurodegenerative diseases as well as psychological disorder or the aging processes. Therefore, maintaining normal cellular ROS

concentrations is vital to the proper physiological function of numerous cell types throughout the body (Oliveira *et al.*, 2004; Abrescia and Golino, 2005; Morrell, 2008).

During times of cell stress, ROS levels can greatly increase and because of their highly reactive nature, ROS can modify other oxygen species, proteins or lipids. Evidence suggests that common risk factors for atherosclerosis increase the risk of production of free ROS not only from the ECs but also from the SMCs (Vogiatzi and Tousoulis, 2009). Thus, hypercholesterolemia, diabetes mellitus, arterial hypertension, smoking, age and nitrate intolerance increase the production of free ROS (Lum and Roebuck, 2001). Several processes are triggered by excessive ROS, including expression of adhesion molecules, the proliferation and migration of SMCs, apoptosis of ECs, oxidation of lipids and the activation of MMPs (Lum and Roebuck, 2001; Förstermann, 2008).

1.8.3 Phagocytosis

Macrophages are phagocytic cells and thus have an important additional role in scavenging of oxLDL, unwanted or dead cells and cellular debris via phagocytosis (Schrijvers *et al.*, 2007). Early atherosclerotic plaques are characterised by an efficient phagocytic clearance of apoptotic cells, unlike advanced plaques where the process is defective leading to the formation of secondary necrosis, expansion of the necrotic core and increased plaque vulnerability (Schrijvers *et al.*, 2007; Thorp *et al.*, 2009; Schrijvers, De Meyer and Martinet, 2012). When cells undergo apoptosis, they express cell-surface and secreted molecules that promote their rapid recognition by phagocytes and influence their phagocytosis (Tabas, 2005). Numerous investigations have shown that phagocytic clearance of apoptotic cells will prevent many pathophysiological consequences of apoptosis like the harmful exposure to inflammatory responses as well as from the immunogenic content of the dying cells after undergoing apoptosis (Tabas, 2005). Protective mechanisms of phagocytosis include the suppression of inflammatory signalling and the activation of anti-inflammatory pathways, these include the stimulation of the production of the anti-inflammatory cytokine IL-10 and the inhibition of secretion of the pro-inflammatory cytokine IL-12, in addition to the inhibition of recruitment, survival and proliferation of macrophages themselves. This involves a suppressive mechanism requiring the

secretion of TGF-β, which in turn inhibits the recruitment of circulating monocytes and the secretion of pro-inflammatory cytokines IL-1β, IL-8 and TNF-α (Reddy *et al.*, 2002; Chung *et al.*, 2006). Moreover, phagocytosis of apoptotic T cells by macrophages results in vascular endothelial growth factor (VEGF) secretion, which can promote ECs proliferation (Reddy *et al.*, 2002).

Previous *in vivo* and *in vitro* studies using ApoE$^{-/-}$ mice showed that an impaired clearance of apoptotic cell remnants results in a systemic pro-inflammatory condition when compared to wild-type controls (Grainger *et al.*, 2004). Therefore, analysis of the cell death and phagocytosis machinery as well as survival strategies of cells in plaques could provide additional insights for the development of new plaque stabilising strategies.

1.8.4 Cellular proliferation and migration

Migration and proliferation are highly integrated multistep processes that occur during vascular development or for tissue repair in response to vascular injury (Louis and Zahradka, 2010). Migration contributes to several important pathological processes, including vascular diseases and chronic inflammatory diseases. Thus, understanding the fundamental mechanisms underlying cell migration holds the promise of effective therapeutic approaches for treating disease, cellular transplantation and the preparation of artificial tissues (Ridley *et al.*, 2003).

Vascular injury and inflammation will stimulate the migration of monocytes and SMCs to the intimal space where they start to proliferate, resulting in the formation of atherosclerotic lesions (Kraemer, 2000). Several different growth factors and cytokines have been identified as mediators of cellular migration in the development of intimal lesions. The principal mediators of monocyte adhesion and recruitment to the injured or activated vascular wall is MCP-1 and ICAM-1 (Kraemer, 2000; Wolf and Lawson, 2012; Ramji and Davies, 2015). Previous studies showed that deficiency of the chemokine MCP-1 leads to almost complete attenuation of atherosclerosis in mouse model systems (Wolf and Lawson, 2012; Moore and Sheedy, 2013).

1.9 The use of animal models for the investigation of the ERK1: STAT1 serine 727 phosphorylation axis in the regulation of atherosclerosis and analysis of nutraceutical actions

Modern biomedical research requires robust animal models to understand the pathogenesis, progression and mechanisms underlying disorders such as human CVD. Animal models have been used to address a variety of scientific questions, encourages researchers to investigate a broad range of mechanisms and assess novel therapies before translation to humans (Getz and Reardon, 2012; Kramer *et al.*, 2018). In this context, the availability of numerous genetically modified animal models of human vascular disease allows the isolation of primary cells directly from these animal, thereby providing the opportunity to evaluate the functional, structural and molecular roles of various factors on the disease associated events in detail (Krame *et al.,* 2018).

As mentioned earlier, atherosclerosis is a chronic inflammatory disorder of the vasculature that is initiated by various risk factors that ultimately leads to the development of atherosclerotic plaques (Libby *et al*. 2016). Cytokine signalling plays a critical role in the disease and it is therefore important to gain a deeper mechanistic insight for both advancing our understanding of the molecular basis of the disease and for the identification of novel targets for therapeutic intervention. Previous studies in the laboratory investigated the molecular mechanisms underlying IFN-γ actions on macrophage expression of key genes implicated in atherosclerosis together with the uptake of modified LPs in relation to the disease (Harvey and Ramji, 2005; McLaren and Ramji, 2009; Ramji and Davies, 2015). The most extensive inhibition of the IFN-γ-induced STAT1 serine 727 phosphorylation was observed using the ERK1/2 pharmacological inhibitor PD 98059 (Li *et al.*, 2010). Additional biochemical studies and RNA interference assays showed that ERK1/2 was integral to the IFN-γ-induced STAT1 serine 727 phosphorylation, the expression of key genes induced by this cytokine and the uptake of modified LPs by human macrophages (Li *et al.*, 2010). The role of the ERK1:STAT1 serine 727 phosphorylation axis on atherosclerosis is unclear and was therefore investigated in another project in the laboratory using the $LDLR^{-/-}$ model system. Because ERK2 deficiency is embryonic lethal (Muslin, 2008), the studies focused on $ERK1^{-/-}$ mice and STAT1 knock-in mice in which serine 727 had been changed to alanine (S727A).

The availability of these animals allowed an excellent opportunity to use primary murine BMDMs from them to further probe the role of the ERK1:STAT1 serine 727 phosphorylation axis on key cellular processes implicated in atherosclerosis. The existence of such mouse models or BMDMs from them are not only useful for studying the roles of specific genes or signalling pathways in atherosclerosis but also help in understanding the mechanisms underlying the anti-inflammatory actions of numerous nutraceuticals in the prevention and treatment of atherosclerosis (Moss and Ramji, 2016). One of the major nutraceuticals that has shown potent anti-inflammatory effects is hydroxytyrosol (HT), a poly phenolic compound found in olive oil (Vilaplana-Pérez *et al.*, 2014). Previous unpublished research in the laboratory showed that HT inhibited a number of macrophage processes associated with atherosclerosis: monocytic migration, pro-atherogenic gene expressions, ROS production, uptake of modified LDL and inflammasome stimulation. In addition, HT stimulated the efflux of cholesterol from foam cells and the expression of the ABCA1 gene. Interestingly, HT was also found to inhibit the IFN-γ-mediated phosphorylation of STAT1 on serine 727 without affecting that on tyrosine 701 (supplementary figure S-1). This suggested a potentially important role for the ERK1:STAT1 serine 727 phosphorylation axis in the anti-atherogenic action of HT, which could be probed further using BMDM from existing animals. Therefore, the role of HT in the context of current and potential therapies for atherosclerosis together with its effect on atherosclerosis-associated events will be discussed in detail in the next section in both *in vitro* and *in vivo* experimental models.

1.10 Current and potential therapies for atherosclerosis

A healthy lifestyle that includes beneficial changes to diet (such as increasing fruit and vegetable consumption, reducing saturated fat and dietary salt intake), increasing physical exercise, weight and stress management, and stopping smoking reduces the adverse clinical consequences of CVDs and the need for cholesterol lowering therapies (Chyu and Shah, 2011).

In the past few years, statins have been considered as the most commonly and successfully used cholesterol-lowering class of pharmaceutical therapies. It has also been found to modulate immune cell activation and to exert anti-inflammatory effects

on the vascular wall by increased expression of atheroprotective genes and inhibition of the actions of pro-inflammatory mediators, and therefore decreasing the number of inflammatory cells in atherosclerotic plaques (Vaughan *et al.*, 2000; Zhou and Liao, 2009). Previous animal studies showed that statins also reduce thrombus formation (Masanori *et al.*, 2001).

Statins act by inhibition of the enzyme involved in the rate limiting step during cholesterol biosynthesis, 3-hydroxy-3-methylglutaryl-CoA (HMG CoA) reductase, resulting in a reduction in circulating LDL cholesterol and possible increase in HDL levels (Zhou and Liao, 2009; Ramkumar *et al.,* 2016). However, the maximum reduction in CVD mortality that can be attributed to statins is approximately 30% of subjects already receiving therapy (Mclaren *et al.*, 2011). Recently, concern has also been expressed regarding the over-prescription of statins as well as the potential adverse effects of statin therapy. This has resulted in several patients stopping taking statins due to concerns about the potential risk of long-term statin use (Logue *et al.*, 2015). High-dose statin therapy is known to exert side effects such as nose bleeds, non-allergic rhinitis, headaches, muscle pain and an increased risk of developing diabetes and hepatic dysfunction. In addition, higher doses have been associated with toxicity. The interactions between statins and other drugs is a very strong risk factor in the development of such toxicity (Collaboration *et al.*, 2010; Navarese *et al.*, 2013; Russo *et al.*, 2014; Logue *et al.*, 2015). Thus, the need for additional lipid-lowering compounds or other therapeutic agents is required to further reduce the risk.

Ezetimibe acts at the brush border of the small intestine and inhibits the uptake of dietary and biliary cholesterol through the inhibition of the Niemann-Pick C1-like protein (NPLC1L1) in the intestine and therefore reduces cholesterol uptake (van Heek *et al.*, 2001; Phan *et al.*, 2012). Ezetimibe therapy can be used alone or in combination with statins to enhance the lipid lowering potential, especially in those individuals that are unable to achieve target plasma LDL levels whilst receiving the maximal dose of statins (Zhou and Liao, 2009). Several clinical trials have been carried out to investigate the effect of ezetimibe alone or in combination with statins (Baigent *et al.*, 2011; Cannon *et al.*, 2015; Tsujita *et al.*, 2015; Banach *et al.*, 2016). IMPROVE-IT was the first trial to show a significant reduction in cardiovascular events when ezetimibe was added to statin therapy, demonstrating a significant additional effect of

ezetimibe to statins in terms of both serum LDL reduction and reduction of cardiovascular events (Cannon *et al.*, 2015). The study found that the addition of ezetimibe to simvastatin resulted in a significant reduction of the serum LDL and that the cardiovascular event rate at 7 years was 32.7% in patients receiving simvastatin with ezetimibe compared with 34.7% in patients receiving simvastatin monotherapy (Cannon *et al.*, 2015). This provided evidence that ezetimibe has a protective benefit against major cardiovascular events when used with statins in high-risk patients through further reducing serum LDL levels (Cannon *et al.*, 2015)

Another potential therapy for CVD is targeting Proprotein convertase subtilisin/kexin type 9 (PCSK9) enzyme, where increased plasma levels predicts for CVD (Huijgen *et al.*, 2012). It acts by reducing LDL intake from circulation by enhancing LDLR degradation and preventing LDLR recycling to the cell surface (Levy *et al.*, 2013; Tavori *et al.*, 2013). Previous studies using human ECs showed that PCSK9 silencing significantly reduced oxLDL-induced apoptosis (Wu *et al.*, 2011). In addition, PCSK9 silencing could inhibit vascular inflammation and atherosclerosis via decreasing toll like receptor 4/ nuclear factor kappa B (TLR4/NF-κB) signalling pathway in $ApoE^{-/-}$ mice (Tang *et al.*, 2017). Furthermore, PCSK9 inhibition reduced endothelial dysfunction, ApoB secretion and atherosclerotic lesion size (Sun *et al.*, 2018). PCSK9 inhibitors have been approved for patients with either familial hypercholesterolemia or atherosclerosis, who require additional reduction of serum LDL (Lin *et al.*, 2018). In addition, PCSK9 inhibition combined with statins has been used as a new approach to help reduce serum LDL levels in patients with either statin intolerance or unattainable LDL goal (Kuehnast *et al.*, 2014).

Manipulating cytokine signalling represents another potential therapeutic avenue. Since the inflammatory response in atherosclerosis is regulated by both the innate and adaptive immune responses via the action of cytokines, generation of small molecule inhibitors or other agents that attenuate the action of pro-inflammatory components or promote the actions of anti-inflammatory cytokines have been explored (Ramji and Davies, 2015).

Previous studies on animal models showed that methotrexate, which has proved beneficial in the treatment of rheumatoid arthritis, and the monoclonal

antibody (MLN1202), which targets the interaction of CCL2 with its receptor and reduces the levels of C-reactive protein (CRP), showed potential effects in reducing atherosclerotic events (Pierre *et al.*, 2007; Gilbert *et al.*, 2011; Li *et al*. 2011; Ridker *et al.*, 2011; Everett *et al.*, 2013; Bäck and Hansson, 2015; Moss, 2015; Ramji and Davies, 2015). In CANTOS (Canakinumab Anti-Inflammatory Thrombosis Outcome Study), a randomised, double-blinded, placebo-controlled trial that investigated the use of canakinumab (monoclonal antibody targeting IL-1β), on high-risk patients with established atherosclerotic disease who had high CRP plasma levels and already survived MI, there was a significant reduction in the rate of recurrent cardiovascular events in patients receiving 150 mg of canakinumab subcutaneously than placebo with no significant reduction in lipid levels from baseline (Baylis *et al.*, 2017; Ridker *et al.*, 2017).

Despite the successes detailed above, monoclonal antibody therapies are expensive and will therefore have to be restricted to high-risk individuals (Baylis *et al.*, 2017). In addition, manipulating inflammation often leaves individuals disposed to infection. Beyond the successes detailed above, many promising pharmaceutical agents against various targets, such as CETP and ACAT1, have failed at the clinical level (Chyu and Shah, 2011). As therapies for CVD have to be taken for a prolonged period of time, it is difficult to measure safety profiles of agents unless genetic evidence exists (Bays and Stein, 2003; Förstermann, 2008; Chyu and Shah, 2011; Bäck and Hansson, 2015; Kramer, Just and Zeller, 2018) . One potential avenue being explored for the prevention of atherosclerosis and as add-on with current pharmaceutical therapies is the use natural products given their demonstrated excellent profile (Moss and Ramji, 2016).

Nutraceuticals are classified as food products that have health benefits beyond their nutritional value. It has been shown that diets that are rich in fruit, vegetables, fish, cereal grains or olive oil have all been associated with cardiovascular health benefits (Sosnowska *et al.*, 2017). Many nutraceuticals have been shown to have anti-inflammatory properties (Moss and Ramji, 2016). There are several nutraceuticals being explored as potential anti-atherogenic therapies. Table 1.4 lists some of these nutraceuticals along with their roles in attenuating atherosclerosis-associated events.

Table 1.4 Potential nutraceutical therapies for atherosclerosis

Nutraceutical	Source	Role	Reference
Omega-3 /6 poly-unsaturated fatty acids (PUFA) and Dihomo-γ-linolenic acid (DGLA)	Omega-3 (fish oils, flax seeds, and nuts) Omega-6 (vegetable oils and animal fat)	Regulation of blood pressure and clotting and modulation of the inflammatory response. Improves atherosclerotic plaque stability by increasing the thickness of the fibrous cap. Increases vasodilatation and reduces monocyte migration and adhesion to SMCs. Reduces blood pressure.	(Engler, 1993; Das, 2008; Takai *et al.*, 2009; Wall *et al.*, 2010; Moss and Ramji, 2016)
HT	Olive oil phenolic compound	Reduces the production of several proinflammatory markers, ROS production and monocyte adhesion-mediated by the expression of adhesion molecules. Reduces atherosclerotic plaque size and increases plasma HDL.	(Mangas-cruz *et al.*, 2001; Rosignoli *et al.*, 2013; Moss and Ramji, 2016)
Allicin	Garlic	Attenuates the expression of several pro-inflammatory cytokines. Has antioxidant effects and inhibits monocyte adhesion and foam cell formation.	(Lee *et al.*, 2012; Moss and Ramji, 2016)
Flavanols/ Catechin	Fruit and vegetables, green tea and cocoa	Reduces vascular inflammation and endothelial cell exocytosis. Attenuates cell migration and reduces atherosclerotic lesion size.	(Falcone Ferreyra *et al.*, 2012; Moss and Ramji, 2016)

As detailed above, it is often difficult to predict the safety profiles of pharmaceuticals in the treatment of CVD as patients receive them for several years whereas nutraceuticals are natural products, which are generally considered safe. Therefore, nutraceuticals may represent effective preventatives that are given to individuals before traditional pharmaceuticals are used (Moss and Ramji, 2016; Sosnowska *et al.*, 2017).

1.10.1 Mediterranean diet and their impact on CVD

Current strategies for the prevention of CVD mainly focus on improving blood lipid profiles. As the oxidative modification of LDL seems to be a major trigger of the atherosclerotic process, prevention of LP oxidation by antioxidants can be important in terms of limiting the onset and progression of the disease (Lusis, 2000). To "neutralise" the excess free radicals and to protect the cells against their toxic effects, the body has developed several mechanisms to counteract oxidative stress by producing anti-oxidants, either naturally generated antioxidants (endogenous anti-oxidants) or externally supplied through foods (exogenous anti-oxidants) for disease prevention (Pham-Huy and He, 2008).

Anti-oxidants from our diet play an important role in helping endogenous anti-oxidants for the neutralisation of oxidative stress. Apparent health benefits have been partially ascribed to the dietary consumption of virgin olive oil by Mediterranean populations (Cicerale and Lucas, 2010). The health benefits of the Mediterranean diet are popularly known and are supported by numerous studies which highlight the reduced CVD-related mortalities in Mediterranean regions compared with other countries with distinct dietary habits (Kromhout *et al.*, 1989). Previous studies showed that the Mediterranean diet is associated with a lower incidence of atherosclerosis, CVD, neurodegenerative diseases and certain types of cancer (Cicerale *et al.*, 2010; Vilaplana-Pérez *et al.*, 2014). Mediterranean diet is known by its high proportion of plant foods where the main source of fat is olive oil, resulting in a higher proportion of mono-unsaturated/poly-unsaturated fats relative to saturated ones (Buckland and González, 2010).

The average intake of olive oil ranges around 30–50 g/day in the Mediterranean countries. This would be an estimated intake of around 9 mg of

phenolic compounds per day (Vissers and Zock, 2004). In a population from Southern Spain, an estimated intake of tyrosol and HT from virgin olive oil in the range of 88.5–237.4 μg/day has been suggested (de la Torre-Robles *et al.*, 2014). Another study of Greek origin with six types of olive oil, which analysed the concentration of phenolic compounds, concluded that the daily intake of HT in the Mediterranean area would be about 2 mg (considering the maximum 50 mg/day of olive oil consumption) (Vissers and Zock, 2004).

Many *in vivo* and *in vitro* studies on humans and animals have focused on the active phenolic compounds present in virgin olive oils to aid in explaining the reduced mortality and morbidity observed in the studies detailed above. Among the various polyphenols, two isolated compounds, oleuropein and HT, have received special attention (Bulotta *et al.*, 2014). These compounds show several anti-inflammatory and anti-atherogenic activities, such as the inhibition of LDL oxidation, platelet aggregation and other promoting factors involved in the development of atherosclerosis (Cicerale and Lucas, 2010). However, oleuropein undergoes almost complete degradation during olive ripening and, therefore, is unlikely to contribute to the cardiovascular health benefits associated with the Mediterranean diet (Cristina Soler-Rivas *et al.*, 2000).

1.11 HT

HT (3,4-dihydroxyphenyl-ethanol) is a major o-diphenol with a molecular weight of 154.16. HT has demonstrated the strongest radical-scavenging properties *in vitro* of olive oil polyphenols (Visioli and Bellomo, 1998).

A previous study concluded that HT supplementation has cardioprotective effects *in vivo* by analysing the effects of HT on blood lipids, antioxidant status and the progression of aortic lesions in hyperlipidemic rabbits after receiving an atherogenic HFD versus another group receiving the same diet together with purified HT dissolved in sterile saline (González-Santiago *et al.*, 2006). They reported a decrease in the plasma levels of total cholesterol and TG together with a 2.3-fold increase in HDL-cholesterol levels in the HT-supplemented groups with improvement in their antioxidant status. In addition, reduction was seen in the size of atherosclerotic lesions

measured as intimal layer areas of the aortic arch when compared with control animals (González-Santiago *et al.*, 2006).

1.11.1 Sources and metabolism

The amount of phenolic compounds present in olive oil greatly varies depending on the cultivar, the degree of maturation, climate and the manufacturing process (Cristina Soler-Rivas *et al.,* 2000). Thus, extra virgin olive oil obtained from the cold pressing or centrifugation of the olives is the one with a higher content of total phenolic compounds. An early study showed a total phenolic content of 232 mg/kg in virgin olive oil versus 62 mg/kg value is refined olive oil (up to 80% usually lost during the refining process) (Owen *et al.*, 2000). Depending on the variety of olive and the type of processing, the phenolic content varies significantly (Vilaplana-Pérez *et al.*, 2014). As an example, the total phenolic content estimated in black olives varies from that extracted from green olives with black olives containing more of HT and other phenolic compounds such as tyrosol, phloretic acid, dihydrocaffeic acid, acteoside, luteolin and apigenin (Romero *et al.*, 2004).

HT is one of the main components of virgin olive oil, olive mill wastewater and olive leaf extract (OLE) and shown to have the strongest *in vitro* anti-oxidant potential among all the olive oil polyphenols (Visioli *et al.* , 1998). HT in oil is found in the free form, in an acetate form or as a part of more complex compounds like oleacein, oleuropein and verbascoside (Figure 1.8) (Boskou *et al*., 2008). Oleuropein is responsible for the bitter taste of olives and decreases as the fruit ripens, turning into an unglycosylated form, oleuropein aglycone, by enzymatic hydrolysis, and finally converts to HT, making this one of the indicator of the maturation of olives (Figure 1.9) (Esti *et al.*, 1998; Charoenprasert and Mitchell, 2012).

In addition to natural sources, commercial products are already in the market containing HT, which are generally recognised as safe drugs. These include Mediteanox®, Hydrox® and Hytolive® in the form of capsules, elixir, creams, and even as extra virgin olive oil with a very high content of HT (over 500 mg/kg) (Vilaplana-Pérez *et al.*, 2014). Some of these products have been tested successfully showing some of the previously described health benefits (Visioli *et al.*, 2009; Giordano, Dávalos and Visioli, 2014).

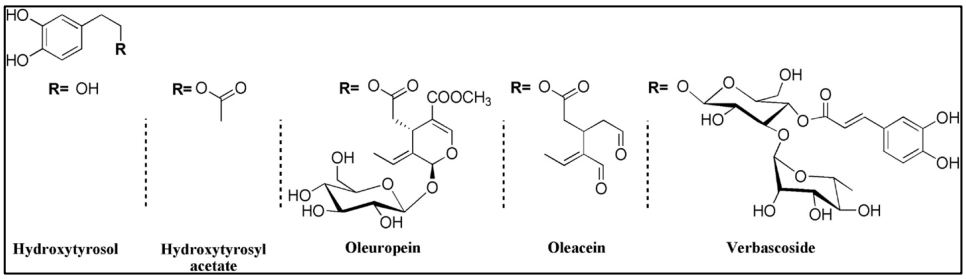

Figure 1.8 HT and derivatives

Chemical structure of HT derivatives present in olive and olive oil (taken from Buckland and González, 2010).

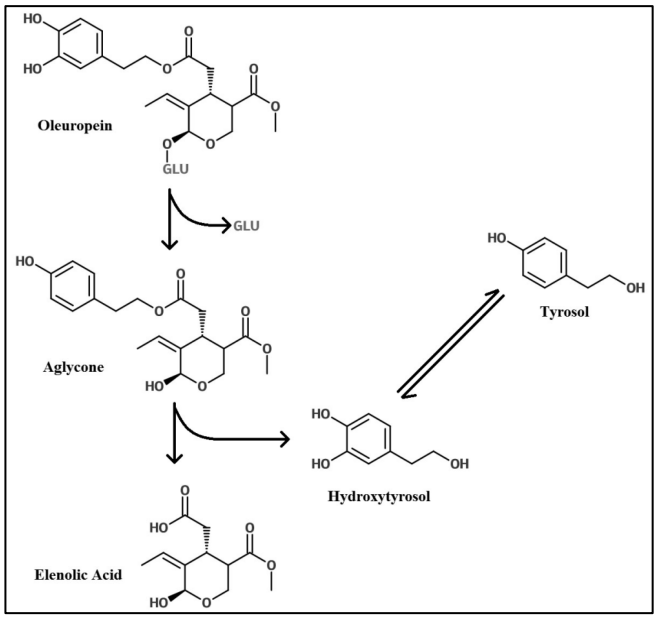

Figure 1.9 HT synthesis from oleuropein

During the maturation of olive oil, oleuropein undergo deglycosylation to produce aglycone, which is then converted to oleanolic acid and HT. HT, in turn, can be hydrolysed to tyrosol (taken from Boss *et al.*, 2016).

1.11.2 HT bioavailability

The term bioavailability is commonly used to indicate the proportion of a substance that reaches the systemic circulation after oral administration considering both its absorption and its local metabolic transformation (Vilaplana-Pérez *et al.*, 2014). In general, hydrophilic phenolic compounds of olive oil are absorbed in a dose-dependent manner in animals and humans and are excreted in the urine mainly as glucuronide conjugates (Visioli and Bellomo, 1998).

Absorption of HT takes place in the small intestine and colon (Vissers *et al.*, 2002). It has been suggested that transport through the intestinal epithelium can occur through passive bi-directional diffusion (Manna *et al.*, 2000). The absorption of this compound is rapid with maximum plasma concentration being reached 5–10 minutes after ingestion, followed by a rapid decline (Bai *et al.*, 1998). A previous study found that administration of extra virgin olive oil to humans was associated with a 44.2% urinary recovery of the administered free HT (Visioli and Bellomo, 1998).

Studies using different techniques to determine the amount of absorbed HT that had been isotopically labelled estimated absorption around 99% of the total intake in oil and 75% in aqueous solution being <3 % in fecal content (Tuck *et al.*, 2001). The absorption of HT differs according to the vehicle in which it is carried. In human beings, HT absorption was higher when subjects ingested virgin olive oil than in refined oil (phenol-free) enriched with phenolic compounds or when HT was incorporated into a yogurt as a functional food, with urinary recoveries of 44, 23 and 5.8%, respectively (Visioli and Bellomo, 1998; Venza *et al.*, 2015). Almost all the phenolic content was present in the plasma and the urine in conjugated forms, mainly glucurono-conjugates. Taking into account that the amount of free HT in the plasma and the urine was almost undetectable, some authors attribute the biological activity to metabolites of HT (Visioli *et al.*, 2000; Romero *et al.*, 2004; Vilaplana-Pérez *et al.*, 2014). Overall, the various data provide indications of the bioavailability of HT and highlight that olive oil phenolics are well absorbed at the intestinal level and suggest that the intestinal/hepatic metabolism of the ingested phenols is extensive (Vilaplana-Pérez *et al.*, 2014).

In terms of the safety profile, the toxicity of HT was analysed in a series of toxicological studies (Angelo *et al.*, 2001; Christian *et al.*, 2004; Chiara Maiuri *et al.*, 2005; Auñon-Calles *et al*., 2013). A study in a rat model analysed toxicity levels, weight gain, food consumption and reproductive capabilities of hydrolysed aqueous olive pulp extract (HAOP) (a water extract product of organically grown olives containing high concentrations of polyphenol antioxidants, especially HT; 1000, 1500 and 2000 mg/kg/day). The study showed that there were no adverse clinical, haematological and biochemical effects observed with normal organ weight and reproductive parameters when compared to the control animals (Christian *et al.*, 2004; Richard *et*

al., 2011a). In another study in rats, administration of HT produced small decreases in body weight at 2000 mg/kg/day in the male animal with no significant effects in females again indicating its safety profile. Food consumption was comparable to the controls (Christian *et al.*, 2004). Significant increases in red blood cells were observed in females with 2000 mg/kg/day but this induction was interpreted as a slight but beneficial erythropoietic stimulation of the bone marrow (Christian *et al.*, 2004). On the other hand, a significant decrease in serum enzymes synthesised by the liver were observed in most of the treated groups of male and female rats though these were considered to be beneficial and not toxic. It was suggested that this was as a result of the biliary excretion of large dosages of olive extract that may also account for the slightly decreased serum cholesterol levels in both male and female rats (significantly decreased in females at 2000 mg/kg/day) (Christian *et al.*, 2004). In a more recent study, pure HT was investigated where oral administration of different dosages (5, 50 and 500 mg/kg/day) to rats once a day for 13 weeks did not lead to any death or induce effects that can be considered as toxicological relevance (Auñon-Calles *et al.,* 2013).

Based on the studies detailed above and many more that have not been addressed here in detail (Angelo *et al.*, 2001; Christian *et al.*, 2004; Chiara Maiuri *et al.*, 2005; Auñon-Calles *et al.*, 2013; Moss and Ramji, 2016), it can be concluded that HT has an excellent safety profile.

1.12 Project aims and objectives

CVD-related events are predicted to rise as a result of the adoption of a westernised diet in developing countries and the increase in the prevalence of risk factors such as obesity, diabetes and hypertension. Atherosclerosis is a chronic inflammatory disease of medium-sized and large arteries and the major cause of CVD, which develops as a result of an inflammatory process initiated by EC damage/activation. It is characterised by the accumulation of cholesterol, connective tissue components, infiltration of macrophages and proliferation of SMC at the site of the inflammatory lesion, which can lead to the formation of a thrombus that will eventually lead to stroke or MI.

Signalling pathways play important roles in the pathogenesis of atherosclerosis and could be of major significance for understanding the mechanism of atherogenesis and establishing new effective parameters for diagnosis, which include finding a range of new biomarkers, and drug targets that has a high potential in the treatment of the disease. Several signalling pathways have been implicated in the initiation, progression and development of atherosclerosis such as MAPK and JAK-STAT pathways. Recent studies in our laboratory using knockdown approaches have shown a key role for ERKs in the IFN-γ-mediated regulation of expression of key genes implicated in atherosclerosis and the uptake of modified LDL by human macrophages (Li *et al.*, 2010). The action of ERKs was potentially mediated via phosphorylation of STAT1 on serine 727, which is required for maximal transcriptional activation.

The effect of the ERK1: STAT1 serine 727 phosphorylation axis on key cellular processes associated with atherosclerosis *in vitro* remains to be determined and would complement ongoing *in vivo* studies. The availability of ERK1 deficient mice and STAT1 S727A knock-in mice together with control C57BL/6J mice provides great opportunity to use BMDM from them to probe the effects on macrophage gene expression and key cellular processes associated with atherosclerosis. The initial aim of this project was therefore to:

Investigate the role of ERK1: STAT1 serine 727 phosphorylation axis on key cellular processes associated with atherosclerosis (Chapter 3), including:

- Regulation of expression of key genes implicated in atherosclerosis using an array of 84 genes associated with this disease; and Molecular and cellular processes involved in plaque development and progression, including the production of ROS, foam cell formation (phagocytosis, macropinocytosis and cholesterol efflux), chemokine-driven macrophage migration, and cellular viability and proliferation.

Previous studies had shown that HT attenuated the IFN-γ-induced phosphorylation of STAT1 on serine 727 without affecting that on tyrosine 727. The role of the ERK1:STAT1 serine 727 phosphorylation axis in the actions of HT therefore formed the focus of studies presented in Chapter 4. This involved the use of BMDM from C57BL6/J control mice, ERK1$^{-/-}$ mice and STAT1 S727A mice to investigate the effect of HT on:

- The regulation of expression of key genes implicated in atherosclerosis using an array of 84 genes associated with the disease; and Molecular and cellular processes involved in plaque development and progression, including production of ROS, foam cell formation (phagocytosis and macropinocytosis), chemokine-driven macrophage migration and cellular viability and proliferation.

Once the potential anti-atherogenic effect of HT were identified and validated using mouse cells, it was then used in an initial short term *in vivo* study to determine its effects on wild-type C57BL6/J mice fed a HFD for 3 weeks and given a daily gavage of 10 mg/kg/day HT or the vehicle (water) (Chapter 5). The concentration of HT employed was based on survey on its used in a range of metabolic diseases (Acín *et al.*, 2006; López-Villodres *et al.*, 2016). The study involved investigation of the effects of HT on:

- Changes in weight;

- Plasma lipid profile (total cholesterol, LDL/VLDL, HDL and TG), ROS production and plasma cytokine profile; and expression of key atherosclerosis associated genes in the liver using an array of 84 genes associated with the disease.

Once the potential cardiovascular protective effects of HT on wild-type mice were identified, it was then used in a long term *in vivo* study using hyperlipidemic atherosclerotic model; male and female $LDLR^{-/-}$ mice fed a HFD for 12 weeks with 10 mg/kg/day HT or vehicle control (water) (Chapter 6). The study involved investigation of the effect of HT on:

- Changes in weight;

- Plasma lipid profile (total cholesterol, LDL/VLDL, HDL and TG) and ROS production; and proportion of haematopoietic stem/progenitor cells within the bone marrow.

Tissues were also stored for future investigation of plaque burden, lipid and cellular content and expression of key genes.

1.13 Experimental Aims

Details of specific methodologies for each experimental aim are outlined in Chapter 2 and the *in vitro* and *in vivo* experimental strategies for Chapters 3-6 are presented in Figures 1.10- 1.25

1.13.1 Experimental strategies for *in vitro* studies

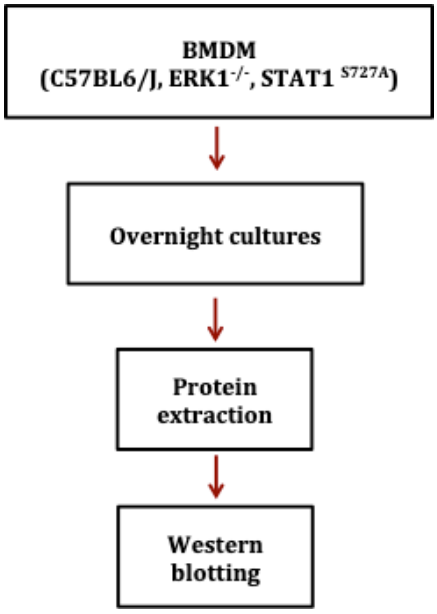

Figure 1.10 Experimental strategy for analysis of protein expression

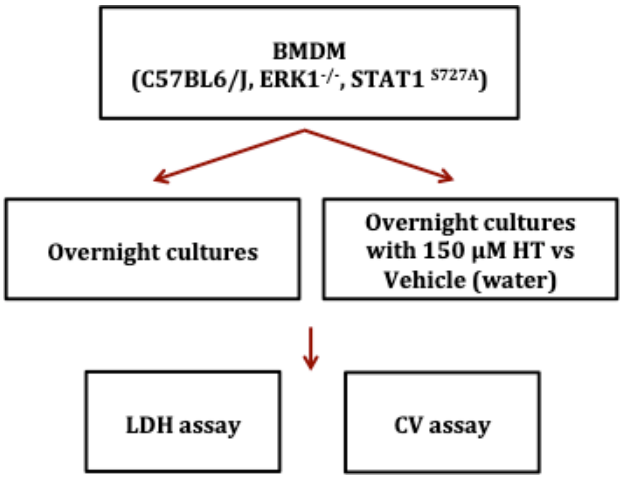

Figure 1.11 Experimental strategy for analysis of cell viability and proliferation

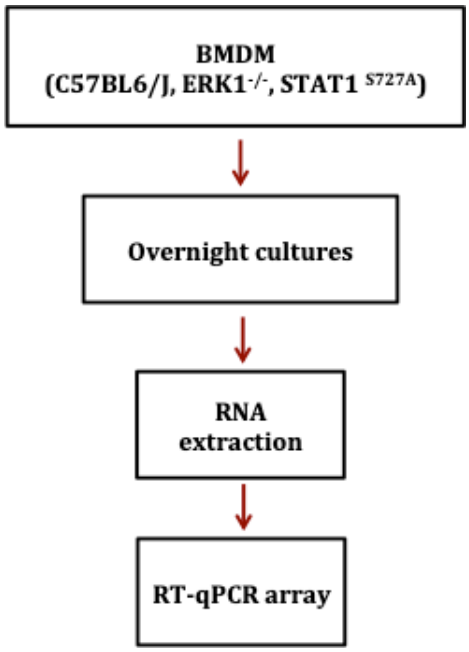

Figure 1.12 Experimental strategy for analysis of RNA expression

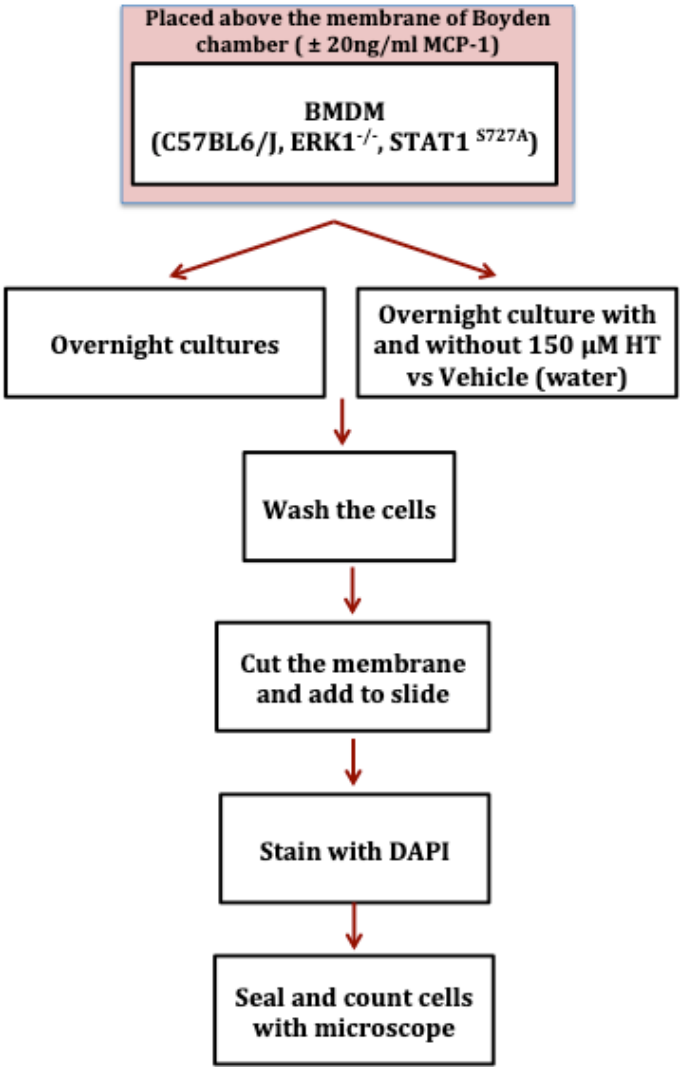

Figure 1.13 Experimental strategy for investigating chemokine-driven migration

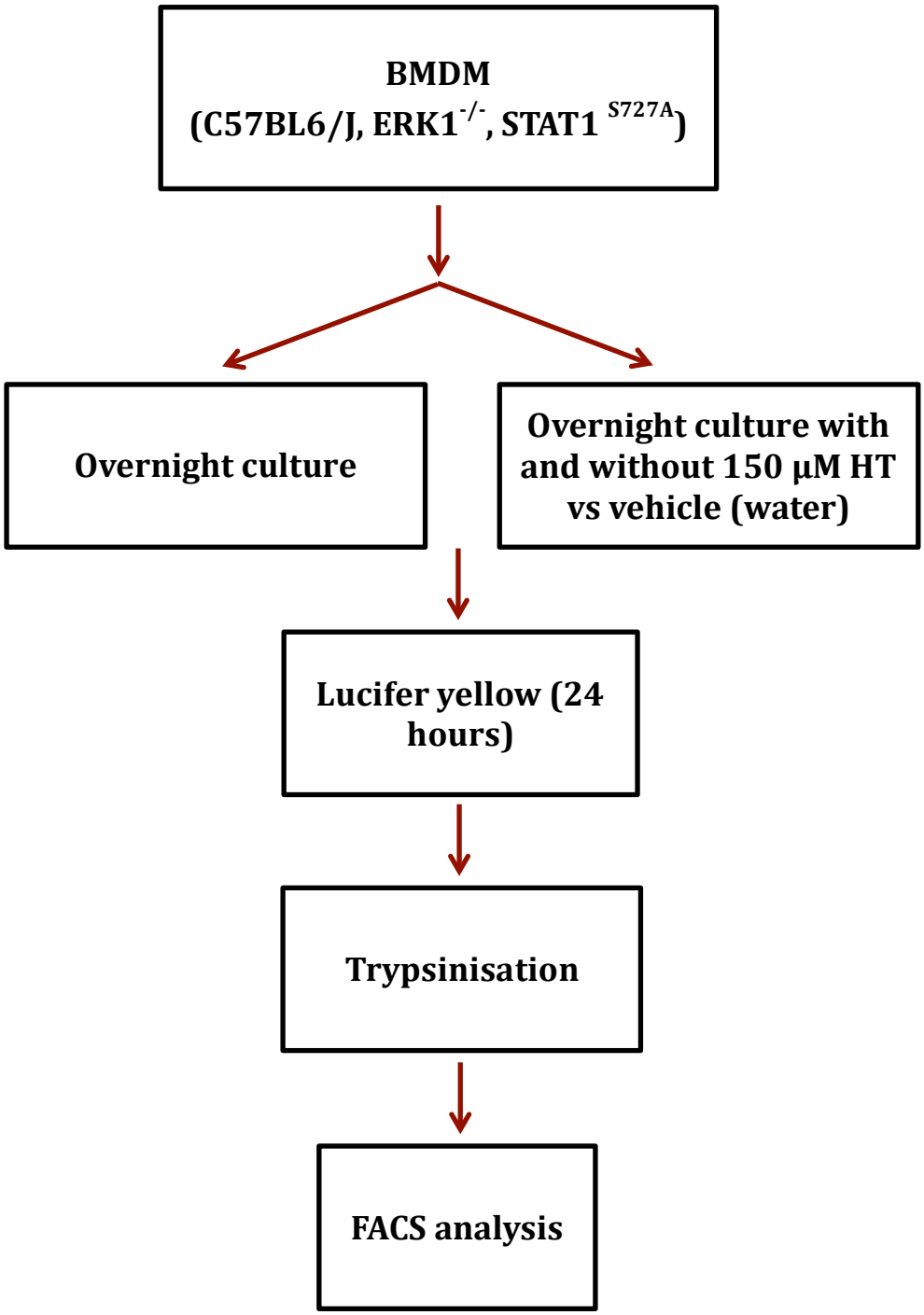

Figure 1.14 Experimental strategy for assessing macropinocytosis

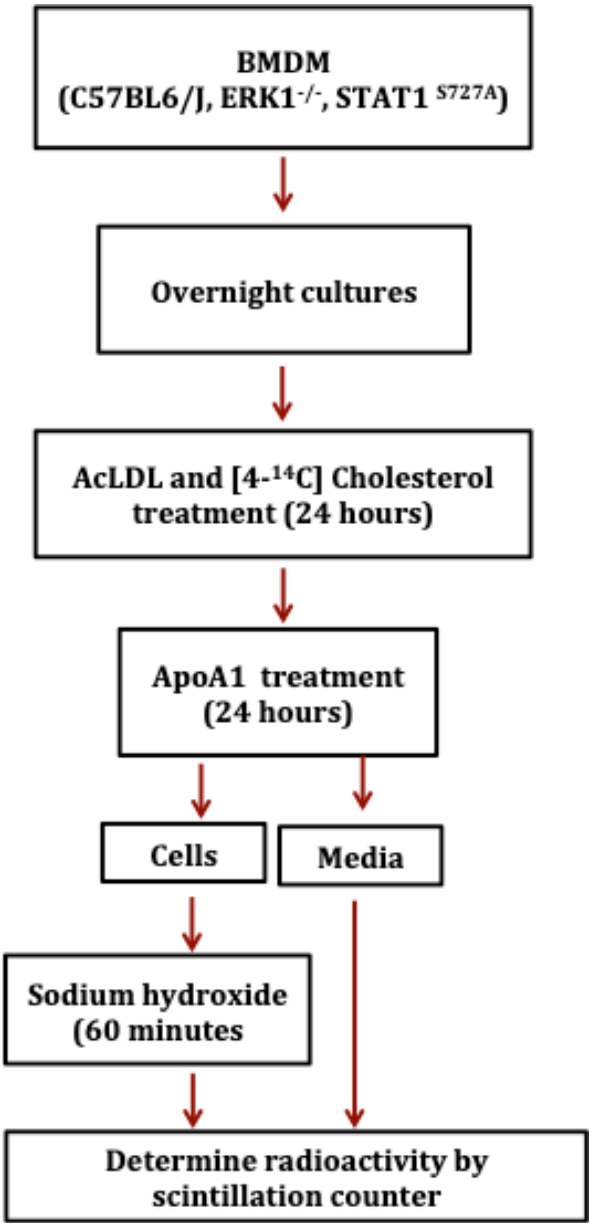

Figure 1.15 Experimental strategy for determining macrophage cholesterol efflux

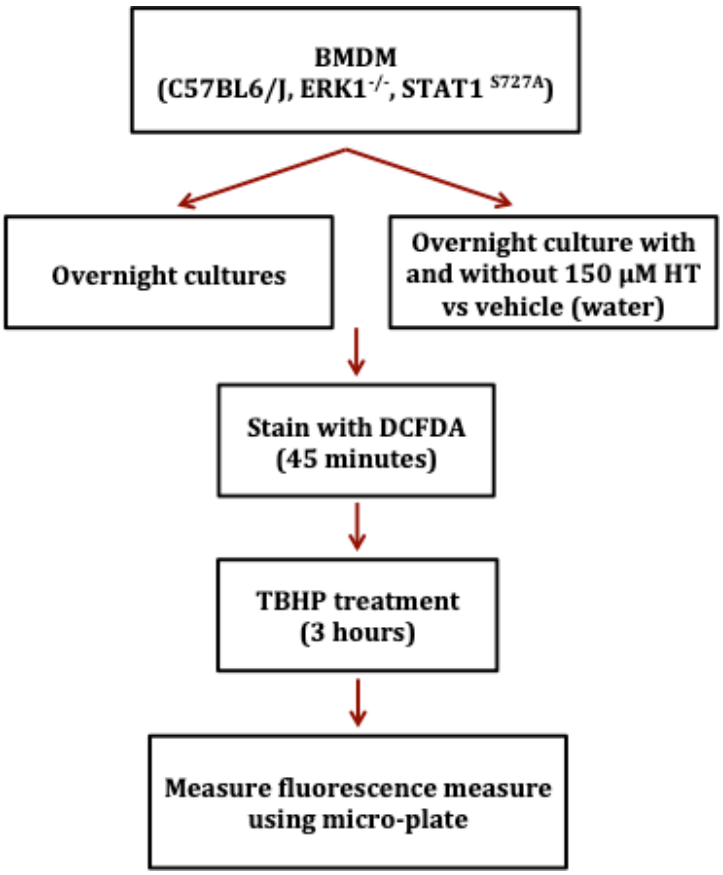

Figure 1.16 Experimental strategy for determining ROS production

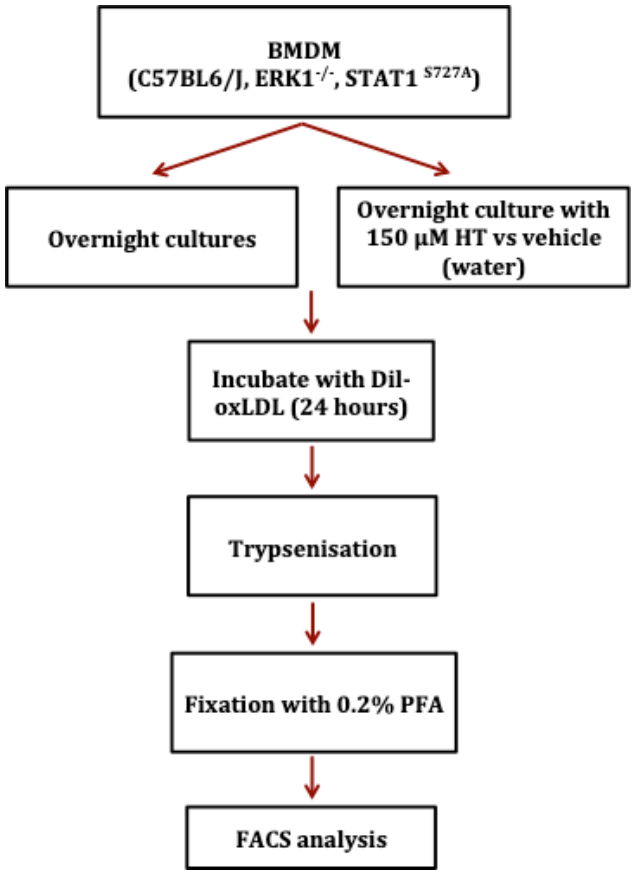

Figure 1.17 Experimental strategy for monitoring oxLDL uptake

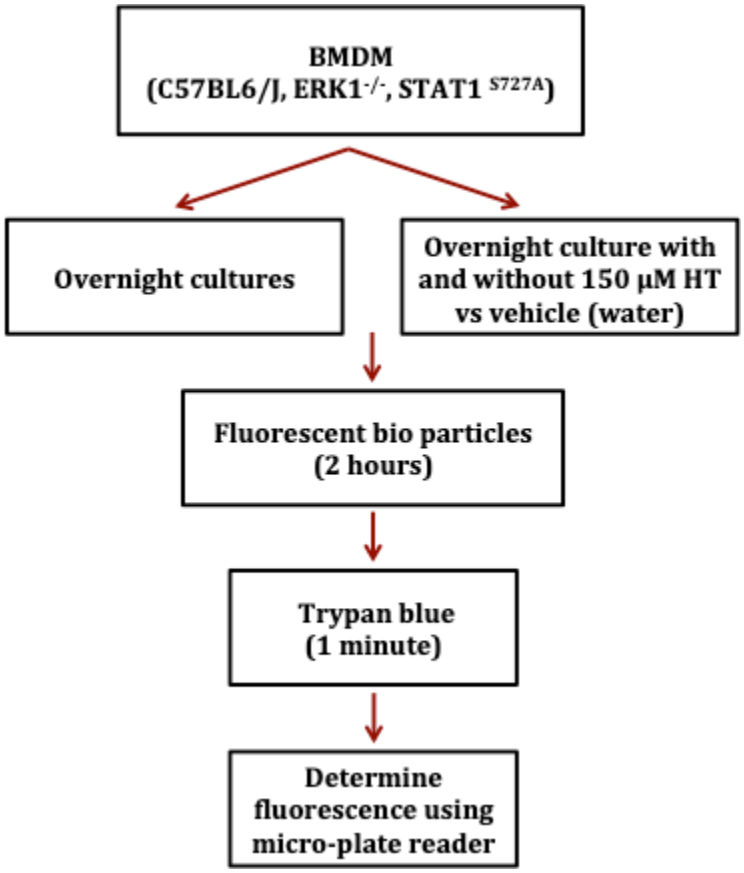

Figure 1.18 Experimental strategy for monitoring Phagocytosis

1.13.2 Experimental strategy for *in vivo* studies

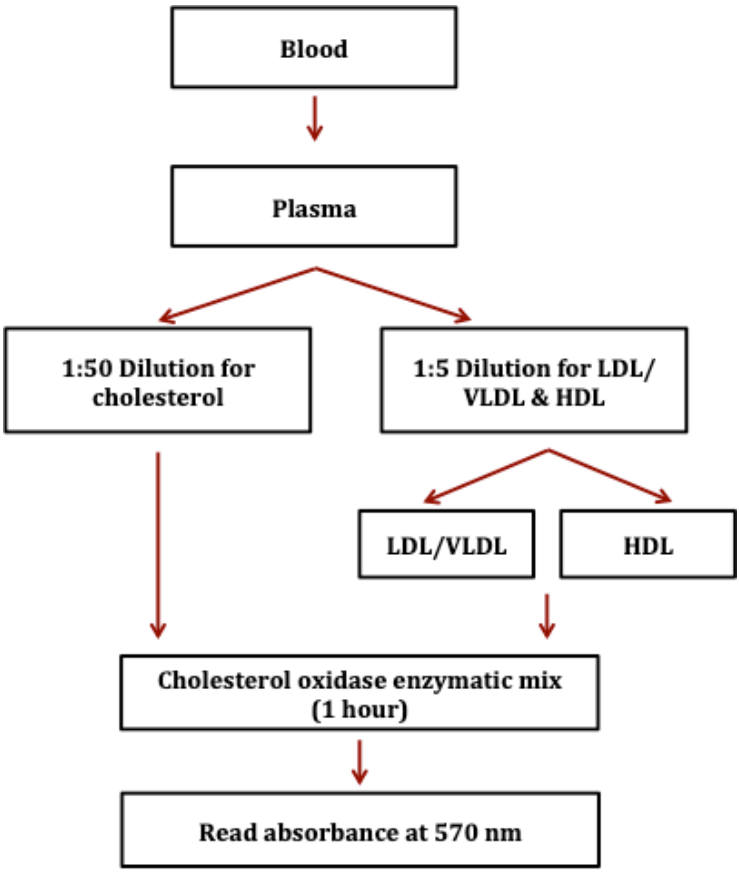

Figure 1.19 experimental strategy for determining plasma levels of total cholesterol, LDL/VLDL and HDL

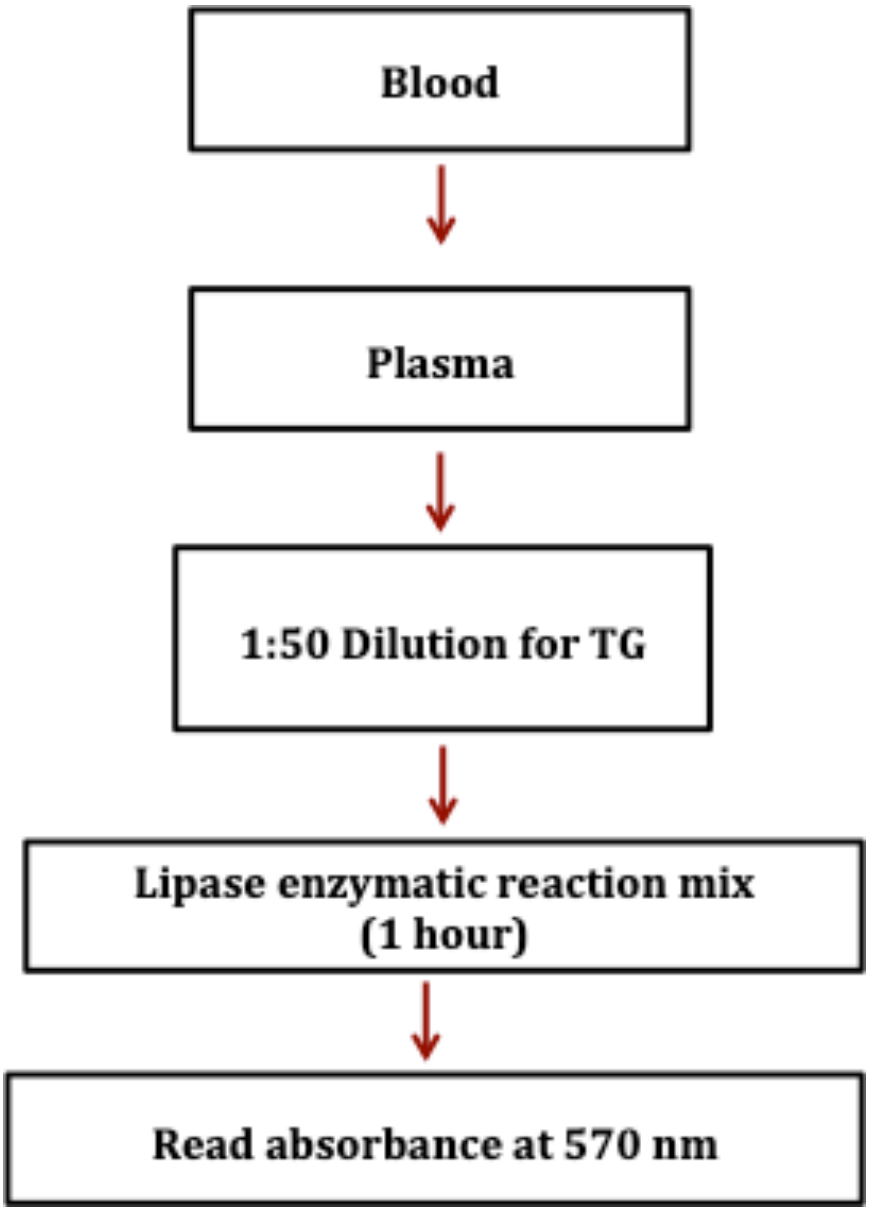

Figure 1.20 Experimental strategy for determining plasma TG levels

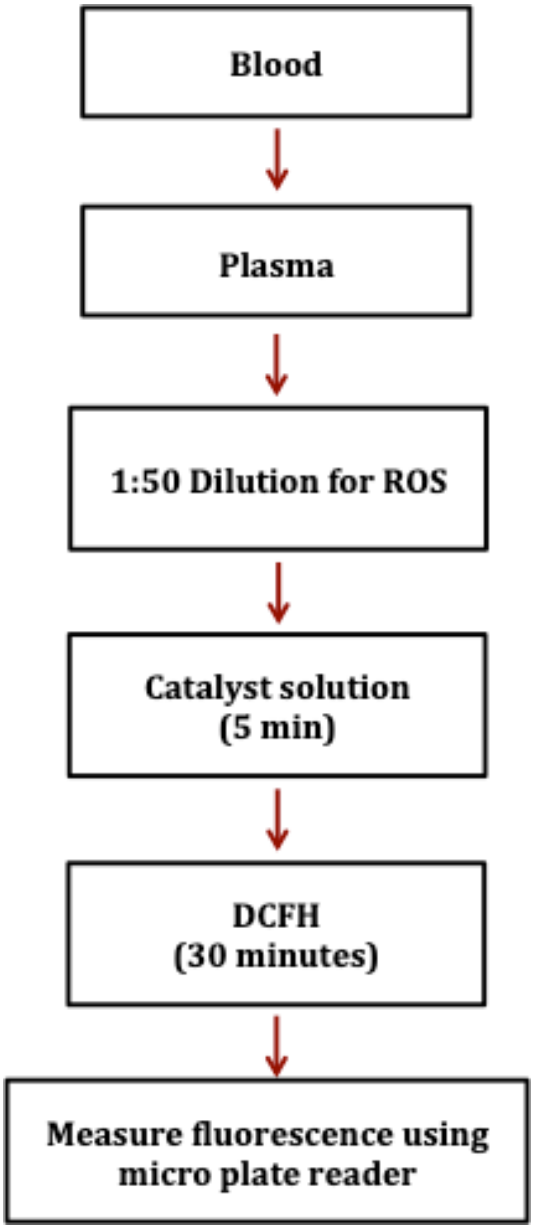

Figure 1.21 Experimental strategy for determining plasma ROS levels

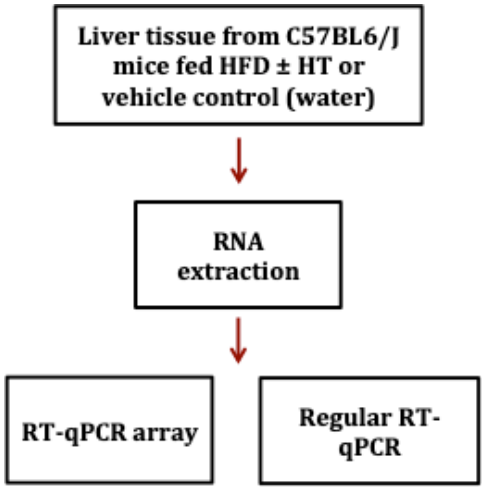

Figure 1.22 Experimental strategy for determining gene experiment *in vivo*

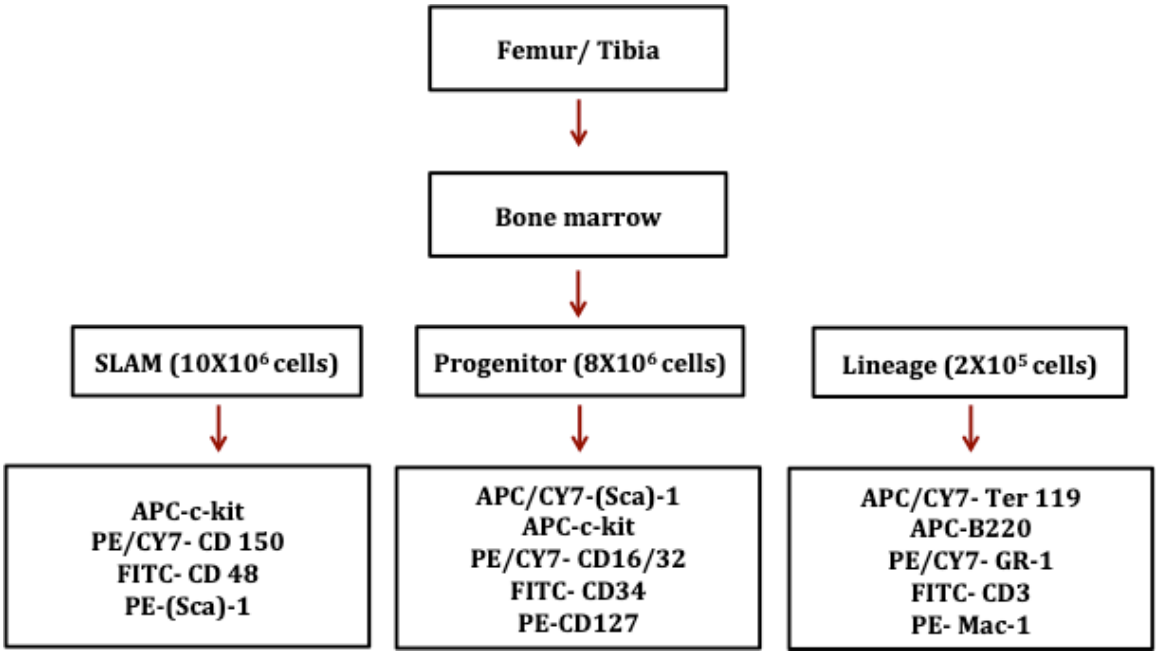

Figure 1.23 Bone marrow cell population detection experimental strategy

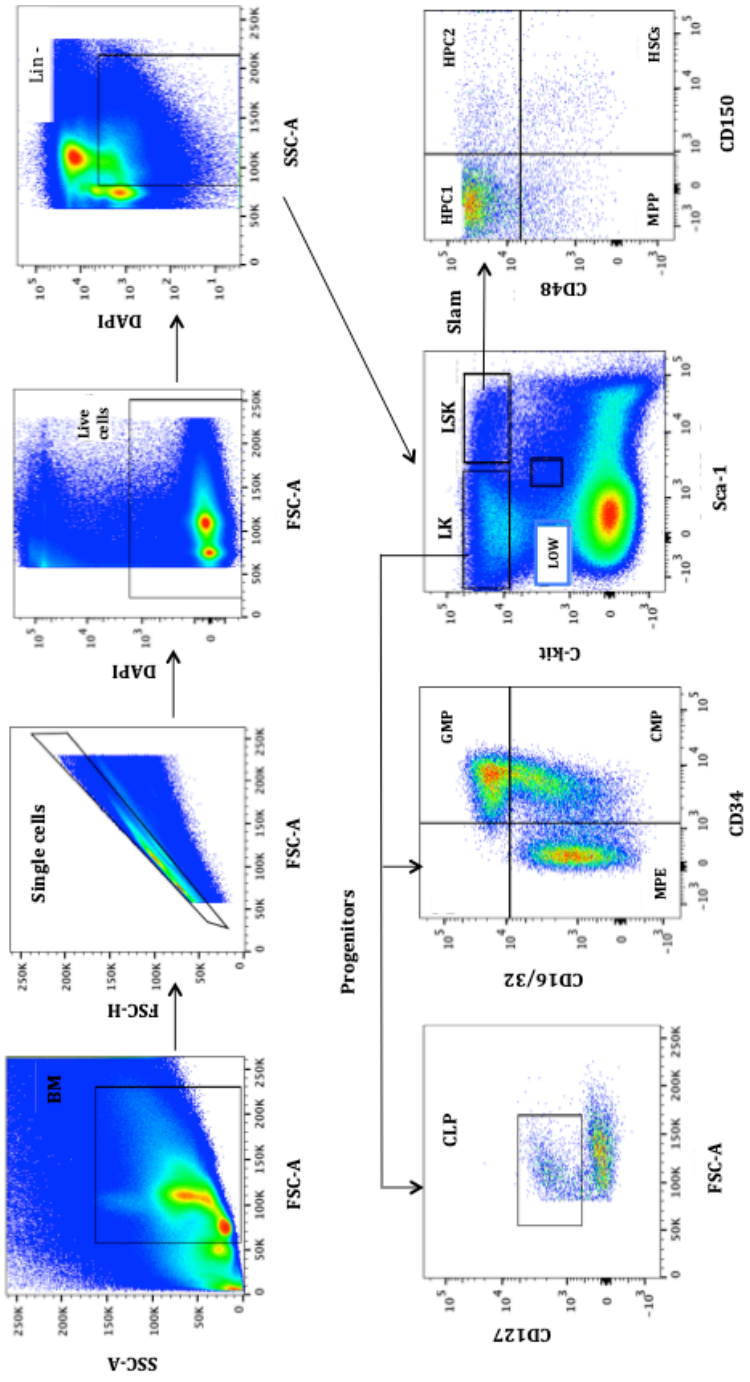

Figure 1.24 Bone marrow cell population gating strategy (Lineage negative)

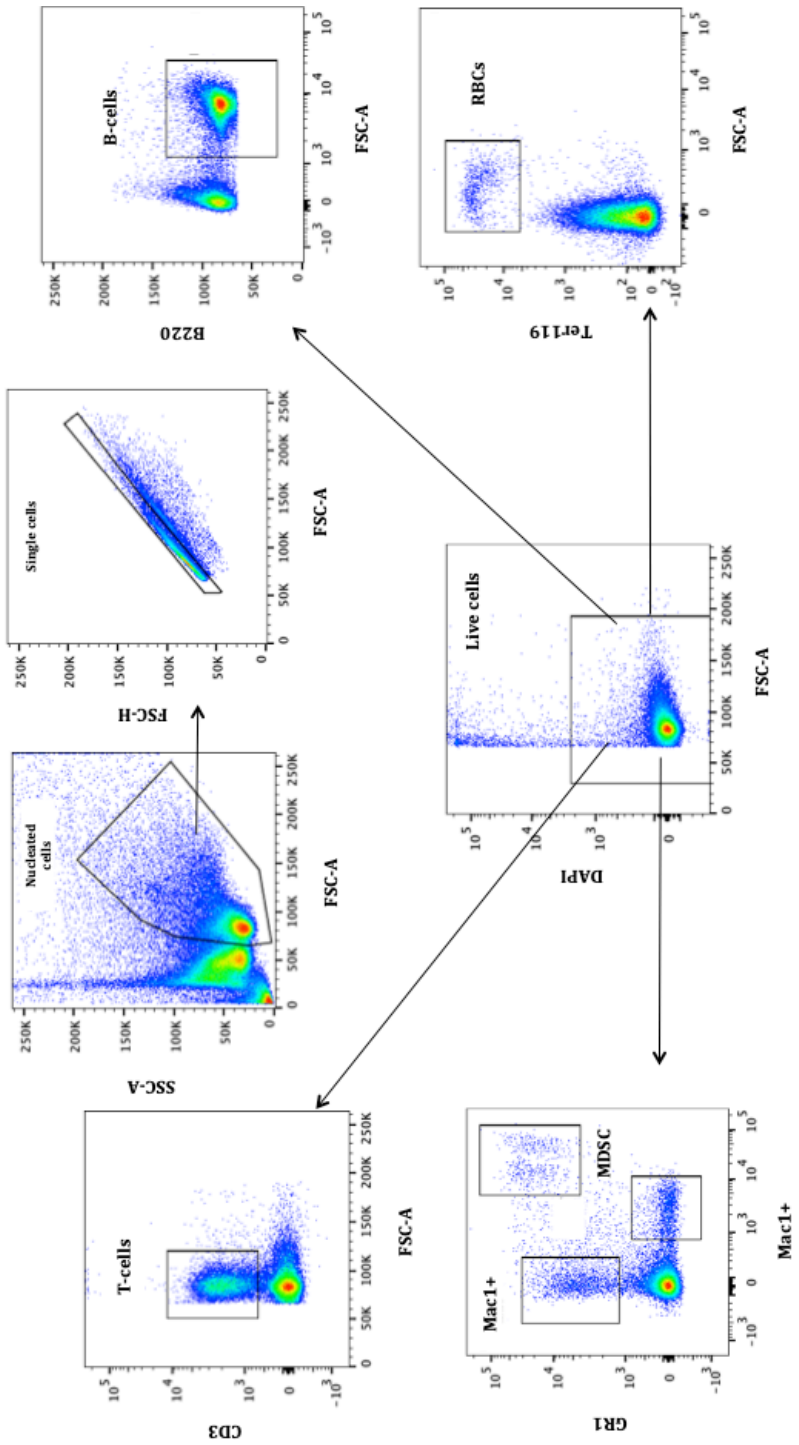

Figure 1.25 Bone marrow cell population gating strategy (Lineage positive)

Chapter 2

2.1 Materials and methods

Table 2.1 Materials and suppliers

Company	Reagent
Abcam, UK	2',7' –dichlorofluorescin diacetate (DCFDA) cellular ROS detection assay kit
	HDL and LDL/VLDL cholesterol assay kit
	Phospho-STAT6 (Y641) Ab (ab28829)
	Anti-rabbit secondary antibody IgG-AP (ab98048)
	Anti-goat secondary antibody IgG-AP (ab6702)
	Triglyceride quantification assay kit
Amersham, UK	[4-^{14}C] cholesterol
BD Bioscience, UK	40/70 μm sterile cell strainer
	FITC-conjugated anti-mouse CD34 (260238)
Biolegend, USA	APC-conjugated anti-mouse c-Kit (105811)
	APC/Cy7-conjugated anti-mouse Sca-1 (108125)
	BV650-conjugated anti-mouse CD127 (121111)
	FITC-conjugated anti-mouse CD48 (130403)
	PE-conjugated anti-mouse Sca-1 (108107)
	PE/Cy7-conjugated anti-mouse CD150 (115913)
	PE/Cy7-conjugated anti-mouse CD16/32 (101317)
Biotrend, Germany	Acetylated LDL
	Dil-oxLDL
Cell Biolabs, USA	OxiSelect *in vitro* ROS/RNS assay kit (green fluorescence)

Cell Signaling Technology, UK	Phospho-STAT1 (Ser727) Ab (9177s)
Fisher Scientific, UK	Agarose Chloroform DAPI Dulbecco's Modified Eagle's Medium (DMEM) Methanol Nuclease-free water Scalpel
Helena Biosciences, UK	Cell scraper
Jackson Laboratory, USA	Male C57BL/6J wild-type mice ERK1$^{-/-}$ mice.
Life Technologies, UK	Fetal calf serum qPCR plate seals TBE Penicillin Streptomycin
Lonza, UK	RPMI 1640 with L-Glutamine media
Marienfeld, UK	Haemocytometer
Millipore, UK	Polyvinylidene difluoride membrane (PVDF)
Peprotech, UK	IFN-γ MCP-1 M-CSF
Perkin-Elmer, USA	Opti-FLUOR® Scintillation analyser
Professor Thomas	STAT1 knock-in S727A mice

Decker	
Promega, UK	dNTPs MMLV reverse transcriptase MMLV RT 5x buffer Random primers RNasin ribonuclease inhibitor
Qiagen, UK	Atherosclerosis RT^2 Profiler PCR Arrays (mouse/human)
Roche, UK	Roche light cycler
Sigma-Aldrich, UK	10/25 ml pipettes 12/24/96-well plates 15/50 ml Falcon tubes Apolipoprotein A-I Bovine serum albumin (BSA) Cell culture plates Crystal violet Dimethyl sulfoxide (DMSO) Ethanol Ethidium bromide Ethylenediaminetetraacetic acid (EDTA) HT Isopropanol Lucifer yellow CH dipotassium salt (LY) PCR primers Phosphate buffer saline (PBS) tablets Ponceau S Protease inhibitor cocktail Red blood cells lysis buffer RNA Zap

	Sodium hydroxide Sybr® Green Jumpstart Taq polymerase Tissue culture flasks (25/75 cm^2) Tris-borate EDTA (TBE) Trypsin EDTA X-ray film
Special Diets Services, UK	High fat diet [21% (w/w) pork lard and 0.15% (w/w) cholesterol]
Starlabs, UK	qPCR 96-well plates
Thermo Fisher Scientific, UK	2x RNA loading dye Bis-Tris gel 4-12% (w/v) 1.0mm (x10) Cryoprotected tissue freezing reagent (OCT) Gel sample buffer (GSB) IBT blocking buffer in PBS Tween Magic marker XP western protein standard Micro BCATM Protein Assay Kit Nanodrop™ ND2000 Nu Page MOPS running buffer Nu Page MOPS transfer buffer NuPage ™ Novex gel tank system blotting module Paraformaldehyde (PFA) PBS Tween Pierce lactate dehydrogenase (LDH) cytotoxicity assay kit RiboRuler high range RNA ladder Ribozol RIPA buffer SDS polyacrylamide gel electrophoresis (SDS-PAGE gel) Streptavidin

	Stripping buffer
	Tropix® CDP-Star detection reagent
	Vybrant™ Phagocytosis Assay Kit
	X cell sure-lock mini cell
VWR Jencons, UK	Falcon® 12-well companion plates
	Falcon®cell culture inserts (8 μm pore size)
	Glass slides

2.2 Preparation of glassware and solutions

Glassware and solutions were autoclaved (if necessary) for 20-30 minutes at 121˚C (95 kPa).

2.3 Animal models

Several animal models were used in this study. C57BL/6J wild-type mice, ERK1$^{-/-}$ mice (obtained from The Jackson Laboratory) and STAT1 knock-in S727A mice (obtained from Professor Thomas Decker), all in the C57BL/6J background, were used for studies on BMDM. Wild-type C57BL/6J mice were used for the short-term studies involving feeding a HFD for 3 weeks. LDLR$^{-/-}$ mice were used for long term studies investigating the effect of vehicle or HT.

The breeding and the maintenance of all mice was carried out at the animal facilities of Cardiff University (Heath Hospital) in accordance with approved guidelines. They were kept under appropriate 12 hours day/night cycles and fed a normal diet unless or otherwise stated. All studies and protocols were approved by the Cardiff University Institutional Ethics Review Committee and the United Kingdom Home Office. All experiments were performed in accordance with the Guide for the Care and Use of Laboratory Animals (NIH Publication No. 85–23, revised 1996; Experimental license 30/3365).

2.3.1 Tissue collection

Animals were weighed before being euthanised by increasing the levels of CO_2. Following cessation of breathing, death was confirmed by palpitation. Animals were subjected to cardiac puncture of the heart in order to obtain approximately 1 ml of whole blood. The heart was then flushed with PBS. The subcutaneous fat, gonadal fat, spleen, thymus, and liver were taken, snap frozen and stored at -80°C for subsequent isolation of RNA or proteins. The heart, the brachiocephalic artery and a section of the liver were also taken and stored in Shandon Base molds, covered in optimum cutting temperature formulation (OCT) and stored at -80°C. The descending aorta was also isolated from the aortic arch to the subclavian arteries and stored in PBS. Legs were also taken and stored in PBS with 2% (v/v) FCS for the isolation of BMDM and analysis of cell populations in the bone marrow.

2.3.2 Cell culture and maintenance

Macrophages play a key role in atherogenesis and the overall macrophage functionality is critical for the balance between plaque progression and regression (Bisgaard, et al. 2016). For *in vitro* experiments, BMDM were used throughout the study as they exhibit similar traits to HMDM both *in vitro* and *in vivo* (Chanput *et al.*, 2014). They are primary macrophage cells derived from the bone marrow *in vitro* and cultured in the presence of the growth factor M-CSF (Weischenfeldt and Porse, 2008). Macrophages were isolated and cultured as described in Section 2.3.3.

2.3.2.1 *In vitro* HT assays

HT has a molecular weight of 154.16 and is a white powder with a melting point around 55°C that is fairly soluble in water and polar organic solvents such as low-molecular-weight alcohols (Owen *et al.*, 2003). HT stock solution of 100 mM was prepared in water and further dilutions were carried out according to experimental protocols.

Prior to experiments BMDM were cultured according to the experimental conditions required in presence of either 150 μM HT or vehicle control (water) for 24 hours (see Figure 4.1).

2.3.3 BMDM isolation

Following the isolation of mouse tibiae and femur, muscles and cartilage were carefully removed from the bones before sterilising them in 70% (v/v) methanol. Bone ends were cut and the marrow was flushed out with RPMI 1640 media only using a 25G syringe with a needle until the entire bone marrow had been flushed out. The extracted marrow was pelleted by centrifugation at 250 x g for 5 minutes. Pellets were then suspended in 1 ml of red blood cells lysis buffer (150 mM NH_4Cl, 10 mM $KHCO_3$, 0.1 mM Na_2EDTA, pH 7.4) and left for about 1 minute. The mixture was then "topped up" to 10 ml with RPMI complete media [containing 2 mM L-glutamine supplemented with 10% (v/v) heat-inactivated fetal calf serum (HI-FCS)(FCS heated at 56 °C for 10 minutes) and penicillin (100U/ml)/streptomycin (100µg/ml) (Pen/Sep)].

Clumped cells debris was then removed by passing the cell suspension through a 40 µm cell strainer before centrifuging once again as described above. The pellet was washed three times (with centrifugation steps in between) in RPMI media only. After washing, the cells were re-suspended in 20 ml of differentiation medium [DMEM containing 10% (v/v) HI-FCS, 100 U/ml penicillin/100 µg/ml streptomycin and 20 ng/ml M-CSF]. Cells were plated in 5 ml differentiation medium across three 25 cm^2 tissue culture flasks and left to begin differentiation for three days at 37°C in a humidified atmosphere containing 5% (v/v) CO_2 before addition of an additional 5 ml differentiation medium to each flask.

On day six, cells were washed briefly with PBS (to remove M-CSF) followed by harvesting by gentle scraping of the cell monolayer from the plate and centrifugation at 250 x g for 5 minutes. Macrophages were counted as described in Section 2.3.4 and plated in complete DMEM media containing 10% (v/v) HI-FCS, 100 U/ml penicillin and 100 µg/ml streptomycin as needed for experiments.

2.3.4 Counting cells

A haemocytometer was used to count cells in order to seed the correct number of cells for each experiment. The haemocytometer was covered with a glass coverslip and 10 µl of the cell suspension was applied. The numbers of cells contained within

the four outer grids of the haemocytometer were then counted. The number of cells/ml was calculated by multiplying the number of cells counted by 10^4.

2.4 Protein analysis and western blotting

Western blotting is an extensively used technique for the qualitative and semi-quantitative analysis of single proteins and protein modifications. In this study, it was used to confirm the genetic modifications (knockout of ERK1 and STAT1 S727 knock in leading to loss of serine 727 phosphorylation site) in the animal models used. A list of all the reagents used together with their composition is shown in Table 2.2.

Table 2.2 Composition of buffers used in western blotting

Reagents	Composition
RIPA buffer	150 mM NaCl 1% (v/v) IGEPAL® CA-630 0.5% (v/v) sodium deoxycholate 0.1% (w/v) SDS 50 mM Tris, pH 8.0
Gel sample buffer (GSB)	63 mM Tris HCl, pH 6.8 10% (v/v) glycerol 5% (v/v) β mercaptoethanol 2% (w/v) SDS, 0.0025% (w/v) bromophenol blue
PBS Tween	1 L ddH_20 10 PBS Tablets 2 ml Tween20
NuPAGE® MOPS SDS Running Buffer	50 mM MOPS 50 mM Tris Base 0.1% (w/v) SDS

	1 mM EDTA, pH 7.7
NuPAGE® Transfer buffer	500 mM Bicine 500 mM Bis-Tris, PH 7.2 20.5 mM EDTA
IBT Blocking buffer	0.5% (w/v) I BLOCK in PBS Tween
Ponceau S	0.1% (w/v) Ponceau S 5% (v/v) acetic acid ddH_20

2.4.1 Protein isolation from tissues

Liver tissues were collected as described in Section 2.3.1 (all procedures were carried out with pre-chilled reagents on ice). An appropriate amount of RIPA buffer (typically 1-2 ml) was added to 50 mg of liver tissue and ground until homogenised using a pestle and mortar. The homogenised tissue was placed into a clean tube and vortexed thoroughly for 30 seconds followed by centrifugation at 2000 x g for 3 minutes at 4°C. The supernatant was then transferred into a clean tube. A small aliquot was removed for protein quantitation as described in Section 2.4.2.

2.4.2 Determination of protein concentrations

Total protein concentration was determined using the Micro bicinchoninic acid (BCA) Protein Assay Kit. Briefly, a standard curve was produced by serial dilutions (5 to 200 µg/ml) of purified BSA in 0.9% (w/v) saline (2 mg/ml) provided in the kit. Then, to 25 µL of BSA standards, protein samples along with a blank (RIPA buffer), 100 µl of BCA working reagent (provided in the kit) was added to a 96 well plate and incubated for 30 minutes at 37°C. The BCA working reagent was prepared for each sample by mixing 49 parts of reagent A, 49 parts of reagent B and 2 parts of reagent C (all provided in the kit) as stated in the manufacturer's instructions. Following incubation, the absorbance was read at 595 nm on a Dynex Technology MRX Model 680 Micro-plate reader. A standard curve was compiled, and the unknown protein concentrations were determined from this.

2.4.3 Protein separation

SDS-PAGE is commonly used for the separation of denatured proteins on the basis of their relative molecular mass. The protein samples (typically 60 µg) were mixed with an equal volume of GSB containing SDS followed by heating at 95^0C for 5 minutes. The samples were then chilled on ice for 2 minutes and loaded onto a pre-cast NuPAGE 4-12% Bis-Tris gel (1.0 mm thick, 10-well) (Thermo-Fisher Scientific). These pre-cast gels allow for optimum separation of small to medium-sized proteins in a neutral pH environment. The electrophoresis tank was filled with 1 x NuPAGE® MOPS SDS Running buffer. Magic markers were also used to determine the size of the proteins on the membranes following blotting. Samples were subjected to electrophoresis for 2 hours at 120 V and 400 mA.

2.4.4 Blotting

After the electrophoretic separation, the proteins were transferred onto a membrane. The process involves the use of an electric field, porous pads and filter papers to facilitate the transfer. When an electric field is applied, the proteins move out of the gel and onto the surface of the membrane, where the proteins become tightly attached. The result is a membrane with a "copy" of the proteins present on the gel.

In brief, the gel was removed from its casing and placed on top of methanol-activated PVDF membrane using XCell Surelock® Mini-Cell via XCell II™ Blot Module filled with 1X NuPAGE®Transfer buffer, which was used to "top up" the inner chamber. The assembly of the transfer cell is detailed in Figure 2.1. The transfer was performed at 30 V and 300 mA for 2 hours.

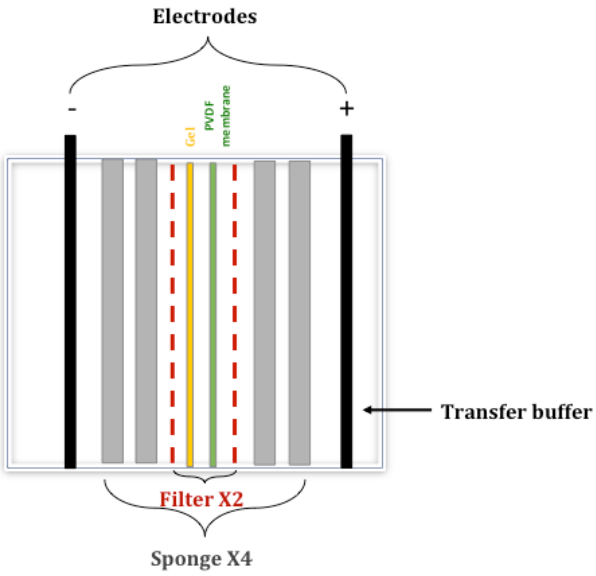

Figure 2.1 The assembly of protein transfer unit

PVDF membrane (0.45 µm pore size, Millipore) was cut to the size of the gel and activated in methanol (100%) for 2 minutes before being placed in transfer buffer. The membrane was placed on top of the gel and both were sandwiched between Whatman 3 mm filter paper and sponge pads that had also been soaked in 1 x transfer buffer. The whole assembly was then placed into a Mini Trans-Blot Cell. Electro-blotting was carried out at 30 V, 300 mA for 2 hours.

2.4.5 Immuno-detection of proteins

After completion of the transfer process, the proteins could be visualised on the membrane by staining with Ponceau S to confirm that successful transfer had occurred. Following visualisation of the proteins, the membrane was washed in 2% (v/v) PBS-Tween® until all the stain had been removed. It is important to then "block" the remaining surface of the membrane to prevent non-specific binding of the detection antibodies during subsequent steps. The membrane was therefore "blocked" with IBT solution for 1 hour at room temperature with constant shaking. Following this, the membrane was treated with a primary antibody for 1 hour at room temperature or overnight at 4 ˚C (the antibodies used are listed in Table 2.3). After incubation with a primary antibody, the membrane was washed three times with 2% (v/v) PBS-Tween® at room temperature with constant shaking. Next, the membrane was treated with a corresponding alkaline phosphate (AP)-conjugated secondary antibody diluted in IBT solution at room temperature, with constant shaking for 1

hour. The membrane was then washed again as above and incubated for 30 minutes with Tropix®CDP Star®, a chemiluminescent substrate for AP that allows for the rapid and reproducible detection of AP-labelled molecules. Following this step, the membrane was secured into a lightproof cassette, exposed to chemiluminescent X-ray film and several exposures at various time points were taken (exposure time varied between 5 minutes to overnight).

Table 2.3 Antibodies and conditions used in western blot analysis

Primary antibody	Dilution	Incubation time	Secondary antibody	Dilution	Size (kDa)
Rabbite Polyclonal-Phospho STAT1 (Ser727)	1/250	Overnight	Anti-Rabbit-AP	1:1000	91
Rabbite Polyclonal-p44/42 MAPK	1/250	Overnight	Anti-Rabbit-AP	1:1000	44/42
Goat polyclonal-GAPDH	1/5000	1 hour	Anti-Goat-AP	1:20,000	36

2.5 Pro-inflammatory gene expression

The expression of a specific gene into mRNA molecules can be determined by real-time quantitative polymerase chain reaction (RT-qPCR) using cDNA against isolated RNA.

2.5.1 RNA isolation

BMDM were produced as described in Section 2.3.3 and seeded into 12 well plates (0.5 x 10^6 cells/well) in complete DMEM media and left for 24 hours to adhere at 37°C in a humidified incubator containing 5% (v/v) CO_2. Prior to RNA extraction, the media was aspirated and the cells were washed gently with PBS.

RNA was isolated using RiboZol™, a single-phase phenol that homogenises the cells and inhibits RNase activity, according to the manufacturer's instructions (Amresco). Briefly, 1 ml of RiboZol™ was added to cells per well and incubated for 15 minutes at room temperature with constant shaking to guarantee complete lysis.

Then, 200 µl of chloroform per 1 ml of RiboZol™ was added and mixed vigorously for 15 seconds. This was followed by centrifugation at 12,000 x g for 15 minutes at 4°C. The colourless upper aqueous phase, containing the RNA, was then transferred into a new RNase-free tube. The RNA was then precipitated by adding 1:1 volume of isopropanol and incubated for 10 minutes on ice, followed by centrifugation at 12,000 x g for 10 minutes at 4 °C to pellet the RNA. The isopropanol was decanted carefully from the tube without disturbing the RNA pellet. The pellet was then washed three times with 75% (v/v) ethanol. Following the final wash, the pellet was left to air dry to evaporate any excess ethanol. Dried RNA pellet was dissolved in 15-20 µl nuclease free water and incubated for 10 minutes at 56°C to completely dissolve the RNA.

NanoDrop™ ND2000 was used to measure the RNA concentration. The A_{260}/A_{280} and the A_{230}/A_{260} ratios were used to assess RNA purity and quality respectively. In addition, the quality of RNA was checked by size-fractionation of a small aliquot by agarose gel electrophoresis as described in Section 2.5.2.

2.5.2 Resolving RNA

The RNA was size-fractionated on an agarose gel as an additional check for the quality (Figure 2.2). For this, 1.5% (w/v) gel was made by dissolving agarose in 1 x TBE buffer (0.98 M Tris-borate, 890 mM Boric acid, 20 mM EDTA, pH 8) followed by the addition of 0.5 µg/ml of ethidium bromide to aid visualisation. The gels were loaded with 200-500 ng/µl of RNA that had been mixed with 2 x RNA loading dye (95% formamide, 0.025% SDS, 0.025% bromophenol blue, 0.025% xylene cyanol). Electrophoresis was carried out using a horizontal gel unit at 100 V in 1 x TBE for 45 minutes. The quality of RNA was judged as good when two distinct bands were observable with no obvious smearing, the band corresponding to the 28S rRNA being twice as intense as that for 18S rRNA.

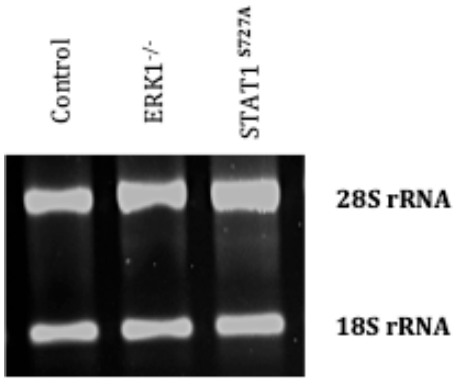

Figure 2.2 RNA gel electrophoresis fractionation

Electrophoresis was carried out using 1.5% (w/v) agarose gel with 500 ng/µl of RNA mixed with 2 x RNA loading dye. The quality of RNA was judged as good when two distinct bands were observable with no obvious smearing, the band corresponding to the 28S rRNA being twice as intense as that for 18S rRNA. Representative samples are shown here with RNA from control C57/BL6J, ERK1$^{-/-}$ and STAT1^{S727A} mice.

2.5.3 cDNA synthesis

In order to be able to assess gene expression, the extracted RNA had to be reverse transcribed into cDNA for RT-qPCR analysis. RNA (1-5 µg depending on the concentration of the isolated RNA) was mixed with 0.5 µl of random hexamer primers (200 pmol) and nuclease-free water to make a total volume of 11 µl. The mixture was then incubated at 70°C for 5 minutes on a Biometric Thermos Block, followed by a 5-minute period on ice. The reagents listed in Table 2.4 were then added to the reaction mixture.

Table 2.4 The composition of the master mix used in reverse transcription reaction

Reagent	1 x master mix (µl)
10 mM dNTPs mixture	1
5 x MMLV buffer	4
RNase inhibitor (40 U/µl)	1
MMLV reverse transcriptase (200 U/µl)	1

Abbreviations: MMLV, Moloney murine leukaemia virus.; dNTP's (dATP, dTTP, dCTP, dGTP)

The final reaction mix was incubated at 37°C for 1 hour, followed by a termination period at 95°C for 5 minutes to inactivate the reverse transcriptase enzyme. The cDNA was diluted to 350 ng with nuclease-free water and kept at 4°C for short-term storage or -20°C if long-term storage was required.

2.5.4 Real-time quantitative PCR (RT–qPCR)

RT-qPCR is a reliable detection method for the measurement of products generated during each cycle of the PCR process that is directly proportional to the amount of mRNA for the gene of interest at the start. The method allows for the direct detection of PCR products during the exponential phase of the reaction, combining amplification and detection in one single step. The fluorescent signal is plotted as a function of cycle number (Ginzinger, 2002).

In this study, the mRNA expression levels of several genes were analysed using the SYBR® Green JumpStart™ Taq Ready Mix kit (Sigma-Aldrich). The SYBR® Green intercalates into double-stranded DNA (dsDNA) and therefore the strength of the fluorescent emission is proportional to the amount of cDNA template. The amplification of products throughout the different PCR cycles were monitored.

During the project, two forms of RT-qPCR were utilised. The first will be referred to as 'regular RT-qPCR' and was performed using the method outlined below and the sequences of the primers shown in Table 2.5. All the primers used for regular

RT-qPCR were intron-spanning and were designed and used extensively by other members of the laboratory. A reverse transcriptase negative control was included in regular RT-qPCR experiments to confirm that the signals obtained did not arise because of any contamination of the samples with genomic DNA. The second form of RT-qPCR will be referred to as 'RT-qPCR array'. RT-qPCR arrays use special plates (Atherosclerosis RT^2 Profiler PCR Arrays), which contain the primers for 84 atherosclerosis-associated genes and 5 housekeeping gene(s) (HKG) as well as 3 negatives, 3 positive and 1 genomic DNA contamination controls. The advantage of RT-qPCR arrays is that they are able to provide a large volume of data compared to regular RT-qPCR in the same time frame. Melting curve analysis was used for both regular RT-qPCR and RT-qPCR array to ensure that the primers produced a single product.

Table 2.5 Primer sequences used for RT-qPCR

Primer	Species	Forward sequence (5'-3')	Reverse Sequence (5'-3')
β-actin	Mouse	ACACCCGCCACCAGTTCGCCAT	CACACCCTGGTGCCTAGGGCGGCCCACG ATG
ABCA1	Mouse	TGGAAAACAGTTAATGACCAGCCA	TCCAGTAACAGCTGACATGTTTGT
ABCG5	Mouse	CGTGGCGGACCAAATGATT	CCACTGGAAATTCCCCCAAA
ABCG8	Mouse	GAGCTGCCCGGGATGATA	CGGAAGTCATTGGAAATCTG
HMGCR	Mouse	AAGGGTACGGAGAAAGCACT	AATGACGCTTCACAAACCA
NPC1L1	Mouse	GGCTCCATCTGGAGTAGCTG	ATCGCACTACCATCCAGGAC

Abbreviations: ATP-binding cassette transporter (ABCA1), ATP Binding Cassette Subfamily G Member 5 and 8 (ABCG5 and ABCG8), 3-Hydroxy-3-Methylglutaryl-CoA Reductase (HMGCR), Niemann-Pick C1-Like 1 (NPC1L1).

RT-qPCR samples were prepared as 25 µl reactions in a 96-well plate. The reaction mix is detailed in Table 2.6. The cycling conditions for the RT-qPCRs are shown in Table 2.7.

Table 2.6 Reaction mix for RT-qPCR using SYBR® Green

Reagent	Regular RT-qPCR 1 x master mix (µl)	RT-qPCR array 1 x master mix (µl)
SYBR® Green	12.5	12.5
Forward primer (2.5 µM)	0.5	-
Reverse primer (2.5 µM)	0.5	-
cDNA	1	1
Water	10.5	10.5

Table 2.7 RT-qPCR conditions

PCR step	Regular RT-qPCR		Array RT-qPCR	
	Temperature (°C)	Time (seconds)	Temperature (°C)	Time (seconds)
Pre-incubation	94	120	95	600
Melting	95	30	95	15
Annealing	60	60	60	60
Extension	72	60	-	-

The regular RT-qPCR is a three-step amplification process and cycles 40 times whereas the RT-qPCR arrays involve two-step amplification (as the annealing and extension steps occur simultaneously) and cycles 45 times.

A relative quantification method was used to describe the changes in the expression of a target transcript in a treatment group to that of the controls after normalisation of samples with HKG whose expression was not altered under the experimental conditions. The HKG used for regular RT-PCR was β-actin whereas the most stable ones from five HKG were employed for RT-qPCR assays. The quantification method used determines when the fluorescent emission reaches a pre-

set threshold value (C_t value) within the amplification stage, using the comparative C_t ($\Delta\Delta C_t$) method (Livak and Schmittgen, 2001). Once the PCR reaction was completed, Ct values were recorded and analysed in Microsoft Excel. All PCRs were performed at least five times using Roche light cycler.

2.6 Cell-based assays

2.6.1 Cell viability and proliferation assays

2.6.1.1 Lactate dehydrogenase (LDH)

An LDH assay kit was used to assess the viability of BMDM. Briefly, the cells were incubated with a reaction mixture containing lactate and NAD^+, which will react with the released LDH (cytosolic enzyme) upon cell rupture or damage, producing pyruvate and nicotinamide adenine dinucleotide (NADH). Subsequently, pyruvate and NADH reacts with the water-soluble salt 2-(4- iodophenyl)-3-94-nitrophenyl)-5-phenyl-2H-tetrazolium chloride (INT) contained in the reaction mixture and will be reduced to an insoluble red formazan salt. The darker the red colour the more LDH leakage indicating a reduction in cell viability.

Differentiated BMDM (2.5 x 10^5 cells/well) were plated in 96 wells plate and left to adhere overnight. After 24 hours, 20 µl of 10 x lysis buffer (provided in the kit) was added to the positive control wells to achieve 100% cellular lysis and left to incubate at 37^{o}C. A negative control was also included containing the media alone for a background reading.

In order to compensate for the increased volume in the positive control wells, 20 µl of dH_2O was added to all of the other wells. The plate was then incubated for 45 minutes and then 50 µl of the supernatant from each well was transferred into a new 96 well plate. Then, 50 µl of the reaction mixture (provided in the kit and made according to manufacturer's instructions) was added and incubated for 30 minutes followed by 50 µl of stop solution (provided in the kit). The LDH absorbance was read immediately at 490 nm on a Dynex Technology MRX Model 680 Micro-plate reader from BioRad. Negative control values were subtracted from the readings and arbitrary assigned as 100% in comparison to the control.

2.6.1.2 Crystal violet (CV)

The proliferation of BMDM was assessed using the CV assay. In the method, adhered cells are stained with the crystal violet dye, which binds to proteins and DNA. Cells that undergo cell death lose their adherence and are subsequently lost from the population of cells during the washing steps, thereby reducing the amount of CV staining of the culture (Feoktistova, et.al, 2016). Therefore, the darker the purple color the more proliferationof the cells.

The cells were cultured as described in Section 2.6.1.1 Once the supernatant was removed from the original 96 wells plate for the LDH assay, the remaining media was aspirated and the cells washed with 300 µl PBS. A CV solution [0.2% (w/v) in 10% (v/v) ethanol] was prepared and 100 µl was added to each well followed by incubation for 5 minutes at room temperature to stain the cells. The CV solution was then removed and the cells were washed three times with 300 µl PBS. Then, 100 µl of solubilisation buffer [0.1 M NaH_2PO_4 in 50% (w/v) ethanol] was added to each well and incubated for 5 minutes with constant rocking at room temperature. The absorbance of CV was read in a microplate reader at 570 nm. The results were expressed as a percentage of viable cells in comparison to the control conditions, which was arbitrarily assigned as 1.

2.6.2 Migration assay

Migration of BMDM was determined using a modified Boyden chamber (Figure 2.3), which involves the use of a porous membrane that mimics the endothelium layer in the artery. Cells were plated on the topside of an 8 µm pore size membrane that split the wells of the companion plate into separate halves but still allowed the cells to migrate. The level of migration was determined by the percentage of cells that move across the membrane in response to a key atherosclerosis-associated macrophage chemoattractant molecule, MCP-1.

BMDM (5×10^5 cells) were suspended in cell culture DMEM media containing 0.2% (w/v) fatty acid-free BSA and 1% (v/v) pen/strep and placed on top of the cell culture insert. Complete DMEM media (0.5 ml) was added to the bottom chamber. The assay included a negative control without MCP-1 and that containing the chemokine

MCP-1 (20 ng/ml) to stimulate migration. The set up was incubated for 24 hours in a humidified incubator at 37°C containing 5% (v/v) CO_2.

The media in the top chamber and non-migrated cells were removed gently using cotton swap. The membrane was then cut with a scalpel and placed over 10 µl of Fluoroshield Mounting Medium with DAPI on a glass slide, covered with a coverslip and sealed. The numbers of fluorescently stained, migrated cells in 5 different fields on each slide were counted using an Olympus BX61 fluorescence microscope. The results were expressed as fold fluorescence change in relation to the MCP-1 positive control, which was arbitrarily assigned as 1.

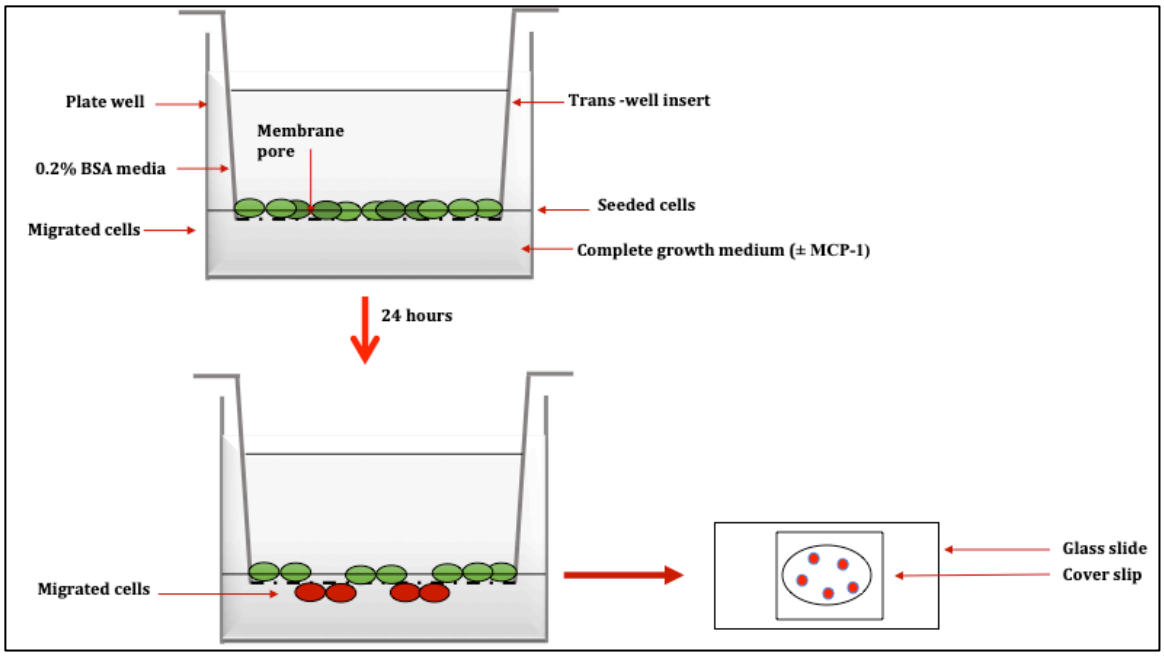

Figure 2.3 Cell migration

Pre-cultured BMDM were added on top of a trans-well migration insert with the lower chamber containing complete DMEM media with 20 ng/ml MCP-1 to stimulate cell migration. Negative control without MCP-1 was also included. The migrated cells were stained and analysed by microscopy.

2.6.3 *In vitro* ROS production assay

In vitro measurement of ROS was performed using a DCFDA-Cellular Reactive Oxygen Species Detection Assay Kit (Abcam). The assay employs the use of a cell-

permeant reagent 2', 7' –dichlorofluorescein diacetate (DCFDA), a fluorogenic dye that measures ROS activity within the cells.

BMDM were cultured in 96 wells as described in Section2.6.1.1 as recommended by the manufacturer's protocol (the reagents provided in the kit were brought up to room temperature at the time of use). The cells were washed with PBS to remove all traces of the media. Then, 100 µl/well of 1 x buffer (provided in the kit) was added to the cells and incubated for 1 minute. The 1 x buffer was then removed and the cells stained with 100 µl/well of 25 µM DCFDA (provided in the kit) for 45 minutes at 37°C in a humidified incubator containing 5% (v/v) CO_2. The stain was then removed and the cells were washed again with 1 x buffer. The cells were then treated with 50 µM tert-butyl hydrogen peroxide (TBHP; provided in the kit) for 3 hours to induce ROS production (buffer blank was also included to measure background). Following this, the reaction was stopped by removing the media and washing the cells with 1 x buffer. The fluorescence was then read using a fluorescent plate reader with excitation wavelength at 490 nm and emission wavelength at 520 nm. The results were expressed as fold fluorescence change between TBHP positive control, which was arbitrarily assigned as 1, and the other samples following background subtraction.

2.7 Cholesterol homeostasis

2.7.1 Macropinocytosis

Macropinocytosis is a mechanism by which cholesterol may be taken up into macrophages during foam cell formation. LY is a fluorescent dye, which enters the cells via macropinocytosis. Determining the fluorescent signal within macrophages treated with LY by FACS analysis can therefore be used as an indication of the levels of macropinocytosis that has occurred within the cells.

For the assay, BMDM were cultured as described in Section 2.5.1 the cells were then treated with 100 µg/ml LY in 0.2% (w/v) BSA and 1% (v/v) pen/strep cell culture DMEM media and left to incubate for 24 hours. The overlying media was then discarded and cells were detached using 0.5 ml of Trypsin-EDTA (0.05% w/v), which was added to each well and incubated for 30 minutes. Then, 0.5 ml of complete

culture medium was added to each well to inactivate the Trypsin-EDTA to prevent cell lysis. The resulting mixture was then pipetted up and down several times to ensure that the cells were no longer adherent to the surface of the well and subjected to centrifugation at 9,000 x g for 5 minutes to pellet the cells. The supernatant was removed and the pellets were re-suspended in 2% (w/v) paraformaldehyde (PFA). LY incorporation was analysed by flow cytometry on a BD FACS Canto flow cytometer. At least 5,000 events were counted for each sample. The results were expressed as fold fluorescence change calculated in relation to the vehicle control, which was arbitrarily assigned as 1.

2.7.2 Dil-oxidised LDL uptake

Reduced cholesterol uptake results in decreased foam cell formation. Any changes that are capable of attenuating cholesterol uptake would represent potential anti-atherogenic therapy. Using fluorescently labeled oxLDL, the uptake into cells can be assessed by flow cytometry as the stronger the fluorescent signal, the more cholesterol uptake has occurred.

BMDM were cultured as described in Section 2.5.1 and then treated with 5 μg/ml Dil-oxLDL in 0.2% (w/v) fatty acid-free BSA and 1% (v/v) pen/strep cell culture DMEM medium for 24 hours. The overlying media was discarded and the cells were detached using 0.5 ml Trypsin-EDTA (0.05%, w/v) that was added to each well and incubated for 30 minutes. Then, 0.5 ml of complete culture medium was added to each well to inactivate the Trypsin EDTA in order to prevent cell lysis. The resulting mixture was then pipetted up and down several times to ensure that the cells were no longer adherent and subjected to centrifugation at 9,000 x g for 5 minutes to pellet the cells. The pellets were re-suspended in 2% (w/v) PFA. Dil-oxLDL incorporation was analysed by flow cytometry on a BD FACS Canto flow cytometer. At least 5,000 events were counted for each sample. The results were expressed as fold fluorescence changes in relation to the control, which was arbitrarily assigned as 1.

2.7.3 Cholesterol efflux

Cholesterol efflux can be measured using radioactively labeled cholesterol. Cells are allowed to take up the radioactive cholesterol during foam cell formation for

24 hours before the addition of ApoA1, a key apolipoprotein on HDL particles, to stimulate its efflux into the surrounding media. The more radioactive cholesterol found within the media compared to the amount found within the cell indicates increased cholesterol efflux and therefore a possible reduction in foam cell formation. The cholesterol efflux assay was adapted from a previously reported protocol (McLaren *et al.* 2010a).

Initially, BMDM cells were cultured as described in Section 2.5.1 and the media was replaced with 0.2% (w/v) fatty acid-free BSA and 1% (v/v) pen/strep cell culture DMEM media supplemented with acetylated LDL (acLDL, 25 µg/ml) and [4-^{14}C] cholesterol (0.5 µCi/ml). No HI-FCS was used in the culture media because of the ability of FCS to stimulate cholesterol efflux from the cells and thereby affecting the accuracy of the assay. Following incubation for 24 hours, the cells were washed with PBS (1 x, pH 7) and the media was replaced with that containing 10 µg/ml ApoA1 followed by incubation for another 24 hours. The media was then removed into clean tubes for use in scintillation counting. The remaining cells were treated with 0.2 M NaOH to solubilise the cells and again removed to clean tubes for use for scintillation counting.

For scintillation counting, samples were placed into 20 ml polyethylene vials with 10 ml OPTI-FLUOR®. Samples were counted on a Liquid Scintillation Analyser (TriCarb 2800TR, Perkin Elmer) and recorded using Quanta Smart. Radioactivity was determined by the number of disintegrations per minute (d.p.m) within the samples. Cholesterol efflux was calculated as the fold change of radioactivity in the supernatant versus total radioactivity (cells and supernatant). The results were normalised to the vehicle control, which was arbitrarily assigned as 1.

2.7.4 Phagocytosis

Phagocytosis levels in BMDM were assessed using Vybrant® Phagocytosis Assay Kit (from Invitrogen and supplied by Thermo-Fisher Scientefic), a highly sensitive, simple and quantitative fluorometric assay method for monitoring the process. The assay principle is based on the internalisation of killed *E. coli* (K-12 strain) cells that have been labeled with the fluorescent dye fluorescein followed by

the use of trypan blue solution which will quench the fluorescence from particles that were not internalised as described in the manufacturer's protocol.

BMDM (2.5 x 10^5 cells/well) were plated in 96 wells plate and left to adhere overnight (negative control wells with media only were also included). After 24 hours incubation, the media was aspirated and 100 µl of Fluorescent BioParticle suspension (prepared according to manufacturer's protocol) was added to all the wells. The plate was then transferred back to the incubator. After 2 hours incubation, the media was aspirated and 100 µl of 0.25 mg/ml trypan blue suspension was added to all the wells followed by incubation at room temperature for 1 minute. Excess trypan blue was aspirated and fluorescence was determined using a fluorescence plate reader with 490 nm excitation and 520 nm emissions.

Net phagocytosis under normal physiological conditions and in response to treatment was calculated after subtracting the average fluorescence intensity from negative-control wells. The data were presented as fold fluorescence changes in relation to the vehicle control, which was arbitrarily assigned as 1.

2.8 *In vivo* studies

2.8 .1 Feeding of mice

To assess the effect of HT in short-term studies *in vivo*, 8 weeks old male C57/BL6J mice (weight 25-35g) were used (Section 2.3). Thus, 16 mice were distributed randomly between two groups (n=8 per group) and fed a HFD [21% (w/w) pork lard and 0.15% (w/w) cholesterol] for 3 weeks with daily administration by gavage of vehicle control (water) or 10 mg/kg/day HT. For long-term studies on atherosclerosis, 8 weeks old male or female $LDLR^{-/-}$ mice were used. The numbers of animals used were dictated in part by the availability at the time that the experiments were carried out. For the study on male mice, 22 animals were used (10 vehicle control and 12 HT whereas 21 female mice were used (10 vehicle control and 11 HT). They were given HFD mixed with vehicle or 10mg/kg/day HT for 12 weeks.

The body weight was measured at the start of the study and then approximately every 3 days using an electronic scale. At the end of the study, all mice were sacrificed by increasing the levels of CO_2 and the death confirmed by an absence

of a pulse (See section 2.3.1).

2.8.2 Blood and tissue collection

Blood from cardiac puncture was collected into Eppendorf tubes containing 20 µl heparin and the plasma was obtained by centrifugation (12,000 x g) for 5 minutes at room temperature. Tissues (Liver, spleen, thymus, heart, aorta and bone marrow) were also isolated from each animal (See section 2.3.1) and kept at –80°C until further analysis.

2.9 Plasma lipid profile

2.9.1 Plasma cholesterol levels

As high levels of LDL cholesterol and low levels of HDL cholesterol are considered to be pro-atherogenic, it was essential to determine the effect that HT treatment exerted on cholesterol levels in mice receiving a HFD. Total cholesterol, HDL and LDL/VLDL levels were determined in plasma using HDL and LDL/VLDL cholesterol assay kit (Abcam), an enzymatic colourimetric based cholesterol assay kit (Figure 2.4).

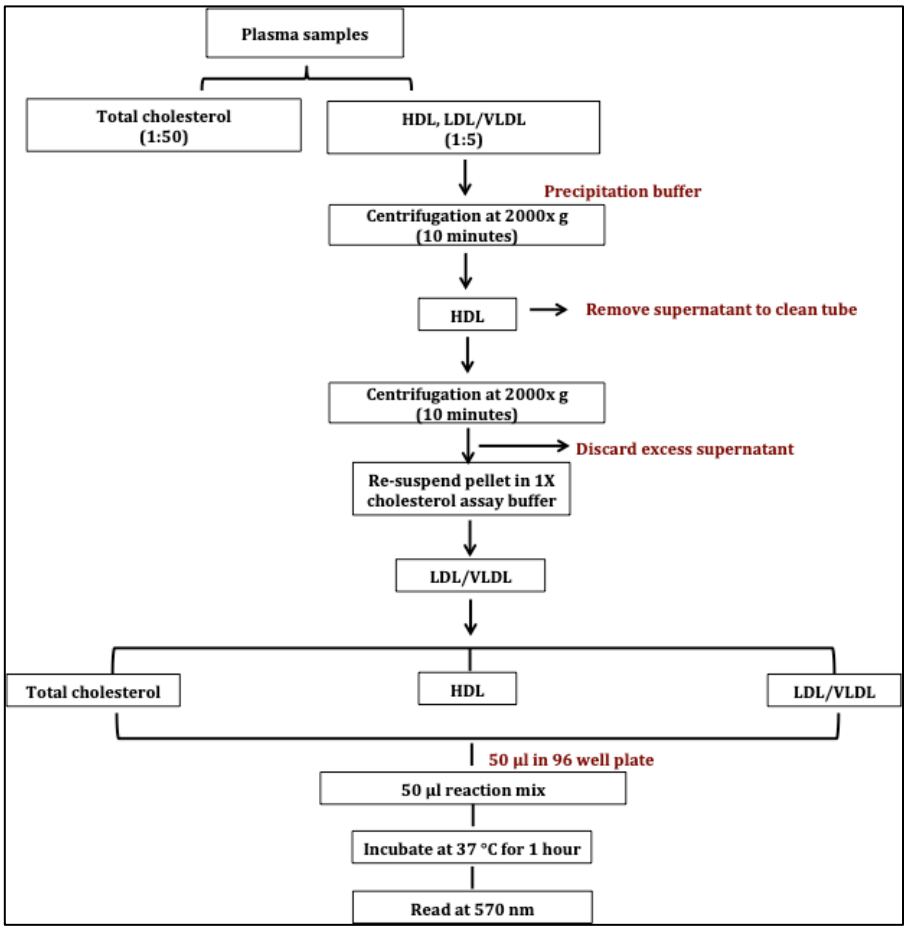

Figure 2.4 Schematic representation of the assay used for determining the levels of plasma total cholesterol, HDL and LDL/VLDL

Initially, serial dilutions of 0.25 µg/ml of cholesterol standards were carried out to obtain a standard curve for determination of cholesterol concentration in unknown plasma samples. On the basis of initial optimisation experiments, the plasma samples for total cholesterol assay were diluted 1:50 in 1 x cholesterol assay buffer (provided in the kit) whereas the plasma samples for HDL/LDL/VLDL were diluted 1:5.

A master mix for total cholesterol and free cholesterol was prepared in accordance with the manufacturer's instructions as shown in Table 2.8. Diluted plasma samples were directly incubated with the cholesterol oxidase enzymatic mix whereas HDL was first separated from LDL/VLDL in the plasma samples using a precipitation buffer (provided in the kit). The mixture was then incubated at room temperature for 10 minutes followed by centrifugation at 2,000 x g for 10 minutes.

The HDL fractions were present in the supernatant, which was removed and placed into a clean tube. The remaining samples were re-centrifuged under the same conditions and any remaining supernatant was removed. The pellet was re-suspended in 1 x cholesterol assay buffer and designated as the LDL/VLDL fraction.

Table 2.8 Composition of cholesterol oxidase enzymatic reaction mixture

Component	Reaction mix (µl)
Cholesterol assay buffer	44
Cholesterol probe	2
Enzyme mix	2
Cholesterol esterase	2

The diluted samples (50 µl) were transferred into 96 wells plate (background wells of 50 µl of water were also included) and 50 µl of the reaction mix was added to each well. The plate was then incubated at 37°C for 1 hour in the dark. The cholesterol oxidase enzymatic mix specifically recognises free cholesterol and produces a component that will react with a probe to generate a colour that can be measured spectrophotometrically at 570 nm. The levels of total cholesterol were measured and the unknown concentrations were obtained from the standard curve. Data were presented after background subtraction and adjusted to the dilution factors.

2.9.2 Plasma TG levels

TG levels were measured using an enzymatic colourimetric-based TG Quantification Assay kit (Abcam) according to manufacturer's protocol. Serial dilutions of TG were used to prepare a standard curve to calculate TG concentrations in the plasma samples. Plasma samples were diluted 1:50 (based on initial optimisation experiments) and incubated with a reaction mixture containing an enzyme (lipase) as shown in Table 2.9 and transferred to 96 wells plate (background wells of diluted plasma samples without the reaction mixture were also included).

Table 2.9 Preparation of TG reaction mixture

Component	Reaction mix (µl)	Back Ground Reaction mix (µl)
TG assay buffer	46	46
TG probe	2	2
TG enzyme mix	2	0

The enzyme lipase will digest the TG within the plasma into FFAs and glycerol. The glycerol is then oxidised to produce a product that is capable of interacting with the target probe and induce a colour within 1 hour of incubation at room temperature in the dark. The generated colour was measured spectrophotometrically at 570 nm. The greater the colour change, the more TGs are present in the plasma. Data were presented after background subtraction and adjusted to dilution factor.

2.10 ROS production

To assess the levels of ROS production in the plasma of mice, an OxiSelect *in vitro* ROS/Reactive Nitrogen Species (RNS) assay kit (green fluorescence) (Cell Biolabs) was used. The principle of the assay is similar to that described in Section 2.6.3. The dichlorodihydrofluorescein (DCFH) probe is oxidised by ROS into a highly fluorescent probe and therefore the stronger the fluorescent signal detected, the more the ROS present in the plasma. The DCFH-DiOxyQ probe was first primed with a quench removal reagent and subsequently stabilised in the highly reactive DCFH form. In this reactive state, H_2O_2 can react with DCFH, which is rapidly oxidised to the highly fluorescent 2', 7'- dichlorodihydrofluorescein (DCF). Fluorescence intensity was measured using a fluorescent plate reader at 480 nm excitation/530 nm emission. The intensity is proportional to the total H_2O_2 levels within the sample.

Initially, serial dilutions of H_2O_2 were used to prepare a standard curve to calculate H_2O_2 concentration in unknown plasma samples. Plasma samples were diluted 1:50 with PBS (based on initial optimisation experiments) and 50 µl of the

samples and H_2O_2 standards (made according to manufacturer's instructions) were transferred to a 96-well plate (background wells of 50 µl water were also included). An equal volume of the catalyst solution (provided in the kit) was added to each well and the plate incubated for an additional 5 minutes at room temperature in the dark. The samples were then mixed with a DCFH solution (provided in the kit), a probe that breaks down in the presence of H_2O_2 into a fluorescent form, for 30 minutes in the dark. The fluorescence was measured in a fluorescence microplate reader with excitation at 490 nm and emission detected at 520 nm and compared to the H_2O_2 standard curve. Data were presented as a percentage of fluorescence changes in relation to the vehicle control, which was arbitrarily assigned to 100 after background subtraction and adjusted to dilution factor.

2.11 Plasma cytokine levels

Plasma cytokine levels were determined by the Central Biotechnology Services at the School of Medicine of Cardiff University using a V-PLEX Plus Pro-inflammatory Panel1 Mouse Kit and 25 µl of plasma from each mouse.

2.12 Liver gene expression

Approximately 20-50 mg of liver was placed in a mortar along with 1 ml of RiboZol™ and the tissue samples were homogenised with a pestle. RNA was then extracted following the method outlined in Section 2.5.1. The RNA was then used in a reverse transcription reaction as described in Section 2.5.3 before assessment of gene expression by a RT-qPCR (Section 2.5.4).

2.14 Analysis of cell populations within the bone marrow

Haematopoietic Signaling lymphocyte activation molecule (SLAM) and progenitors cell population levels were assessed in the bone marrow of $LDLR^{-/-}$ mice after 12 weeks of administration of HFD with either a vehicle control or 10 mg/kg/day of HT. This was to determine whether HT was capable of preventing HFD induced changes in HSC populations (Table 2.10).

Table 2.10 Markers used to identify HSC populations within the bone marrow.

Class	Cell type	Marker
SLAM	LSK	Lin^- $Sca\text{-}1^+$ $c\text{-}Kit^+$
	HSC	$CD150^+$ $CD48^-$ LSK
	MPP	$CD150^-$ $CD48^-$ LSK
	HPC1	$CD150^-$ $CD48^+$ LSK
	HPC2	$CD150^+$ $CD48^+$ LSK
Progenitor	LK	Lin^- $Sca\text{-}1^-$ $c\text{-}Kit^+$
	CMP	$CD34^+$ $CD16/32^-$ LK
	MEP	$CD34^-$ $CD16/32^-$ LK
	GMP	$CD34^+$ $CD16/32^+$ LK
	CLP	$CD127^+$
Lineage	Granulocytes	$R1^+$ $Mac1^-$
	Macrophages	$GR1^-$ $Mac1^+$
	MDSCs	$GR1^+$ $Mac1^+$
	T-cells	$CD3^+$
	B-cells	$B220^+$
	RBCs	$Ter119^+$

Abbreviations: HSC, haematopoietic stem cell; MPP, multipotent progenitors; HPC, haematopoietic progenitor cell; CMP, common myeloid progenitor; MEP, megakaryocyte-erythroid progenitor; GMP, granulocyte-macrophage progenitor; MDSC, myeloid-derived suppressor cells; CLP, common lymphoid progenitor; SLAM, signalling lymphocytic activation molecule; RBC, red blood cells.

The day after collection, the tibia and femur were placed in a mortar along with 10 ml of PBS supplemented with HI-FCS (2% v/v). The bones were then crushed with a pestle until no visible bone marrow remained and the extracted marrow had been homogenised. The mixture was placed on a sterile filter (pore size of 70 μm) and allowed to pass through into a large Falcon tube. Further 2% (v/v) PBS was added to the filter until a final volume of 30 ml had been collected in the Falcon tube.

Cell suspension was then centrifuged at 2000 x g for 10 minutes and the pellet was re-suspended in 1 ml red blood cells lysis buffer (150 mM NH_4Cl, 10 mM $KHCO_3$, 0.1 mM Na_2EDTA, pH 7.4) for 1 minute. Cells were washed three times with 2% (v/v) PBS and the final pellet was re-suspended in 30 ml of 2% (v/v) PBS. The total number of cells was then calculated and 10 or 8 million cells were placed in separate Falcon tubes to analyse the SLAM and progenitor cell populations respectively. In addition, 200 μl (2-5 x 10^5 cells/ml) of the cells suspension was used for lineage positive cell population analysis.

As the SLAM and progenitor cells form a small proportion of the total number of cells in the bone marrow, large cell numbers were required to ensure that a sufficient number of target cells were detected during FACS analysis. The cells were then centrifuged at 5,000 x g for 5 minutes at 4 °C (these setting were used for centrifugation throughout the procedure unless otherwise stated). Cells from the bone marrow were stained at 4°C for 30 minutes with a biotinylated mix of lineage marker antibodies present within the SLAM, progenitor and lineage cell populations (Table 2.11).

Table 2.11 Antibodies used for lineage markers

Population	Antibody	Volume (µl)	2% HI-FCS PBS (µl)
SLAM	PE/Cy7-conjugated anti-mouse CD150	1	32
	FITC-conjugated anti-mouse CD48	2	
	Allophycocyanin (APC)-conjugated anti-mouse c-Kit	1	
	PE-conjugated anti-mouse stem cell antigen (Sca)-1	4	
Progenitors	PE-conjugated anti-mouse CD127	1	75
	PE/Cy7-conjugated anti-mouse CD16/32	10	
	FITC-conjugated anti-mouse CD34	4	
	APC-conjugated anti-mouse c-Kit	1	
	APC/Cy7-conjugated anti-mouse Sca-1	4	
Lineage	APC-conjugated anti-mouse B220	0.5	497.5
	FITC-conjugated anti-mouse CD3	0.5	
	PE/Cy7-conjugated anti-mouse Gr1	0.5	
	PE-conjugated anti-mouse Mac1	0.5	
	APC/Cy7- conjugated anti-mouse Ter119	0.5	

After the initial staining of the cells with the fluorescent antibodies for SLAM, progenitors and lineage cell surface markers, the cells were washed with 2% (v/v) PBS and only SLAM and progenitor cells were re-suspended in 50 µl PerCP-Cy5.5-conjugated streptavidin and incubated for a further 15 minutes at 4°C. Then, 1 ml of 2% (v/v) PBS was added followed by a quick centrifugation (5,000 x g) for 2 minutes. The supernatant was decanted carefully from the tube without disturbing the cell

pellet. The pellet was then re-suspended in 400 µl of 2% (v/v) PBS. The SLAM and progenitor cell populations were now ready to be analysed by FACS. For lineage cell analysis, the cells were washed and re-suspended in 200 µl of 2% (v/v) PBS. Before the samples could be analysed on the FACS machine, they were vortexed and filtered (pore size 40 µm) to prevent the cells from clumping together. Then, 0.5 µl of 1µg/ml DAPI stain was added to all of the SLAM, progenitor and lineage samples in order to identify viable cells. A BD FACS Fortessa flow cytometer (BD LSR Fortessa™) was then used to assess the composition of the cell populations and all possible cell counts were collected from each sample.

The process of back gating was performed to ensure the accuracy of the gating strategy. This was achieved by overlaying the final gated population over the preceding parent population in order to determine whether all of the target cells had been isolated correctly (See figure 1.24).

2.15 Data Analysis

All data analysis was performed using the Prism statistical software package. Data were tested for normality using the Shapiro-Wilk test and represented as mean ± standard error and single comparisons were carried out using the Student's *t* test (two-tailed, paired or unpaired). For multiple comparisons One-way ANOVA was employed accompanied with Tukey's post-hoc test or Dunnett post-hoc analysis. Data values outside two standard deviations of the mean were classed as outliers and removed before statistical analysis. The results were regarded as significant where *p≤0.05, **p≤0.01, ***p≤0.001.

Chapter 3

3.1 Introduction

MAPK signalling cascades play an important role in the pathogenesis of CVD. Previous research has focused on the identification and characterisation of the components of the MAPK cascades and attempt to link this to CVD (Muslin, 2008; Plotnikov *et al.*, 2011). Many of the details of the organisation of the MAPK pathway and the activation of the various components have now been defined (Muslin, 2008). However, the roles of the individual signalling proteins in the pathogenesis of atherosclerosis and CVD is still being investigated in order to identify new therapeutic targets (Moss and Ramji, 2015).

Previous studies showed that ERK1/2 plays an important role in two critical steps in the control of macrophage cholesterol homeostasis: uptake of modified LPs and the efflux of cholesterol from foam cells (Li *et al.*, 2010; Zhou *et al.*, 2010). In addition, ERK1/2 were found to be integral to the IFN-γ-mediated activation of STAT1 by phosphorylation on serine 727, the expression of several key genes implicated in atherosclerosis and the uptake of modified LDL by human macrophages (Li *et al.*, 2010). The role of the ERK1/2: STAT1 S727 phosphorylation axis in early atherosclerosis development via the modulation of macrophage inflammatory responses in mouse model systems has not been investigated. At the time of this study, another project in the laboratory was investigating this using ERK1 deficient mice and STAT1 S727A knock-in mice in the LDLR$^{-/-}$ model system.

In this study, the impact of ERK1 deficiency and STAT1 S727A mutation on several macrophage parameters relevant to CVD *in vitro* were investigated using BMDMs from these animals. Figure 3.1 provides an overview of the approaches used.

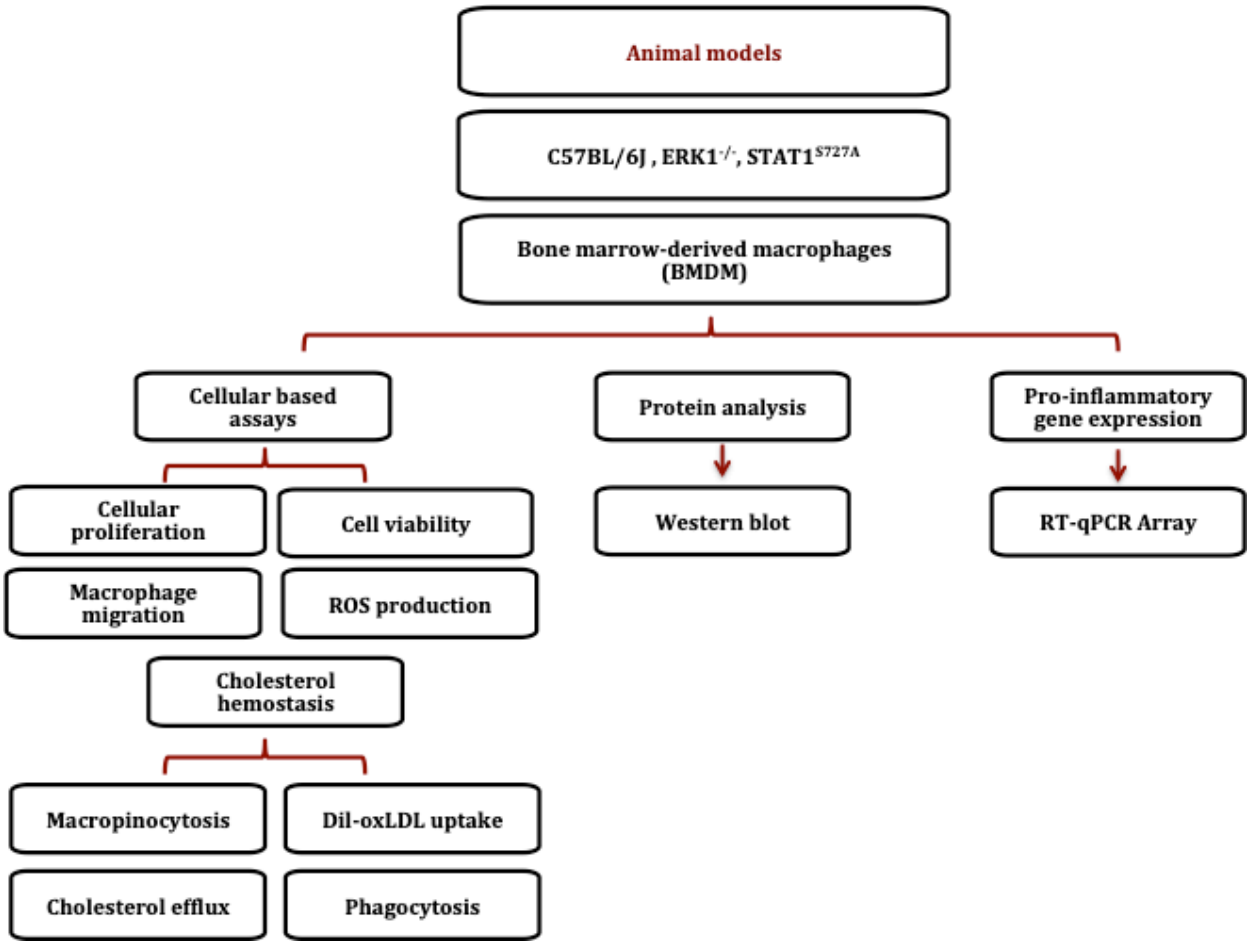

Figure 3.1 Overall summary of the *in vitro* assays used to determine the role of the ERK1: STAT1 S727 phosphorylation axis on key macrophage processes and gene expression associated with atherosclerosis.

3.2 Results

3.2.1 Confirmation of the genetic background of mice

Before carrying out further studies, Western blot analysis was performed on liver tissue protein lysates from C57BL/6J mice (control), ERK1 knockout mice (ERK1$^{-/-}$) and STAT1 S727A knock-in mice (STAT1^{S727A}) in order to validate that the mice had the expected changes in protein expression from the genetic manipulation**.** As expected, signals for ERK1, ERK2 and phospho-STAT1 S727 were present in liver extracts from C57BL/6J control mice (Figure 3.2 A-B). In contrast, the ERK1 protein was undetectable in tissue lysates from ERK1$^{-/-}$ mice whereas the ERK2 protein was present (Figure 3.2A). Tissue lysates from STAT1 S727A mice expressed both ERK1 and ERK2 proteins (Figure 3.2A) but not phospho-STAT1 S727 (Figure 3.2B). These results confirm the expected changes in protein levels from the genetic modifications in the mice used.

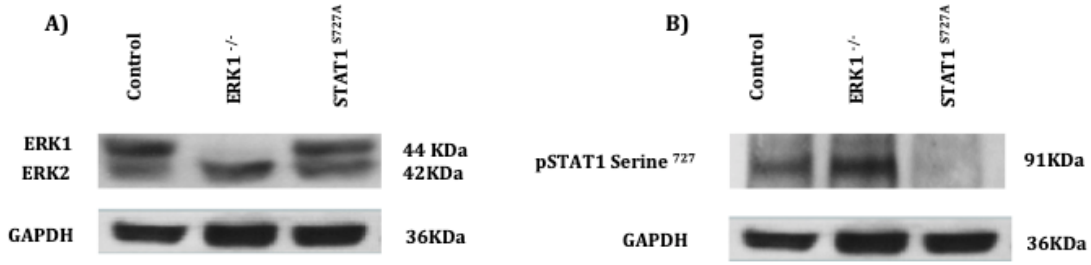

Figure 3.2 Confirmation of genetic modifications by western blotting.

Total protein lysates from the liver of C57BL/6J mice (Control), ERK1 knockout mice (ERK1$^{-/-}$) and STAT1 S727A knock-in mice (STAT1^{S727A}) were prepared and separated by SDS-PAGE. The proteins were then transferred onto PVDF membrane and subjected to Western blot analysis using antibodies specific for ERK1/2 (A), phospho-STAT1 Serine 727(B) and GAPDH as HKG control. The membrane was then treated with IBT solution for 5 minutes followed by exposure to an X-ray film. The image shows the immuno-reactive proteins with the corresponding molecular weights shown on the right side.

3.2.2 The effect of the genetic modifications on cellular viability of BMDM *in vitro*

The viability of BMDM from C57BL/6J control, ERK1$^{-/-}$ and STAT1^{S727A} mice was determined by the LDH assay. As shown in Figure 3.3, no significant reduction in cell viability was obtained with both genetic modifications. There was a slight but significant increase of about 20% *(p*<0.001) seen with ERK1 deficiency.

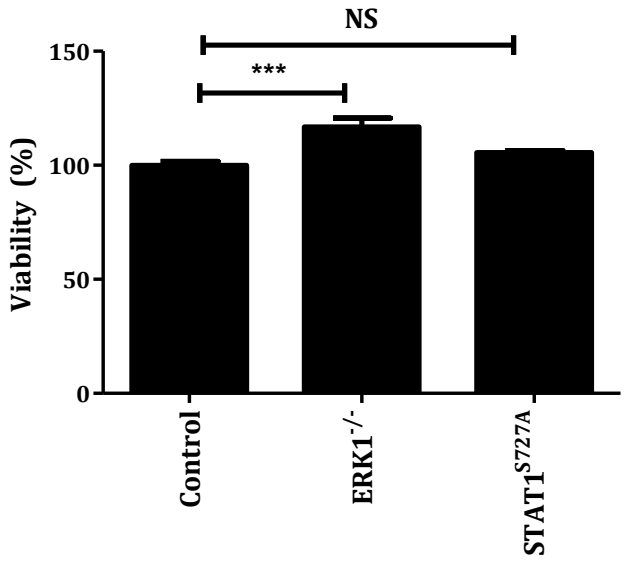

Figure 3.3 Cellular viability of BMDM *in vitro*.

The LDH assay was used to asses cellular viability in an overnight culture of BMDM from C57BL/6J (Control), ERK1$^{-/-}$ and STAT1^{S727A} mice as described in Materials and Methods (Section 2.6.1.1). The absorbance of LDH was measured at 490 nm. Background wells with media only were included and the values subtracted from the others. Data were normalised to the control that has been arbitrary assigned as 100%. Graph displays means ± SEM from four independent experiments. Statistical analysis was carried out using One-way ANOVA with Dunnett post-hoc analysis. *** $P \leq 0.001$; NS, not significant.

3.2.3 The effect of the genetic modifications on cellular proliferation of BMDM *in vitro*

Cellular proliferation of BMDM from C57BL/6J control, ERK1$^{-/-}$ and STAT1^{S727A} mice were determined using a CV assay. As shown in Figure 3.4, there was a significant 30% reduction (p=0.049) in cellular proliferation levels of ERK1$^{-/-}$ BMDM compared to the wild type counterpart. In contrast, there was no significant difference in the proliferation level with STAT1^{S727A} BMDM when compared to the control.

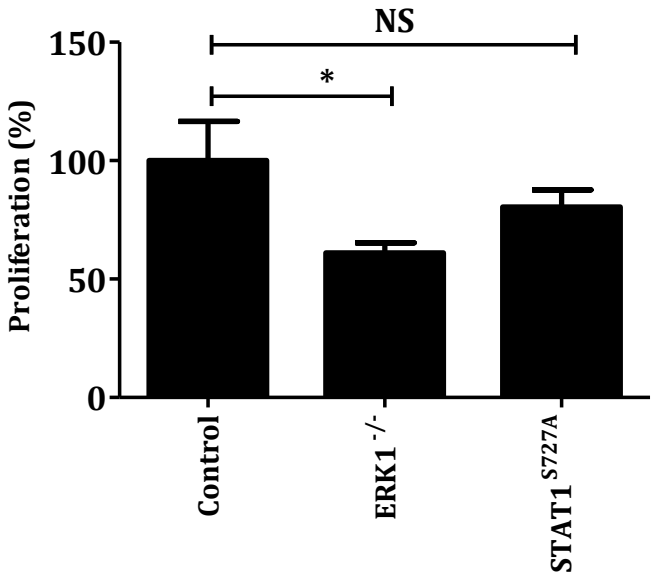

Figure 3.4 Cellular proliferation of BMDM *in vitro*.

CV assay was used to asses cellular proliferation in an overnight culture of BMDM from C57BL/6J (Control), ERK1$^{-/-}$ and STAT1^{S727A} mice. Adhered cells were stained with the CV dye as described in Materials and Methods (Section 2.6.1.2). The absorbance of CV was measured in a microplate reader at 570 nm. Background wells with media only were also included (background intensity). Data were normalised to the control that has been arbitrary assigned as 100% after subtracting the background. Graph displays means ± SEM from four independent experiments. Statistical analysis was carried out using One-way ANOVA with Dunnett post-hoc analysis. * $P \leq 0.05$; NS, not significant.

3.2.4 The effect of the ERK1: STAT1 S727 phosphorylation axis on the mRNA expression of key genes implicated in atherosclerosis

Genetic modifications of key signalling components such as ERKs and STAT1

usually impact cellular processes that are associated with changes in the expression of key genes. RT-qPCR array analysis for 84 genes involved in the regulation of different cellular process in atherosclerosis was performed to determine the expression of which genes implicated in key cellular processes, was affected by the ERK1$^{-/-}$ and STAT1^{S727A} modifications.

Table 3.1 and 3.2 shows the significant and non-significant gene expression changes, clustered according to their known functions in atherosclerosis, in BMDM from ERK1$^{-/-}$ and STAT1^{S727A} mice when compared to the control mice. The mRNA levels were calculated using the comparative Ct method and normalised to HKGs whose expressions were found to be stable during the assay and not affected by test conditions, as judged by their Ct values and standard errors of the means (SEM). The best candidates were those genes with the lowest SEM (Kozera and Rapacz, 2013). Samples with Ct values above 35 were removed from the analysis.

In the case of BMDM from ERK1$^{-/-}$ mice, the most stable genes were β-actin (*ACTB*), β-Glucuronidase (*GUSB*) and Heat shock protein HSP 90-β (*HSP90AB1*) (Table 3.1; SEM of 0.01-0.02 and approximately 5-7% change in expression). For BMDM from STAT1^{S727A} mice, the most stable genes were β-2-Microglobulin (*B2M*) and *ACTβ* (Table 3.2; approximately 1-3% changes in expression). The normalised values from control cells were given an arbitrary value of 1 to determine the changes in the gene expression levels between control and test samples.

Table 3.1 Gene expression levels in ERK1 deficient BMDM.

			Control	ERK1 $^{-/-}$		
#	**Gene**	**N**	**Mean ± SEM**	**Mean ±SEM**	**Change (%)**	***p*-value**
Stress response						
1	**APOE**	**6**	1 ± 0.09	3.21 ±1.23	221 ↑	0.12
2	**BAX**	**6**	1 ± 0.02	0.89 ± 0.25	11 ↓	0.99
3	**BCL2L1**	**6**	1 ± 0.05	0.57 ± 0.12	43 ↓	0.17
4	**CCL2**	**6**	1 ± 0.00	1.86 ± 0.52	86 ↑	0.14
5	**CCL5**	**6**	1 ± 0.00	2.09 ± 1.04	109 ↑	0.35
6	**CCR1**	**5**	1 ± 0.01	0.68 ± 0.28	32 ↓	0.46
7	**CCR2**	**5**	1 ± 0.00	0.30 ± 0.08	70 ↓	0.09
8	**CXCL1**	**4**	0.00 ± 0.00	0.00 ± 0.00	00	NA
9	**FN1**	**6**	1 ± 0.00	1.40 ± 0.63	40 ↑	0.590
10	**IFNγ**	**6**	1 ± 0.00	0.54 ± 0.16	46 ↓	0.04 (*)
11	**1L1α**	**6**	1 ± 0.00	2.78 ± 1.10	178 ↑	0.17
12	**IL1β**	**6**	1 ± 0.00	1.17 ± 0.64	17 ↑	0.84
13	**IL2**	**6**	1 ± 0.00	0.79 ± 0.29	21 ↓	0.47
14	**IL4**	**4**	1 ± 0.00	0.46 ± 0.13	54 ↓	0.01 (**)
15	**ITGβ2**	**6**	1 ± 0.03	1.30 ± 0.39	30 ↑	0.49
16	**PPARγ**	**6**	1 ± 0.04	0.69 ± 0.20	31 ↓	0.45
17	**SELP**	**5**	1 ± 0.00	0.85 ± 0.08	15 ↓	0.12
18	**SPP1**	**6**	1 ± 0.13	4.62 ± 1.51	362 ↑	0.06
19	**SOD1**	**6**	1 ± 0.04	0.67 ± 0.17	33 ↓	0.34
20	**TGFβ1**	**3**	1 ± 0.13	0.86 ± 0.21	14 ↓	0.71
21	**TNF**	**5**	1 ± 0.01	1.18 ± 0.33	18 ↑	0.56
Apoptosis						
22	**BCL2**	**4**	1 ± 0.00	0.60 ± 0.17	40 ↓	0.09
23	**BCL2 A1A**	**6**	1 ± 0.00	2.27 ± 0.81	127 ↑	0.16
24	**BID**	**6**	1 ± 0.01	0.74 ± 0.18	26 ↓	0.41
25	**BIRC3**	**6**	1 ± 0.00	0.88 ± 0.27	12 ↓	0.63
26	**FAS**	**6**	1 ± 0.00	1.27 ± 0.38	27 ↑	0.51
27	**NFKβ1**	**6**	1 ± 0.01	0.64 ± 0.21	36 ↓	0.21
28	**TNFαIP3**	**4**	1 ± 0.00	1.77 ± 0.43	77 ↑	0.12
29	**VEGFα**	**6**	1 ± 0.01	0.44 ± 0.12	56 ↓	0.004 (**)
Blood coagulation and circulation						
30	**NPY**	**4**	1 ± 0.01	5.06 ± 1.61	414 ↑	0.05 (*)
31	**PTGS1**	**6**	1 ± 0.00	0.96 ± 0.22	4 ↓	0.98
32	**VWF**	**3**	1 ±0.01	1.37 ± 0.46	37 ↑	0.48

Cell adhesion						
33	**CD44**	**6**	1 ± 0.09	0.68 ± 0.17	32 ↓	0.44
34	**CDH5**	**6**	1 ± 0.00	0.43 ± 0.11	57 ↓	0.002 (**)
35	**ICAM1**	**6**	1 ± 0.01	1.52 ± 0.52	52 ↑	0.37
36	**VCAM1**	**6**	1 ± 0.00	2.80 ± 1.15	180 ↑	0.20
37	**CTGF**	**6**	1 ± 0.00	5.63 ± 2.32	463 ↑	0.10
38	**ENG**	**6**	1 ± 0.01	0.75 ± 0.17	25 ↓	0.40
39	**ITGα2**	**5**	1 ± 0.00	0.40 ± 0.09	60 ↓	<0.001 (***)
40	**ITGα5**	**4**	1 ± 0.03	0.71 ± 0.17	29 ↓	0.40
41	**ITGαX**	**4**	1 ± 0.07	0.56 ± 0.18	44 ↓	0.27
42	**LAMA1**	**6**	1 ± 0.00	0.45 ± 0.15	55 ↓	0.01 (**)
43	**SELE**	**4**	1 ± 0.00	0.40 ± 0.16	60 ↓	0.01 (**)
44	**SELL**	**5**	1 ± 0.00	0.84 ± 0.02	16 ↓	0.07
45	**SELPG**	**6**	1 ± 0.05	0.43 ± 0.09	57 ↓	0.018 (*)
46	**THBS4**	**3**	1 ± 0.00	0.65 ± 0.33	35 ↓	0.39
Lipid transport and metabolism						
47	**ABCA1**	**6**	1 ± 0.02	0.89 ± 0.28	11 ↓	0.90
48	**APOA1**	**6**	1 ± 0.00	0.38 ± 0.13	62 ↓	0.003 (**)
49	**APOB**	**6**	1 ± 0.00	0.62 ± 0.18	38 ↓	0.09
50	**FABP3**	**6**	1 ± 0.00	2.21 ± 0.81	121 ↑	0.17
51	**LDLR**	**4**	1 ± 0.02	0.77 ± 0.17	33 ↓	0.58
52	**LPL**	**6**	1 ± 0.13	1.42 ± 0.30	42 ↑	0.39
53	**LYPLα1**	**6**	1 ± 0.01	0.82 ± 0.20	18 ↓	0.72
54	**MSR1**	**4**	1 ± 0.10	0.66 ± 0.16	34 ↓	0.46
55	**NR1H3**	**5**	1 ± 0.01	0.86 ± 0.29	14 ↓	0.79
56	**PLIN2**	**6**	1 ± 0.09	1.61 ± 0.47	61 ↑	0.27
57	**PPAR α**	**6**	1 ± 0.00	0.31 ± 0.11	69 ↓	<0.001(***)
58	**PPARD**	**5**	1 ± 0.00	0.90 ± 0.27	10 ↓	0.89
59	**RXRα**	**6**	1 ± 0.01	0.76 ± 0.25	24 ↓	0.53
Cell growth and proliferation						
60	**CSF2**	**3**	1 ± 0.00	0.43 ± 0.09	57 ↓	<0.001(***)
61	**ELN**	**4**	1 ± 0.00	0.19 ± 0.04	81 ↓	<0.001(***)
62	**FGF2**	**6**	1 ± 0.00	0.82 ± 0.18	18 ↓	0.34
63	**HBEGF**	**6**	1 ± 0.00	0.56 ± 0.16	44 ↓	0.04 (*)
64	**IL3**	**3**	1 ± 0.00	0.23 ± 0.05	77 ↓	<0.001(***)
65	**IL5**	**3**	1 ± 0.00	0.24 ± 0.06	76 ↓	<0.001(***)
66	**KDR**	**6**	1 ± 0.00	1.97 ± 0.69	97↑	0.19
67	**LIF**	**4**	1 ± 0.00	1.00 ± 0.31	0	0.96
68	**PDGFA**	**5**	1 ± 0.00	1.11 ± 0.31	11 ↑	0.55
69	**PDGFB**	**5**	1 ± 0.02	0.61 ± 0.13	39 ↓	0.13

70	**PDGFRβ**	**6**	1 ± 0.00	0.86 ± 0.32	14 ↓	0.66
71	**TGFβ2**	**5**	1 ± 0.00	0.97 ± 0.26	3 ↓	0.85
			Transcription regulation			
72	**KLF2**	**6**	0.00 ± 0.00	0.00 ± 0.00	00	NA
			Extracellular matrix (ECM)			
73	**ACE**	**5**	1 ± 0.00	0.59 ± 0.14	41 ↓	0.04 (*)
74	**CFLAR**	**6**	1 ± 0.02	0.92 ± 0.28	8 ↓	0.94
75	**COL3α1**	**4**	1 ± 0.00	4.34 ± 1.54	334 ↑	0.10
76	**FGα**	**6**	1 ± 0.00	0.68 ± 0.18	32 ↓	0.16
77	**FGβ**	**6**	1 ± 0.00	0.38 ± 0.10	62 ↓	0.001 (***)
78	**IL1R1**	**6**	1 ± 0.00	0.96 ± 0.31	4↓	0.91
79	**IL1R2**	**5**	1 ± 0.00	0.65 ± 0.37	34 ↓	0.35
80	**MMP1α**	**6**	1 ± 0.14	1.74 ± 0.37	74 ↑	0.24
81	**MMP3**	**4**	1 ± 0.00	3.70 ± 1.45	270 ↑	0.14
82	**SERPINβ2**	**4**	1 ± 0.00	1.81 ± 0.75	81 ↑	0.31
83	**SERPINE1**	**6**	1 ± 0.01	2.40 ± 1.01	140 ↑	0.23
84	**TNC**	**6**	1 ± 0.00	2.01 ± 0.89	101 ↑	0.32
			HKGs			
1	**ACTβ**	**6**	1 ± 0.02	1.07 ± 0.01	7 ↑	0.6
2	**B2M**	**6**	1 ± 0.05	1.08 ± 0.03	8 ↑	0.64
3	**GAPDH**	**6**	1 ± 0.04	1.09 ± 0.01	9 ↑	0.68
4	**GUSB**	**6**	1 ± 0.02	1.05 ± 0.01	5 ↑	0.51
5	**HSP90AB1**	**6**	1 ± 0.02	1.06 ± 0.01	6 ↑	0.55

Abbreviations: Apolipoprotein E (APOE), BCL2 associated X (BAX), BCL-2 like protein 1 (BCL2L1), C-C motif chemokine ligand 2 (CCL2), C-C motif chemokine ligand 5 (CCL5), C-C motif chemokine receptor 1(CCR1), C-C motif chemokine receptor 2 (CCR2), C-X-C motif chemokine ligand 1 (CXCL1), Fibronectin 1 (FN1), Interferon gamma (IFN-γ), Interleukin 1 alpha (1L1α), Interleukin 1 beta (IL1β), Interleukin 2 (IL2), Interleukin 4 (IL4), Integrin subunit beta 2 (ITGβ2), Peroxisome proliferator activated receptor gamma (PPARγ), Selectin P (SELP), Secreted phosphoprotein 1 (SPP1), Superoxide dismutase 1 (SOD1), Transforming growth factor beta1 (TGFβ1), Tenascin F (TNF), B-cell lymphoma 2 (BCL2), B-cell leukemia /lymphoma 2 related protein A1a (BCL2 A1A), BH3 interacting domain death agonist (BID), Baculoviral IAP repeat containing 3 (BIRC3), FAS cell surface death receptor (FAS), Nuclear factor kappa B subunit 1 (NFKβ1), Tumor necrosis factor alpha induced protein 3 (TNFαIP3), Vascular endothelial growth factor alpha (VEGFα), Neuropeptide Y (NPY), Prostaglandin endoperoxide synthase 1 (PTGS1), Von Willebrand factor (VWF),Cell surface glycoprotein (CD44), Cadherin 5 (CDH5), Intracellular adhesion molecule1 (ICAM1), Vascular cell adhesion molecule 1 (VCAM1), Connective tissue growth factor (CTGF), Endoglin (ENG), Integrin subunit alpha 2 (ITGα2), Integrin subunit alpha 5 (ITGα5), Integrin subunit alpha X (ITGαX), Laminin subunit alpha 1(LAMA1), Selectin E (SELE), Selectin L (SELL), Selectin P glycoprotein (SELPG), Thrombospondin 4 (THBS4), ATB-binding cassette transporter A1(ABCA1), Apolipoprotein A1 (APOA1), Apolipoprotein B (APOB), Fatty acid binding protein 3 (FABP3), Low density lipoprotein receptor (LDLR), Lipoprotein lipase (LPL), Lysophospholipase (LYPLα1), Macrophages scavenger receptor1 (MSR1), Nuclear receptor subfamily 1 group H member 3 (NR1H3), Perilipin 2 (PLIN2), Peroxisome proliferator activated receptor alpha (PPAR α), Peroxisome proliferator activated receptor delta (PPARD), Retinoid X receptor alpha (RXRα), Colony stimulating factor 2 (CSF2), Elastin (ELN), Fibroblast growth factor (FGF2), Heparin binding EGF like growth factor (HBEGF), Interleukin 3 (IL3), Interleukin 5 (IL5), Kinase insert domain receptor (KDR), Interleukin 6 family cytokine (LIF), Platelet derived growth factor subunit A (PDGFA), Platelet derived growth factor subunit B (PDGFB), Platelet derived growth factor receptor subunit A (PDGFRβ), Transforming growth factor beta2 (TGFβ2), Kruppel like factor 2 (KLF2), Angiotensin I converting enzyme (ACE),

CASP8 & FADD like apoptosis regulator (CFLAR), Collagen type III alpha 1 chain (COL3α1), Fibrinogen alpha chain (FGα), Fibrinogen beta chain (FGβ), Interleukin 1 receptor 1 (IL1R1), Interleukin 1 receptor 2 (IL1R2), Matrix metallopeptidase 1 (MMP1α), Matrix metallopeptidase 2 (MMP3), Serpin family beta member 2 (SERPINβ2), Serpin family E member 1(SERPINE1), Tenascin C (TNC). ↓ = Down regulation of gene expression , ↑ = Up regulation of gene expression ,*P ≤ 0.05, **P ≤ 0.01, ***P ≤ 0.001, NA= Not available.

Table 3.2 Gene expression levels in BMDM from STAT1^{S727A} mice.

			Control	STAT1^{S727A}		
#	**GENE**	**N**	**Mean ± SEM**	**Mean ± SEM**	**Change (%)**	***p*-value**
			Stress response			
1	**APOE**	4	1 ± 0.008	0.87 ± 0.68	13 ↓	0.86
2	**BAX**	6	1 ± 0.265	0.54 ± 0.22	46 ↓	0.09
3	**BCL2L1**	5	1 ± 0.195	0.30 ± 0.13	70 ↓	0.01 (**)
4	**CCL2**	4	1 ± 0.226	0.09 ± 0.08	91 ↓	0.002 (**)
5	**CCL5**	5	1 ± 0.072	0.86 ± 0.69	14 ↓	0.85
6	**CCR1**	4	1 ± 0.042	0.13 ± 0.13	87 ↓	0.01 (**)
7	**CCR2**	4	1 ± 0.000	0.01 ± 0.01	99 ↓	<0.001 (***)
8	**CXCL1**	3	1 ± 0.255	0.01 ± 0.00	99 ↓	<0.001(***)
9	**FN1**	5	1 ± 0.011	0.71 ± 0.48	29 ↓	0.57
10	**IFNγ**	4	1 ± 0.058	0.09 ± 0.09	91 ↓	0.01 (**)
11	**1L1α**	4	1 ± 0.148	0.01 ± 0.01	99 ↓	<0.001 (***)
12	**IL1β**	5	1 ± 0.019	0.21 ± 0.12	79 ↓	0.01 (**)
13	**IL2**	5	1 ± 0.016	0.35 ± 0.24	65 ↓	0.06
14	**IL4**	5	1 ± 0.039	0.47 ± 0.46	53 ↓	0.32
15	**ITGβ2**	6	1 ± 1.108	0.73 ± 0.46	27 ↓	0.59
16	**PPARγ**	5	1 ± 2.014	0.95 ± 0.77	5 ↓	0.95
17	**SELP**	4	1 ± 0.035	0.40 ± 0.27	60 ↓	0.11
18	**SOD1**	6	1 ± 0.420	0.52 ± 0.33	48 ↓	0.21
19	**SPP1**	4	1 ± 0.023	1.56 ± 0.84	54 ↑	0.55
20	**TGFβ1**	6	1 ± 0.025	0.37 ± 0.18	63 ↓	0.02 (*)
21	**TNF**	5	1 ± 0.156	0.25 ± 0.16	75 ↓	0.01 (**)
			Apoptosis			
22	**BCL2**	3	1 ± 0.025	0.00 ± 0.00	100 ↓	<0.001 (***)
23	**BCL2 A1A**	3	1 ± 0.254	0.01 ± 0.01	99 ↓	<0.001 (***)
24	**BID**	5	1 ± 1.290	0.50 ± 0.30	50 ↓	0.17
25	**BIRC3**	3	1 ± 0.097	0.31 ± 0.31	69 ↓	0.11
26	**FAS**	5	1 ± 0.111	0.19 ± 0.13	81 ↓	<0.001 (***)
27	**NFKβ1**	5	1 ± 0.213	0.48 ± 0.20	52 ↓	0.06
28	**TNFαIP3**	5	1 ± 0.410	0.26 ± 0.26	74 ↓	0.04 (*)
29	**VEGFα**	6	1 ± 0.003	0.40 ± 0.23	60 ↓	0.05 (*)
			Blood coagulation			
30	**NPY**	4	1 ± 0.213	0.41 ± 0.34	51 ↓	0.18
31	**PTGS1**	4	1 ± 0.252	0.09 ± 0.06	91 ↓	<0.001 (***)
32	**VWF**	3	1 ± 0.036	0.00 ± 0.00	100 ↓	<0.001 (***)

Cell adhesion molecules						
33	**CDH5**	3	1 ± 0.021	0.02 ± 0.02	98 ↓	0.01 (*)
34	**CD44**	6	1 ± 0.739	0.42 ± 0.25	58 ↓	0.07
35	**CTGF**	6	1 ± 0.119	0.10 ± 0.05	90 ↓	<0.001 (***)
36	**ENG**	5	1 ± 0.077	0.53 ± 0.35	47 ↓	0.24
37	**ICAM1**	4	1 ± 0.090	0.42 ± 0.29	58 ↓	0.14
38	**ITGα2**	5	1 ± 0.077	0.32 ± 0.26	68 ↓	0.06
39	**ITGα5**	6	1 ± 0.244	0.41 ± 0.17	59 ↓	0.02 (*)
40	**ITGαX**	5	1 ± 0.890	0.24 ± 0.14	76 ↓	0.01 (**)
41	**LAMA1**	4	1 ± 0.051	0.18 ± 0.18	82 ↓	0.02 (*)
42	**SELE**	4	1 ± 0.038	2.19 ± 2.13	119 ↑	0.61
43	**SELL**	5	1 ± 0.001	0.05 ± 0.05	95 ↓	<0.001 (***)
44	**SELPG**	6	1 ± 6.754	0.29 ± 0.13	71 ↓	<0.001 (***)
45	**THBS4**	5	1 ± 0.012	0.01 ± 0.00	99 ↓	<0.001 (***)
46	**VCAM1**	4	1 ± 0.133	0.00 ± 0.00	100 ↓	<0.001 (***)
Lipid transport and metabolism						
47	**ABCA1**	6	1 ± 0.367	0.45 ± 0.17	55 ↓	0.02 (*)
48	**APOA1**	4	1 ± 0.039	0.06 ± 0.05	94 ↓	<0.001 (***)
49	**APOB**	5	1 ± 0.046	0.41 ± 0.30	59 ↓	0.12
50	**FABP3**	5	1 ± 0.278	0.71 ± 0.56	29 ↓	0.63
51	**LDLR**	6	1 ± 0.136	0.62 ± 0.31	38 ↓	0.28
52	**LPL**	6	1 ± 0.486	0.51 ± 0.24	49 ↓	0.09
53	**LYPLα1**	6	1 ± 0.113	0.28 ± 0.13	72 ↓	0.003 (**)
54	**MSR1**	6	1 ± 0.322	1.13 ± 0.45	13 ↓	0.78
55	**NR1H3**	5	1 ± 0.111	0.32 ± 0.18	68 ↓	0.02 (*)
56	**PLIN2**	5	1 ± 0.535	0.26 ± 0.13	74 ↓	0.004 (**)
57	**PPAR α**	5	1 ± 0.026	0.17 ± 0.14	83 ↓	0.004 (**)
58	**PPARδ**	5	1 ± 0.472	0.11 ± 0.08	89 ↓	<0.001 (***)
59	**RXRα**	6	1 ± 1.853	0.41 ± 0.24	69 ↓	0.053
Cell growth and proliferation						
60	**CSF2**	5	1 ± 0.018	0.01 ± 0.00	99 ↓	<0.001 (***)
61	**ELN**	5	1 ± 0.047	0.39 ± 0.31	61 ↓	0.12
62	**FGF2**	4	1 ± 0.046	0.14 ± 0.14	86 ↓	0.01 (**)
63	**HBEGF**	5	1 ± 0.062	0.28 ± 0.17	72 ↓	0.01 (*)
64	**IL3**	5	1 ± 0.040	0.36 ± 0.22	64 ↓	0.04 (*)
65	**IL5**	4	1 ± 0.4548	0.03 ± 0.02	97 ↓	<0.001 (***)
66	**KDR**	5	1 ± 0.205	0.46 ± 0.35	54 ↓	0.20
67	**LIF**	4	1 ± 0.020	0.10 ± 0.10	90 ↓	0.002 (**)

68	**PDGFA**	5	1 ± 0.354	0.13 ± 0.09	87 ↓	0.001 (***)
69	**PDGFB**	5	1 ± 0.149	0.27 ± 0.13	73 ↓	0.001 (**)
70	**PDGFRβ**	6	1 ± 0.163	0.20 ± 0.15	80 ↓	0.01 (**)
71	**TGFβ2**	5	1 ± 0.157	0.10 ± 0.10	90 ↓	0.001 (***)
			Transcriptional regulation			
72	**KLF2**	6	1 ± 0.000	0.00 ± 0.00	00	NA
			Extracellular matrix (ECM)			
73	**ACE**	4	1 ± 0.002	0.00 ± 0.00	100 ↓	<0.001 (***)
74	**CFLAR**	6	1 ± 0.029	0.97 ± 0.67	3 ↓	0.97
75	**COL3α1**	1	1 ± 0.008	0.00 ± 0.00	100 ↓	<0.001 (***)
76	**FGα**	5	1 ± 0.017	0.14 ± 0.08	86 ↓	<0.001 (***)
77	**FGβ**	5	1 ± 0.025	0.08 ± 0.07	92 ↓	0.01 (**)
78	**IL1R1**	4	1 ± 0.077	0.33 ± 0.23	77 ↓	0.06
79	**IL1R2**	5	1 ± 0.087	0.23 ± 0.18	77 ↓	0.01 (*)
80	**MMP1α**	6	1 ± 6.998	0.44 ± 0.20	56 ↓	0.03 (*)
81	**MMP3**	5	1 ± 0.044	0.38 ± 0.23	62 ↓	0.06
82	**SERPIN β2**	5	1 ± 0.010	0.71 ± 0.58	29 ↓	0.64
83	**SERPINE1**	5	1 ± 0.010	0.48 ± 0.34	52 ↓	0.20
84	**TNC**	4	1 ± 0.168	0.06 ± 0.06	94 ↓	<0.001 (***)
			HKGs			
1	**ACTB**	6	1.00 ± 0.05	0.99 ± 0.00	1 ↓	0.49
2	**B2M**	3	1.00 ± 0.04	0.97 ± 0.01	3 ↓	0.32
3	**GAPDH**	6	1.00 ± 0.03	0.8 ± 0.02	20 ↓	0.06
4	**GUSB**	6	1.00 ± 0.02	0.82 ±0.01	18 ↓	0.16
5	**HSP90AB1**	6	1.00 ± 0.03	0.09 ± 0.02	10↓	0.07

See table 3.2 for list of abbreviations; ↓ = Down regulation of gene expression, ↑ = Up regulation of gene expression, *P ≤ 0.05, **P ≤ 0.01, ***P ≤ 0.001, NA = Not available.

Overall, the expression of 20 genes was affected in BMDM from ERK1$^{-/-}$ mice and 50 genes using cells from STAT1 ^{S727A} mice compared to the wild type control (Table 3.1-3.2). The common reduced expressions of 18 genes were observed with BMDM from ERK1$^{-/-}$ and STAT1^{S7S7A} mice compared to the wild type counterpart. Table 3.3 lists those genes according to their function in atherosclerosis.

Table 3.3 Common genes whose expression was significantly altered by deficiency of ERK1 and STAT1 S727 phosphorylation when compared to wild type control mice.

Stress response
CXCL-1
IFN-γ
IL-4
Apoptosis
VEGF-α
Blood coagulation
NPY
Cell adhesion molecules
CDH5
ITG-α2
LAMA-1
SELPG
Lipid transport and metabolism
APOA-1
PPAR-α
Cell growth and proliferation
CSF-2
HBEGF
IL-3
IL-5
Transcriptional regulation
KLF-2
Extracellular matrix
ACE
FG-β

In addition to the use of tables, another common method of visualising gene expression data was employed. “Genesis software” was used to generate a heat map

with combination of clustering methods (hierarchical clustering), which group genes together based on the similarity of their gene expression pattern. The relationships among genes are represented by a tree whose branch lengths reflect the degree of similarity between the genes (Eisen *et al.*, 1998). Hierarchical clustering is useful for identifying genes that are commonly regulated, or biological signatures associated with a particular condition (Eisen *et al.*, 1998).

In the heat maps, data are presented as log2 and displayed in a grid where each row represents a gene and each column represents a sample (ERK1$^{-/-}$ and STAT1 S727A). The colour and intensity of the boxes of the heat map is used to represent changes of gene expression, where red represents up-regulated genes and green represents down-regulated genes. Black represents unchanged expression. The expressions of some genes were undetectable and are shown by grey boxes.

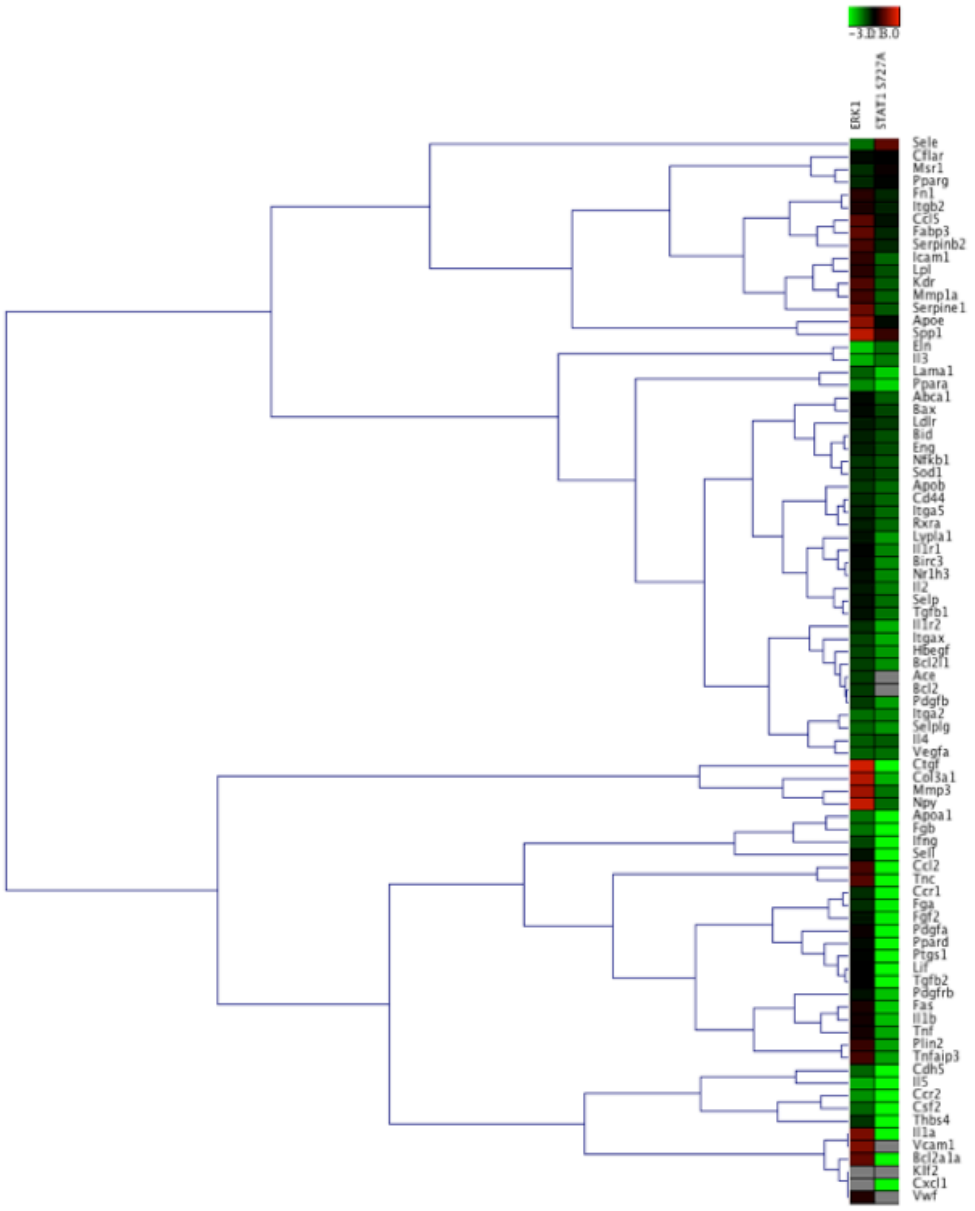

Figure 3.5 Heat map representing colour-coded expression levels of differentially expressed genes.

Heat map of hierarchical clustering of gene transcript levels of 84 genes were assessed in BMDM from ERK1$^{-/-}$ and STAT1^{S727A} mice. The heat maps present the log2 fold change in the expression in BMDM from genetically modified mice after normalisation with the C57BL/6J control that was arbitrary assigned as 1. Genesis software was used to assess gene expression signals and clustering. A scale of colour changes presenting the intensity of gene expression are presented on top of the figure. All genes present in the Qiagen RT^2 profiler PCR Array were plotted.

3.2.5 Genetic modifications attenuate MCP-1 driven migration of BMDM

Cell migration during atherosclerosis is a key mechanism in lesion formation (Charo and Taubman, 2004). MCP-1 is a key chemokine in atherosclerosis and was used to stimulate cellular migration (Wain et al. 2002). As shown in Figure 3.6 A-B, the inclusion of 20 ng/ml MCP-1 significantly induced the migration of BMDM from C57BL/6J control mice, ERK$^{-/-}$ mice and STAT1^{S727A} mice (p=0.004, p=0.05 and p<0.001 respectively). The MCP-1-driven migration was significantly lower in BMDM from ERK1$^{-/-}$ mice (p=0.006) and STAT1^{S727A} mice (p=0.03) when compared to the C57BL/6J mice.

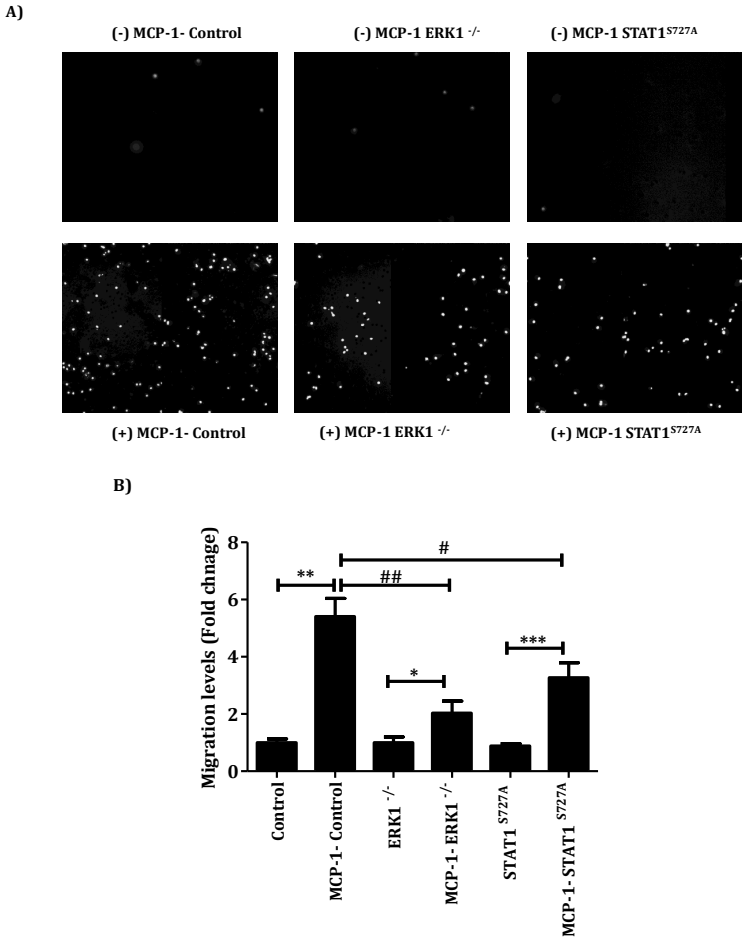

Figure 3.6 The effect of genetic modifications on MCP-1 driven migration of BMDM *in vitro*.

BMDM from C57BL/6J mice (Control), ERK1$^{-/-}$ and STAT1^{S727A} mice were cultured overnight in trans-wells with migration inserts in the absence or presence of 20 ng/ml MCP-1 to stimulate cellular migration as described in Section 2.6.2. The migration of the cells was assessed by counting the migrated cells using fluorescence microscope after staining them with the nuclear stain DAPI. Representative images of membranes are shown in panel A. Graphs display mean ± SEM from four independent experiments performed in triplicate for each condition (B), where the values from each control have been arbitrary assigned as 1. Statistical analysis was carried out using One-way ANOVA with Tukey's post-hoc analysis for each condition [* $P \leq 0.05$, ** $P \leq 0.01$ *** $P \leq 0.001$ compared to control (no MCP-1) in each case; # $P \leq 0.05$, ## $P \leq 0.01$ compared to MCP-1 treated cells].

3.2.6 The effect of the genetic modifications on ROS production in BMDM *in vitro*.

ROS plays an important role in the pathology of atherosclerosis by modifying LDL, which can then be taken up by macrophages via SRs (Moore and Freeman, 2006). The effect of the genetic modifications on ROS production in response to stimulation of BMDM with TBHP was therefore determined. As shown in Figure 3.7, TBHP significantly induced ROS production by 100% in BMDM from C57BL/6J control mice (p<0.001) and by about 80% (p=0.01) in cells from both ERK1$^{-/-}$ and STAT1^{S727A} mice. The genetic modifications had no significant effect on TBHP-induced ROS production when compared to BMDM from control mice.

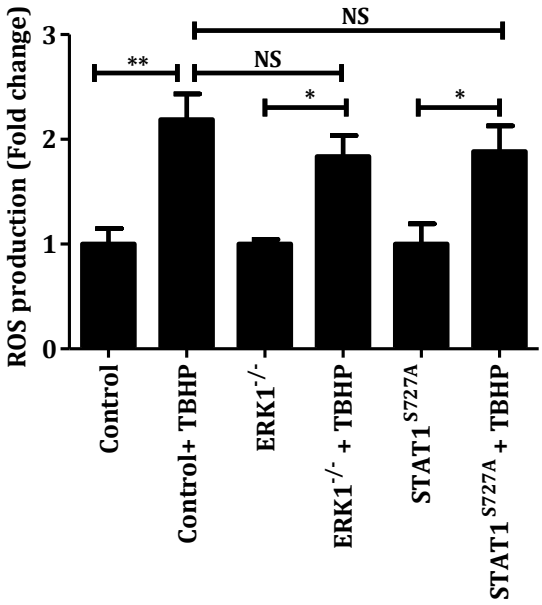

Figure 3.7 Genetic modifications have no effect on ROS production *in vitro*.

Ros production was assessed in BMDM from C57BL/6J (Control), ERK1$^{-/-}$ and STAT1^{S727A} mice that were either treated with vehicle (water) or TBHP (50 µM) to initiate ROS production as described in Section 2.6.3. Fluorescence was measured after 3 hours incubation using fluorescence plate reader at a wavelength 490 nm and 520 nm for excitation and emission spectra respectively. Graph displays mean ± SEM from three independent experiments performed in triplicate for each condition where the values from each control have been arbitrary assigned as 1. Statistical analysis was carried out using One-way ANOVA with Tukey's post-hoc analysis (*p≤ 0.05, **p≤ 0.01 when compared to non-treated control in each case, and NS=not significant when compared to TBHP control).

3.2.7 The effect of the genetic modifications on LY uptake by macropinocytosis *in vitro*

In addition to the receptor-mediated uptake by SRs, macrophages have been shown to take up large amounts of native LDL and oxLDL by bulk fluid phase macropinocytosis (Kruth *et al.*, 2005). The endocytic pathway has also been implicated to play an important role in foam cell formation (Yao *et al.*, 2009). The effect of the genetic modifications on macropinocytosis, as judged by the uptake of widely used LY dye (Kruth *et al.*, 2005), was therefore determined. As shown in Figure 3.8, there were no significant changes in the uptake levels of LY with BMDM from ERK1$^{-/-}$ and STAT1^{S727A} mice when compared to those from control mice.

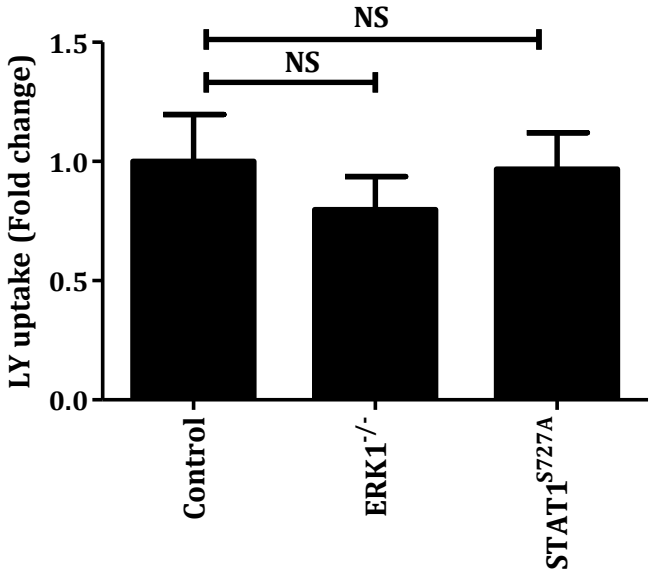

Figure 3.8 Genetic modifications have no significant effect on macropinocytosis in BMDM.

BMDM from C57BL/6J (Control), ERK1$^{-/-}$ and STAT1^{S727A} mice were cultured overnight in the presence of 100 µg/ml LY as described in Section 2.7.1. Macropinocytosis levels were assessed by measuring LY uptake using BD FACS Canto flow cytometer with at least 5,000 counts for each sample. Cells incubated without LY were also included to determine background fluorescence intensity. Graphs display mean ± SEM from three independent experiments performed in triplicate for each condition after subtracting the background. The value in BMDM from control mice has been arbitrarily assigned as 1 with normalisation of the remaining data to this. Statistical analysis was carried out using One-way ANOVA with Dunnett post-hoc analysis (NS =not significant).

3.2.8 The effect of the genetic modifications on oxLDL uptake by BMDM *in vitro*.

To determine the effect of the genetic modifications on oxLDL uptake, oxLDL labelled with a fluorescent dye (Dil-oxLDL) was incubated for 24 hours with BMDM cultures from C57BL/6J control, ERK1$^{-/-}$ and STAT1^{S727A} mice. Upon 24 hours treatment with Dil-oxLDL, the uptake levels were measured using a BD FACS Canto flow cytometer. As shown in Figure 3.9, a significant 100% induction in uptake (p<0.001) was observed with cells from ERK1$^{-/-}$ mice when compared with the control. On the other hand, there was no significant change detected with STAT1^{S727A} modification when compared to the control.

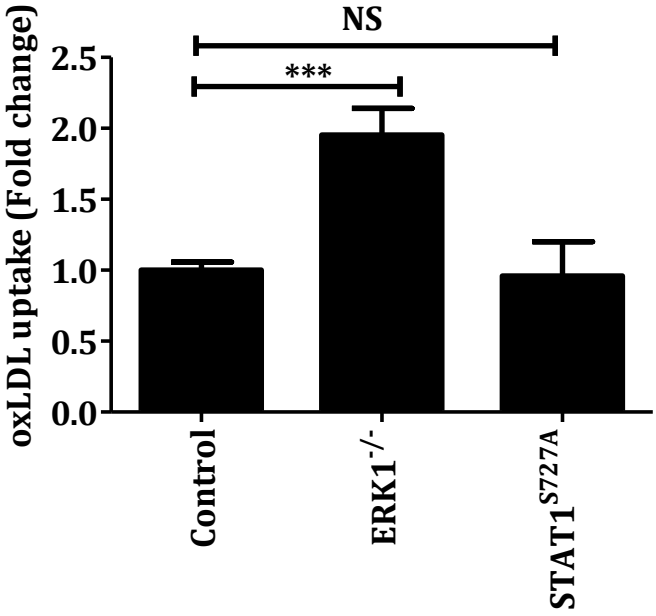

Figure 3.9 The effect of the genetic modifications on oxLDL uptake by BMDM *in vitro*.

BMDM from C57BL/6J (Control), ERK1$^{-/-}$ and STAT1^{S727A} mice were treated with 0.5 μg/ml Dil-oxLDL as described in Section 2.7.2. The uptake of Dil-oxLDL was assessed after 24 hours incubation using a BD FACS Canto flow cytometer with at least 5,000 counts measured for each sample. Cells incubated in the absence of Dil-oxLDL were also included for the determination of background fluorescence intensity. Graph displays mean ± SEM from four independent experiments performed in triplicate for each condition after subtracting the background. The value of Dil-oxLDL uptake with BMDM from control mice has been arbitrary assigned as 1 with the remaining data represented to this. Statistical analysis was carried out using One-way ANOVA with Dunnett post-hoc analysis (*** $P \leq 0.001$, NS = not significant).

3.2.9 The effect of the genetic modifications on cholesterol efflux from foam cells *in vitro*.

Cholesterol efflux plays a major role in limiting atherogenesis and enhancing this may provide new therapeutic approach for CVD (Phillips, 2014). Evaluation of serum cholesterol efflux capacity is a predictor of the extent of atherosclerosis (Klucken *et al.*, 2000). Figure 3.10 show that the genetic modifications had no significant effect on cholesterol efflux when compared to BMDM from control mice.

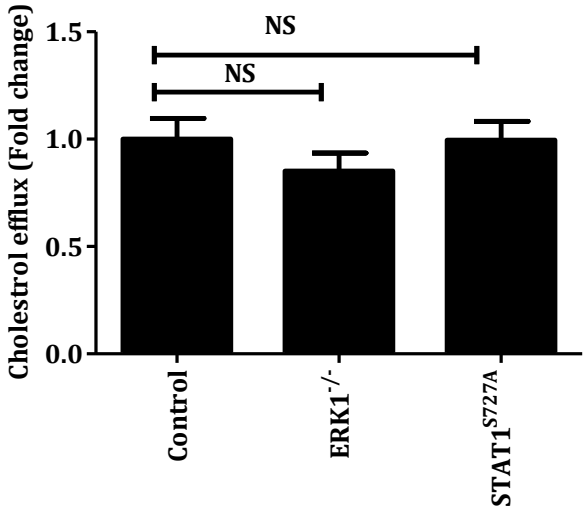

Figure 3.10 Genetic modifications have no effect on cholesterol efflux by BMDM.

BMDM from C57BL/6J (Control), ERK1$^{-/-}$ and STAT1^{S727A} mice were converted into foam cells by incubation with 0.5 µCi/ml [4-^{14}C] cholesterol and 25 µg/ml acLDL for 24 hours prior to a further 24-hour treatment with ApoA1 (10 µg/ml) as described in Section 2.7.3. The level of efflux was assessed using a liquid scintillation counter (TriCarbi 2800TR). Radioactivity was determined by the number of disintegrations per minute (d.p.m) within the samples. Cholesterol efflux was calculated as the fold change between radioactivity in the media versus total radioactivity (cells and supernatant). The cholesterol efflux in control cells was arbitrary assigned as 1 with the remaining data normalised to this. Graph displays mean ± SEM from four independent experiments performed in triplicate for each condition. Statistical analysis was performed using a One-way ANOVA with Dunnett post-hoc analysis (NS= not significant).

3.2.10 The effect of genetic modifications on phagocytosis by BMDM *in vitro.*

Macrophages are phagocytic cells and have an important role in the scavenging of modified LP, unwanted or dead cells and cellular debris via phagocytosis, all of which play a crucial role in plaque destabilisation and rupture (Schrijvers *et al.*, 2007). The levels of phagocytosis of BMDM from C57BL/6J control, ERK1$^{-/-}$ and STAT1^{S727A} mice were therefore determined. Data presented in Figure 3.11 shows that there were no significant changes in phagocytosis with cells from ERK1$^{-/-}$ mice when compared to the control. In contrast, there was a significant 200% induction (p=0.004) in the phagocytosis levels of BMDM from STAT1^{S727A} mice when compared to the control.

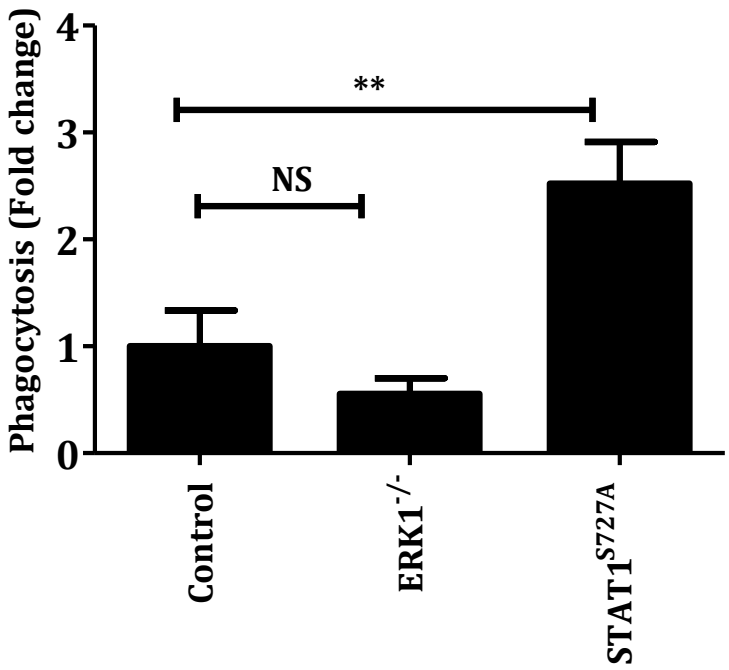

Figure 3.11 The effect of the genetic modifications on phagocytosis by BMDM *in vitro.*

BMDM from C57BL/6J (Control), ERK1$^{-/-}$ and STAT1^{S727A} mice were pre-incubated with fluorescent bio-particle suspension for 2 hours followed by 5-minute incubation with trypan blue as described in Section 2.7.4. Excess trypan blue was aspirated and fluorescence was determined using fluorescence plate reader with 490 nm excitation and 520 nm emissions. Background wells were also included to determine background fluorescence intensity. Graph displays mean ± SEM from four independent experiments performed in triplicate for each condition after subtracting the background. The value from control cells has been arbitrary assigned as 1 with the remaining data normalised to this. Statistical analysis was carried out using One-way ANOVA with Dunnett post-hoc analysis (** $P \leq 0.01$; NS, not significant).

3.3 Discussion:

Previous studies showed that ERKs regulate gene expression through STAT1 Ser727 phosphorylation (Li *et al.*, 2010). It was found that the most extensive inhibition of STAT1 Ser727 phosphorylation was observed following inhibition of ERKs and these findings were extended by analysis of ERK activity and the effect on the expression of IFN-γ inducible genes (Li *et al.*, 2010). *In vitro* studies using BMDM presented here have advanced our understanding of the roles of ERK1 and STAT1 Ser727 phosphorylation on cellular processes associated with atherosclerosis. Table 3.4 Summaries all the processes that were analysed.

Table 3.4 Summary of the effect of the genetic modifications on various cellular processes implicated in atherosclerosis.

Cellular processes	**ERK1$^{-/-}$**		**STAT1^{S727A}**	
	Effect	***P*-value**	**Effect**	***P*-value**
ROS production	NC	NS	NC	NS
Cellular migration	↓	0.006 (**)	↓	0.03 (*)
Macropinocytosis	NC	NS	NC	NS
Cholesterol efflux	NC	NS	NC	NS
OxLDL uptake	↑	<0.001 (***)	NC	NS
Phagocytosis	NC	NS	↑	0.004 (**)

Abbreviations: NC-No changes in relation to control; NS- no significant effect;↓Down regulation;↑Up regulation.

The results show that the deficiency of ERK1 and STAT1 Ser727 phosphorylation in BMDM had no effect on TBHP-induced ROS production, macropinocytosis and cholesterol efflux from foam cells when compared to cells from control mice (Figures 3.7-3.8 and 3.10). In contrast, both modifications attenuated the MCP-1-drived migration of BMDM when compared to the control (Figure 3.6). The genetic modifications had differential effects on oxLDL uptake and phagocytosis. Thus, BMDM from ERK1$^{-/-}$ mice showed increased oxLDL uptake when compared to control mice (Figure 3.9) whereas BMDM from STAT1 S727A knock-in mice had higher phagocytic activity compared to the control (Figure 3.11). These studies allow for a greater understanding on the role of these two factors in the development of

atherosclerosis.

Deletions or modifications of key genes such as ERK1 affect cellular processes by modulating the expression of downstream genes. In this study, the use of a RT-qPCR array of 84 genes associated with atherosclerosis (Table 3.1) showed that ERK1 was potentially required for the constitutive expression of key genes involved in many cellular processes. Genes whose expression was significantly altered include those that play important roles in blood coagulation and circulation, cell-adhesion, lipid transport and metabolism, stress responses, cellular growth and proliferation and the regulation of ECM production and function. The down regulation of expression of these genes is potentially likely to alter atherosclerotic plaque progression and stability, for example, attenuating cellular migration, pro-inflammatory cytokine production and thrombus formation. Table 3.5 lists the important roles of these genes in the disease that can potentially aid in understanding the changes seen in cellular processes investigated as part of studies presented in this chapter.

Table 3.5 The key functions of genes regulated by ERK1 deficiency in atherosclerosis.

#	Gene	Role in atherosclerosis	References
1	**ACE**	Regulates blood pressure and the balance of fluids and salts in the body. Induces the expression of inflammatory mediators such as cytokines, chemokines and adhesion molecules.	(Pacurari *et al.*, 2014; Zeinali *et al.*, 2015)
2	**FG-β**	Involved in blood clot formation (coagulation), increases blood viscosity, stimulates fibrin formation and increases platelet-platelet interactions.	(Cerit, 2017)
3	**IL-3**	Promotes haematopoietic cell proliferation, survival and differentiation, stimulates adhesion and cell migration, and facilitates leukocyte extravasation. Augments macrophage activation, smooth muscle cell accumulation and neovascularisation in advanced plaques.	(Nishinakamura *et al.*, 1995; Von der Thüsen *et al.*, 2003)

4	**IL-4**	Considered to be potentially anti-atherogenic by suppressing pro-inflammatory cytokine production.	(Huber *et al.*, 2001)
5	**IL-5**	Anti-inflammatory cytokine that induces the differentiation and survival of B-cells and eosinophils.	(Kouro and Takatsu, 2009)
6	**APOA1**	Mediates reverse cholesterol transport.	(Smith, 2010)
7	**PPARα**	Inhibits the expression of inflammatory genes and adhesion molecules.	(Erbel *et al.*, 2011)
8	**CDH5**	Pro-atherogenic and plays a role in leukocyte rolling and adhesion, endothelial cell dysfunction and vascular inflammation.	(Nus *et al.*, 2016)
9	**ITG-α 2**	Adhesion molecule that promotes platelet aggregation and contributes to the development of blood clots.	(Rivera *et al.*, 2009)
10	**LAMA-1**	Involved in cell adhesion, differentiation, migration, signalling and metastasis.	(Sookoian *et al.*, 2011)
11	**SELE**	Responsible for the accumulation of blood leukocytes at sites of inflammation by mediating the adhesion of cells to the vascular wall.	(Elena and Klaus, 2007)
12	**SELPL-γ**	Recruits leukocytes to the endothelium.	(Tregouet *et al.*, 2003)
13	**CSF-2**	Promotes advanced plaque progression by increasing macrophage apoptosis susceptibility.	(Subramanian *et al.,* 2015)
14	**ELN**	Increases arterial stiffness and blood pressure. Stimulates migration and proliferation of monocytes.	(Stoka *et al.*, 2018)
15	**CXCL1**	Chemokine that plays a role in chemoatraction of neutrophils and in leukocyte recruitment.	(Zernecke and Weber, 2010)
16	**IFN-γ**	Involved in the pathogenesis of atherosclerosis. Promotes foam cell formation, plaque development and T_h1-driven adaptive immune responses.	(McLaren and Ramji, 2009)

17	**VEGF-α**	Growth factor active in angiogenesis, vasculogenesis and endothelial cell growth. Induces endothelial cell proliferation, promotes cell migration, inhibits apoptosis and induces permeabilisation of blood vessels.	(Camaré *et al.*, 2017)
18	**KLF-2**	Anti-inflammatory, anti-thrombotic and anti-migratory. Inhibits both the expression of inflammatory cytokines and the production of adhesion molecules that are critical for leukocyte recruitment.	(Parmar *et al.*, 2006)
19	**NPY**	Involved in vascular endothelial cell dysfunction, formation of foam cells, proliferation of vascular smooth muscle cells, local inflammatory responses of plaques and activation and aggregation of platelets.	(Zhu *et al.*, 2016)
20	**HBEGF**	Promotes smooth muscle cell proliferation and macrophage-mediated cellular proliferation and differentiation.	(Vinante and Rigo, 2013)

Deficiency of ERK1 appears to affect only some of the steps in atherosclerosis disease development rather than all of them. *CSF-2, ELN, HBEGF, IL-3, IL-5, LAMA-1, VEGF-α, SELE, SELPL-γ, ACE, CDH-5, ITG-α* and *CXCL-1* are genes involved in the control of cellular proliferation, growth and migration. The expression of these genes was found to be significantly attenuated in BMDM from ERK1$^{-/-}$ mice (Table 3.1) and this might be responsible for the reduction in cellular proliferation and migration observed without any effect on cellular viability (Figures 3.3, 3.4 and 3.6). These findings imply that ERK1 knockout has the potential to reduce atherosclerotic lesion size *in vivo* by reducing their cellular content by inhibiting both proliferation of existing cells and the recruitment of immune cells from elsewhere (e.g. blood).

As mentioned earlier, maintaining plasma cholesterol homeostasis is an important step in the prevention of atherosclerosis (Pennings *et al.*, 2006). Macrophage foam cell formation represents a promising therapeutic target (Ohashi *et al.*, 2005). Previous *in vitro* research provided evidence that pro-inflammatory factors such as IFN-γ, endotoxin, TNF-α and IL-1β can be atherogenic by stimulating oxLDL

uptake and impairing cholesterol efflux and RCT (Ohashi *et al.*, 2005). The use ERK1/2 inhibitors has shown induced expression of "cholesterol efflux" gene ABCA1, which is then associated with increased macrophage cholesterol efflux to ApoA1 and HDL (Zhou *et al.*, 2010). In this study, no significant reduction were seen in the expression of ABCA1 and that of ApoA1, which promotes cholesterol efflux (Table 3.1). Despite this, ERK1 deficiency had no effect on macrophage cholesterol efflux (Figure 3.10). This suggests potential functional redundancy between ERK1 and ERK2 with the latter potentially compensating for ERK1 deficiency. In terms of LDL and oxLDL uptake, processes such as macropinocytosis and phagocytosis were also not affected by ERK1 deficiency (Figure 3.8 and 3.11, respectively), whereas SR-mediated uptake of oxLDL was stimulated (Figure 3.9), despite no significant reduction in the expression of SR-A1, thus suggesting potential involvement of other SRs not present in the arrays on the response. Future investigation on the impact of both ERK1 and ERK2 deficiency on macrophage lipid homeostasis and changes in gene expression should be carried out.

As shown in Table 3.1, knocking-out of ERK1 was found to significantly reduce the expression of *IFN-γ* and this could potentially have a major anti-atherogenic effect as this cytokine is often regarded as a master regulator of the disease (Harvey and Ramji, 2005). In addition to *IFN-γ*, the expression of *IL-3, IL-4* and *IL-5* was inhibited. The role of IL-3 in atherosclerosis has not been investigated in detail whereas both pro-and anti-atherogenic actions have been found for IL-4 in mouse model systems (Lee *et al.*, 2010; Ramji and Davies, 2015). On the other hand, IL-5 is considered anti-atherogenic (Ait-Oufella *et al.*, 2011). It is therefore difficult to conclude whether ERK1 deficiency is pro- or anti-inflammatory though the reduction in migration (Figure 3.6) suggests that the latter is likely to be the case.

Previous research showed that increased levels of phosphorylated ERK1/2 led to an increase in ROS generation (Myhre *et al.*, 2004). In this study, the deficiency of ERK1 had no effect on the ROS production levels (Figure 3.7). The exact reason for such a discrepancy is currently unclear though functional redundancy between ERK1 and ERK2 might have contributed.

The effect of STAT1 S727A modification on the expression of atherosclerosis-associated genes was also carried out (Table 3.2). The expression of 50 genes was significantly attenuated thereby informing on the importance of STAT1 serine phosphorylation in the regulation of expression of key genes implicated in the control of macrophage function during atherosclerosis. Table 3.6 summaries the functions of these genes.

Table 3.6 Function of genes whose expression was significantly altered by the STAT1 S727A modification.

	Gene	Role in atherosclerosis	References
1	**ABCA1**	Stimulates cholesterol efflux and RCT.	(Oram and Heinecke, 2005)
2	**APOA1**	See Table 3.5.	
3	**APOE**	Mediates the binding, internalisation and catabolism of lipoprotein particles.	(Greenow *et al.,*2005)
4	**MSR-1**	Mediates the endocytosis of modified LDL.	(Manning-Tobin *et al.*, 2009)
5	**NR1H3**	Maintains cellular cholesterol homeostasis by regulating the expression of genes involved in RCT as well as hepatic lipogenesis and inflammation.	(Dave and Kaul, 2010)
6	**PPARδ**	Anti-inflammatory mediator that attenuates lesion progression and suppresses chemoattractant signalling by down-regulation of chemokine expression.	(Barish *et al.*, 2008; Ehrenborg and Skogsberg, 2013)
7	**PPARγ**	Modulates the recruitment of leukocytes to endothelial cells, controls the inflammatory response and lipid homeostasis of monocytes/macrophages and regulates inflammatory cytokine production by smooth	(Duval *et al.*, 2002)

		muscle cells.	
8	**RXR-α**	Regulates cholesterol biosynthesis, cell proliferation and immune-responses.	(Rőszer *et al.*, 2013)
9	**ACE**	See Table 3.5.	
11	**CSF-2**	See Table 3.5.	
12	**ELN**	See Table 3.5.	
13	**IL-1α**	Pro-inflammatory cytokine and induces the production of cytokines and chemokines, increases the expression of adhesion molecules on endothelial cells, stimulates the recruitment of inflammatory cells and promotes cell proliferation and release of MMPs.	(Dinarello, 1996; Merhi-Soussi *et al.*, 2005)
14	**IL-1R-α**	Modulates inflammatory responses.	(Arend *et al.*, 1998)
15	**IL-1R-2**	Modulates inflammatory responses.	(Peters *et al.,* 2013)
16	**IL-2**	Pro-atherogenic cytokine that contributes to inflammatory responses and activation of cell proliferation.	(Ramji and Davies, 2015)
17	**IL-3**	See Table 3.5.	
18	**MMP1-α**	Promotes breakdown of ECM.	(Vacek *et al.*, 2015)
19	**MMP3**	Promotes breakdown of ECM.	(Vacek *et al.*, 2015)
20	**LPL**	Regulates lipid metabolism and transport. Responsible for catalysing the hydrolysis of TG transported in the bloodstream by chylomicrons and VLDL.	(Mead and Ramji, 2002)
21	**TNC**	Promotes MMP production and VSMC proliferation. Promotes the development of atherosclerosis.	(Golledge *et al.*, 2011)
22	**BCL-2**	Suppresses apoptosis.	(Thorp *et al.*, 2009)

23	**BCL2L1**	Suppresses apoptosis.	(Gustafsson and Gottlieb, 2007)
24	**BID**	Suppresses apoptosis.	(Gustafsson and Gottlieb, 2007)
26	**CCL-2**	Chemotactic factor that is involved in the recruitment of monocytes into the arterial wall during atherosclerosis.	(Winter *et al.*, 2018)
27	**CXCL-1**	See Table 3.5.	
28	**FAS**	Promotes cell apoptosis.	(Kubo *et al.*, 2015)
29	**FG-α**	See Table 3.5.	
30	**FG-β**	Regulates blood clot formation (coagulation), increases blood viscosity, stimulates fibrin formation and increases platelet-platelet interactions.	(Zhou *et al.*, 2013)
31	**FGF-2**	Regulates cell proliferation, differentiation, survival, adhesion and migration. Modulates processes such as vasculogenesis, angiogenesis and blood vessel remodelling.	(Oulion *et al.*, 2012; Liu *et al.*, 2013)
33	**IFN-γ**	See Table 3.5.	
36	**TNF**	Modulates cell death, survival, differentiation and proliferation. Increases leukocyte adhesion, transendothelial migration and vascular leak, and promotes thrombosis.	(Bradley, 2007)
37	**VEGF-α**	See table 3.5.	
38	**CTGF**	Enhances monocyte migration and plays a role in plaque stabilisation.	(Iwona *et al.*, 2005)
39	**ICAM-1**	Modulates the attachment of leukocytes to the endothelium and subsequent transmigration into	(Frank and Lisanti, 2008)

		peripheral tissues.	
40	**ITG-α2**	See Table 3.5.	
42	**ITG-α5**	Regulates cell surface adhesion and signalling.	(Turner *et al.*, 2015)
43	**ITG-β2**	Regulates cell surface adhesion and signalling.	(Turner *et al.*, 2015)
44	**LAMA-1**	See Table 3.5.	
45	**SELP**	See Table 3.5.	
46	**THBS-4**	Modulates cellular proliferation, migration, adhesion and attachment together with inflammatory responses. Regulates vascular inflammation and adaptive responses.	(Frolova *et al.*, 2012)
47	**VCAM-1**	Plays a role in the development of atherosclerosis. Mediates leukocyte-endothelial cell adhesion and signal transduction.	(Ley and Huo, 2001)
48	**NPY**	See Table 3.5.	
49	**PTGS-1**	Regulates angiogenesis in endothelial cells.	(Lee *et al.*, 2008)
50	**VWF**	Controls adhesion of platelets to the sites of vascular injury. Modulates blood coagulation.	(van Galen *et al.*, 2012)

As shown in Table 3.2, the expression of many pro-inflammatory genes was down regulated, which is then likely to attenuate the inflammatory response and reduce the atherosclerotic events. Such genes include cytokines and their receptors (e.g. *IFN-γ, IL-1α, IL-1R-α and IL-1R-2*), chemokines and their receptors (e.g. *CCL-2, CCR1, CCR2 and CXCL-1*) and adhesion proteins (e.g. *ICAM-1, ITG-α2, ITG-α5, ITG-β2, SELP and VCAM-1*), all of which are likely to have a major impact on vascular inflammation and the recruitment of immune cells (Table 3.6). IFN-γ is potentially a master regulator of atherosclerosis and responsible for modulating the expression of 30% of the macrophage transcriptome (McLaren and Ramji, 2015). Such attenuation

of the expression of the IFN-γ gene is likely to subsequently inhibit the expression of key genes whose expression is induced by this cytokine such as MCP-1, ICAM-1 and MMPs (McLaren and Ramji, 2015), which may ultimately impact the significant reduction in the levels of cell migration shown in Figure 3.6.

Previous studies have shown that STAT1 is required for optimal foam cell formation and atherosclerotic lesion development *in vivo* and *in vitro* (Agrawal *et al.*, 2007). Indeed, the expression of many key genes implicated in the control of lipid transport and metabolism such as *APOA1, ABCA1, APOE, MSR1* and members of the *PPAR* family was down regulated in BMDM from STAT1 S727A mice when compared to the wild type counterpart. Despite this, there were no significant changes in the uptake of oxLDL, macropinocytosis or efflux of cholesterol from foam cells (Figures 3.8-3.10). This suggests that STAT1 serine phosphorylation is not a major regulator of these processes and there is potentially compensation by tyrosine phosphorylated STAT1. On the other hand, phagocytosis was significantly greater in BMDM form STAT1 S727A mice when compared to control mice (Figure 3.11), thereby suggesting a dominant role for serine phosphorylated STAT1 in this process. Phagocytosis is also involved in the uptake of LPs (McLaren *et al.*, 2011) so it is possible that such regulation by serine phosphorylated STAT1 may be responsible for the reduced foam cell formation seen *in vivo* (Agrawal *et al.*, 2007).

This study shows that ERK 1 and STAT1 Ser727 phosphorylation plays a key role in MCP-1 driven migration of macrophages (Figure 3.6). Other processes are either unaffected or only affected by ERK1 deficiency or STAT1 S727A modification (Table 3.4). Migration of immune cells is critical for the resolution of an inflammatory response and continued migration is likely to lead to a state of chronic inflammation seen in atherosclerosis (Louis and Zahradka, 2010). Indeed, many of the key genes whose expression was affected by ERK1 deficiency or STAT1 S727A modification play important roles in cellular migration and immune cell recruitment (Table 3.1-3.2). These findings inform on the importance of the ERK1:STAT1 serine 727 phosphorylation axis in cellular migration and immune cell recruitment associated with inflammation and suggest that they may represent promising therapeutic targets against atherosclerosis.

Most of the current pharmaceutical therapies against atherosclerosis target plasma lipid levels (e.g. statins) and prevent clinical complications such as thrombosis (e.g. aspirin). Statin therapy has been successful in reducing the morbidity and mortality from CVD (Zhou and Liao, 2009). However, statin therapy is associated with substantial residual risk for CVD with typical reduction of cardiovascular events of about 20–30% (Catapano *et al.*, 2014). Statin therapy is also associated with various side effects (Ramkumar *et al.,* 2016). Beyond statins, although there have been some successes (e.g. expensive monoclonal antibodies against PCSK9), many promising pharmaceutical leads have failed at the clinical level (Ladeiras-Lopes et al., 2015). The safety profile of agents taken to limit atherosclerosis is of paramount importance given the long period in the life span of an individual that these have to be taken.

Natural products represent an important source of new bioactive compounds and generally have excellent safety profile (Moss and Ramji, 2016). Nutraceuticals, food products with health benefits beyond their nutritional value, have potential in the prevention and treatment of atherosclerosis but require an in-depth understanding of the mechanisms underlying their actions and large clinical trials (Moss and Ramji, 2016; Moss et al., 2018). There is a strong belief that phenolic compounds modulate different components of inflammatory-associated signalling pathways and by regulating the expression of pro-inflammatory mediators (Costa *et al.*, 2012). However, only a restricted number of studies have addressed the effect of polyphenols on a specific signal transduction pathway (Costa *et al.*, 2012).

Previous unpublished research in the laboratory has shown that the polyphenol HT attenuates several pro-atherogenic cellular processes (e.g. IFN-γ induced gene expression) and stimulates anti-atherogenic processes (e.g. cholesterol efflux). In relation to IFN-γ-induced gene expression, HT attenuated the levels of STAT1 phosphorylated on serine 727 induced by the cytokine without affecting that on tyrosine 701 (Supplementary figure S-1). This suggests a potentially key role for the ERK1:STAT1 serine phosphorylation axis in HT actions. This was investigated in the next chapter using BMDM from C57BL/6J control mice, ERK1$^{-/-}$ mice and STAT1 S727A knock-in mice.

Chapter 4

4.1 Introduction

Several *in vitro* and *in vivo* studies on HT have reported a wide range of protective biological activities, including anti-microbial, anti-hypertensive, anti-glycaemic, anti-platelet aggregation, cardio-protective, anti-oxidant, anti-proliferative and anti-inflammatory (Jemai et al., 2008). Previous unpublished *in vitro* studies in the laboratory on human macrophages showed that HT attenuated several key pro-atherogenic processes (e.g. monocytic migration, oxLDL uptake, inflammasome activation and ROS production) and stimulated cholesterol efflux from foam cells. Such promising findings suggest that it is essential that further in-depth studies be carried out on the anti-atherogenic actions of HT.

In relation to the IFN-γ-induced pro-inflammatory gene expression, HT attenuated the phosphorylation of STAT1 on serine 727 induced by this cytokine without affecting that on tyrosine 701 (Supplementary figure S-1). Since ERK1 plays an important role in the phosphorylation of STAT1 on serine 727 (Li *et al.*, 2010), these data suggest a potential role for the ERK1: STAT1 serine 727 phosphorylation axis in the anti-atherogenic actions of HT. The availability of ERK1 deficient mice and $STAT1^{S727A}$ knock-in mice allows probing of this issue in more detail and hence was investigated. The approaches used to address this are summarised in Figure 4.1.

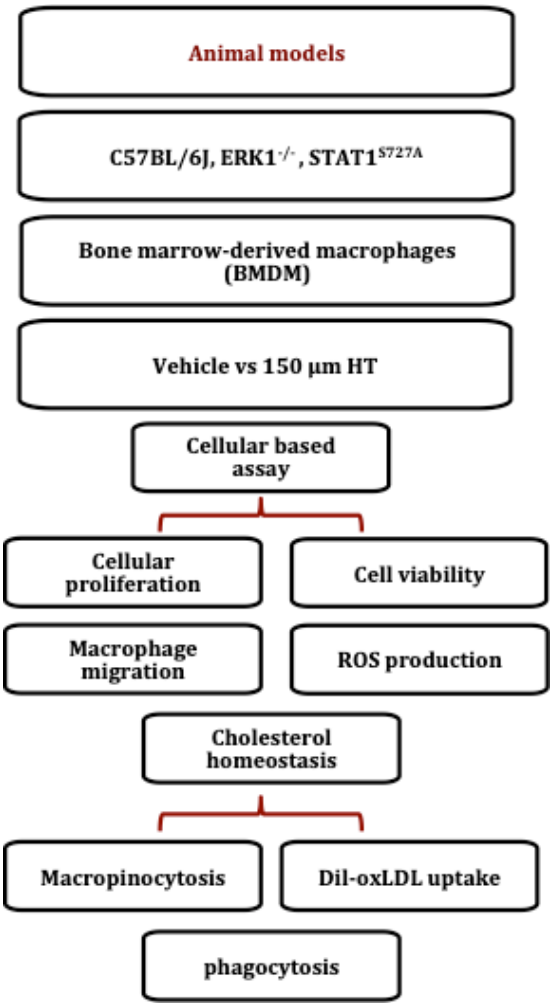

Figure 4.1 Overall summary of the assays used to determine the role of the ERK1: STAT1 S727 phosphorylation axis on the HT-mediated regulation of macrophage processes associated with atherosclerosis.

4.2 Results

4.2.1 HT has no effect on cell viability of BMDM from wild- type or genetically modified mice.

The viability of BMDM from C57BL/6J control, ERK1$^{-/-}$ and STAT1^{S727A} mice was determined by the LDH assay following stimulation of the cells for 24 hours with 150 μM of HT or the vehicle control (water). The concentration of HT used together with the incubation time was based on previous dose response and time course studies in the laboratory on human macrophages. As shown in Figure 4.2, HT had no significant effect on the viability of the cells in all cases when compared to the vehicle control.

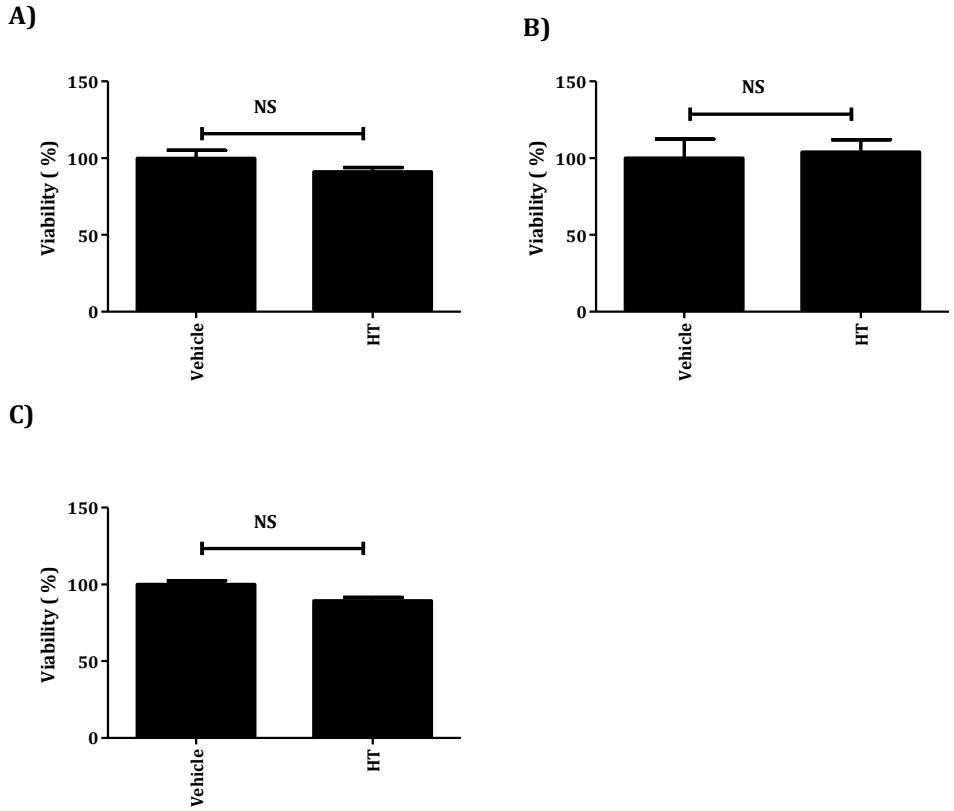

Figure 4.2 HT has no effect on cellular viability of BMDM from wild- type or genetically modified mice.

The release of LDH was used to asses cellular viability in BMDM from C57BL/6J (Control) (A), ERK1$^{-/-}$ (B) and STAT1^{S727A} (C) mice as described in (Section 2.6.1.1) following incubation with vehicle or 150 µM HT for 24 hours. In each case, the value in vehicle treated cells has been arbitrarily assigned as 100% and the treated samples have been normalised to this. Graphs display the mean ± SEM from four independent experiments. Statistical analysis was performed using an unpaired Student's t-test (NS= not significant; HT v/s Vehicle).

4.2.2 The effect of HT on cellular proliferation of BMDM from wild- type and genetically modified mice.

Cellular proliferation of BMDM from C57BL/6J control, ERK1$^{-/-}$ and STAT1^{S727A} mice was determined using the CV assay following stimulation of the cells for 24 hours with 150 µM of HT or the vehicle control (water). As shown in Figure 4.3A and C**,** HT caused a significant 23% reduction in proliferation with BMDM from C57BL6/J control mice (p=0.035) and a 25% decrease in proliferation with cells from STAT1^{S727A} mice (p=0.037) when compared to the vehicle control. In contrast, HT had

no significant effect on the proliferation of BMDM from ERK1$^{-/-}$ mice (Figure 4.3B), thereby indicating a potential requirement for this kinase in HT-mediated changes in the proliferation of macrophages.

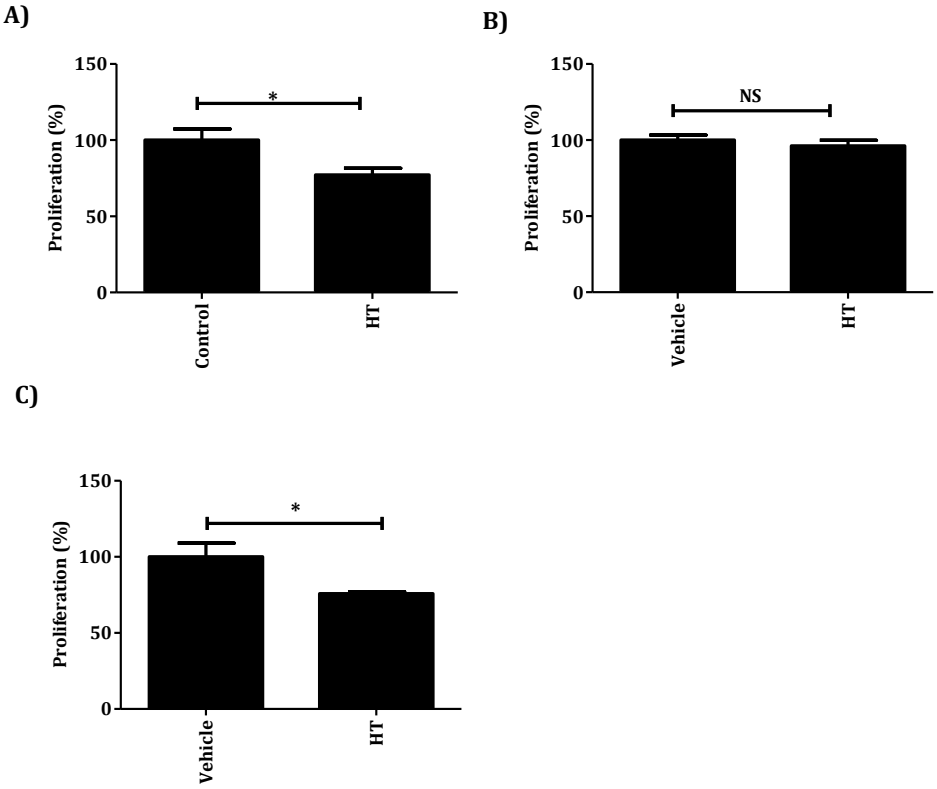

Figure 4.3 The effect of HT on cellular proliferation of BMDM from wild-type or genetically modified mice.

The CV assay was used to assess cell proliferation in BMDM from C57BL/6J (Control) (A), ERK1$^{-/-}$ (B) and STAT1^{S727A} (C) mice as described in (Section 2.6.1.2) following 24 hours incubation with vehicle or 150 μM HT. In each case, the value in vehicle treated cells has been arbitrarily assigned as 100% and treated samples were normalised to this. Graphs display the mean ± SEM from four independent experiments. Statistical analysis was performed using an unpaired Student's t-test (* $P \leq 0.05$; NS=not significant; HT v/s Vehicle).

4.2.3 HT attenuates the MCP-1 driven migration of BMDM from wild-type and genetically modified mice.

Previous studies showed that HT had significant inhibitory effects on EC migration (Fortes *et al.*, 2012). In the light of this finding and those in our laboratory that HT attenuated monocyte migration, the effect of HT on the migration of BMDM

from wild type and genetically modified mice was determined. As shown in Figure 4.4, HT significantly decreased the MCP-1 driven migration by 75% in BMDM from C57BL/6J control mice (p=0.001), by 76% in BMDM from ERK1$^{-/-}$ mice (p=0.006) and by 62% in BMDM from STAT1^{S727A} mice (p=0.002) compared to the vehicle control.

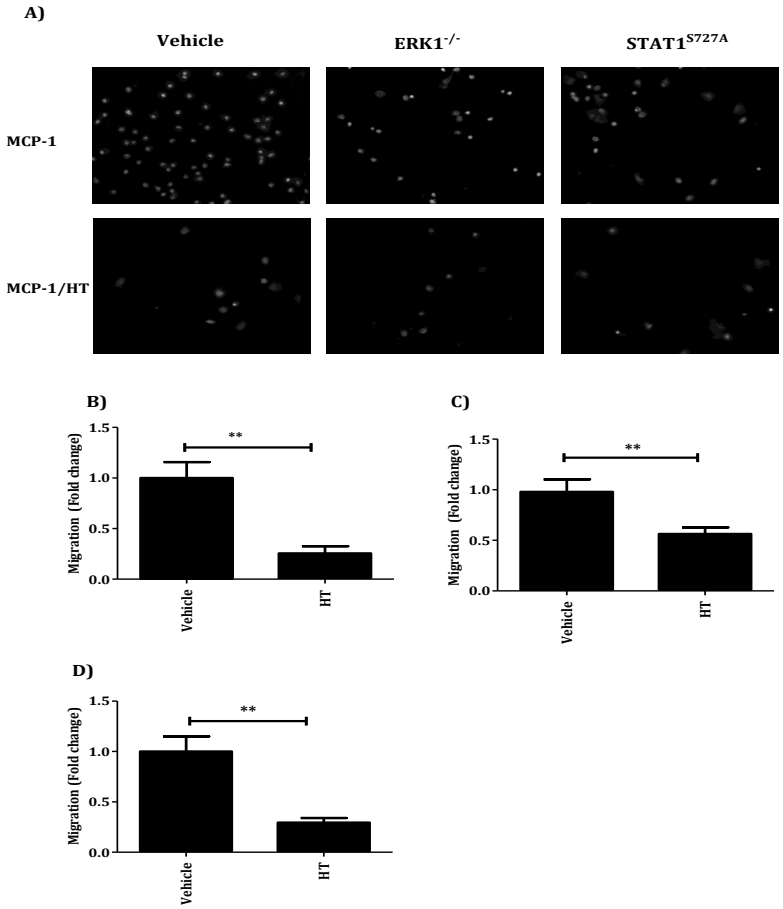

Figure 4.4 The effect of HT on the MCP-1 driven migration of BMDM from wild-type and genetically modified mice.

BMDM from C57BL/6J (Control), ERK1$^{-/-}$ and STAT1^{S727A} mice were cultured overnight in a trans-well migration chamber with vehicle or 150 μM HT. MCP-1 (20 ng/ml) was added to the lower chamber to stimulate cellular migration. Migration of the cells was assessed 24 hours later using a fluorescence microscope after staining of the cells with the nuclear stain DAPI. Representative images are shown in panel A. Graph displays mean ± SEM from four independent experiments performed in triplicate for each condition: C57BL/6J control (B); ERK1$^{-/-}$ (C); and STAT1^{S727A} (D). In each case, the values from the vehicle-treated cells have been arbitrary assigned as 1. Statistical analysis was carried out using an unpaired Student's t-test (**p≤0.01, HT v/s Vehicle).

4.2.4 HT attenuates ROS production in BMDM from wild-type or genetically modified mice

Several studies have demonstrated a potentially protective role for HT and its derivatives in oxidative-related diseases by reducing ROS production through the inhibition of oxidases, reduction in the production of superoxide radicles and inhibiting oxLDL formation (Vilaplana-Pérez *et al.*, 2014; Y.-C. Cheng *et al.*, 2017). In the light of these findings, the effect of HT on TBHP-induced ROS production was determined. As shown in Figure 4.5, HT significantly attenuated TBHP-induced ROS levels in BMDM from C57BL/6J mice by 73% ($p \leq 0.001$), by 64% from ERK1$^{-/-}$ mice ($p=0.006$) and by 75% from STAT1^{S727A} mice ($p=0.002$) when compared to the vehicle control.

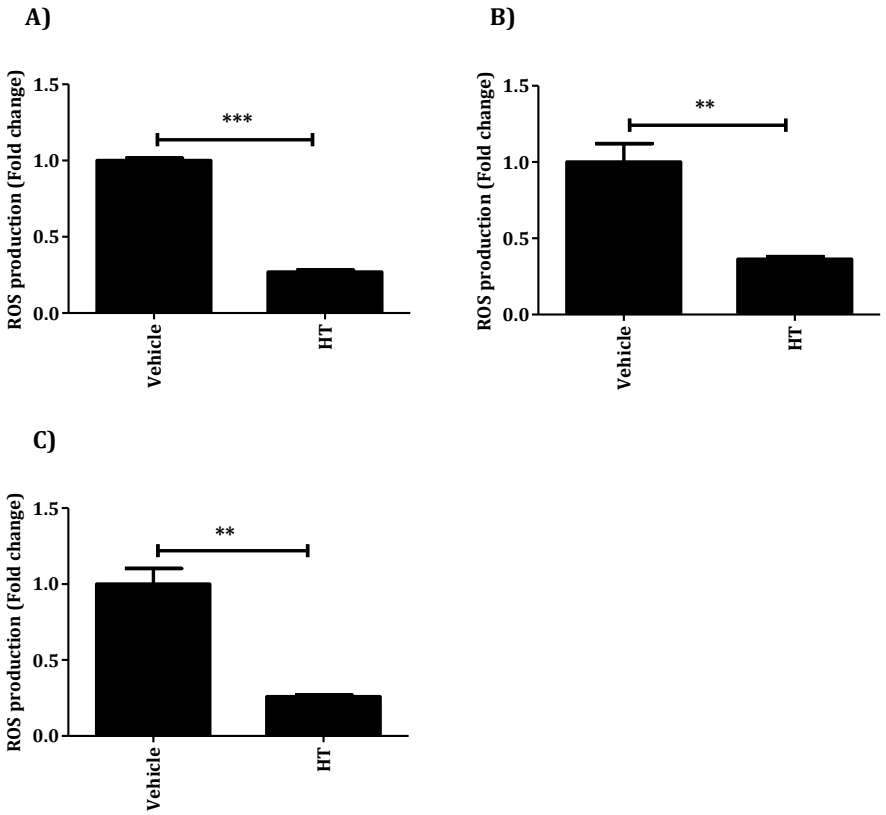

Figure 4.5 The effect of HT on ROS production in BMDM from wild-type and genetically modified mice.

BMDM from C57BL/6J (Control) (A), ERK1$^{-/-}$ (B) and STAT1^{S727A} (C) mice were cultured overnight in the presence of 150 μM HT or vehicle. *In vitro* ROS production was assessed as described in (Section 2.6.3) by measuring fluorescence using fluorescence plate reader at a wavelength of 490 nm and 520 nm for excitation and emission spectra respectively. Graph display mean ± SEM from four independent experiments performed in triplicate for each condition after subtracting the background (cells without DCFDA). In each case, the values in the TBHP vehicle controls have been arbitrary assigned as 1 and treated samples were normalised to this. Statistical analysis was carried out using an unpaired Student t-test (**p≤0.01, ***p≤0.001; HT v/s Vehicle).

4.2.5 The effect of HT on macropinocytosis in BMDM from wild-type and genetically modified mice.

The effect of HT on macropinocytosis was investigated by monitoring the uptake levels of LY in BMDM from C57BL/6J control, ERK1$^{-/-}$ and STAT1^{S727A} mice following incubation with vehicle or 150 μM HT. As shown in Figure 4.6A, the LY

uptake was significantly reduced by 20% (p=0.014) by HT in BMDM from wild- type mice when compared to the vehicle control. For BMDM from ERK1$^{-/-}$ mice, HT caused a significant 40% increase in LY uptake (p=0.035) whereas a non-significant change was seen with BMDM from STAT1^{S727A} mice (Figure 4.6B-C). This suggests a potential requirement for ERK1 and STAT1 serine727 phosphorylation in HT-mediated changes in LY uptake by macrophages.

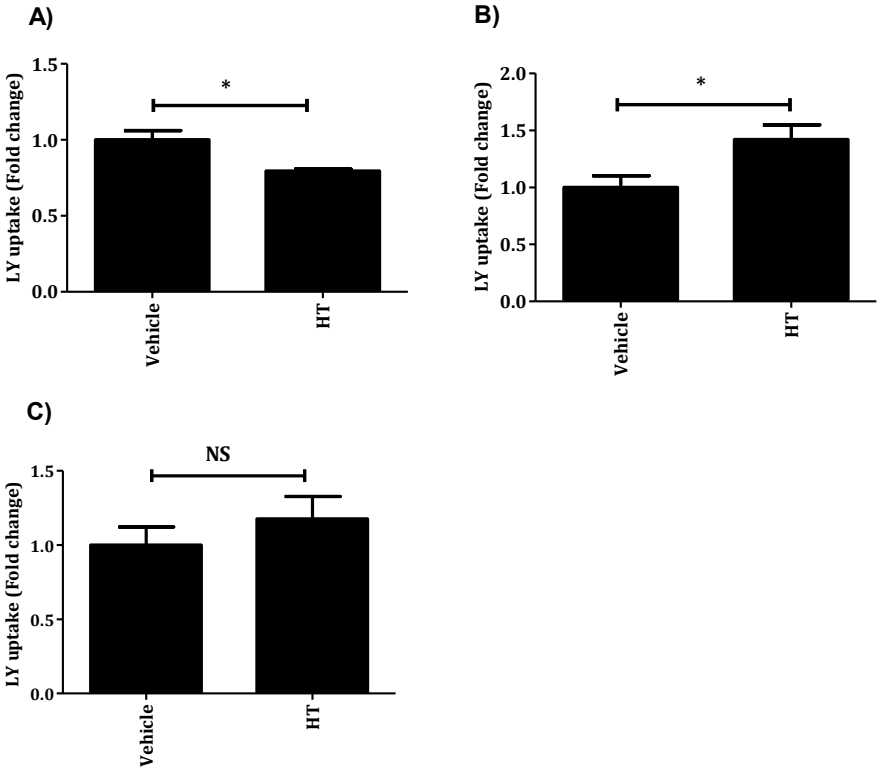

Figure 4.6 The effect of HT on macropinocytosis in BMDM from wild type and genetically modified mice.

BMDM from C57BL/6J control (A), ERK1$^{-/-}$ (B) and STAT1^{S727A} (C) mice were cultured overnight in the presence of 150 µM HT or vehicle. The following day, LY was added to the cells and incubated for another 24 hours. LY uptake levels were assessed as described in (Section 2.7.1) by BD FACS Canto flow cytometer with at least 5,000 counts measured for each sample. Cells incubated without LY were also included to determine background fluorescence intensity. Graph displays mean ± SEM from three independent experiments performed in triplicate for each condition after subtracting the background. In each case, the value in vehicle treated cells has been arbitrary assigned as 1 with treated samples normalised to this. Statistical analysis was carried out using an unpaired Student's t-test (*p≤ 0.05; NS= not significant; HT v/s Vehicle).

4.2.6 HT attenuates oxLDL uptake in BMDM from wild- type and genetically modified mice.

The effect of HT on the uptake of oxLDL was determined in BMDM from C57BL/6J control, ERK1$^{-/-}$ and STAT1^{S727A} mice using labelled oxLDL (Dil-oxLDL) following stimulation of the cells with 150 μM of HT or vehicle. As shown in figure 4.7, HT significantly reduces the uptake of Dil-oxLDL by 95% in BMDM from wild- type control mice, by 88% in those from ERK1$^{-/-}$ mice and by 97% from those of STAT1^{S727A} mice (p<0.001 in all cases) when compared to the vehicle control.

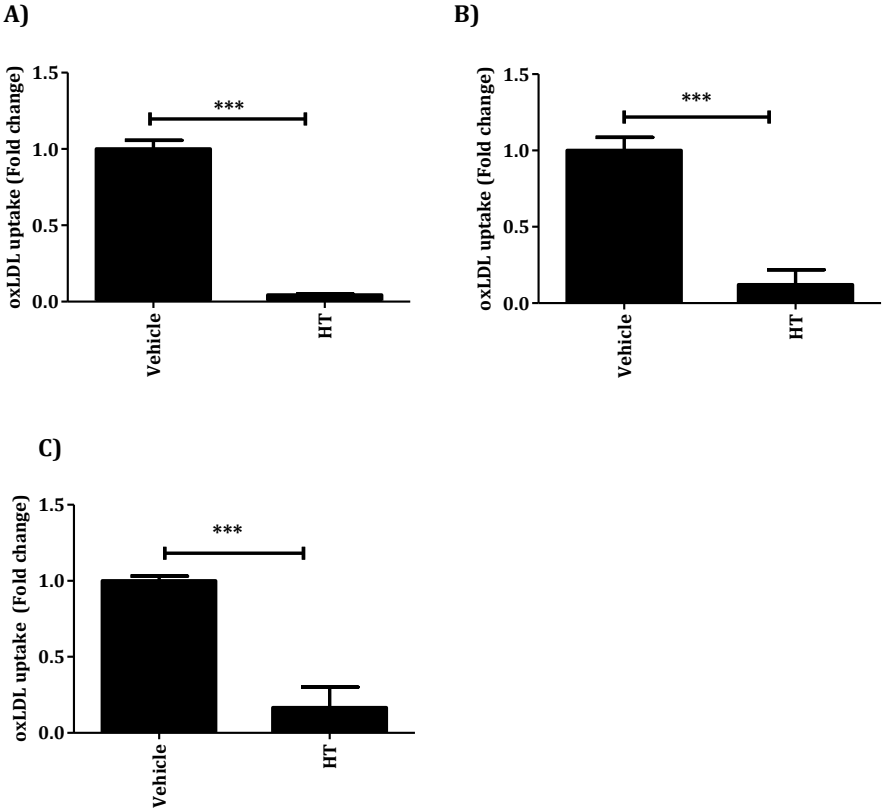

Figure 4.7 HT inhibits oxLDL uptake in BMDM from wild-type and genetically modified mice.

BMDM from C57BL/6J control (A), ERK1$^{-/-}$ (B) and STAT1^{S727A} (C) mice were pre-treated with 150 μM HT or vehicle for 6 hours prior to incubation with 0.5 μg/ml Dil-oxLDL for an additional 18 hours. The uptake of Dil-oxLDL was then assessed by BD FACS Canto flow cytometer with at least 5,000 counts measured for each sample as described in (Section 2.7.2). Cells incubated in the absence of Dil-oxLDL and HT were also included to determine background fluorescence intensity. Graphs display mean ± SEM from three independent experiments performed in triplicate for each condition after subtracting the background. In each case, the values in the vehicle control have been arbitrary assigned as 1 and treated sample were normalised to this. Statistical analysis was carried out using an unpaired Student's t-test (*** $P \leq 0.001$; HT v/s Vehicle).

4.2.7 HT attenuates phagocytosis in BMDM from wild-type and genetically modified mice

The effect of HT on phagocytosis of fluorescently-labelled killed *E. coli* (K-12 strain) cells in BMDM from C57BL/6J control, ERK1$^{-/-}$ and STAT1^{S727A} mice was determined following incubation of the cells with 150 μM HT or vehicle. HT caused a

significant 60% reduction in phagocytosis in BMDM from control mice (p=0.016), by 88% in BMDM from ERK1$^{-/-}$ mice (p=0.005) and by 77% in BMDM from STAT1^{S727A} mice (p=0.002) when compared to the vehicle control.

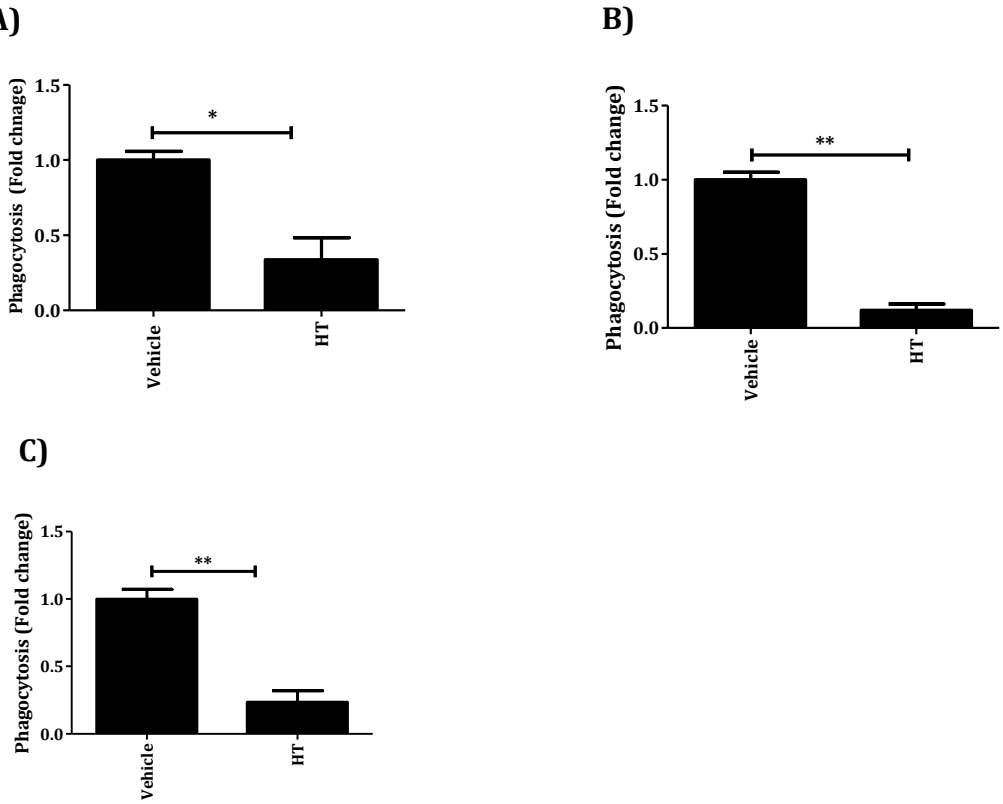

Figure 4.8 HT inhibits phagocytosis in BMDM from wild-type and genetically modified mice.

BMDM from C57BL/6J control (A), ERK1$^{-/-}$ (B) and STAT1^{S727A} (C) mice were cultured for 18 hours with 150 μM HT or vehicle. Phagocytosis was assessed as described in (Section 2.7.4). Fluorescence was determined using fluorescence plate reader with 490 nm excitation and 520 nm emission. Background wells with cells only were also included to determine background fluorescence intensity. Graphs display mean ± SEM from three independent experiments performed in triplicate for each condition after subtracting the background. In each case, the values in vehicle treated cells have been arbitrary assigned as 1 and treated samples were normalised to this. Statistical analysis was carried out using an unpaired Student's t-test (* P ≤ 0.05, ** P ≤ 0.01; HT v/s Vehicle).

4.3 Discussion

Controlling the inflammatory process has the potential to prevent and treat disorders such as atherosclerosis. However, side effects and high costs of current anti-inflammatory drugs implicate the need for the development and use of new drugs/agents (Dinarello, 2010). The protective effects of naturally extracted phenolic compounds are often attributed not only to their antioxidant capacity but also to the modulation of the inflammatory response (Ambriz-Pérez *et al.*, 2016; Moss and Ramji, 2016). Thus, phenolic compounds exert anti-inflammatory activity by inhibiting the expression of pro-inflammatory mediators, immune cell activation or oxidative stress (Emerit *et al.,* 2004; Alarcón de la Lastra and Villegas, 2005; Chuang and McIntosh, 2011). This has led to an increase in interest for the use of dietary phenolic compounds as a potential natural alternative to pharmaceutical drugs for the prevention and treatment of inflammation and related diseases with minimal side effects (Ambriz-Pérez *et al.*, 2016). However, more in-depth studies are required in relation to their mechanisms of actions.

Signal transduction pathways are integral to the changes in the expression of inflammatory mediators and their subsequent ability to control the inflammatory response following interaction with their cell surface receptors. The anti-inflammatory properties of phenolic compounds were often found due to modulation of such signal transduction pathways (Santangelo *et al.*, 2007). However, only a restricted number of studies have addressed the effect of polyphenols on specific signal transduction pathways associated with inflammation and further studies are required.

HT has been reported to have protective anti-oxidant and anti-inflammatory actions in preclinical studies against several diseases, especially CVD and metabolic disorders (Bulotta *et al.*, 2014). It was found that HT inhibits the ERK pathway and decreases its phosphorylation-mediated activation (Zhao *et al.*, 2014). Previous studies in the laboratory showed that the IFN-γ induced phosphorylation of STAT1 on serine 727 but not tyrosine 701 in human macrophages was attenuated by HT (Supplementary figure S-1). As ERKs are major contributors to STAT1 serine 727 phosphorylation (Li *et al.*, 2010), BMDM from genetically modified mice ($ERK1^{-/-}$,

STAT1^{S727A}) were used to further probe the role of ERK1:STAT1 serine 727 phosphorylation axis on HT actions.

HT is rapidly metabolised upon ingestion so its concentrations in the plasma tend to be relatively low to undetectable (Visioli *et al.*, 2000; Auñon-Calles *et al.*, 2013; Vilaplana-Pérez *et al.*, 2014). The biological activity of HT *in vivo* is therefore often associated to its metabolites (Visioli *et al.*, 2000). It's therefore difficult to correlate the concentration of HT added to the cells with those present in the plasma. It is hence possible that the concentration of HT added to the cells may be on the higher side. Nevertheless, this concentration had no effect on cell viability and, as shown later in the studies, correlation was seen in responses *in vitro* and *in vivo*.

Previous research in the laboratory showed that the most effective dose of HT on human macrophages *in vitro* was 150 μM and had no effect on cell viability. The studies presented in this chapter also found no changes in cellular viability by this concentration of HT in BMDM from wild-type or genetically modified mice (Figure 4.2). On the other hand, a previous study has shown that HT is able to decrease cellular proliferation by arresting the cell cycle (Reboredo-Rodríguez *et al.*, 2018) and this was also found with BMDM cultures from C57BL/6J mice (Figure 4.3A). HT also significantly reduced cell proliferation in BMDM culture from STAT1^{S727A} mice (Figure 4.3B), which suggests that the process does not require STAT1 serine phosphorylation. In the previous chapter, we showed that knocking out of ERK1 significantly induces cellular proliferation (Figure 3.3) and no HT-mediated reduction in cellular proliferation was seen with BMDM from ERK1 deficient mice when compared to the control (Figure 4.3). This indicates a potential requirement for ERK1 in HT-mediated changes in proliferation of macrophages.

It has been suggested in a previous study that HT is a potent angiogenesis inhibitor via suppressing effects on specific auto phosphorylation sites that control EC proliferation and migration (Lamy *et al.*, 2014). Here we showed that macrophage cellular migration in response to the chemokine MCP-1 was also significantly attenuated with BMDM from control, ERK1 deficient and STAT1 ^{S727A} mice (Figure 4.4). Such attenuation of macrophage migration may make a significant contribution

to the anti-atherogenic actions of HT. However, the ERK: STAT1 serine 727 phosphorylation axis appears not to be involved in the process though functional redundancy cannot be ruled out at present.

HT is often considered as an active polyphenol scavenger of ROS in olive oil (O'Dowd *et al.*, 2004) and should therefore have anti-oxidant activity. In this study, the TBHP-mediated ROS production was attenuated by HT in BMDM from wild-type control, ERK1$^{-/-}$ and STAT1^{S727A} mice, thereby confirming the anti-oxidant properties of this polyphenol. However, the genetic modifications had no effect on the HT-mediated ROS production, thereby suggesting either no requirement of the ERK:STAT1 serine 727 phosphorylation axis or the potential existence of functional redundancy.

Foam cell formation due to excessive uptake of oxLDL and subsequent imbalance in lipid efflux is key to atherosclerotic lesion formation (McLaren *et al.*, 2011; Yu *et al.*, 2013). polyphenolic compounds have been shown previously to have a lipid-lowering activity and inhibit of foam cell formation (Wu *et al.*, 2016). In this study, HT inhibited oxLDL uptake and phagocytosis in BMDM from C57BL/6J, ERK1$^{-/-}$ and STAT1^{S727A} mice (Figures 4.7-4.8). This shows a potentially key role for HT in the inhibition of macrophage foam cell formation. In addition, the results indicate either no requirement of the ERK: STAT1 serine 727 phosphorylation axis or the potential existence of functional redundancy in these processes.

Macropinocytosis represents another key process in foam cell formation (Kruth *et al.*, 2005). HT was found to inhibit macropinocytosis in BMDM from control but not those from ERK1$^{-/-}$ or STAT1^{S727A} mice (Figure 4.6). These results suggest a potentially key role for the ERK1:STAT1 serine 727 phosphorylation axis in macropinocytosis. Interestingly, previous studies have shown that the entry of human immunodeficiency virus type 1 (HIV-1) into brain microvascular endothelia by macropinocytosis was dependent on lipid rafts and ERK signalling (Liu *et al.*, 2002). In addition, an interferon stimulated, STAT1 responsive gene, ADP ribosylation factor-GAP with Dual PH Domain-Containing Protein 2 (ADAP2), which is involved in the control of macropinocytosis, restricts RNA virus entry (Shu *et al.*, 2015). Thus, the role of the ERK: STAT1 axis in macropinocytosis may extend to other modes.

The findings provided by the *in vitro* experiments carried out in the studies presented in this chapter support HT as a potential therapeutic agent that can help in limiting atherosclerosis by controlling several key processes such as macrophage migration and foam cell formation. In the light of these findings, we carried out *in vivo* experiments to investigate the impact of HT on atherosclerosis risk factors in wild-type mice fed a HFD. The outcome of these *in vivo* studies is presented in the next chapter.

Chapter 5

5.1 Introduction

Current strategies for the prevention of CVD mainly focus on improving blood lipid profiles. Several epidemiological studies have reported a correlation between increased levels of olive oil in the diet and a lower risk of developing atherosclerosis and other CVD (Peyrol *et al.,* 2017). These studies have also demonstrated a potentially important role for phenolic compounds, particularly HT, in the protection of LDL oxidation (Echeverría *et al.*, 2017). The European Food Safety Authority (EFSA) published a scientific opinion in 2011 that 5 mg of HT and its derivatives should be consumed per day to protect from oxidative damage of LDL particles. HT also contributes to the maintenance of normal blood HDL cholesterol concentration, blood pressure, function of the gastrointestinal tract, health of the upper respiratory tract and the body's defence against external agents (Carlo Agostoni *et al.*, 2011).

In a previous *in vivo* study using hyperlipidaemic rabbits, the effects of HT on the antioxidant status, lipid profile and the progression of aortic lesions were assessed in different groups of animals receiving different diets. The mix was as follows: 97% standard chow diet, 3% sunflower oil (control group); 96% standard chow diet, 1.3% cholesterol and 3% lard to induce atherosclerosis (atherogenic diet) and 97% standard chow diet, 3% virgin olive oil containing 5.6 mg/kg of pure HT (HT diet). A 50% and 42% decrease in total cholesterol and TG levels respectively were observed together with an increase in HDL cholesterol levels and a reduction of the size of atherosclerotic lesions with HT diet when compared with the control animals (González-Santiago *et al.*, 2006).

Other studies have also described HT as a powerful anti-inflammatory compound amongst the various polyphenols of olive oil, showing an effective down regulation in the expression of enzymes involved in oxidative stress, cytokines, chemokines and several other pro-inflammatory genes (Zhang *et al.*, 2009; Killeen *et al.*, 2014; Echeverría *et al.*, 2017).

Liver is an immunologically complex organ that plays key roles in the changes of metabolism and inflammation during atherosclerosis, as producer of acute phase

plasma proteins and components of the complement system, in the control of leukocyte migration into tissues and secretion of mediators that regulate an inflammatory response (cytokines and chemokines). Liver is essential for the maintenance of tissue and organ homeostasis and dysregulated function leads to chronic infection, autoimmunity and malignancy. Controlling inflammation is essential for the maintenance of liver homeostasis otherwise this can lead to pathological inflammation and disrupted tissue homeostasis characterised by the progressive development of fibrosis, cirrhosis and eventual liver failure (O'Farrelly and Crispe, 1999; Crispe, 2009). Because of such important functions, liver gene expression levels have been studied intensively (Kleemann *et al.*, 2007; Robinson *et al.* , 2016).

In the previous chapter, we showed that HT has several anti-inflammatory and anti-atherogenic activities *in vitro* such as the inhibition of LDL oxidation, macrophage migration and proliferation, and modified LDL uptake and foam cell formation. The data obtained were very promising concerning the potential health benefits of HT. It was therefore important that the analysis of the beneficial actions of HT was extended *in vivo*. Numerous *in vivo* studies have used 10 mg/kg/day HT as the most effective dose and this has been shown to reduce the inflammatory responses via inhibition of production of NO, prostaglandins, pro-inflammatory cytokines, chemokines and MMPs in different animal models (Acín *et al.*, 2006; Echeverría *et al.*, 2017; Peyrol *et al.,* 2017). It was therefore decided to carry out a short-term study on the protective and potential anti-atherogenic activity of HT in wild-type male C57BL/6J mice that received HFD for 21 days with daily gavage of 10 mg/kg/day of HT or vehicle to analyse its effects on plasma lipid profile, oxidation levels and liver expression of key genes implicated in atherosclerosis. Figure 5.1 summarises the experimental approach that was used for the studies.

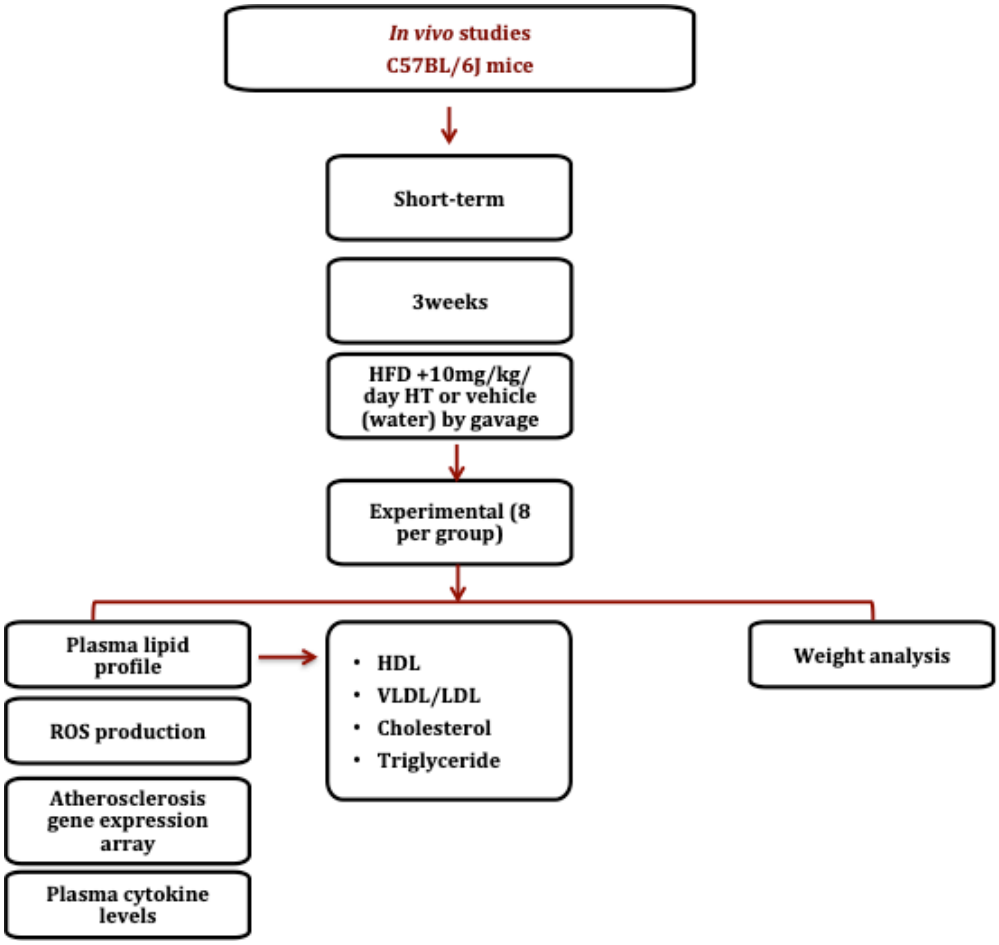

Figure 5.1 Summery of the experimental approach used to investigate the protective actions of HT in C57BL/6J mice *in vivo*

5.2 Results

5.2.1 Weight analysis.

The weight of C57BL/6J mice fed a HFD with administration of 10 mg/kg/day of HT or vehicle control (water) was monitored every 5 days throughout the study (21 days). Table 5.1 shows the weight of the mice as determined during the duration of the study. HT produced no significant changes in the weight gain of the mice when compared to the vehicle control (Figure 5.2).

Table 5.1 Weight analyses in mice receiving HT vs control.

		Days					
	Mouse	**1**	**6**	**11**	**17**	**21**	**Weight changes at day 21 compared to day 1 (g)**
Vehicle	1	31	31	31	31	31	0
	2	31	28	29	30	30	1 ↓
	3	31	31	30	30	30	1 ↓
	4	25	26	27	28	28	3 ↑
	5	24	25	26	26	27	3 ↑
	6	26	26	27	27	26	0
	7	28	28	29	30	29	1 ↑
	8	29	29	29	30	29	0
HT	1	33	31	31	31	32	1 ↓
	2	29	29	29	28	28	1 ↓
	3	34	34	32	33	33	1 ↓
	4	27	28	28	28	29	2 ↑
	5	25	26	25	26	26	1 ↑
	6	35	35	34	33	32	3 ↓
	7	30	30	31	30	31	1 ↑
	8	39	39	40	39	39	0

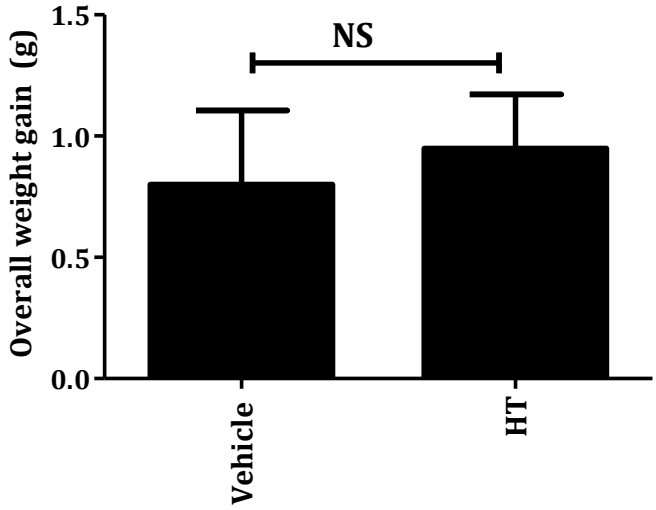

Figure 5.2 HT has no significant effect on weight of mice fed a HFD

C57BL/6J mice (n=8 per group) were fed a HFD for 21 days with daily administration by gavage of vehicle (water) or 10 mg/kg/day of HT. Weight was monitored regularly throughout the study (see Table 5.1) Graph displays mean ± SEM of the average differences in weight gain between the groups at the end of the experimental period. Statistical analysis was carried out using a paired Student's t test (NS=not significant; HT v/s Control).

5.2.2 HT reduces ROS levels in C57BL/6J mice fed a HFD *in vivo*.

Several studies have demonstrated that olive oil polyphenol compounds, including HT and its derivatives, as protectors of LDL oxidation (Vilaplana- Pérez and Aunon, 2014). In this study, the animal groups that received HT showed a significant 30% reduction (p=0.002) in plasma ROS levels compared to the vehicle control (Figure 5.3), thereby demonstrating the anti-oxidant properties of HT *in vivo*.

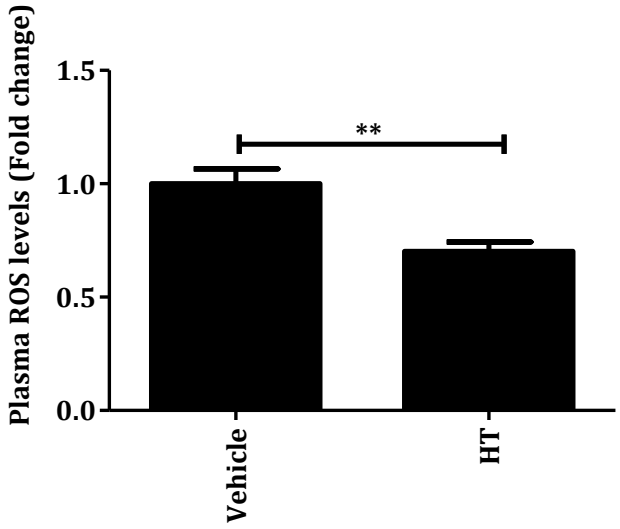

Figure 5.3 *In vivo* effect of HT on plasma ROS levels in C57BL/6J mice fed a HFD.

Male C57BL/6J mice (n=8 per group) were fed a HFD for 21 days with daily administration by gavage of vehicle (water) or 10 mg/kg/day of HT. The plasma levels of ROS were determined as described in (Section 2.10). The values for the vehicle control group were arbitrarily assigned as 1. The graph displays mean ± SEM for each group. Statistical analysis was carried out using an unpaired Student's t test (**$P \leq 0.01$; HT v/s Control).

5.2.3 HT modulates plasma lipid levels in C57BL/6J mice fed a HFD.

The effect of HT on plasma levels of total cholesterol, LDL/VLDL and HDL was analysed since they play important roles in the pathogenesis of atherosclerosis (Gofman *et al.*, 1950). Generally, total cholesterol and LDL/VLDL cholesterol are regarded as pro-atherogenic and HDL as anti-atherogenic (Barter, 2005). Compared to the vehicle control, HT significantly decreased the plasma levels of total cholesterol by 27% (p=0.02), LDL/VLDL cholesterol levels by 26% (p<0.001) and HDL levels by 30% (p=0.002) (Figure 5.4A-C)

Ratios of plasma LPs and total cholesterol have also been suggested to provide additional parameter for risk of atherosclerosis in some cases (Lemieux *et al.*, 2001). The effect of HT on such ratios in comparison to the vehicle control was therefore determined. As shown in Figure 5.4D-F, there were no significant changes in the ratios of total cholesterol: HDL, total cholesterol: LDL/VLDL and LDL/VLDL: HDL.

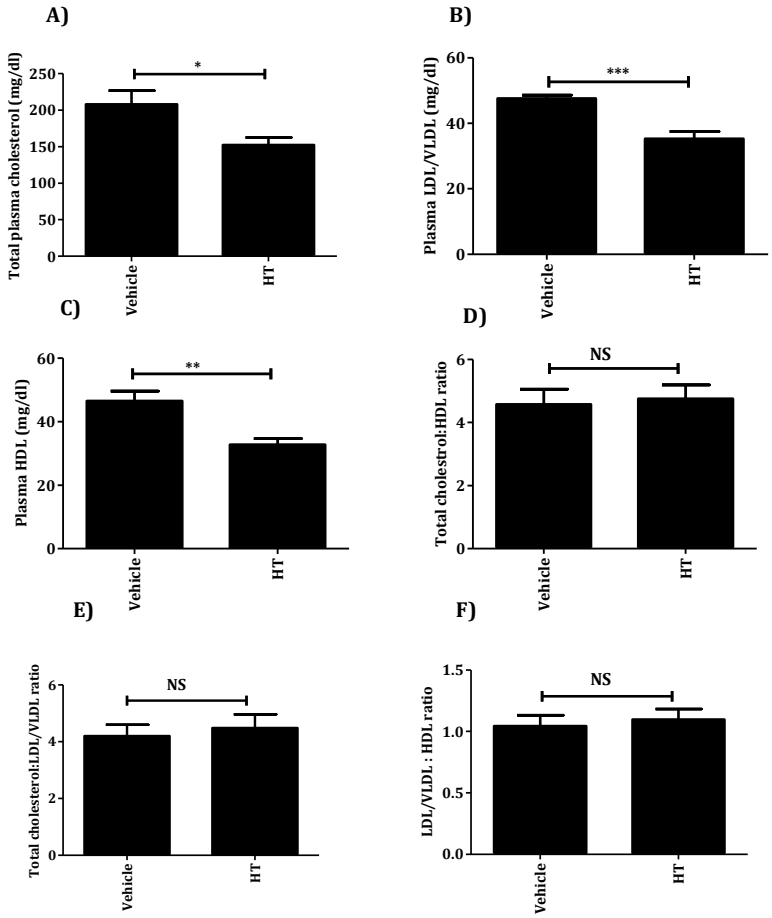

Figure 5.4 *In vivo* effect of HT on total cholesterol; LDL/VLDL and HDL levels together with various ratios in C57BL/6J mice fed a HFD.

Total cholesterol (A), LDL/VLDL (B) and HDL (C) from C57BL/6J mice (n=8 per group) was measured after 21 days of receiving a HFD with daily administration by gavage of vehicle (water) or 10 mg/kg/day HT as described in (Section 2.9.1). The ratios of total cholesterol: HDL (D), total cholesterol: LDL/VLDL (E) and LDL/VLDL: HDL (F) were also assessed. Graphs display mean ± SEM for each group. Statistical analysis was carried out using an unpaired Student's t test (*$P \leq 0.05$, **$P \leq 0.01$, *** $P \leq 0.001$, NS=not significant; HT v/s Control).

5.2.4 HT significantly induces TG levels in C57BL/6J mice fed a HFD.

Increased plasma TG levels is an independent risk factor for developing atherosclerosis and CVD-related events (Talayero and Sacks, 2011). HT treatment significantly increased TG levels by 27% (p=0.005) in C57BL/6J mice receiving HFD along with gavage of 10 mg/kg/day of HT for 21 days compared to the vehicle control

(Figure 5.5A). The ratios of TG: total cholesterol, TG: LDL/VLDL and TG:HDL were also assessed because they can often provide additional parameter for risk of atherosclerosis development (Millán *et al.*, 2009). HT produced increases of 90% in the TG: total cholesterol ratio, 122% in the TG: LDL/VLDL ratio and 100% in the TG: HDL cholesterol ratio (p=0.01, p<0.001 and p<0.001 respectively) when compared to the vehicle control (Figure 5.5B-D).

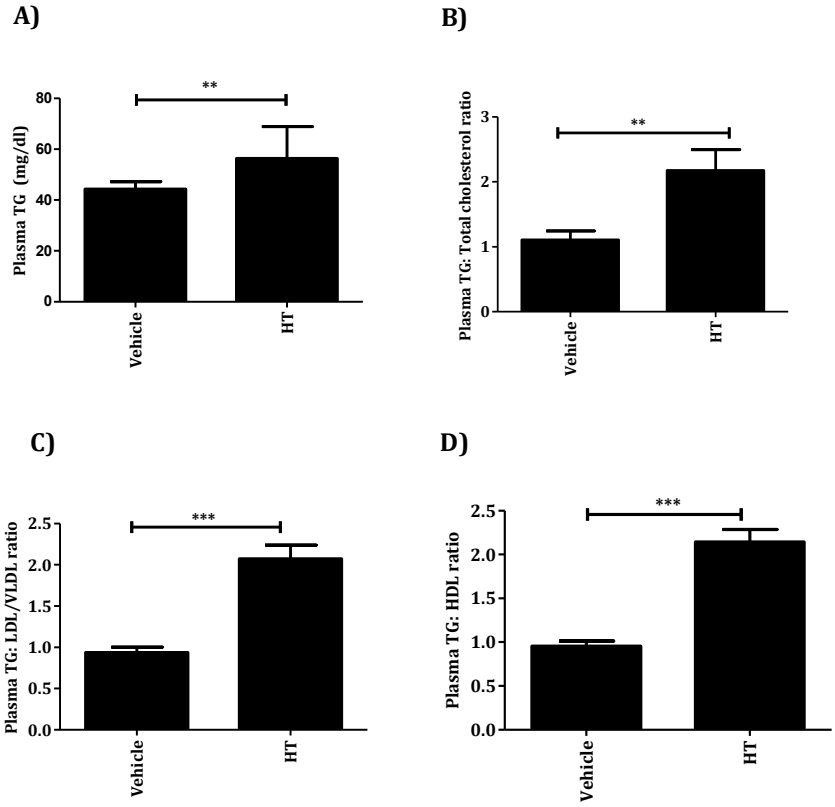

Figure 5.5 The *in vivo* effect of HT on TG levels in C57BL/6J mice following feeding of a HFD

TG levels from C57BL/6J mice (n=8 per group) were measured after 21 days of receiving a HFD with daily administration by gavage of vehicle (water) or 10 mg/kg/day of HT (A) as described in (Section 2.9.2). The ratios of TG: total cholesterol (B), TG: LDL/VLDL cholesterol (C) and TG: HDL cholesterol (D) were also assessed. Graphs display mean ± SEM and statistical analysis was carried out using an unpaired Student's t test (**P≤0.01, ***P≤0.001; HT v/s Control).

5.2.5 Array analysis of liver gene expression

To assess the effect of HT on liver expression of key genes implicated in atherosclerosis, mRNA was isolated from C57BL/6J mice fed a HFD with gavage of 10 mg/kg/day of HT or vehicle for 21 days and used for Atherosclerosis RT^2 Profiler PCR arrays and regular RT-qPCR analysis. Table 5.2 shows the significant and non-significant changes in the expression of genes in the RT-qPCR array clustered according to their known function in atherosclerosis. The analysis of the data was carried out as described previously in Section 3.2.4.

The expression of five HKGs present in the array (*ACTβ*, *GUSB*, *HSP90AB1*, *B2M* and *GAPDH*) was found to be stable (see Section 3.2.4) during the assay and were therefore used to normalise the test genes. A total of 55 genes were found to have their expression altered by at least 10% with the expression of 20 genes significantly reduced by HT (*BCL2L1, CCL2, IL-2, IL-4, TGFβ1, VWF, SELE, APOA1, FABP3, LDLR, ELN, IL-5, LIF, PDGFA, TGFβ2, KLF2, IL1R1, IL1R2, MMP3 and SERPINβ2*) and the expression of two genes was significantly induced (*MSR1* and *COL3α1*) (Table 5.2). In addition, there was a trend towards reduced expression of 8 genes by HT [*CCl5* (p=0.09), *IFN-γ* (p=0.08), *SOD1* (p=0.08), *BCL2A1A* (p=0.09), *BIRC3* (p=0.08), *PLIN2* (p=0.09), *PPARα* (p=0.06) and *PPARδ* (p=0.07)] and a trend towards increased expression of one gene [*TNFαIP3* (p=0.06)].

A heat map was also generated (Figure 5.6) as described previously in Section 3.2.4. The data are presented as log2 of the averages where green indicates reduced expression, black indicates unaltered expression, red indicates increased expression and grey indicates no expression. Mice with undetectable assay readings were removed before statistical analysis and the values from the vehicle control groups were arbitrary assigned as 1.

Table 5.2 The effect of HT on the liver expression of atherosclerosis-associated genes.

			Vehicle	HT		
#	**GENE**	**N**	**Mean ± SEM**	**Mean ± SEM**	**Change (%)**	***p*-value**
			Stress response			
1	**APOE**	5	1 ± 0.04	1.05 ± 0.15	5↑	0.74
2	**BAX**	4	1 ± 0.05	0.74 ± 0.15	26 ↓	0.17
3	**BCL2L1**	4	1 ± 0.05	0.67 ± 0.09	33 ↓	0.04 (*)
4	**CCL2**	4	1 ± 0.05	0.61 ± 0.1	39 ↓	0.03 (*)
5	**CCL5**	4	1 ± 0.05	0.64 ± 0.14	36 ↓	0.09
6	**CCR1**	5	1 ± 0.04	1.9 ± 0.42	90 ↑	0.1
7	**CCR2**	3	1 ± 0.07	1.6 ± 0.7	60 ↑	0.52
8	**CXCL1**	3	1 ± 0.13	1.5 ± 0.8	50↑	0.59
9	**FN1**	5	1 ± 0.25	0.86 ± 0.18	14↓	0.49
10	**IFNγ**	3	1 ± 0.07	0.57 ± 0.13	43 ↓	0.08
11	**1L1α**	5	1 ± 0.03	0.9 ± 0.16	10 ↓	0.55
12	**IL1β**	4	1 ± 0.06	0.92 ± 0.3	8 ↓	0.82
13	**IL2**	3	1 ± 0.04	0.24 ± 0.06	76 ↓	0.006 (**)
14	**IL4**	4	1 ± 0.04	0.47 ± 0.14	53 ↓	0.03 (*)
15	**ITGβ2**	4	1 ± 0.05	0.79 ± 0.2	21 ↓	0.37
16	**PPARγ**	5	1 ± 0.06	0.84 ± 0.17	16 ↓	0.41
17	**SELP**	5	1 ± 0.08	0.78 ± 0.17	22 ↓	0.27
18	**SOD1**	5	1 ± 0.2	0.61 ± 0.16	39 ↓	0.08
19	**SPP1**	5	1 ± 0.07	0.87 ± 0.15	13 ↓	0.44
20	**TGFβ1**	3	1 ± 0.05	0.78 ± 0.04	22 ↓	0.03 (*)
21	**TNF**	5	1 ± 0.03	0.99 ± 0.23	1 ↓	0.99
			Apoptosis			
22	**BCL2**	3	1 ± 0.07	0.59 ± 0.23	41 ↓	0.3
23	**BCL2 A1A**	3	1 ± 0.06	0.56 ± 0.13	44 ↓	0.09
24	**BID**	4	1 ± 0.06	0.72 ± 0.14	28 ↓	0.15
25	**BIRC3**	4	1 ± 0.03	0.78 ± 0.08	22 ↓	0.08

26	**FAS**	4	1 ± 0.06	0.71 ± 0.16	29 ↓	0.18
27	**NFKβ1**	3	1 ± 0.05	0.93 ± 0.18	7 ↓	0.74
28	**TNFαIP3**	4	1 ± 0.04	2.7 ± 0.43	170 ↑	0.06
29	**VEGFα**	5	1 ± 1.08	0.82 ± 0.14	18 ↓	0.27
			Blood coagulation			
30	**NPY**	4	1 ± 0.06	0.98 ± 0.55	2 ↓	0.97
31	**PTGS1**	4	1 ± 0.05	0.77 ± 0.23	23 ↑	0.4
32	**VWF**	3	1 ± 0.05	0.64 ± 0.07	36 ↓	0.04 (*)
			Cell adhesion molecules			
33	**CDH5**	3	1 ± 0.06	0.45 ± 0.2	54 ↓	0.10
34	**CD44**	4	1 ± 0.06	0.91 ± 0.3	9 ↓	0.78
35	**CTGF**	5	1 ± 0.08	1.12 ± 0.11	12 ↑	0.32
36	**ENG**	5	1 ± 0.08	0.91 ± 0.23	9 ↓	0.71
37	**ICAM1**	3	1 ± 0.07	0.84 ± 0.27	16 ↓	0.62
38	**ITGα2**	4	1 ± 0.05	0.6 ± 0.18	40↓	0.11
39	**ITGα5**	3	1 ± 0.07	0.69 ± 0.12	31 ↓	0.1
40	**ITGαX**	4	1 ± 0.06	0.73 ± 0.17	27 ↓	0.22
41	**LAMA1**	3	1 ± 0.03	1.1 ± 0.11	10 ↑	0.56
42	**SELE**	4	1 ± 0.07	0.45 ± 0.05	55 ↓	0.001 (**)
43	**SELL**	3	1 ± 0.03	1.2 ± 0.11	20 ↑	0.13
44	**SELPG**	3	1 ± 0.05	0.6 ± 0.17	40 ↓	0.11
45	**THBS4**	3	1 ± 0.06	0.78 ± 0.32	22↓	0.6
46	**VCAM1**	6	1 ± 0.04	0.81 ± 0.19	19↓	0.38
			Lipid transport and metabolism			
47	**ABCA1**	4	1 ± 0.12	1.24 ± 0.16	24 ↑	0.23
48	**APOA1**	4	1 ± 0.07	0.5 ± 0.14	50 ↓	0.04 (*)
49	**APOB**	6	1 ± 0.10	0.76 ± 0.13	24 ↓	0.14
50	**FABP3**	6	1 ± 0.04	0.74 ± 0.06	26 ↓	0.02 (*)
51	**LDLR**	4	1 ± 0.12	0.67 ± 0.06	33 ↓	0.01 (*)
52	**LPL**	5	1 ± 0.13	0.78 ± 0.19	22 ↓	0.33
53	**LYPLα1**	6	1 ± 0.16	0.98 ± 0.17	2 ↓	0.93

54	**MSR1**	4	1 ± 0.04	1.66 ± 0.19	66 ↑	0.04 (*)
55	**NR1H3**	5	1 ± 0.04	1.01 ± 0.1	1 ↑	0.77
56	**PLIN2**	5	1 ± 0.4	0.69 ± 0.13	31 ↓	0.09
57	**PPAR α**	4	1 ± 0.09	0.75 ± 0.08	25 ↓	0.06
58	**PPARD**	4	1 ± 0.04	0.6 ± 0.14	40 ↓	0.07
59	**RXRα**	5	1 ± 0.26	0.73 ± 0.14	27 ↓	0.13
		Cell growth and proliferation				
60	**CSF2**	3	1 ± 0.05	0.77 ± 0.26	23↓	0.44
61	**ELN**	4	1 ± 0.06	0.59 ± 0.1	41 ↓	0.03 (*)
62	**FGF2**	5	1 ± 0.03	0.8 ± 0.14	20 ↓	0.32
63	**HBEGF**	4	1 ± 0.05	0.68 ± 0.24	32 ↓	0.28
64	**IL3**	3	1 ± 0.08	0.64 ± 0.34	36 ↓	0.41
65	**IL5**	3	1 ± 0.06	0.41 ± 0.08	59 ↓	0.02 (*)
66	**KDR**	3	1 ± 0.07	0.84 ± 0.25	16 ↓	0.6
67	**LIF**	4	1 ± 0.03	0.35 ± 0.08	65 ↓	0.004 (**)
68	**PDGFA**	4	1 ± 0.05	0.43 ± 0.09	57 ↓	0.01 (*)
69	**PDGFB**	4	1 ± 0.06	0.71 ± 0.18	29 ↓	0.22
70	**PDGFRβ**	5	1 ± 0.05	0.76 ± 0.16	24 ↓	0.22
71	**TGFβ2**	5	1 ± 0.03	0.6 ± 0.1	40 ↓	0.02 (*)
		Transcriptional regulation				
72	**KLF2**	6	1 ± 0.000	0.00 ± 0.00	0	NA
		Extracellular matrix (ECM)				
73	**ACE**	3	1 ± 0.04	0.8 ± 0.45	20 ↓	0.71
74	**CFLAR**	3	1 ± 0.1	0.64 ± 0.08	36 ↓	0.052
75	**COL3α1**	4	1 ± 0.07	1.7 ± 0.10	70 ↑	0.006 (**)
76	**FGα**	4	1 ± 0.07	0.87 ± 0.2	13 ↓	0.5
77	**FGβ**	6	1 ± 0.04	0.83 ± 0.12	17 ↓	0.22
78	**IL1R1**	4	1 ± 0.13	0.53 ± 0.14	47 ↓	0.04 (*)
79	**IL1R2**	5	1 ± 0.05	0.3 ± 0.13	70 ↓	0.03 (*)
80	**MMP1α**	4	1 ± 0.1	0.6 ± 0.18	40 ↓	0.12
81	**MMP3**	4	1 ± 0.05	0.22 ± 0.08	88 ↓	0.002 (**)

82	**SERPINβ2**	4	1 ± 0.05	0.31 ± 0.17	69 ↓	0.03 (*
83	**SERPINE1**	5	1 ± 0.05	0.6 ± 0.19	40 ↓	0.23
84	**TNC**	6	1 ± 0.02	0.85 ± 0.14	15 ↓	0.38
			HKG			
1	**ACTB**	6	1.00 ± 0.02	0.99 ± 0.02	1 ↓	NA
2	**B2M**	6	1.00 ± 0.03	0.97 ± 0.02	3 ↓	NA
3	**GAPDH**	**4**	1.00 ± 0.01	1.03 ± 0.01	3 ↑	NA
4	**GUSB**	**4**	1.00 ± 0.01	1.00 ± 0.01	0	NA
5	**HSP90AB1**	**6**	1.00 ± 0.01	1.02 ± 0.01	2 ↑	NA

See table 3.1 for list of abbreviations, ↓ = Down regulation of gene expression, ↑ = Up regulation of gene expression, *P ≤ 0.05, **P ≤ 0.01, ***P ≤ 0.001, NA= Not available.

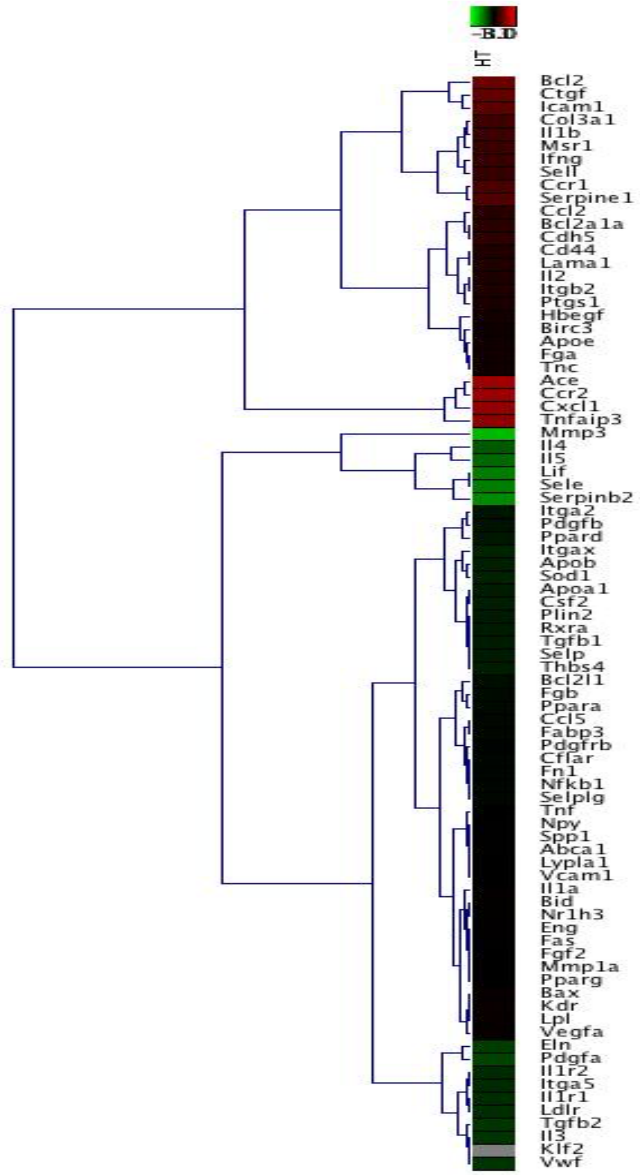

Figure 5.6 Heat map representing colour-coded expression levels of differentially expressed genes.

Heat map of hierarchical clustering showing the expression of 84 key atherosclerosis-associated gene transcripts from liver tissues of C57BL/6J mice fed a HFD with daily gavage of 10 mg/kg/day of HT or vehicle for 21 days. The heat maps present the log2 fold change. Genesis software was used to assess gene expression signals and clustering. A colour-coded scale of the intensity of gene expression is presented on top of the figure. All the genes present on the Qiagen RT^2 Profiler PCR Array were plotted.

5.2.6 Regular RT-qPCR analysis of key genes associated with cholesterol synthesis, transport and metabolism

Atherosclerosis is now considered to be a chronic inflammatory disease where increased expression of genes by the liver may play key roles in accelerating the disease process and associated inflammatory responses. Some such key genes code for proteins that are involved in the maintenance of cholesterol homeostasis (Laguna and Alegret, 2012). Many of these were not present in the arrays used so specific primers were employed to measure their expression levels using standard RT-qPCR. Table 5.3 shows the significant and non-significant changes in the expression of genes in the regular RT-qPCR analysis. The analysis of the data was carried out as described previously in Section 3.2.4 with *ACTβ* used as a HKG for data normalisation. Studying the changes of expression of these genes could shed light on more targets that are potentially used by HT to reduce the atherosclerotic events.

Table 5.3 The effect of HT on the expression of key genes associated with cholesterol synthesis, transport and metabolism by regular RT-qPCR

			Vehicle	HT		
#	**GENE**	**N**	**Mean ± SEM**	**Mean ± SEM**	**Change (%)**	***p*-value**
1	**ABCA1**	**7**	1 ± 0.44	3.65 ± 1.3	265 ↑	0.035 (*)
2	**ABCG5**	**7**	1 ± 0.07	2.22 ± 0.36	122 ↑	0.005 (**)
3	**ABCG8**	**6**	1 ± 0.06	1.46 ± 0.17	46 ↑	0.026 (*)
4	**SERBP1**	**7**	1 ± 0.3	1.77 ± 0.21	77 ↑	0.05 (*)
5	**HMGCR1**	**5**	1 ± 0.25	3.4 ± 0.9	240 ↑	0.026 (*)
6	**NPC1L1**	**6**	1 ± 0.13	2.75 ± 0.57	175 ↑	0.012 (*)
7	**ACTβ**	**7**	1± 0.01	1.02 ± 0.01	2 ↑	0.1

5.2.6.1 HT induces the expression of "cholesterol efflux" genes.

Three members of the ABC transporter family play important roles in the modulation of excess cellular cholesterol export from cells to HDL particles and reduce cholesterol accumulation in macrophages (Oram and Heinecke, 2005). As shown in Table 5.2, the expression of ABCA1 was non-significantly induced by 24%.

The effect of HT on the liver expression of other efflux genes ABCG5 and ABCG8 along with ABCA1 (to confirm the change seen in array analysis) was therefore determined. As shown in Figure 5.7, feeding the mice a HFD with HT for 21 days caused a significant induction in the expression of ABCG5 by 122% (p=0.005), ABCG8 by 46% (p=0.02) and ABCA1 by 260% (p=0.03). The induction of ABCA1 was therefore observed by regular RT-qPCR and RT-qPCR arrays, therefore providing validation of the latter.

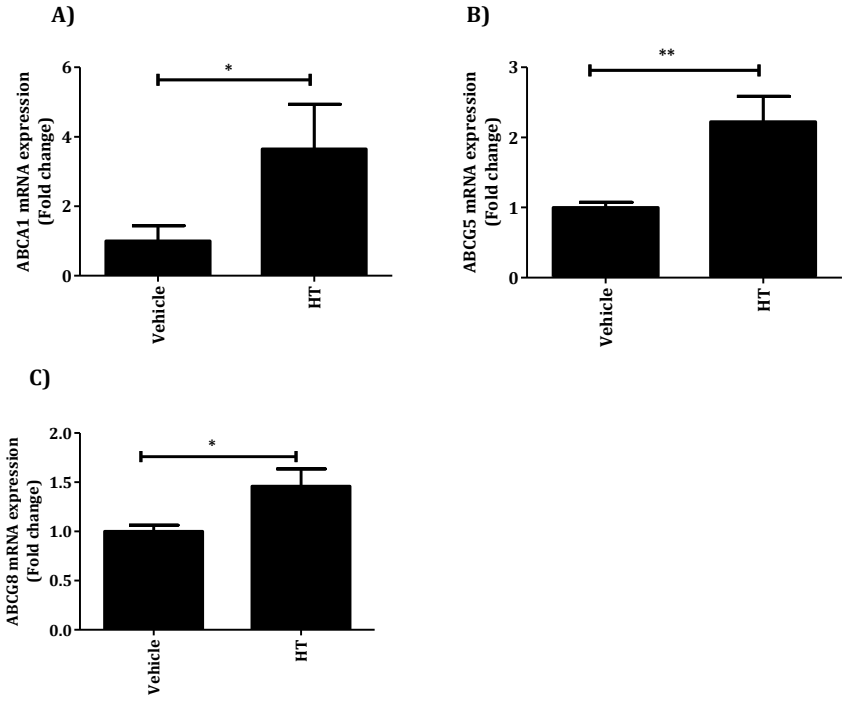

Figure 5.7 The effect of HT on the expression of "cholesterol efflux" genes in the liver.

The expression levels of "cholesterol efflux" genes ABCA1 (A), ABCG5 (B) and ABCG8 (C) were assessed using RNA extracted from liver tissues of male C57BL/6J mice fed a HFD for 21 days with daily administration by gavage of vehicle (water) or 10 mg/kg/day of HT. The expression levels were calculated using the comparative Ct method where β-actin was used as a HKG. Mice with undetectable assay readings were removed before statistical analysis and the values from the vehicle control groups were arbitrary assigned as 1. Graphs display mean ± SEM from (ABCA1; Vehicle 7; HT 7), (ABCG5; Vehicle 7; HT 6), (ABCG8; Vehicle 6; HT 6). Statistical analysis was carried out using an unpaired Student's t test (*p≤0.05, **P≤0.01; HT v/s Control).

5.2.6.2 HT induces the liver expression of genes implicated in cholesterol homeostasis.

As shown in Table 5.2, HT controls the expression of many genes implicated in the control of cholesterol homeostasis. The expression levels of other genes that play a key role in the control of cholesterol synthesis and metabolism such as HMGCR1, NPC1L1 and Sterol-Regulatory Element-Binding Protein (SREBP-1) were therefore determined using the same liver tissue lysate of the C57BL/6J mice that had been fed a HFD with daily gavage of 10 mg/kg/day HT or vehicle (Table 5.3). As shown in Figure 5.8, a significant increase in the expression of HMCGR1 by 270% (p=0.03), of NPC1L1 by 170% (p=0.01) and SREBP1 by 70% (p=0.05) was seen by HT when compared to the vehicle control.

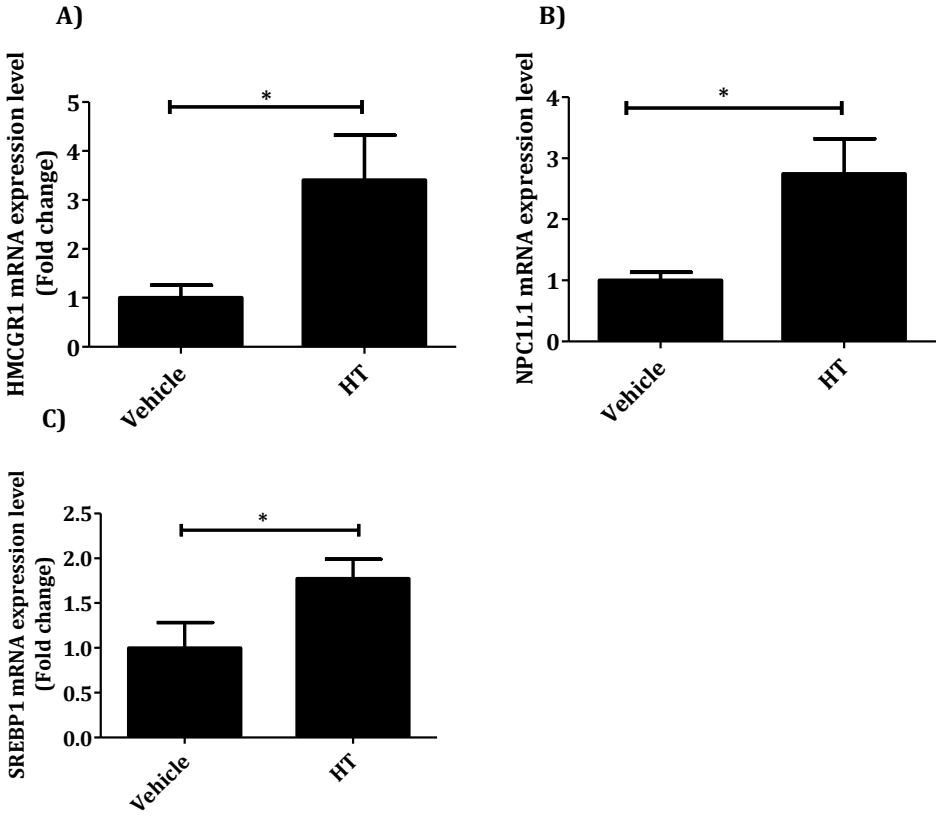

Figure 5.8 The effect of HT on the expression of key genes implicated in the control of cholesterol synthesis and metabolism in the liver.

Gene expression levels of HMCGR1 (A), NPC1L1 (B) and SREBP1 (C) were assessed using RNA extracted from the liver tissues of male C57BL/6J mice that were fed a HFD for 21 days with daily administration by gavage of vehicle (water) or 10 mg/kg/day of HT. The expression levels were determined using the comparative Ct method where β-actin was used as a HKG for data normalisation. Mice with undetectable assay readings were removed before statistical analysis and the values from the vehicle control groups were arbitrary assigned as 1. Graphs display mean ± SEM from (HMGCR1; Vehicle 5; HT 7), (NPC1L1; Vehicle 6; HT 6), (SERBP-1; Vehicle 7; HT 7). Statistical analysis was carried out using an unpaired Student's t test (*p≤0.05; HT v/s Control).

5.2.7 HT has no effect on the levels of several pro- and anti-inflammatory cytokines in the plasma of C57BL/6J mice fed a HFD.

The protein levels of pro- and anti-inflammatory cytokines IFN-γ, IL-2, IL-5, IL-6, IL-10 and TNF-α were assessed in the plasma of C57BL/6J mice fed a HFD for 21 days and given daily gavage of 10mg/kg/day HT or vehicle (water). There were non-significant reduction seen in the plasma levels of IFN-γ (13%), TNF-α (20%) and IL-6

(18%) (Figure 5.9) when compared to the vehicle control. On the other hand, there was a non-significant induction in the levels of IL-10 (6%), IL-2 (20%) and IL-5 (16%) when compared to the vehicle control (Figure 5.8).

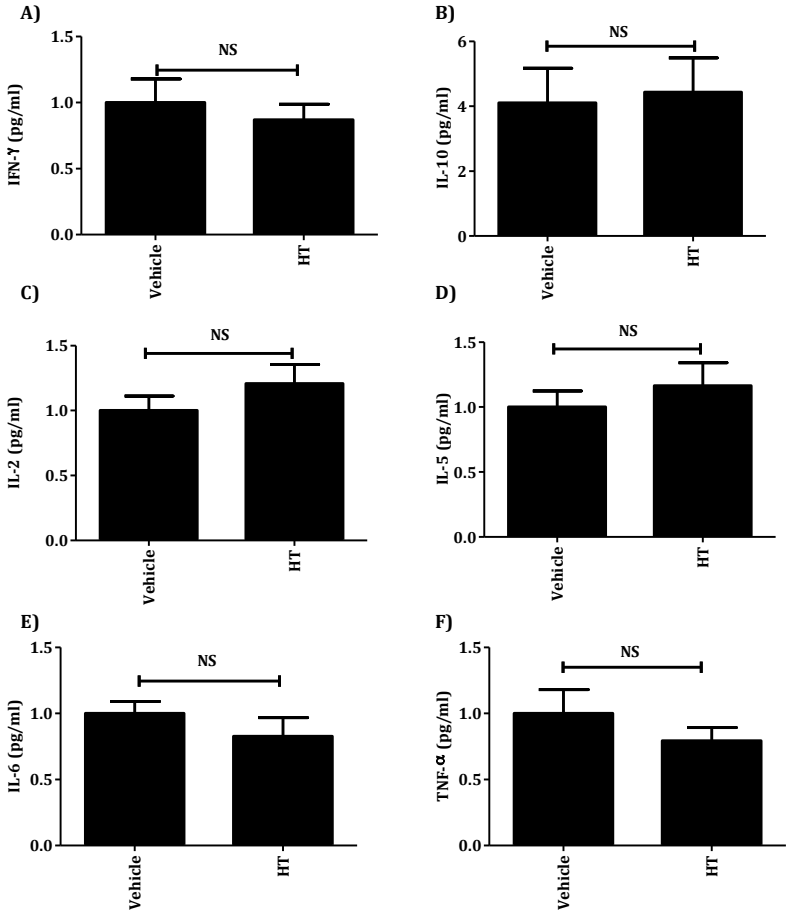

Figure 5.9 The effect of HT on plasma cytokine levels in mice receiving a HFD.

Plasma levels for the cytokines IFN-γ (A), IL-10 (B), IL-5 (C), IL-6 (D), IL-2 (E) and TNF-α (F) were measured after 21 days feeding of HFD with daily gavage of either a vehicle control or 10 mg/kg/day HT. The data presented are the mean ± SEM from 16 mice (8 per group). Mice with undetectable assay readings were removed before statistical analysis and the values from the vehicle control groups were arbitrary assigned as 1. Statistical analysis was performed using an unpaired student's t-test (NS=not significant; HT v/s Control).

5.3 Discussion

It has been reported that oxidative stress is one of the causative factors that links hypercholesterolemia with the pathogenesis of atherosclerosis (Prasad and Kalra, 1993). This stress results from an imbalance between the production of free radicals and the effectiveness of the antioxidant defence system (Halliwell, 1994). Several studies have examined the biological actions of HT, including in human and animal model systems and *in vitro*, all of which have pointed to its anti-oxidant effects, its high bioavailability and its health promoting activities (Tuck and Hayball, 2002; Moss and Ramji, 2016). The studies presented in this chapter have investigated the effects of HT in C57BL/6J mice fed a HFD for 21 days and found beneficial effects on plasma lipid and ROS levels together with gene expression in the liver (Figure 5.3-5.4 and Table 5.2-5.3).

Initially the effect of HT on weight change was assessed (Table 5.1 and figure 5.2). After 21 days of a HFD, both the vehicle control and HT treated mice increased weight at the same rate, indicating that there were no detrimental effects as a result of HT (Table 5.1). As this was a short term feeding study, beneficial changes in weight gain may occur gradually over time and should therefore be continued to be explored in future long-term feeding studies. However, the absence of any effect on weight is consistent with several studies using different animal models (González-Santiago *et al.*, 2006; Jemai *et al.*, 2008; Hmimed *et al*., 2016). Nevertheless, one study showed a beneficial effect of 50 mg/kg/day of HT supplementation against HFD-induced weight gain though this was for a considerably longer period of 17 weeks (Cao *et al.*, 2014).

HT has antioxidant properties that can counteract reactive oxygen and nitrogen species, thereby potentially protecting against the pathogenesis of CVD (Visioli *et al.*, 1995; Tuck and Hayball, 2002; Dreosti, 2016). In this study, mice that received HFD for 21 days and given a daily gavage of vehicle had significantly increased plasma ROS levels compared to mice that were receiving the same diet along with the administration of 10 mg/kg/day of HT. These data suggest that mice treated with HT are less susceptible to oxidative damage under the challenge of dietary-induced oxidative stresses, which includes oxidation of LDL and subsequent promotion of foam cell formation.

As mentioned earlier, increased levels of total cholesterol and LDL have been established as risk factors for atherosclerosis whereas elevated HDL levels are believed to have protective, anti-inflammatory properties (Gordon *et al.*, 1981). Analysis of lipid profile in this study demonstrated that HT administration induced protective effects against HFD-induced risk factors implicated in atherogenesis such as decreased plasma levels of total cholesterol and LDL/VLDL (Figure 5.4). In addition, HT significantly increased the expression of three key transporters involved in cellular cholesterol efflux (Figure 5.7). The effluxed cholesterol can then be accepted by HDL particles, which then promote its loss via the RCT system. However, not all the actions of HT were anti-atherogenic since it produced significant induction in plasma TG levels and a significant attenuation of HDL levels (Table 5.2-5.3).

To understand how HT could potentially act in controlling changes in blood lipids and the inflammatory state, the liver expression of key atherosclerosis–associated genes was determined especially as under hypercholesterolaemic conditions, the liver switches to predominantly an inflammatory state (Kleemann *et al.*, 2007). RT-qPCR array of 84 genes that play a key role in atherosclerosis was used (Table 5.2) together with regular RT-qPCR (Table 5.3). The results demonstrate that HT treatment was able to alter the expression of genes involved in stress responses, cholesterol homeostasis, cellular growth and proliferation, blood coagulation and the regulation of the inflammatory response. Most of these genes were described in Chapter 3 in relation to the important roles they play as pro- and anti-inflammatory mediators. Table 5.4 lists the genes whose expression was significantly altered by HT *in vivo*, and includes those determined by standard RT-qPCR.

Table 5.4 Genes whose expression was significantly altered by HT *in vivo*.

No.	Pro-atherogenic genes	Atheroprotective genes
1	MMP3	BCL2L1
2	CCL2	TGFβ1
3	IL2	APOA1
4	IL4	FABP3
5	SELE	IL5
6	VWF	TGFβ2
7	SELE	COL3α1
8	MSR1	LIF
9	ELN	ABCA1
10	IL1R1/2	ABCG5
12	PDGFA	ABCG8
13	SERPINβ2	NPC1L1
14	KLF2	LDLR

Abbreviations: BCL-2 like protein 1 (BCL2L1), C-C motif chemokine ligand 2 (CCL2), Interleukin 2 (IL2), Interleukin 4 (IL4), Integrin subunit beta 2 (ITGβ2), Von Willebrand factor (VWF), Apolipoprotein A1 (APOA1), Fatty acid binding protein 3 (FABP3), Low density lipoprotein receptor (LDLR), Macrophages scavenger receptor1 (MSR1), Elastin (ELN), Interleukin 5 (IL5), Interleukin 6 family cytokine (LIF), Platelet derived growth factor subunit A (PDGFA), Transforming growth factor beta2 (TGFβ2), Kruppel like factor 2 (KLF2), Collagen type III alpha 1 chain (COL3α1), Interleukin 1 receptor 1 (IL1R1), Interleukin 1 receptor 2 (IL1R2), Matrix metallopeptidase 2 (MMP3), Serpin family beta member 2 (SERPINβ2).

Table 5.4 shows the effect of HT on the expression of some pro-inflammatory genes which contribute to initiating the inflammatory responses [e.g. IL-2, SELE, CCL2 (MCP-1)], and additionally control cellular proliferation, migration and adhesion of leukocytes at the site of inflammation (Lee and Hirani, 2006; Toma and McCaffrey, 2012; Ramji and Davies, 2015; Winter *et al.*, 2018). A previous study assessed the effects of HT from olive extract on gene expression of LPS treated murine macrophages (RAW264.7 cells). HT was able to attenuate the expression of numerous inflammatory genes including CCL-2, which thereby emphasises its anti-inflammatory effect (Richard *et al.*, 2011b). This finding correlates well with the reduction in pro-inflammatory gene expression observed and the decrease in cellular migration we showed previously *in vitro* (Figure 4.4).

A previous study using a cancer cell line showed that HT can alter the expression of proteins involved in the regulation of apoptosis as well as the cell cycle

to induce its growth inhibitory effect (Zubair *et al.*, 2017). In another study using the ApoE$^{-/-}$CD36$^{-/-}$MSR1$^{-/-}$ animal model to define the roles of MSR1 and CD36 in atherogenesis and lesional macrophage apoptosis, the atherosclerotic lesions showed reduced expression of inflammatory genes and a decrease in plaque necrosis in aortic root lesions (Manning-Tobin *et al.*, 2009). This was accompanied by a 30% decrease in macrophage apoptosis as result of up-regulation in the expression of the anti-apoptotic genes *Bcl2* and *Bcl2l1* in these mice. In this study (Table 5.2), the MSR1 expression levels were induced and this might explain the reduction in the anti-apoptotic *BCL2L1* gene expression observed.

VWF controls the adhesion of platelets to the sites of vascular injury and promotes blood coagulation (van Galen *et al.*, 2012). A previous study has shown the anti-thrombotic benefits of olive oil in part via reduction of platelet aggregation. Using rats receiving oral HT for 6 weeks, a delay in platelet aggregation and prevention of blood clots was observed (Brzosko *et al.*, 2002). In this study, HT significantly down regulated the expression of *VWF* (Table 5.2). This suggests a potential attenuation of blood coagulation, adhesion of platelets to the site of vessel injury and subsequent thrombus formation (Rivera *et al.*, 2009).

As mentioned earlier, cholesterol homeostasis is an important factor in controlling the progression of atherosclerosis (Pennings *et al.*, 2006). Several changes in gene expression were consistent with a protective role for HT. For example, the expression of genes encoding *ABCA1*, *ABCG5* and *ABCG8*, which are all considered as anti-atherogenic because of their critical roles in cholesterol efflux and biliary cholesterol secretion (Yu *et al.*, 2002; Iqbal and Hussain, 2009), was induced by HT (Table 5.3).

Cholesterol homeostasis can also be controlled via modulation of intestinal absorption. NPC1L1 plays a critical role in this and the drug ezetimibe is an inhibitor of this transporter (van Heek *et al.*, 2001; Altmann *et al.*, 2004; Betters and Yu, 2010). NPC1L1 is widely expressed in many tissues with the highest levels in the liver and the small intestine and previous studies have suggested a relationship between NPC1L1 expression and intracellular trafficking and cellular cholesterol content, where cholesterol depletion results to its enhanced expression and translocation to

the cell surface (Yu et al., 2006). NPC1L1 therefore plays a potent anti-atherogenic role and its liver expression was induced by HT (Figure 5.8).

Not all of the HT-mediated changes in gene expression relevant to cholesterol homeostasis appeared to be beneficial. For example, HT also significantly down regulated the expression of *LDLR* (Table 5.2), which mediates the uptake LDL. Reduction in the levels of this gene could potentially attenuate foam cell formation and inhibit disease progression. However, this could also promote atherogenesis by decreasing the clearance of plasma LDL. In addition, HT significantly increased the expression of *MSR1* (Table 5.2), which mediates endocytosis of oxLDL, so this could potentially promote foam cell formation. However, as HT inhibited oxLDL uptake and foam cell formation *in vitro* (Figures 4.6-4.7), this induced expression of *MSR1* is unlikely to be functionally significant and compensation by other SRs and genes implicated in non-receptor-mediated uptake of LPs is possible.

The expression of *HMGCR* involved in the biosynthesis of cholesterol together with *SREBP-1*, a key transcription factor implicated in the control of cholesterol homeostasis (Miserez *et al.*, 2002), was also induced (Figure 5.8). As HT inhibited the plasma levels of total cholesterol and LDL/VLDL, this might be a compensatory mechanism to maintain intracellular cholesterol levels. Future studies should investigate the levels of cholesterol in the liver.

The expression of the *ApoA1* gene was significantly attenuated and this correlates well with decreased plasma HDL levels (Figure 5.4) since ApoA1 is a key apolipoprotein in HDL. More studies on a range of other genes involved in cholesterol homeostasis together with correlation between mRNA and protein expression (e.g. by western blot analysis) will be required to fully understand the actions of HT and delineate the existence of any post-transcriptional regulatory mechanisms.

Previous research showed that under disease conditions, mitochondrial oxidation of FAs is impaired and intracellular levels of FAs are significantly induced, which can potentially lead to arrhythmias or MI (van der Vusse *et al.*, 1992). The expression of FA binding protein 3 (*FABP3*) was significantly down regulated after HT treatment (Table 5.3). This could potentially be crucial in the prevention of accumulation of FAs, and thereby tissue damage.

HT also significantly decreased the expression of *PDGFA* (Table 5.3), an important mitogenic stimulant of vascular tissues, which acts upon SMC to enhance their proliferation and migration during the latter stages of atherosclerosis (Li *et al.*, 2011). This occurs in response to inflammation so reduced expression by HT could potentially be because of its anti-inflammatory actions.

IL-5, TGFβ2 and LIF, on the other hand, are anti-atherogenic. As shown in table 5.2, HT significantly decreases the expression of these genes. Previous studies showed that IL-5 and TGFβ2 control many different cellular functions including proliferation, differentiation and cell survival/apoptosis. In addition; LIF has the ability to attenuate EC's proliferation and induce vaso-relaxation within arteries by increasing NO production (Demyanets *et al.*, 2012). The amount of intimal thickening, which occurs following blood vessel injury due to increased level of VSMC proliferation, can be inhibited by LIF (Sheehy *et al.*, 2006; Takatsu, 2011; Demyanets *et al*. 2012; Tennant and McGeachie, 2018). HT was shown to be able to significantly reduce cellular proliferation *in vitro* (Figure 4.3). However the effect of HT on cell proliferation *in vivo* still needs to be determined in future studies.

The expression of genes encoding pro-inflammatory ECM regulators involved in atherogenesis, such as *IL1R1*, *IL1R2*, *MMP3* and *SERPINβ2*, was significantly down regulated (Table 5.3), which are all likely to contribute to the attenuation of the inflammatory events and the progression of the disease. Type III collagen (Col3α1) is important for the development of the cardiovascular system and for maintaining the normal physiological functions of this organ in adult life (Olsen, 1995). The rupture of unstable atherosclerotic plaque frequently causes acute coronary events and collagen plays a key role in determining plaque stability (Nadkarni *et al.*, 2009). In this study, there was an up regulation in its expression levels (Table 5.3), which suggests a potential involvement of HT in plaque stabilisation.

In addition to the significant changes in gene expression detailed above, there was a trend towards reduced expression of 8 genes by HT (*CCl5, IFN-γ, SOD1, BCL2A1A, BIRC3, PLIN2, PPARα* and *PPARδ*) and a trend towards increased expression of one gene (*TNFαIP3*). Some of these changes are anti-atherogenic. For example, CCL5 is a key chemokine in the recruitment of immune cells to an activated

endothelium and IFN-γ is potentially a master regulator of the disease (Moss, 2015). However, transcription factors such as PPARs activate an anti-atherogenic and anti-inflammatory gene expression programme together with the expression of key genes involved in the control of lipid metabolism and glucose homeostasis in several tissues, including adipose tissue, muscle and liver, ultimately influencing circulating lipid and glucose levels (Ricote and Glass, 2007).

There are many potential sources for plasma cytokines, which are major determinants of the inflammatory status of atherosclerotic disease (Ramji and Davies, 2015). Measuring the levels of plasma cytokines aids in determining the systemic inflammatory status in the presence or absence of HT. HT was not found to significantly affect the plasma levels of IFN-γ, IL-10, IL-6, IL-2, IL-5 and TNF-α proteins. Interestingly, HT significantly decreased the mRNA expression of IL-2, IL-5 and IFN-γ in the liver (Table 5.2). Future studies should seek to determine their protein levels in the liver and in the atherosclerotic lesions. Such studies could also inform on the existence of any post-transcriptional mechanisms in the regulation of cytokine expression as has been previously reported (Vogel and Marcotte, 2012).

In conclusion, the anti-inflammatory, anti-oxidant and hypocholestrolemic activity of HT could potentially be important for human atherosclerosis disease prevention and therapy. HT can potentially be used as a supplement for the treatment of inflammatory diseases to decrease the damages caused by chronic inflammation. As demonstrated in the present study, HT treatment was found to be associated with several anti-atherogenic events such as the attenuation of oxidation levels by inhibition of ROS production, decrease in plasma levels of total cholesterol and LDL/VLDL, and generally promoting a beneficial gene expression programme. However, this study also showed a few pro-inflammatory changes with the expression of some pro-atherogenic genes associated with the disease, induced plasma TG levels and attenuated plasma HDL cholesterol levels. Further studies are required to fully evaluate the effectiveness of HT as this will enhance our understanding of HT actions and could ultimately lead to the identification of novel treatment and prevention strategies to reduce the global prevalence of CVD.

Overall this initial study justifies the use of HT in long term feeding studies

using the atherosclerotic mouse models ($LDLR^{-/-}$) to fully decipher the potential of HT for attenuating the rate of atherosclerosis disease development. The use of $LDL^{-/-}$ mice would also allow study of the effects of HT on adipose tissue, plaque size, immune cell profile within the bone-marrow and gene expression. Such studies form the focus of the next chapter.

Chapter 6

6.1 Introduction

After investigating the protective effects of HT in wild-type C57BL/6J mice fed a HFD, it was decided to investigate its anti-atherogenic potential using the LDLR$^{-/-}$ model system also receiving a HFD. Previous studies have shown that sex hormones alter the immune response during atherosclerosis resulting in gender-dependent differences in disease phenotypes in some cases (Regitz-Zagrosek, 2006; Fairweather, 2015). In particular, research focused on the actions of cytokines such as IFN-γ have demonstrated striking differences in responses between male and female mice in the development of the disease (Whitman *et al.,* 2002). Studies on many other agents have also used both male and female mice (Seeland and Regitz-Zagrosek, 2012). However, a number of questions still need to be addressed on the differences in inflammation processes associated with atherosclerosis in males and females. It is therefore important that both male and female mice are used in studies on atherosclerosis to identify any gender-specific differences.

Therefore, in the studies presented in this chapter, and to make maximum utilisation of all mice that were born and additionally satisfy the 3Rs in animal research (Replacement, Reduction and Refinement), the effect of HT on atherosclerosis development and risk factors related to the disease were investigated in both male and female mice. This would also allow comparisons of different parameters between male and female mice and also identify any gender-specific effects in HT actions.

LDLR$^{-/-}$ mice (male and female) were used for these studies because they show more similarity to atherosclerosis development in humans compared to other models (e.g. ApoE$^{-/-}$)(Getz and Reardon, 2012). Diet-induced atherosclerosis was also employed (HFD) because of direct relevance to western-type diet in disease development in humans. Studies under this objective involved in-depth analysis of weight, plasma lipid profile, oxidative stress and bone marrow cell population. Because of time limitations, plaque burden together with content of lipids, immune cells and gene expression could not be carried out. Nevertheless, tissues were

collected for future studies. Figure 6.1 shows a schematic representation of studies carried out in this chapter.

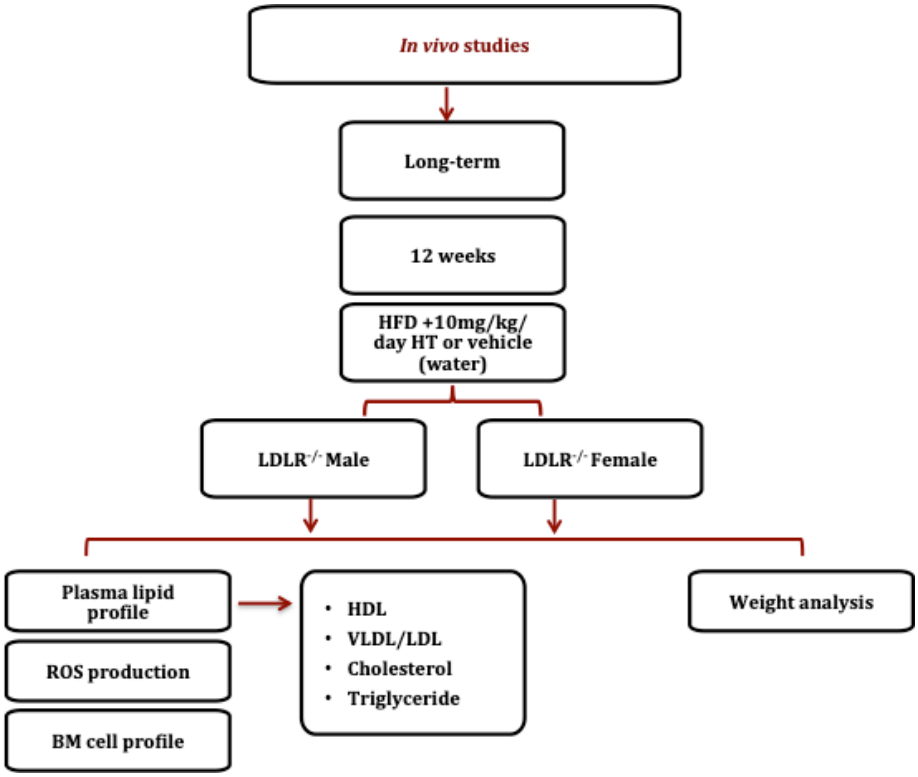

Figure 6.1 Summary of the *in vivo* assays used to determine the protective actions of HT in atherogenesis.

6.2 Studies on the effect of HT in female LDLR$^{-/-}$ mice.

6.2.1 Weight analysis.

The weight of female LDLR$^{-/-}$ mice fed a HFD mixed with 10 mg/kg/day HT or the vehicle control was monitored every 3, 4 or 5 days for 12 weeks. Table 6.1 shows the weight of the mice when determined during the duration of the study and these are depicted in a graphical form on Figure 6.2A. The mouse weight gain correlated with time of HFD feeding in both groups (Table 6.1 and Figure 6.2A). However, there was a trend towards reduction in the overall weight gain (subtracting the mean weight at the end of the experimental period from the mean starting weight) in mice receiving HT when compared to the vehicle control by about 30% (p= 0.09)(Figure 6.2B).

Table 6.1 Weight measurements throughout the study.

Day	Vehicle	HT
	Mean± SEM	**Mean± SEM**
1	20.4 ± 0.3	19.7 ±0.5
4	21.3 ± 0.6	19.9 ± 0.5
12	21.9 ± 1.0	19.8 ± 0.4
15	21.3 ± 0.8	19.5 ± 0.4
18	21.5 ± 1.0	19.6 ± 0.5
23	21.8 ± 1.0	19.9 ± 0.5
26	21.9 ± 0.9	20.1± 0.6
29	22.2 ± 1.0	20.4 ± 0.6
33	22.6 ± 1.1	20.6 ± 0.6
37	23.2 ± 1.2	21.1 ± 0.7
40	23.7 ± 1.2	21.2 ± 0.8
43	23.5 ± 1.0	21.2 ± 0.8
47	23.8 ± 1.1	20.7 ± 0.9
51	23.8 ± 1.1	21.3 ± 0.8
54	23.8 ± 1.0	21.5 ± 0.9

57	24.5 ± 1.1	21.6 ± 1.0
60	24.6 ± 1.1	21.9 ± 1.1
64	24.6 ± 0.9	22.2 ± 1.0
67	24.9 ± 1.0	22.2 ± 1.0
70	24.9 ± 1.0	22.2 ± 1.0
73	25.6 ± 1.1	22.2 ± 1.0
76	26.0 ± 1.1	22.4 ± 1.0
79	25.9 ± 1.4	22.9 ± 1.1
81	26.1 ± 1.4	23.3 ± 1.2
84	26.1 ± 1.5	23.6 ± 1.2

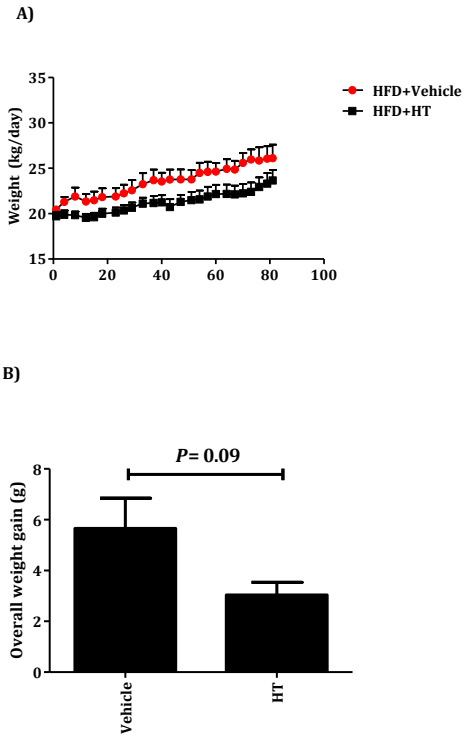

Figure 6.2 HT reduces the average weight gain in female LDLR$^{-/-}$mice fed a HFD.

LDLR$^{-/-}$ mice (vehicle =10, HT= 12) were fed a HFD mixed with vehicle or HT (10/mg/kg/day) for 12 weeks. Weight was monitored regularly throughout the study (every 3-5 days). (A) Graph displays mean ± SEM of average weight of mice during the duration of the study. (B) Average differences in weight gain between the groups at the end of the experimental period. Statistical analysis was carried out using paired Student's t test (*p≤0.05; HT v/s Vehicle).

6.2.2 HT reduces fat pad weight in female LDLR$^{-/-}$ mice fed a HFD.

At the day of termination of the experiment, the weight of the liver, subcutaneous fat pad (Sub-cut) and gonadal fat pad was determined. As shown in Figure 6.3A, HT produced no significant changes in the weight of the livers. In contrast, a trend towards 50% reduction in the weight of the subcutaneous fat depot and a 60% reduction in the weight of gonadal fat pads was observed (p=0.059 and p=0.070 respectively; (Figure 6.3 B-C). This reduction in fat accumulation could be the reason for the possible decrease in mouse weight gain following HT treatment shown previously in Figure 6.2B.

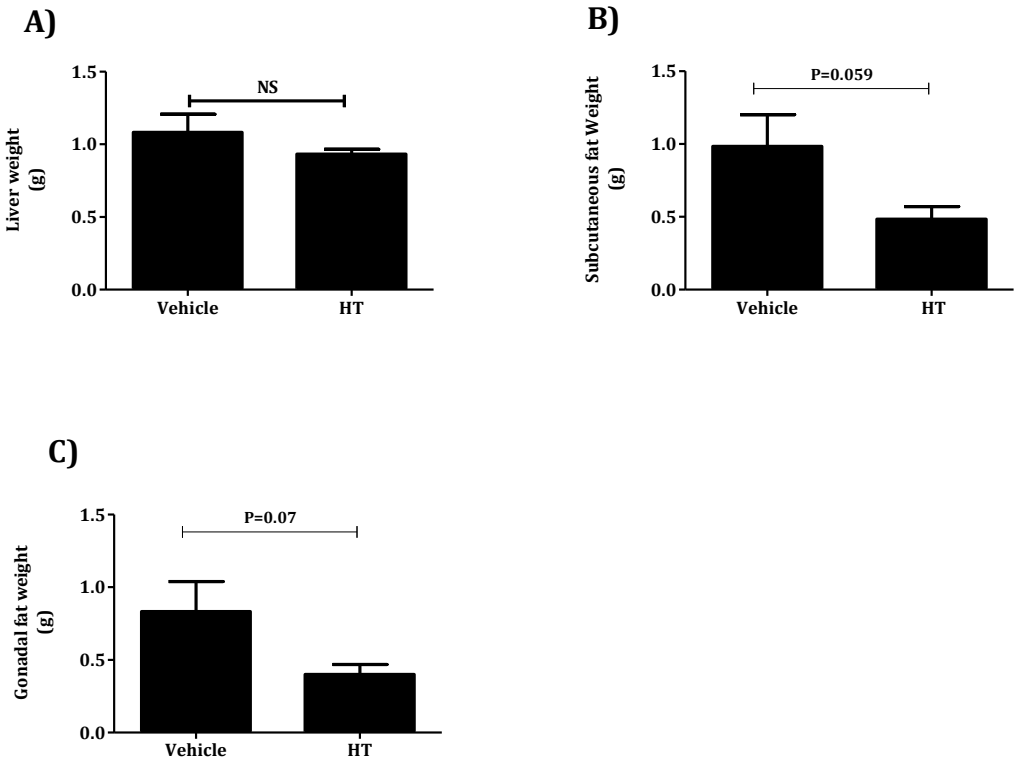

Figure 6.3 HT reduces the fat pad weight in female LDLR$^{-/-}$ mice fed a HFD.

LDLR$^{-/-}$ mice (Vehicle= 10; HT= 12) were fed a HFD mixed with vehicle or HT (10 mg/kg/day) for 12 weeks. The weight of the liver (A), subcutaneous fat pad (B) and gonadal fat pad (C) was determined at the end of the experiment. Graph displays mean ± SEM of the weight of the groups. Statistical analysis was carried out using an unpaired Student's t test (*p≤ 0.05, NS= not significant; HT v/s Vehicle).

6.2.3 HT produces a favourable lipid profile in female LDLR$^{-/-}$ mice fed a HFD.

Plasma levels of total cholesterol, LDL/VLDL and HDL were determined in female LDLR$^{-/-}$ mice after 12 weeks of receiving a HFD mixed with either vehicle or 10 mg/kg/day HT. As shown in Figure 6.4A**,** HT produced a significant 24% reduction in plasma total cholesterol levels (p=0.046) when compared to the control. In addition, HT produced a trend towards a 23% reduction in plasma LDL/VLDL levels that failed to reach significance (p=0.07). In contrast, HT showed no significant changes in the plasma HDL levels together with the total cholesterol: LDL/VLDL ratio, total cholesterol: HDL ratio or LDL/VLDL: HDL ratio (Figure 6.4C-F). These data provide initial evidence for an anti-atherogenic effect of HT via the control of plasma lipid profile.

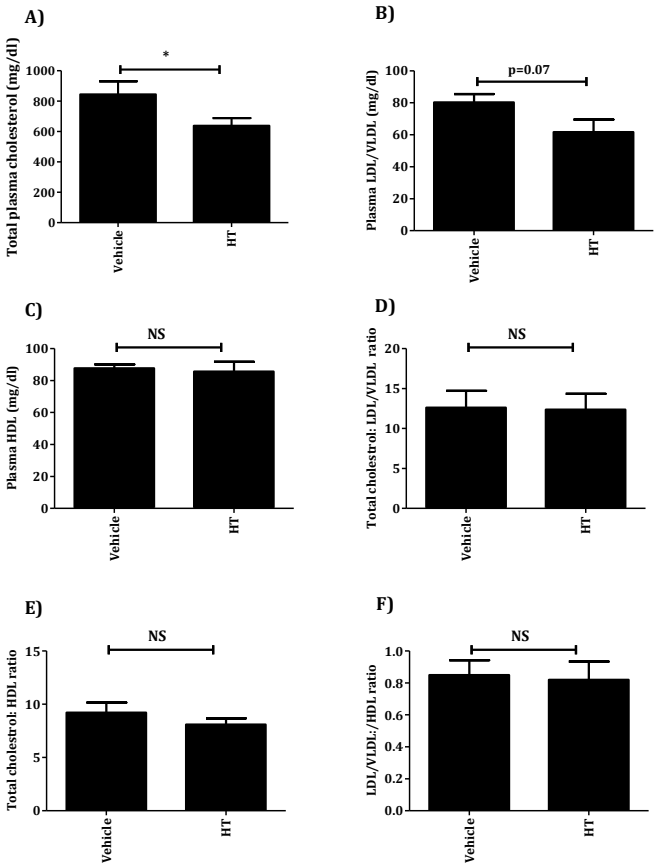

Figure 6.4 The effect of HT on plasma lipid profile in female LDLR$^{-/-}$ mice fed a HFD.

Total cholesterol (A), LDL/VLDL (B) and HDL (C) levels were determined in the plasma of 22 female LDLR$^{-/-}$ mice (vehicle= 10; HT= 12) following 12 weeks feeding of HFD mixed with vehicle or HT (10 mg/kg/day). The ratios of total cholesterol: LDL/VLDL (D), total cholesterol: HDL (E) and LDL/VLDL: HDL (F) were also assessed. Graphs display mean ± SEM for each group. Statistical analysis was carried out using an unpaired Student's t test (*P≤0.05, NS= not significant; HT v/s Vehicle).

6.2.4 HT has no effect on plasma TG levels in female LDLR$^{-/-}$ mice fed a HFD.

Plasma TG levels were determined in female LDLR$^{-/-}$ mice after 12 weeks of receiving a HFD mixed with either vehicle or 10 mg/kg/day of HT. As shown in Figure 6.5A**,** HT had no significant effect on plasma TG levels when compared to the vehicle control. The ratios of TG to total cholesterol, to LDL/VLDL and to HDL levels were also assessed. As shown in Figure 6.5B-D**,** HT had no effect on these ratios when compared to the control.

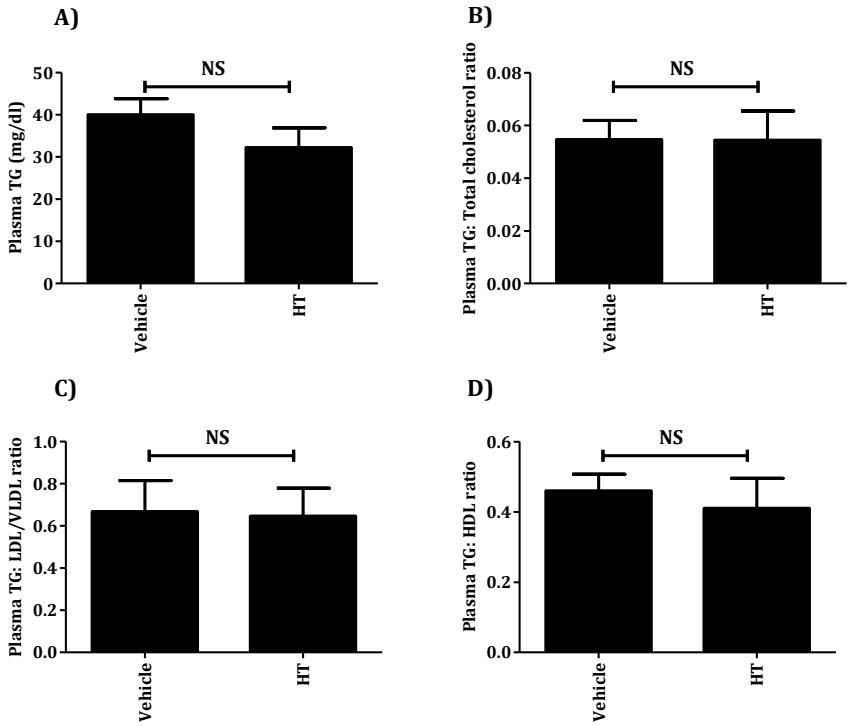

Figure 6.5 HT has no significant effect on plasma TG levels in female LDLR$^{-/-}$ mice fed a HFD.

TG levels (A) from female LDLR$^{-/-}$ mice (Vehicle=10, HT=12) were determined after 12 weeks of receiving a HFD mixed with vehicle or 10 mg/kg/day HT. The ratios of TG: total cholesterol (B), TG: LDL/VLDL (C) and TG: HDL cholesterol (D) were also assessed. Graphs display mean ± SEM for each group. Statistical analysis was carried out using an unpaired Student's t test, (NS=not significant; HT v/s Vehicle).

6.2.5 HT has no effect on ROS production in female LDLR$^{-/-}$ mice fed a HFD.

Previous studies showed that females appear to be less susceptible to oxidative stress than males (Kander *et al.*, 2017). The effect of HT on plasma ROS levels was therefore determined in LDLR$^{-/-}$ mice fed a HFD. As shown in Figure 6.6, HT produced no significant changes in plasma ROS levels when compared to the control.

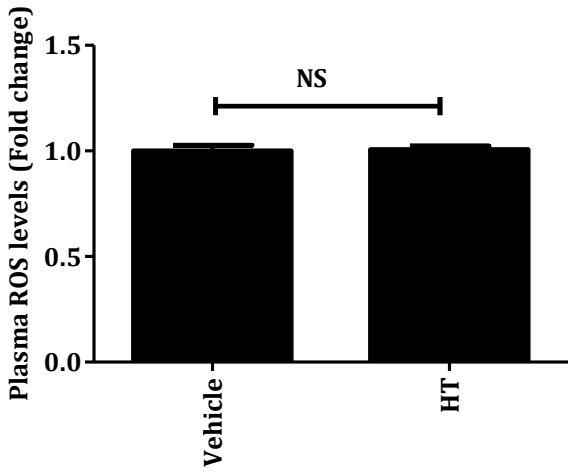

Figure 6.6 Plasma ROS levels were not affected in female LDLR$^{-/-}$ mice following feeding of a HFD with HT.

Female LDLR$^{-/-}$ mice (vehicle=10, HT=12) were fed a HFD mixed with vehicle or HT (10 mg/kg/day) for 12 weeks. The plasma levels of ROS were determined. The graph displays mean ± SEM of each group with values from the vehicle control arbitrarily assigned as 1. Statistical analysis was carried out using an unpaired Student's t test (NS= not significant, HT v/s Vehicle).

6.2.6 The effect of HT administration on the number of white blood cells (WBC) within the bone marrow of female LDLR$^{-/-}$ mice fed a HFD.

The levels of WBC within the bone marrow can be an indicator of the inflammatory state of an individual (Madjid *et al.*, 2004; Madjid and Fatemi, 2013). The WBC cell population in the bone marrow of female LDLR$^{-/-}$ mice following 12 weeks of receiving a HFD mixed with either vehicle or 10 mg/kg/day HT was therefore determined. Haemocytometer was first used to identify the effect of HT on total cellularity of the bone marrow followed by multiplying the total cell count with the frequency of WBC. As shown in Figure 6.7, HT produced no significant changes in WBC in the bone marrow when compared to the control group.

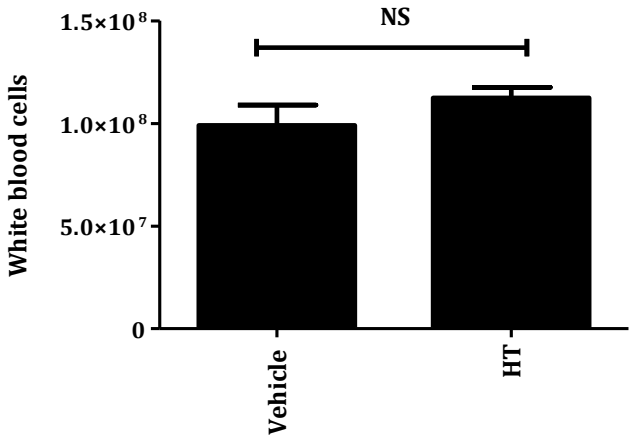

Figure 6.7 HT had no effect on the proportion of WBC present in the bone marrow of female LDLR$^{-/-}$ mice fed a HFD.

The proportion of WBC was assessed in the bone marrow of female LDLR$^{-/-}$ mice (vehicle =4, HT =4) fed a HFD mixed with vehicle or HT (10 mg/kg/day) for 12 weeks. A bar graph displays mean ± SEM of WBC frequency of total cellularity in the bone marrow. Statistical analysis was carried out using an unpaired Student's t test (NS= Not significant; HT v/s Vehicle).

6.2.7 The effect of HT administration on the SLAM cell populations within the bone marrow of female LDLR$^{-/-}$ mice fed a HFD.

SLAM cell population levels were assessed in the bone marrow of female LDLR$^{-/-}$ mice after 12 weeks of receiving a HFD mixed with either vehicle or 10 mg/kg/day of HT. Representative flow plots of the cell populations in the bone marrow gating strategy are presented in Figure 1.24**.** The arrows indicate how each HSC, MPP and HPC 1 and 2 were identified within the preceding gating strategy. The axis represents the various markers used to separate the cell populations (see Table 2.10 for further details). The side scatter (SSC-H) is a measurement of the amount of light that is reflected by the particles within the cells and therefore can be used to determine the granularity of the cells. Panels A-E shows the frequency of LSK, HPC1, HPC2, HSC and MPP cell population respectively. HT had no significant effect on all these cell populations.

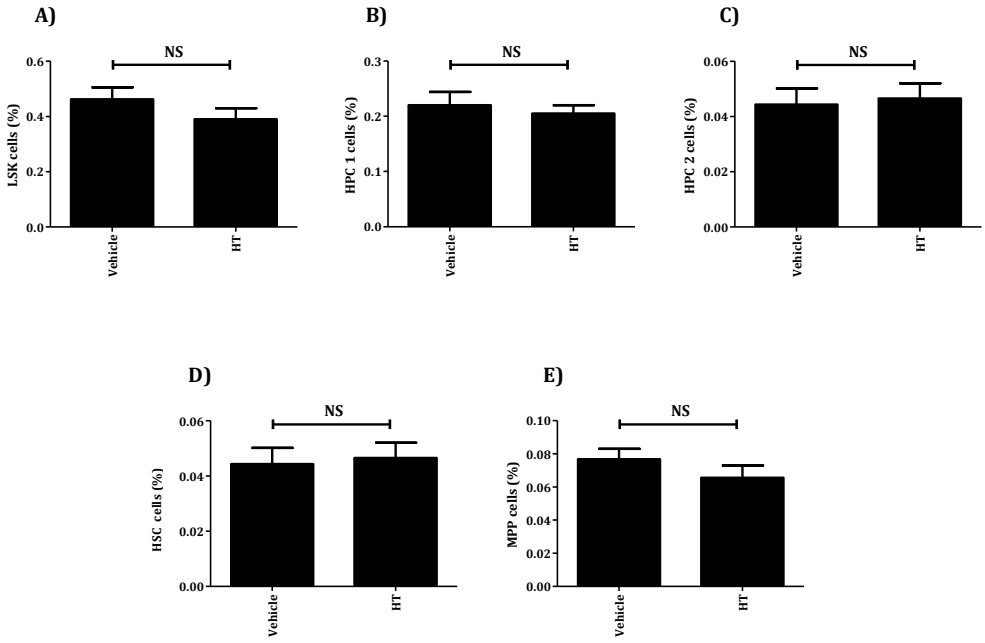

Figure 6.8 The effect of HT administration on the SLAM cell population within the bone marrow of female LDLR$^{-/-}$ mice fed a HFD.

SLAM cell population levels were assessed in the bone marrow of LDLR$^{-/-}$ mice (vehicle= 4, HT= 4) fed a HFD mixed with vehicle or HT (10 mg/kg/day) for 12 weeks. The bar graphs show the frequency (mean ± SEM) of LSK (A), HPC1 (B), HPC2 (C), HSC (D) and MPP (E) cell populations in the bone marrow. Statistical analysis was carried out using an unpaired Student t test (NS= not significant; HT v/s Vehicle).

6.2.8 The effect of HT administration on the progenitor cell population within the bone marrow of female LDLR$^{-/-}$ mice fed a HFD.

The progenitor cell populations were assessed in the bone marrow of female LDLR$^{-/-}$ mice after 12 weeks of receiving a HFD mixed with either vehicle or 10 mg/kg/day of HT. Representative flow plots of the gating strategy are shown in Figure 1.24. The arrows indicate how CMP, MEP, GMP and CLP in the LK-progenitor class were identified within the preceding gating strategy. The axis represents the various markers used to separate the cell populations (see Table 2.10 for further details). The side scatter (SSC-H) is a measurement of the amount of light that is reflected by the particles within the cells and therefore can be used to determine the granularity of the cells. HT had no significant effect on the frequency of total LK cells compared to the vehicle control (Figure 6.9 A). In contrast, HT produced a significant increase in the

frequency of CMP by 34% (p=0.01), GMP by 43% (p=0.02), MEP by 39% (p=0.002) and a significant reduction by 99% of CLP (p<0.001) (Figure 6.9B-E).

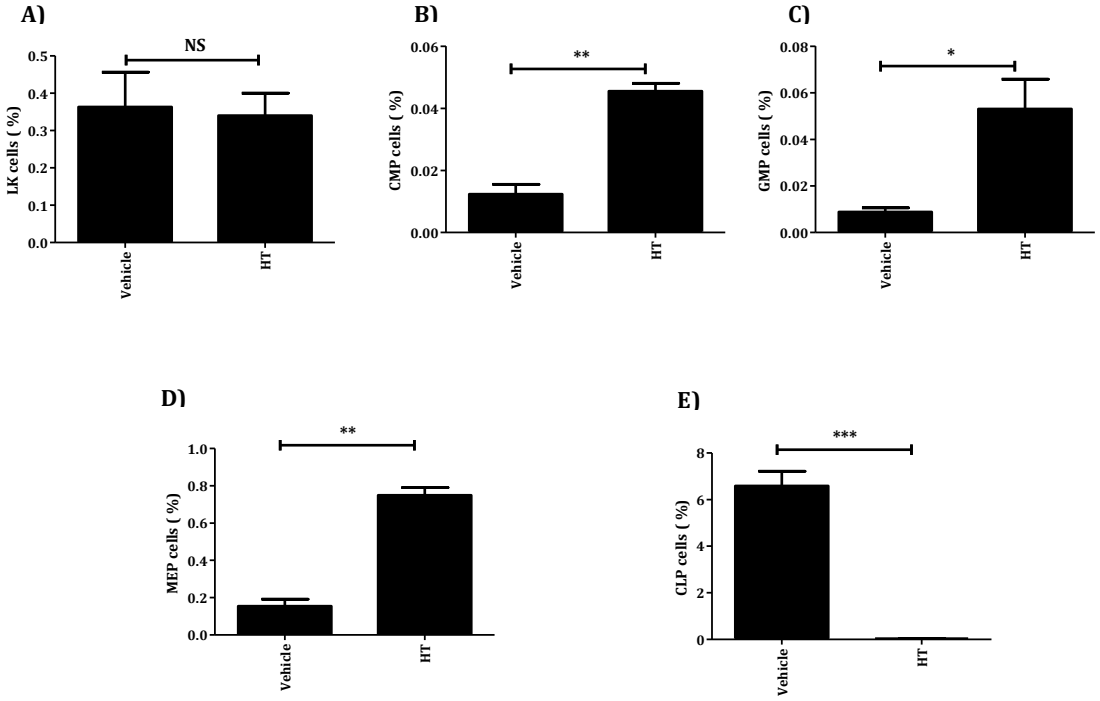

Figure 6.9 The effect of HT on the proportion of progenitor cell population present in the bone marrow of female LDLR$^{-/-}$ mice.

Progenitor cell population levels were assessed in the bone marrow of LDLR$^{-/-}$ mice (vehicle= 4, HT= 4) fed a HFD mixed with vehicle or HT (10 mg/kg/day) for 12 weeks. Bar graphs display the frequency (mean ± SEM) of LK (A), CMP (B), GMP (C), MEP (D) and CLP (E) populations in the bone marrow. Statistical analysis was carried out using an unpaired Student's t test (*P≤0.05; **p≤ 0.01; ***p≤ 0.001, NS= not significant, HT v/s Vehicle).

6.3 Study on the effect of HT on male LDLR$^{-/-}$ mice

6.3.1 Weight analysis

The weight of male LDLR$^{-/-}$ mice fed a HFD mixed with 10 mg/kg/day of HT or vehicle was monitored every 3, 4 or 5 days for 12 weeks. Mouse weight gain was correlated with time (Table 6.2 and Figure 6.10). However, HT had no effect on the overall weight gain by the animals compared to the vehicle control (Figure 6.10B).

Table 6.2 Weight measurements throughout the study.

Day	Vehicle	HT
	Mean± SEM	**Mean± SEM**
1	24.6 ± 0.6	26.0 ±0.2
3	25.4 ± 0.7	27.2 ± 0.4
5	25.9 ± 0.6	27.5 ± 0.4
10	26.5 ± 0.6	28.1 ± 0.4
14	26.8 ± 0.8	28.4 ± 0.4
18	27.4 ± 0.8	28.5 ± 0.6
21	27.9 ± 0.9	29.4 ±0.5
26	28.4 ± 0.9	29.8 ± 0.5
31	28.4 ± 1.1	30.3 ± 0.5
35	29.4 ± 1.0	31.1 ± 0.5
38	29.8 ± 1.1	31.2 ± 0.6
41	30.6 ± 1.1	31.6 ± 0.6
46	31.0 ± 1.1	32.0 ± 0.6
49	31.4 ± 1.1	32.6 ± 0.6
52	31.9 ± 1.1	33.1 ± 0.6
55	31.5 ± 1.3	33.6 ± 0.7
58	32.6 ± 1.2	33.6 ± 0.7
62	32.3 ± 1.4	34.2 ± 0.7
66	32.6 ± 1.5	34.5 ± 1.0
69	33.3 ± 1.4	34.5 ± 0.9
73	33.9 ± 1.5	34.5 ± 1.0
77	33.9 ± 2.2	34.1 ± 0.7
81	33.8 ± 4.7	34.6 ± 1.0
84	38.4 ± 4.7	35.7 ± 1.0

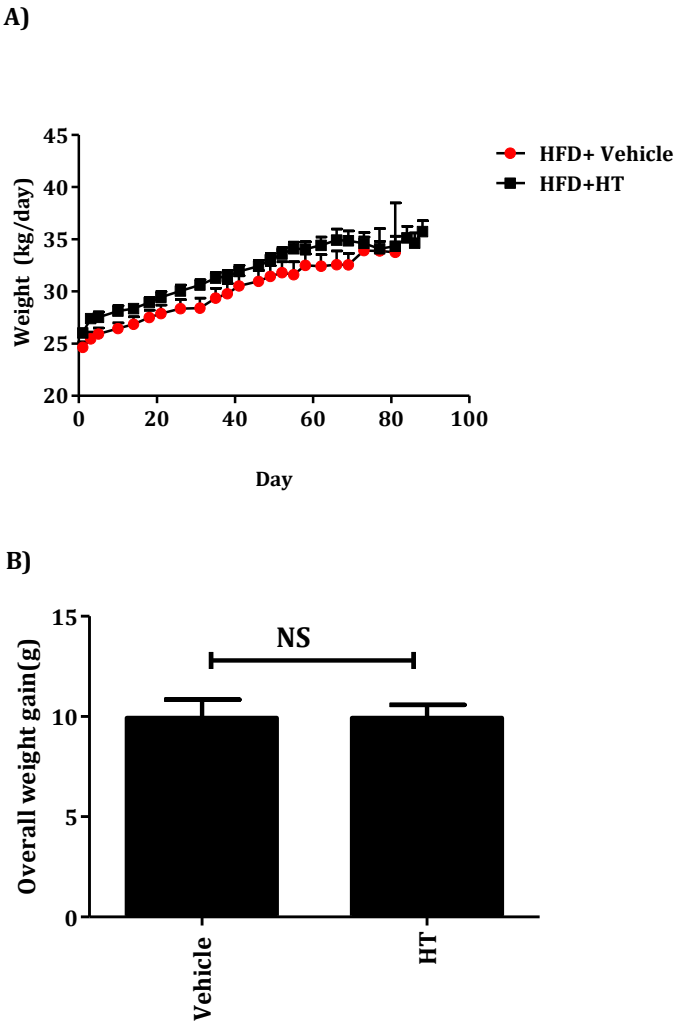

Figure 6.10 HT has no effect on weight gain in male LDLR$^{-/-}$ mice fed a HFD.

Male LDLR$^{-/-}$ mice (vehicle=12; HT=10) were fed a HFD with vehicle control (water) or HT (10 mg/kg/day) for 12 weeks. Weight was monitored regularly throughout the study (every 3-5 days). Panel A displays the weight of the animals whereas panel B shows the overall weight gain (both mean ± SEM). Statistical analysis was carried out using an unpaired Student's t test (NS= not significant; HT v/s Vehicle).

6.3.2 HT reduces the weight of the liver and gonadal fat pad in male LDLR$^{-/-}$ mice fed a HFD.

At the termination of the experiment, the weight of the liver, subcutaneouse fat pad and gonadal fat pad was determined. As shown in Figure 6.11 (panels A and C), HT produced a significant 14% reduction in the weight of the liver (p=0.007) and a 25% decrease in the weight of the gonadal fat pad (p=0.03) when compared to the

vehicle control. In contrast, HT had no significant effect on the weight of the subcutaneous fat pad when compared to the vehicle control (Figure 6.11B).

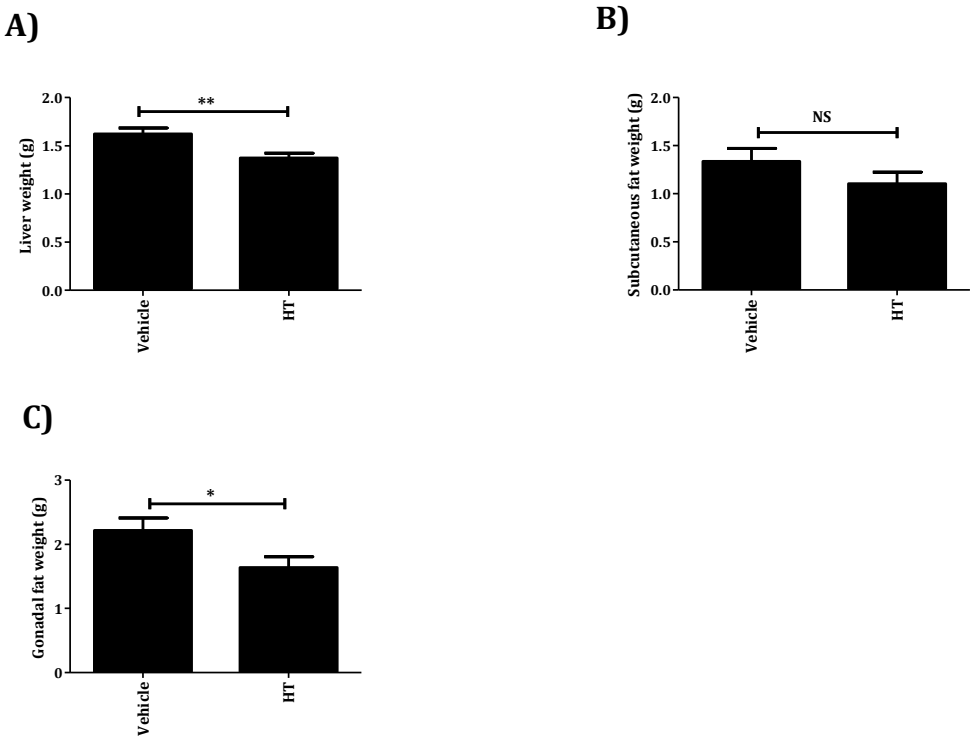

Figure 6.11 HT produces a reduction in the liver and gonadal fat pad weight in male LDLR$^{-/-}$ mice fed a HFD.

Male LDLR$^{-/-}$ mice (vehicle=12, HT=10) were fed a HFD with vehicle or HT (10 mg/kg/day) for 12 weeks. The weight of the liver (A), subcutaneous fat (B) and gonadal fat (C) was determined at the end of the experiment. Graphs display mean ± SEM of organ weight in each group. Statistical analysis was carried out using an unpaired Student's t test (*p≤0.05, **p≤0.01, NS=not significant; HT v/s Control).

6.3.3 The effect of HT on plasma lipid levels in male LDLR$^{-/-}$ mice fed a HFD.

Figure 6.12A shows that the plasma levels of total cholesterol were significantly reduced by 15% (p=0.046) after 12 weeks of administration of HFD mixed with 10 mg/kg/day HT to male LDLR$^{-/-}$ mice compared to those receiving the vehicle. In contrast, HT produced no significant changes in the plasma levels of LDL/VLDL or HDL (Figure 6.12 B-C) along with total cholesterol: LDL/VLDL, total cholesterol: HDL or the LDL/VLDL: HDL cholesterol ratios (Figure 6.12D-F).

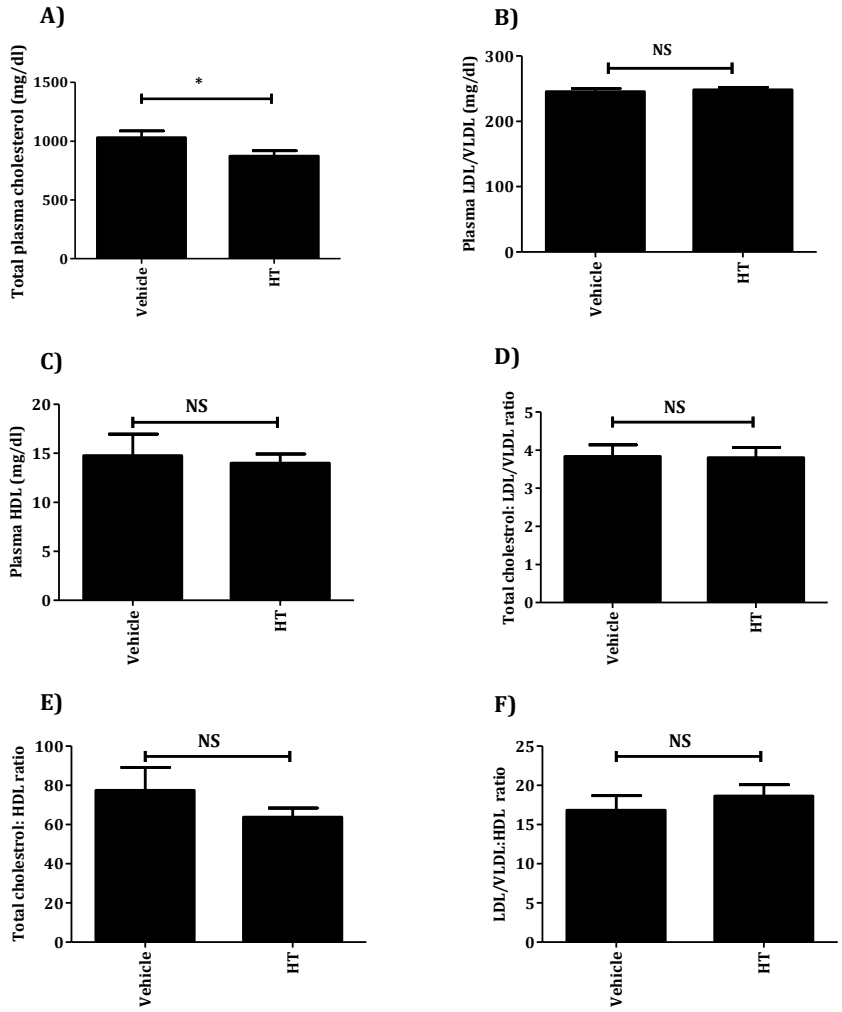

Figure 6.12 The effect of HT on plasma lipid profile in male LDLR$^{-/-}$ mice fed a HFD.

Male LDLR$^{-/-}$ mice (Vehicle=10; HT=11) were fed a HFD mixed with vehicle or HT (10 mg/kg/day) for 12 weeks. The plasma levels of total cholesterol (A), LDL/VLDL (B) and HDL (C) were determined. The ratios of total cholesterol: LDL/VLDL (D), total cholesterol: HDL (E) and LDL/VLDL: HDL cholesterol (F) were also assessed. In each case, graphs display mean ± SEM. Statistical analysis was carried out using an unpaired Student's t test (*P≤0.05, NS=not significant; HT v/s Vehicle).

6.3.4 HT reduces plasma TG levels in male LDLR$^{-/-}$ mice fed a HFD.

TG levels were measured in male LDLR$^{-/-}$ mice after 12 weeks of receiving a HFD mixed with either vehicle or 10 mg/kg/day of HT. As shown in Figure 6.13A, there was a significant 27% reduction in the total TG levels (p=0.03) in mice receiving HT compared to the vehicle. The ratios of TG to total cholesterol, to LDL/VLDL and to

HDL levels were also assessed. As shown in Figure 6.13 (panels B and D), HT produced a significant 33% decrease in the TG: total cholesterol ratio (p=0.04) and a 33% reduction in TG: HDL ratio (p=0.011) when compared to the vehicle control. In contrast, HT produced a trend towards reduction of TG: LDL/VLDL ratio of about 26% that failed to reach significance (p=0.09) (Figure 6.13 C).

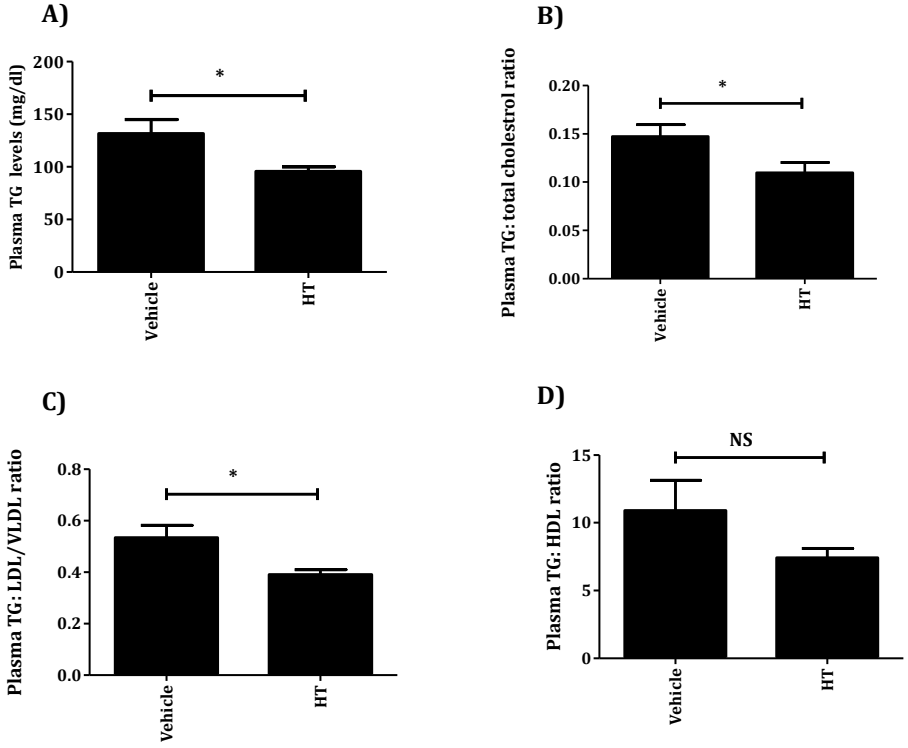

Figure 6.13 The effect of HT on plasma TG levels in male LDLR$^{-/-}$ mice fed a HFD.

Male LDLR$^{-/-}$ mice (Vehicle=10; HT=8) were fed a HFD mixed with vehicle or HT (10 mg/kg/day) for 12 weeks. The plasma levels of TG (A) were determined. The ratios of TG: total cholesterol (B), TG: LDL/VLDL cholesterol (C) and TG: HDL cholesterol (D) were also assessed. In each case, graphs display mean ± SEM. Statistical analysis was carried out using an unpaired Student's t test (*P≤0.05; HT v/s Vehicle).

6.3.5 HT attenuates ROS production in male LDLR$^{-/-}$ mice fed a HFD.

Plasma ROS levels were assessed in male LDLR$^{-/-}$ mice after 12 weeks of receiving a HFD mixed with either vehicle or 10 mg/kg/day of HT. HT produced a significant 15% reduction in the plasma ROS levels (p=0.003) when compared to the vehicle control (Figure 6.14).

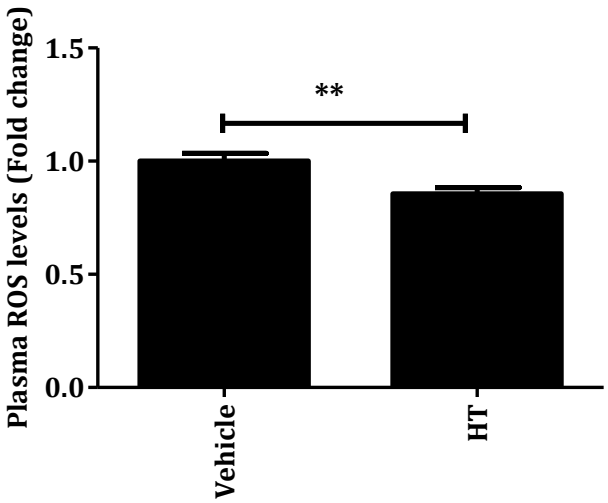

Figure 6.14 The effect of HT on plasma ROS levels in male LDLR$^{-/-}$ mice fed a HFD.

Male LDLR$^{-/-}$ mice (Vehicle= 10; HT= 12) were fed a HFD mixed with vehicle or HT (10 mg/kg/day) for 12 weeks. Graphs display mean ± SEM of plasma ROS levels for each group with values from the vehicle control arbitrarily assigned as 1. Statistical analysis was carried out using an unpaired Student's t test (**P≤0.01; HT v/s Vehicle).

6.3.6 The effect of HT administration on the number of WBC within the bone marrow of male LDLR$^{-/-}$ mice fed a HFD.

WBC in the bone marrow of male LDLR$^{-/-}$ mice were determined after 12 weeks of receiving a HFD mixed with either vehicle or 10 mg/kg/day HT. Haemocytometer was first used to identify the effect of HT on total cellularity of the bone marrow followed by multiplying the total cell count with the frequency of WBC. As shown in Figure 6.15, HT produced no significant changes in WBC in the bone marrow when compared to the control group.

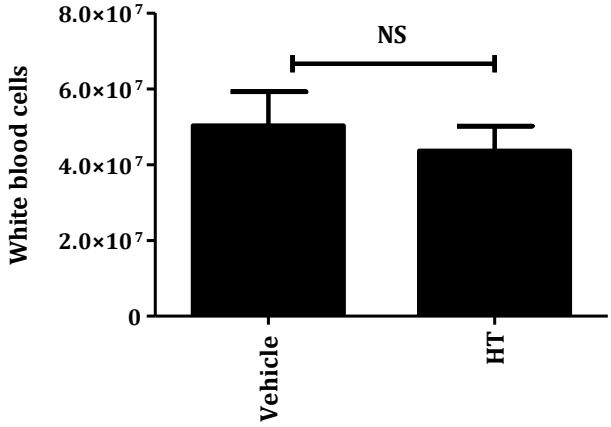

Figure 6.15 HT has no effect on the frequency of WBC present in the bone marrow of male LDLR$^{-/-}$ mice fed a HFD.

WBC population was assessed in the bone marrow of male LDLR$^{-/-}$ mice (vehicle= 10, HT= 12) fed a HFD mixed with the vehicle control or HT (10 mg/kg/day) for 12 weeks. Graph displays mean ± SEM of WBC frequency of total cellularity in the bone marrow. Statistical analysis was carried out using an unpaired Student's t test NS= Not significant; HT v/s Vehicle).

6.3.7 The effect of HT administration on the SLAM cell populations within the bone marrow of male LDLR$^{-/-}$ mice fed a HFD.

SLAM cell population levels were assessed in the bone marrow of male LDLR$^{-/-}$ mice after 12 weeks of receiving HFD mixed with either vehicle or 10 mg/kg/day of HT. Gating strategy was applied as described previously (Figure 1.24 and Section 2.14). HT produced a trend of 15% reduction in the frequency of MPP (p=0.09) (Figure 6.16E). In contrast, HT produced no significant changes in the frequency of HPC1, HPC2, HSC1 or LSK when compared to the vehicle control (Figure 6.16 A-D) though the reduction in LSK almost showed a trend (p=0.12).

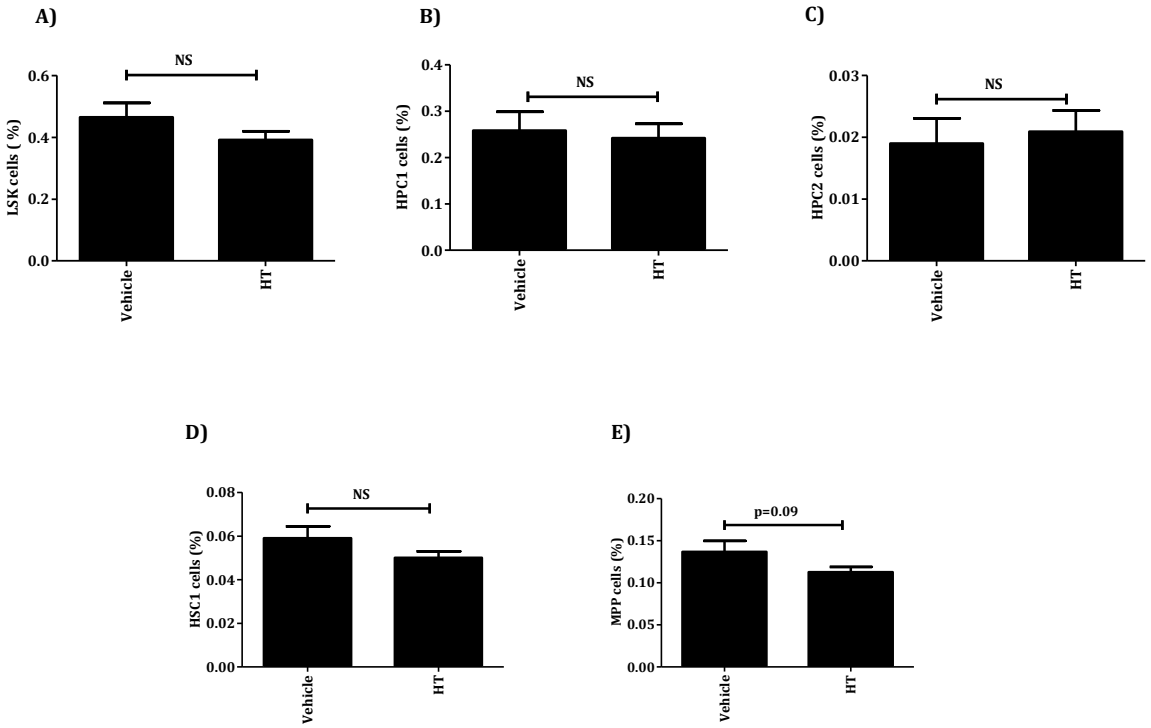

Figure 6.16 The effect of HT on the proportion of LSK, HPC, MPP and HSC present in the bone marrow of male LDLR$^{-/-}$ mice fed a HFD.

SLAM cell populations were assessed in the bone marrow of male LDLR$^{-/-}$ mice (vehicle= 10, HT= 11) fed a HFD mixed with vehicle or HT (10 mg/kg/day) for 12 weeks. Graphs display mean ± SEM of the frequency of LSK (A), HPC1 (B), HPC2 (C), HSC (D), and MPP (E) populations in the bone marrow as a percentage of total WBC cell population. Statistical analysis was carried out using an unpaired Student's t test (NS= not significant; HT v/s Vehicle).

6.3.8 The effect of HT administration on the progenitors cell population within the bone marrow of male LDLR$^{-/-}$ mice fed a HFD.

Progenitor cell populations were assessed in the bone marrow of male LDLR$^{-/-}$ mice after 12 weeks of receiving a HFD mixed with either the vehicle or 10 mg/kg/day of HT. The flow plots for the gating strategy applied was described previously (Figure 1.24 and Section 2.14). HT produced no significant change in the frequency of LK, GMP and CLP when compared to the vehicle control (Fig. 6.17 A, C and E respectively). In contrast, HT produced a significant 40% reduction in the frequency of CMP cells (p=0.022) and a trend towards a 33% decrease in MEP cells (p=0.08) when compared to the vehicle control (Fig. 6.17 B and D respectively).

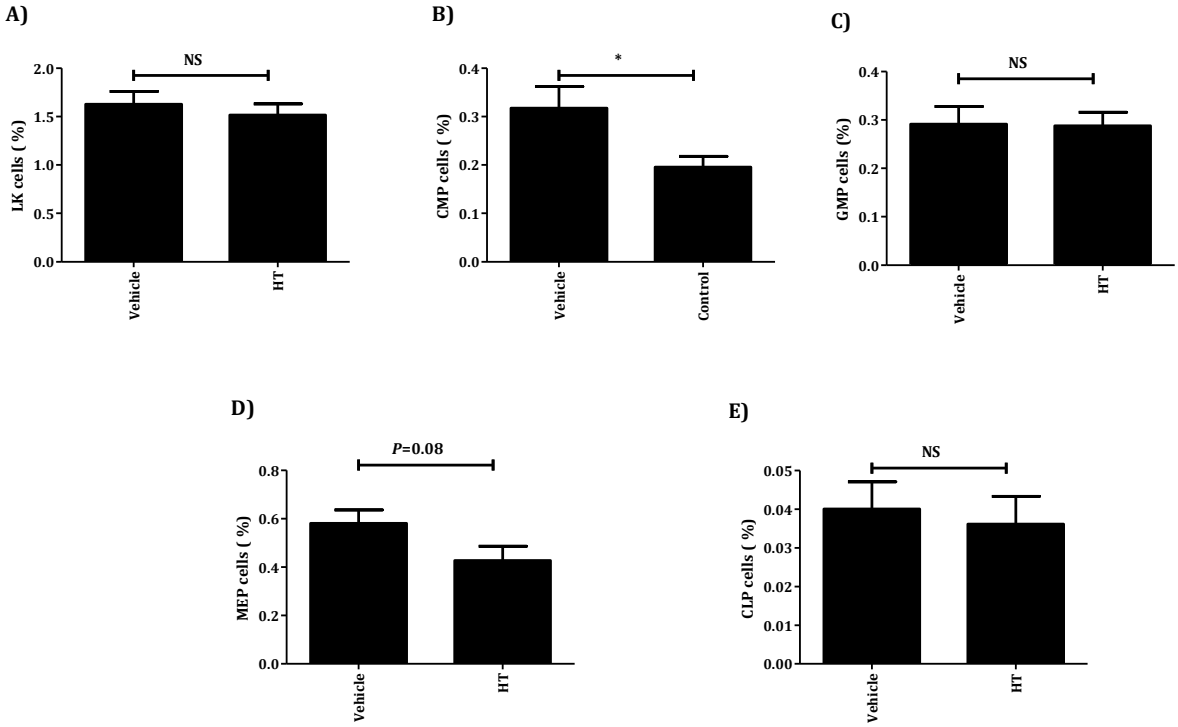

Figure 6.17 the effect of HT on the proportion of progenitor cells present in the bone marrow of male LDLR$^{-/-}$ mice fed a HFD.

The progenitor cell populations were assessed in the bone marrow of male LDLR$^{-/-}$ mice (Vehicle=10, HT=11) after 12 weeks of receiving a HFD mixed with either vehicle or 10 mg/kg/day of HT. Bar graphs display the mean ± SEM of LK (A), CMP (B), GMP (C), MEP (D) and CLP (E) cell populations frequency. Statistical analysis was carried out using an unpaired Student's t test (*P≤0.05; NS=not significant; HT v/s Vehicle).

6.3.9 The effect of HT on macrophages and myeloid-derived suppressor cell (MDSC) populations within the bone marrow of male LDLR$^{-/-}$ mice fed a HFD.

Macrophages (Mac1^{+}), MDSC (Mac1^{+}/Gr1^{+}), B-cells (B220^{+}), T-cells (CD3^{+}) and RBC (Ter119 $^{+}$) populations were also assessed in the bone marrow of male LDLR$^{-/-}$ mice after 12 weeks of receiving HFD mixed with either vehicle or 10 mg/kg/day of HT. A flow plots of the gating strategy of different cell populations are shown in Figure 1.25. HT significantly reduced the level of macrophages by 43% (p=0.04) and produced a trend towards 23% reduction of MDSC that failed to reach significance (p=0.06) (Figure 6.18 A-B). In contrast, HT had no significant effect on the levels of RBC, B-cells and T-cells when compared to the vehicle control (Figure 6.18 C-E).

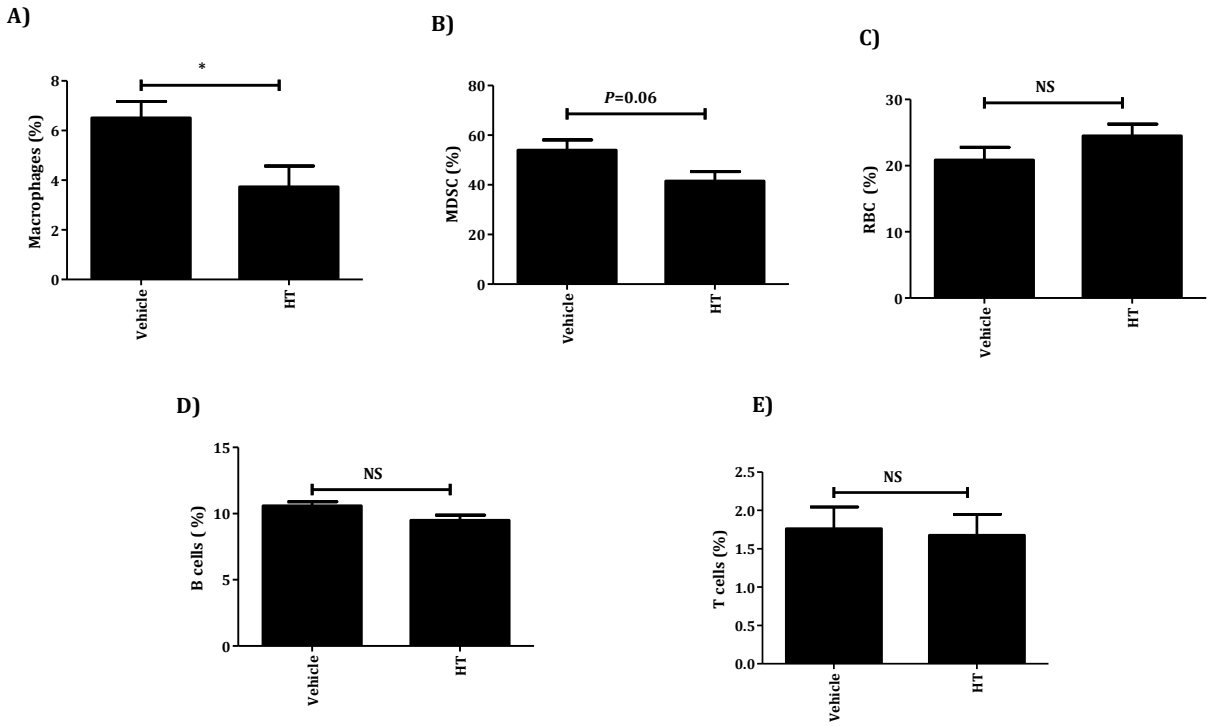

Figure 6.18 HT affects the frequency of lineage cell populations present in the bone marrow of male LDLR$^{-/-}$ mice fed a HFD.

Lineage positive class cell population levels were assessed in the bone marrow of male LDLR$^{-/-}$ mice (vehicle= 5, HT= 5) fed a HFD mixed with vehicle or HT (10/mg/kg/day) for 12 weeks. The bar graphs display the mean ± SEM frequency of macrophages (A), MDSC (B), RBC (C), B-cells (D) and T-cells (E) in the bone marrow. Statistical analysis was carried out using an unpaired Student's t test (*P≤0.05; NS= not significant, HT v/s Vehicle).

6.4 Discussion

Atherosclerosis is the leading cause of death in men and women worldwide, yet more men die from CVD than women and at a relatively younger age (Roger *et al.*, 2011). A number of studies show that women and men differ in their reported symptoms of CVD and drugs that are more effective in men may not be as effective or have unexpected side effects in women (Regitz-Zagrosek, 2006; Seeland and Regitz-Zagrosek, 2012). In the studies presented in this chapter, the *in vivo* effects of HT and the possibility of using it as an anti-atherogenic preventative/treatment was explored in female and male $LDLR^{-/-}$ mice after 12 weeks of receiving a HFD. The results shed light on the action of HT on numerous parameters that can provide additional evidence for its anti-atherogenic properties that were previously observed during *in vitro* and the short-term *in vivo* studies on wild-type mice (Chapters 4 and 5) and how the effect of HT varies between males and females. Table 6.3 summaries the effect of HT in female and male mice based on the findings in this study. Table 6.3 also shows the general gender- specific variations where there were significant differences in the weight, gonadal fat weights, total cholesterol, LDL/VLDL levels, HDL and WBC cell population 'before and after' HT treatment. On the other hand, liver and subcutaneous fat weight, TG and ROS levels showed no significant differences between the genders before and after HT treatment.

	Female				Male				Male vs Female	
Parameter	**Vehicle**	**HT**			**Vehicle**	**HT**			**Vehicle**	**HT**
	Mean ± SEM	**Mean ± SEM**	**Level (%)**	***p*-Value**	**Mean ± SEM**	**Mean ± SEM**	**Level (%)**	***p*-Value**	***p*-Value**	***p*-Value**
Weight gain (g)	5.6± 1.2	3±0.05	30 ↓	0.09	9.9±0.9	9.9±0.6	0	NS	NS	<0.001 (***)
Liver (g)	1.1± 0.12	0.9±0.03	7 ↓	NS	1.6±0.06	1.4±0.05	12.5 ↓	0.007 (**)	NS	NS
Gonadal (g)	0.8± 0.2	0.4±0.06	60 ↓	0.07	2.2±0.2	1.6±0.16	25 ↓	0.03 (*)	0.001 (**)	<0.001 (***)
Sub-cut (g)	1 ±0.2	0.5±0.1	50 ↓	0.06	1.3±0.13	1.1±0.12	7.7 ↓	NS	NS	NS
Total cholesterol (mg/dl)	844 ±86.9	638.4±50.5	24 ↓	0.05 (*)	1030±57.2	872±45.6	15 ↓	0.05 (*)	0.001 (**)	<0.001 (***)
LDL/VLDL (mg/dl)	80.3 ±5.2	61.7±7.8	23 ↓	0.07	245±5.2	248±3.6	1.2 ↑	NS	0.01 (*)	<0.001 (***)
HDL (mg/dl)	87.7 ±2.3	85.6±6.2	2.3 ↓	NS	14.7±2.2	14±0.94	0	NS	NS	<0.001 (***)
TG (mg/dl)	40 ±3.7	32±4.6	20 ↓	NS	131.6±13.2	95±4.4	14 ↓	0.007 (**)	NS	NS
ROS (FC)	1 ±0.03	1±0.02	0	NS	1±0.03	0.85±0.03	15 ↓	NS	NS	NS
WBC	$99X10^6$	$112X10^6$	13 ↑	NS	$50X10^6$	$43X10^6$	14 ↓	NS	<0.001(***)	0.01 (**)

Table 6.3 Summery of the effect of HT in female vs. males $LDLR^{-/-}$ mice fed HFD

Several studies have reported that HT did not exert any effect on body weight levels (González-Santiago *et al.*, 2006). Indeed, as demonstrated in the studies presented in Chapter 5, HT had no effect on weight gain in wild-type mice fed a HFD for 21 days. In the studies presented in this Chapter, HT treatment showed a trend in weight loss in the female model that failed to reach significance (Figure 6.2B). In contrast, no significant detectable changes in weight gain by HT seen in male mice when compared to the vehicle control (Figure 6.10B). The attenuation of weight gain observed in female mice was potentially due to a decrease in the accumulation of the subcutaneous and gonadal fats (Figure 6.3 B-C). A previous *in vitro* study reported that HT dose-dependently reduced adipogenesis during the early stages of differentiation by down regulation of the expression of adipogenesis-related genes implicated in intracellular lipid accumulation (Drira *et al.*, 2011). The adipose tissues were collected as part of this study and could be used in the future for evaluating the effect of HT on the expression of key genes implicated in adipogenesis (e.g. Adipogenesis RT-qPCR arrays).

As discussed earlier, the circulating levels of 'cholesterol, LDL/VLDL cholesterol and HDL cholesterol' within the plasma can all be used as risk markers of atherosclerosis disease development (Rafieian-Kopaei *et al.*, 2014). The plasma levels of total cholesterol, LDL/VLDL and TG were higher in male $LDLR^{-/-}$ mice fed a HFD compared to female mice also fed a HFD (Table 6.3). Despite the high levels of total cholesterol in males compared to the females, HT was able to significantly decrease the levels in both of them (Figure 6.4-6.12A). On the other hand, female LDL/VLDL levels were more susceptible to HT treatment compared to males and showed a trend towards reduction (Figure 6.4-6.12B). Previous studies have reported that total cholesterol: LDL/VLDL, total cholesterol: HDL and LDL/VLDL: HDL ratios are more stronger risk predictors of CVD than each individual lipid parameters (Yang *et al.*, 2011). However, no significant changes in these ratios were observed in both male and female mice (Figures 6.4-6.12 D, E and F).

Numerous studies have shown that circulating TG levels within the plasma can be an indicator of the levels of VLDL, chylomicron remnants and TG-rich LPs, all of which are capable of aggravating atherosclerosis disease progression (Peng *et al.*,

2017). Previous research using Wistar rats fed standard laboratory diet or a HFD for 16 weeks showed that administration of 3 mg/kg of HT and triacetylated HT lowered the serum levels of total cholesterol, TG and LDL while HDL levels were increased (Jemai *et al.*, 2008). The study presented in this chapter HT had no effect on the levels of TG in female mice or the TG: total cholesterol, TG: LDL/VLDL and TG: HDL ratios (Figure 6.5). In contrast, male mice were more susceptible to HT treatment in relation to these parameters as it significantly reduces TG, TG: total cholesterol and TG: LDL/VLDL ratios (Figure 6.13).

Despite the variations in lipid profile between male and female mice (Table 6.3), overall the results show that HT is generally capable of altering the lipid profile to be more anti-atherogenic while receiving a HFD *in vivo*. Further studies need to be carried out using different doses of HT or combining HT with its derivatives for more effectiveness as shown previously where administration of HT and tri-acetylated HT decreased the plasma levels of total cholesterol, TG and LDL significantly and increased the plasma levels of HDL (Jemai *et al.*, 2008). In addition, investigation of the changes in the expression of genes involved in the synthesis, metabolism and transport of lipids will provide a better understanding of the effects of HT on plasma lipid profile.

The association between gender and oxidative stress is important because oxidative stress has been implicated in many diseases that present differently in males and females (Kander *et al.,* 2017). Females appear to be less susceptible to oxidative stress under physiological conditions and previous studies showed apparent changes in myocardial oxidative stress between males and females (Barp *et al.*, 2002; Kander *et al.,* 2017). In the studies presented in previous chapters, HT was shown to protect against LDL oxidation (Chapters 4 and 5). Based on this protective effect, ROS levels were investigated after 12 weeks of HT treatment in male and female $LDLR^{-/-}$ mice fed a HFD. The studies showed that HT had no effect on the levels of ROS production in female mice (Figure 6.6). In contrast, there was a significant reduction in ROS levels in male mice (Figure 6.14). Future studies should seek to correlate these with the expression of key genes implicated in the control of oxidative stress.

Since atherosclerosis has been established as an inflammatory disease, markers of inflammation have been investigated in relation to their potential for predicting risk factors (Libby, 2012). Several inflammatory biomarkers have been proposed as predictors of CVD events such as CRP, fibrinogen, WBC count, cytokines and myeloperoxidase (MPO) (Madji *et al.*, 2007). Indeed, many of the newly identified inflammatory risk markers have not been confirmed by multiple prospective studies and include LP-associated phospholipase A_2, vitamin B_6, IL-6, and soluble thrombomodulin (Madjid and Fatemi, 2013). Further studies on markers of inflammation in relation to atherosclerosis are therefore required.

Numerous studies support the contribution of obesity-induced inflammation to diseases such as CVD via the pro-inflammatory activation of leukocytes in mice and humans together with changes in HSCs and early bone marrow myeloid progenitors that stimulate the production of pro-inflammatory macrophages (Phillips and Perry, 2013; Singer *et al.*, 2014). A growing body of evidence supports the usefulness of the WBC count as an indicator of future CVD events (Madjid *et al.*, 2004; Rana *et al.*, 2007). In addition, changes in the profile of cells within the bone marrow have been observed during the pathogenesis of atherosclerosis and could therefore act as an independent risk predictor (Dotsenko, 2010). The haematopoietic stem and progenitor cell profile within the bone marrow of male and female $LDLR^{-/-}$ mice fed a HFD and either vehicle or HT was therefore determined.

No significant changes in the proportion of WBC within the bone marrow of female $LDLR^{-/-}$ mice was observed after 12 weeks of receiving HFD and HT (Figure 6.7). Neither, the levels of SLAM cell populations were significantly affected by HT (Figure 6.8). Some progenitor cells are the main contributors to the formation of atherosclerotic lesions (Xu, 2006). However, HT produced a significant increase in the frequency of CMP and GMP Figure 6.9), which gives rise to cells like monocytes, macrophages, erythrocytes, platelets, DCs and granulocytes (Manz *et al.*, 2001). Overall, these results would suggest that HT exerts a pro-inflammatory effect by potentially contributing to atherosclerosis development by increasing the numbers of circulating leukocytes and macrophages. However, the frequency of CLP cell population, which gives rise to all the lymphocyte subsets, including T cells, B cells

and natural killer cells, was significantly attenuated (King and Goodell, 2011). Further studies on mature immune cells in the plasma, spleen, thymus and, more importantly, atherosclerotic lesions are required to evaluate the actions of HT.

In contrast to the females, male LDLR$^{-/-}$ mice subjected to the same dietary regime also showed no significant changes in the levels of WBC (Figure 6.15). Furthermore, there was a trend of non-significant reduction in the levels of MPP without an effect on other SLAM populations (Figure 6.16). On the other hand, no detectable changes were observed in other cell populations except for CMP and MEP that showed a significant reduction and a trend of reduction that failed to reach significance respectively (Figure 6.17).

Due to some technical issues during processing of the female bone marrow samples, the effect of HT on the profile of mature cells could only be determined in male mice. The data showed that HT produces a significant reduction in the percentage of macrophages and a trend towards reduction of MDSC that failed to reach significance (Figure 6.18). No significant changes were seen in other cell populations such as B-cells, erythrocytes or T-cells (Figure 6.18). Previous research showed a pro-atherogenic and immune-modulatory activity of MDSC and macrophages and related their accumulation and activation as a response to chronic inflammation in atherosclerosis (Moore and Tabas, 2011; Wang *et al.*, 2015). Reduction in the number and activity of these cells will therefore potentially attenuate disease progression.

In conclusion, the *in vivo* studies presented in this chapter assessed the effects of HT on various parameters related to atherosclerosis in LDLR$^{-/-}$ mice receiving a HFD. Despite the gender-specific variations of HT actions, which should be investigated in more detail in the future, HT was shown to be a promising candidate for the prevention of atherosclerosis in the light of its ability to reduce weight, plasma total cholesterol levels and ROS production together with promoting an anti-atherogenic cell profile in the bone marrow. Furthermore, there was an indication that HT is potentially capable of affecting lipid accumulation and synthesis as shown by reduction in the weight of fat pads and plasma TG levels. Future studies should investigate the plaque burden and lipid content in aortic root and brachiocephalic

arteries of these animals. The tissues are ready for sectioning and such studies will also inform on the potential gender-specific actions of HT on the progression of atherosclerosis development. The efficacy of HT on the regression of existing plaques should also be analysed together with gene expression programs in the arteries, liver and the adipose tissues. These studies will inform on the worth of HT in reducing CVD burden and associated risk factors.

Chapter 7

7 General discussion

CVD remains one of the leading causes of premature mortality and morbidity in developed countries. It takes the lives of 17.9 million people every year, 31% of all global deaths (WHO, 2018). Smoking, obesity, physical inactivity, diabetes and hypertension are all risk factors that trigger CVD such as MI and stroke (WHO, 2018).

Atherosclerosis, the primary cause of CVD, is a progressive, inflammatory disease with complex pathology (Lusis, 2000). A key feature is the formation of lipid-loaded macrophages (foam cells), which accumulate in the walls of large and medium arteries and form the underlying basis for the development of plaques associated with a chronic inflammatory response (Wolf *et al.*, 2014). Targeting the early stages of atherosclerosis and the ongoing inflammatory response is of therapeutic interest in the prevention and management of the disease (Buckley and Ramji, 2015). In addition, the identification of new circulating biomarkers that provide early and specific diagnosis and new therapeutic targets are required to improve diagnosis and treatment (Madjid *et al.*, 2007; Silbiger *et al.*, 2013; Moss and Ramji, 2016).

Inflammation plays a major role at all stages of the atherosclerotic process, from the early events whereby leukocytes are recruited at sites of sub-endothelial LDL cholesterol accumulation to the late events, when plaque rupture occurs leading to thrombus formation and adverse clinical outcomes (Ramji and Davies, 2015). The disease is regulated by both the innate and the adaptive immunity (Prashar *et al.*, 2017). Several signalling pathways have been implicated within the atherosclerotic state and some of the key ones are associated with the inflammatory response such as MAPK and JAK:STAT (Muslin, 2008; Plotnikov *et al.*, 2011). A thorough understanding of these pathways will help in more accurate diagnosis and management of the disease, indeed, detailed mechanistic insights is key for facilitating optimal therapies and preventing disease complications (Ait-Oufella *et al.*, 2011; McLaren *et al.*, 2011; Moss, 2015; Prashar *et al.*, 2017). It is improvement in our understanding of the molecular basis of atherosclerosis that has given researchers knowledge of specific genes and pathways that play a key role in CVD and therefore potential targets for

therapeutic intervention (Wolfram and Donahue, 2013). More studies on the roles of key signalling pathways on key cellular processes associated with atherosclerosis *in vitro* and disease development *in vivo* are therefore required.

Several lipid altering agents that target particular steps in lipid synthesis and metabolism are already being used such as statins (as fixed-dose or in combination with other agents) (Vaughan *et al.*, 2000; Navarese *et al.*, 2013; Cannon *et al.*, 2015; Ramkumar *et al.,* 2016). These have been well documented to have a marked impact in treating the early stages of CVD and in those at elevated risk by inhibiting the enzyme HMG-CoA reductase involved in the initial step of cholesterol synthesis (Taylor *et al.*, 2011; Rabar *et al.*, 2014). The maximum reduction in mortality rates that can be attributed to statins is about 30% and, additionally, there are a number of limitations and side effects associated with them (Bays and Stein, 2003; Ramkumar *et al.*, 2016). Although there have been some successes with alternative pharmaceutical agents (e.g. ezetimibe, and monoclonal antibodies against PCSK9 and IL-1β), many promising leads have failed at the clinical level (Wormald and Hilton, 2004; Fichtlscherer *et al.*, 2006; Yoshimura *et al.*, 2007; Chyu and Shah, 2011; Cannon *et al.*, 2015; Lin *et al.*, 2018).

The limitations of currently available therapies have prompted extensive investigations into other agents. Nutraceuticals are potentially promising alternatives for the prevention of atherosclerosis or as an add-on with current therapies (Moss and Ramji, 2016). HT, a polyphenol present in olive oil, has been shown to exert anti-inflammatory effects *in vitro* and *in vivo* (Fitó *et al.*, 2007; Granados-Principal *et al.*, 2010). In addition, it has an anti-inflammatory protective role in a number of diseases such cancer, acquired immunodeficiency syndrome (AIDS), metabolic syndromes and diabetes, which are addressed in more detail in a later section (Section 7.5.1)(Cao *et al.*, 2014; López-Villodres *et al.*, 2016; Terzuoli *et al.*, 2016). It is therefore important to investigate the athero-protective potential of HT and to understand the molecular mechanisms underlying it actions *in vitro* and *in vivo.*

7.1 The role of the ERK1: STAT1 S727 phosphorylation axis in atherogenesis *in vitro*

MAPK pathways, which include ERK1/2, p38 kinase and JNK, are key signalling cascades that regulate a wide variety of cellular processes, including proliferation, differentiation, survival, apoptosis and stress responses (Figure 1.2) (Wortzel and Seger, 2011). *In vitro* studies using BMDM carried out in Chapter 3 have improved our understanding of the roles of ERK1 and STAT1 Ser727 phosphorylation on key cellular processes associated with atherosclerosis. Thus, deficiency of ERK1 ($ERK1^{-/-}$) and substitution of serine 727 in STAT1 with alanine was found to significantly attenuate the expression of many pro-atherogenic genes associated with monocyte recruitment and migration, differentiation of monocytes into macrophages, foam cell formation, apoptosis, blood coagulation and thrombus formation, cell to cell adhesion, inflammatory mediator production, and lipid transport and metabolism (See Tables 3.1 and 3.2). In addition, analysis of cellular processes *in vitro* showed that macrophage migration and proliferation were significantly attenuated in BMDM from $ERK1^{-/-}$ mice (Figures 3.4 and 3.6) whereas with STAT1 S727A, there was a reduction in macrophage migration (Figures 3.6) and induction in the phagocytosis levels (Figure 3.11). All these significant changes are likely to have a positive impact on the size and stability of the atherosclerotic plaque.

Other atherosclerosis-associated cellular processes, such as macropinocytosis, cholesterol efflux and ROS production, were not affected by ERK1 deficiency or the STAT1 S727A modification. This suggests the potential existence of functional redundancy with other ERK isoforms (e.g. ERK2) or phosphorylation of STAT1 elsewhere (e.g. tyrosine 701). Future studies should investigate these possibilities using macrophages that are deficient in both ERK-1 and -2 or STAT1 or STAT1 where tyrosine 701 has been changed to alanine. It is possible that kinases other than ERKs or transcription factors other than STAT1 might play a more important role.

Overall, the many significant, positive changes that were observed inform on the importance of the ERK1: STAT1 serine 727 phosphorylation axis in cellular migration and immune cell recruitment associated with inflammation in CVD and

suggest that they may represent promising therapeutic targets against atherosclerosis.

7.2 Molecular mechanisms underlying the anti-inflammatory actions of HT in relation to atherosclerosis *in vitro*

Previous studies showed that phenolic compounds could exert their beneficial effects by interacting with molecular targets central to the cell signalling machinery (Yoon and Baek, 2005). These natural compounds exert anti-inflammatory activities through the inhibition of pro-inflammatory gene expression and pro-inflammatory cytokine production together with inhibition of cellular proliferation and migration of immune cells (Santangelo *et al.*, 2007). The role of MAPKs and their involvement in the regulation of inflammatory mediators, at both the transcriptional and post-transcriptional levels, makes them potential targets for novel anti-inflammatory therapies (Santangelo *et al.*, 2007). Similarly, the JAK-STAT pathways play pivotal roles in the regulation of inflammation and inflammatory disorders (Kishore and Verma, 2012; Montecucco *et al.*, 2012).

Several phenolic compounds have been shown to modulate MAPK pathways by acting on several steps of the activation cascade and consequently on downstream effectors by inhibiting ERK, JNK and p38 activities (Santangelo *et al.*, 2007). Some of the actions of phenolic compounds on MAP signalling are cell type-specific or dependent on other parameters such as structure and concentrations (Xagorari *et al.*, 2002; Chen *et al.*, 2004; Soobrattee *et al.*, 2005; Santangelo *et al.*, 2007).

Previous unpublished research in the laboratory has shown that the polyphenol HT attenuates several pro-atherogenic cellular processes (e.g. IFN-γ induced gene expression) and stimulates anti-atherogenic processes (e.g. cholesterol efflux). In addition, HT attenuated the IFN-γ-induced phosphorylation of STAT1 on serine 727 but not tyrosine 701 (supplementary figure S-1). This suggests a potential role of STAT1 S727 phosphorylation together with its upstream kinase, ERK1, in the athero-protective actions of HT. Therefore, in this study, the protective role of HT on several atherosclerosis-associated processes was investigated using BMDM from wild-type control mice, ERK1$^{-/-}$ mice and STAT1 S727A mice.

The findings of the *in vitro* experiments (see Chapter 4) confirm the previous unpublished data on human macrophages to mouse BMDM, thereby ruling out any species-specific differences. The findings generally support the proposition of HT as a potential therapeutic agent that can help in limiting atherosclerosis by attenuating several key processes such as macrophage migration/proliferation, oxLDL uptake, ROS production, phagocytosis and foam cell formation in wild-type control BMDM (Figure 4.3-4.8).

In terms of the ERK1:STAT1 S727 phosphorylation axis, ERK1 was required for the action of HT on macrophage proliferation and macropinocytosis (Figures 4.3 and 4.6). On the other hand, STAT1 S727 phosphorylation was only required in the HT-mediated regulation of macropinocytosis (Figure 4.6). Overall these findings suggest either no requirement of the ERK: STAT1 serine 727 phosphorylation axis on other HT-mediated anti-atherogenic actions or the potential existence of functional redundancy through other kinases present in the cell or other phosphorylation sites on STAT1 (Tyr 701). Again the use of macrophages that are deficient in both ERK-1 and -2 or STAT1 or STAT1 where tyrosine 701 has been changed to alanine will help address these issues.

7.3 The atheroprotective effect of HT in wild- type mice *in vivo*

In the light of the previous positive findings (Chapter 4), the atheroprotective actions of HT were extended to a short term *in vivo* study using wild-type mice fed a HFD with administration of HT or vehicle by gavage (see Chapter 5). HT treatment was found to be associated with a variety of anti-atherogenic actions such as the attenuation of oxidation levels by inhibition of ROS production together with a decrease in plasma levels of total cholesterol and LDL/VLDL (Figures 5.3 and 5.4). Furthermore, HT produced an anti-atherogenic gene expression profile where there was a significant reduction in the expression of genes involved in monocyte recruitment and migration, macrophage differentiation, foam cell formation, apoptosis, blood coagulation and thrombus formation, cell-to-cell adhesion, inflammatory mediator production, cholesterol efflux and lipid transport, and metabolism (see Table 5.2). The altered gene expression profile shows that HT is potentially capable of retarding atherosclerosis disease progression and hence shows

promise in the reduction of atherosclerotic plaque size. However, this study also showed a few pro-inflammatory changes such as the expression of some pro-atherogenic genes associated with the disease (Table 5.2) together with increased plasma TG levels and attenuated plasma HDL cholesterol levels (Figures 5.4- 5.5). Nevertheless, the beneficial actions outweighed the detrimental ones.

7.4 The atheroprotevtive effect of HT in LDLR$^{-/-}$ mice receiving HT for 12 weeks *in vivo*

The initial study presented in Chapter 5 was extended into long term feeding studies using the atherosclerotic (LDLR$^{-/-}$) model (both males and females) to fully decipher the potential of HT for attenuating the rate of atherosclerosis disease development in both genders. A number of studies show that women and men differ in their reported symptoms of CVD and drugs that are more effective in men may not be as effective in women or may have unexpected side effects (Regitz-Zagrosek, 2006; Seeland and Regitz-Zagrosek, 2012). In this part of the study, the *in vivo* effect of HT and the possibility of using it as an anti-atherogenic preventative/treatment were explored in female and male LDLR$^{-/-}$ mice after 12 weeks of receiving HFD with vehicle or HT. The results shed light on the action of HT on numerous parameters that can provide additional evidence for its anti-atherogenic properties that were previously observed during *in vitro* and short-term *in vivo* studies on wild-type mice (Chapters 4 and 5) and how the effect of HT varies between males and females.

As shown in Chapter 6, HT treatment had a positive cardiovascular protective effect in both female and male mice. This included attenuation of plasma total cholesterol and LDL/VLDL levels in female mice (Figures 6.2-6.4) and plasma total cholesterol, TG levels, TG: cholesterol ratio and TG: LDL/VLDL ratio and ROS production in male mice (Figures 6.12-6.14). These changes are anti-atherogenic and potentially likely to reduce the incidence of the disease (Madjid and Fatemi, 2013). Although HT did not affect HDL levels in both models, previous studies have reported changes in biophysical parameters related to HDL function such as remodeling of HDL size towards larger HDL (HDL_2) together with the enhancement of the stability and the oxidative status of the HDL particle. This could potentially improve HDL functionality in addition to the enhancement of HDL-mediated cholesterol efflux by

inducing the expression of ABCA1 seen in the studies presented in this thesis (Figure 5.7)(Álvaro *et al.*, 2014; Berrougui *et al.,* 2015).

A previous study showed that olive leave extract (OLE) HT has beneficial effects against obesity through the regulation of expression of genes involved in adipogenesis and thermogenesis in the adipose tissue of HFD-fed wild-type mice (Shen *et al.*, 2014). In this study, there was a trend of reduction in weight gain in female mice that were associated with a reduction in the fat pad levels in the gonadal and subcutaneous tissues (Figure 6.2-6.3 B-C). In contrast, male mice were resistant to weight lose despite the significant reduction in the liver and gonadal fat pad (Figure 6.10-6.11).

As reported previously, HT is a powerful anti-oxidant agent that reduces ROS generation (Owen *et al.*, 2003; O'Dowd *et al.*, 2004; González-Santiago *et al.*, 2006). This was confirmed in our short term *in vivo* study (Figure 5.3). However, ROS generation was not attenuated in female mice receiving HT (Figure 6.6) whereas male mice showed a significant reduction in plasma ROS levels (Figure 6.14). Gender is often associated with differences in oxidative stress and it has been suggested that females are less susceptible to oxidative stress due to the antioxidant properties of estrogen (Kander *et al.*, 2017).

Studies in Chapter 4 (Figure 4.4) showed that HT was able to attenuate macrophage migration *in vitro*, which is likely to impact the size and stability of the atherosclerotic lesion. A recent study using $LDLR^{-/-}$ mice fed a HFD with or without extra virgin olive oil (EVOO) reported a vascular protective effects of EVOO via reduction of atherosclerotic lesion load in the aortic root, lesion macrophage content and HFD-induced inflammatory gene expression (Luque-Sierra *et al.*, 2018). In another study using hyperlipidaemic rabbits, HT treatment improved their antioxidant status and reduced the size of atherosclerotic lesions when compared with control animals (González-Santiago *et al.*, 2006). Such reduction in lesion size may arise due to the ability of HT treatment to reduce the expression of key genes implicated in immune cell recruitment and proliferation (Table 5.2). Such altered gene expression profile in combination with previous studies showing that HT is capable of retarding atherosclerosis disease progression in rabbits indicate that HT treatment

has the potential to reduce atherosclerotic plaque size in humans (González-Santiago *et al.*, 2006).

Numerous studies have reported the beneficial effects of polyphenols from olive oil intake on stem cell functions, which are now recognised as important promoters of tissue regeneration both *in vivo* and *in vitro* (Fernández del Río *et al.*, 2016). In addition, the intake of a polyphenol-rich olive oil is able to repress the expression of several pro-inflammatory genes *in vivo*, thereby switching the activity of peripheral blood monocytes to a less harmful inflammatory profile (Camargo *et al.*, 2010). Another study showed that OLE, which contain oleuropein and its derivative, HT demonstrated a protective effect by allowing HSCs to survive and give rise to different phenotypes, including enhancing their differentiation potential rather than promoting self-renewal (Samet, 2014). The effect of HT on bone marrow cell populations was therefore investigated and showed a significant increase in the frequency of HSC progenitor cell population in female mice (Figure 6.9), which can be an indicator of the inflammatory state (Madjid *et al.*, 2004; Madjid and Fatemi, 2013). On the other hand, the frequency of CLP cell population, which gives rise to all the lymphocyte subsets, including T cells, B cells and natural killer cells was significantly attenuated (Figure 6.9). However, due to unexpected technical issues, the levels of lineage positive cell population in female mice (i.e. macrophages, erythrocytes, granulocytes, T cells and B cells) could not be determined. In addition, because of sample size, further repetition via use of additional mice will be required to fully evaluate the effect of HT on HSC and lineage positive cell populations.

In male mice, the data showed that HT produces a significant reduction in the percentage of HSC progenitor (CMP and MEP), macrophages and a trend towards reduction of MDSC that failed to reach significance (Figures 6.17-6.18). No significant changes were seen in other cell populations such as B-cells, erythrocytes or T-cells (Figure 6.18). Reduction in the number and activity of the cells observed will therefore potentially attenuate disease progression (Tabas, 2005, 2009; Klaus *et al.*, 2011; Ginhoux and Jung, 2014; Mallat, 2014).

Further studies are required to fully evaluate the molecular mechanisms of action and the effectiveness of HT in several physiological and pathophysiological

processes, as this will enhance our understanding of its actions and could ultimately lead to the identification of novel treatment and prevention strategies to reduce the global prevalence of CVD. In addition, such studies will validate the importance of dietary polyphenol compounds in human health and encourage their use as templates for further structural development of more effective and safe compounds by synthetic chemistry.

7.5 From bench side to clinical trials

This study has demonstrated that HT is an effective natural anti- inflammatory treatment, which has the potential to exert athero-protective effects in our atherosclerotic related *in vitro* and *in vivo* models (Chapters 4-6). Therefore, it can be predicted that HT treatment would be capable of attenuating atherosclerosis plaque formation in humans.

As the majority of nutraceutical therapies will most likely be used for prevention or in combination with other therapies (e.g. statins), the effect of HT needs to be assessed using various atherosclerosis models together with the chosen current therapy (e.g. statins). This would determine whether there are any additional cardiovascular protective effects or any detrimental effects associated with receiving a combination of traditional pharmaceuticals and nutraceutical therapies for atherosclerosis (D'Addato *et al.*, 2017). Only once HT dietary supplementation has been found safe and effective in these studies should it progress into introductory human clinical trials for the assessment as add-on therapy. Results will be able to inform whether HT is most effective when used as a preventative or used in combination with other drugs to achieve greater cardiovascular protective effects.

7.5.1 Current and potential uses of HT in health care

HT has been demonstrated in numerous studies to have strong antioxidant potential (Moss and Ramji, 2016). It acts as a powerful scavenger of free radicals of the superoxide anion, H_2O_2, hypochlorous acid and many others (O'Dowd *et al.*, 2004). In addition, it has a strong chelating effect on metals such as iron and thus attenuates the appearance of ROS derived from reactions associated with this metal (Visioli *et al.*, 2000; Bovicelli, 2010).

Other benefits of HT according to the EFSA reported in 2011 are the maintenance of normal blood HDL-cholesterol concentrations and blood pressure, anti-inflammatory properties, contribution to the upper respiratory tract health, maintenance of a normal function of the gastrointestinal tract and contribution to body's defences against external agents (Carlo Agostoni *et al.,* 2011; Achmon and Fishman, 2015). More conclusive studies are needed to link all these potential benefits with phenolic compounds and thus to identify new lines of research on their potential for the prevention and treatment of various diseases. Table 7.1 lists the beneficial effects of HT in some diseases.

Table 7.1 Beneficial effects of HT in various diseases

Disease	Beneficial effects	References
Cancer	Previous epidemiological studies have reported that changing to a balanced diet might avoid over 30% of all cancers. Lower cancer incidence has been observed in the Mediterranean area. It has been suggested that this reduction is associated with a Mediterranean diet. Recently, many *in vitro* and *in vivo* studies using different animal models and tumour cell lines have demonstrated that HT induces apoptosis and inhibits cell proliferation through the suppression of pro-inflammatory cytokine actions and the expression of genes involved in cell cycle activation, or induces the expression of cell cycle blockers. HT down regulates several phosphokinase enzymes, which are involved in pro-inflammatory signalling pathways such as MAPK pathways.	(Fabiani *et al.*, 2002; Guichard *et al.*, 2006; Fabiani, 2016; Terzuoli *et al.*, 2016; Aydar *et al.,* 2017)

Cardiac dysfunction	Numerous studies have revealed the cardiac protective effects of HT in both *in vitro* and *in vivo* models. HT is a well-known powerful anti-oxidant that positively counteracts oxidative stress and pro-inflammatory gene expression in cardiac dysfunction. Previous study showed that incubation of vascular ECs with HT in the presence of H_2O_2 attenuates intracellular ROS production and induces the expression of anti-oxidant enzymes. Another study reported the effects of HT on the progression of aortic lesions in hyperlipemic rabbits after 1-month of receiving HFD in presence and absence of HT. About 50% and 42% decrease in total cholesterol and TG, respectively, was observed together with a 2.3-fold increase in HDL-cholesterol. The HT-supplemented groups also showed a reduction in the size of atherosclerotic lesions measured as intimal layer areas of the aortic arch when compared with control animals. HT also attenuates the adhesion of monocytes to the activated endothelium, which is a crucial step in early atherogenesis.	(Annunziata *et al.*, 2003; González-Santiago *et al.*, 2006; Khurana *et al.*, 2013)
AIDS	AIDS is a disease of the human immune system caused by infection with human immunodeficiency virus (HIV). Despite the existence of drugs against the HIV virus, they do not cure the infection. The use of natural small molecules together with combining anti-inflammatory and anti-	(Hsiao *et al.*, 2003; Lee-Huang *et al.*, 2003, 2007; Gómez-Acebo *et al.*, 2010)

	viral effects has recently received special attention to prevent HIV infection and associated diseases. HT consumption has an antimicrobial effect that can avoid infections in the respiratory, intestinal and genital systems and boosts the immune system and has recently been recognised as a direct prohibitor of HIV infection. Previous *in vitro* studies demonstrated that HT and oleuropein inhibit acute infection and cell-to-cell transmission between uninfected cells co-cultured with HIV-1 infected lymphocytes in a dose-dependent manner by inhibiting HIV-1 fusion core formation and therefore fusion of the virus with the target cells. Moreover, HT also inhibits HIV-1 replication. In another study, HT exhibited dose-dependent inhibition of the enzyme HIV-1 integrase, which is an essential enzyme for retroviral replication and is involved in the integration of the HIV DNA into the host chromosomal DNA. HT can be easily obtained from olive oil and can be synthesised in the laboratory, which gives it an advantage over the pharmaceutically available HIV fusion inhibitor Furzeon (T-20 or Enfuvirtide), which is difficult to manufacture due to its high-molecular weight.	
Diabetes mellitus	Type 1 diabetic or pre-diabetic patients suffer from hyperglycemia, hyperinsulinaemia and insulin resistance due to an increase in the oxidation levels, which in turn may develop into several adverse effects commonly associated with the disease such as liver and kidny disorders.	(Gonzalez *et al.*, 1993; Allouche and Sayadi, 2003; Hamden *et al.*, 2009; Jemai *et al.*, 2009; Zhang *et al.*, 2009)

Previous studies suggested that using antioxidant-based therapy and certain dietary antioxidants represent promising steps in minimising the complications associated with oxidative stress.

Previous *in vivo* research using diabetic rats with hyperglycemia, hypercholesterolemia, high levels of lipid peroxidation and depletion in the antioxidant enzymes activities showed that administration of 8 and 16 mg/kg/body weight of HT and oleuropein for 4 weeks significantly decreased the plasma glucose and cholesterols levels and restored antioxidant properties.

Another study found a 55% reduction in glucose levels after administration of HT compared to untreated diabetic rats. The hypoglycaemic effect of HT was suggested to be due to:

1- regeneration and protection of pancreatic cells from damages;

2- enhancement of insulin secretion;

3- inhibition of potassium channels and induction of voltage-dependent calcium channels;

4- increased peripheral uptake of glucose;

5- scavenging of the 1,1-diphenyl-2-picrylhydrazyl (DPPH) radicals;

6- induction of glucose phosphorylation enzymes, such as hexokinase, pyruvate kinase, and attenuation of their dephosphorylation.

In addition to the hypoglycaemic effect, administration of HT to diabetic rats reduces

	plasma levels of urea and creatinine, thereby preventing kidney toxicity. Furthermore, hypocholesteremic effects of HT was observed in these diabetic rats as evidenced by low levels of total cholesterol and increase in HDL.	
Hypertension	Clinical trials have demonstrated that olive oil is more efficient than any other oil at reducing blood pressure along with a reduction in saturated fat intake, and lowers the daily dosage of antihypertensive drugs required. Previous *in vivo* research reported a reduction of both systolic and diastolic blood pressure with HT in pre-hypertensive subjects after 6 weeks of combined administration of 6 mg/kg/day of HT plus 136mg/kg/day of oleuropein. Similar findings were reported in hypertensive rats after 5 weeks of receiving 30 mg/kg/day of HT. Another study using diabetic rats showed that 10 mg/kg/day of HT supplementation for 2 months increased the levels of nitrites and nitrates, which are vasorelaxing agents. In addition, administration of 10 μM HT attenuated hyperglycemia-induced expression of endothelin-1, a well-known hypertensive agent.	(Ferrara *et al.*, 2000; Storniolo *et al.*, 2014; López-Villodres *et al.*, 2016; Romero *et al.*, 2016; Lockyer *et al.*, 2017)
Obesity	Clinical studies demonstrated that HT alters key components of metabolic syndromes. However, contradictory results have been reported for obesity probably resulting from differences in the study design, administered doses and type of animals.	(Drira, Chen and Sakamoto, 2011; Warnke *et al.*, 2011; de Bock *et al.*, 2013; Cao *et al.*, 2014; Lutfi *et al.*, 2017; Peyrol *et al.*,

	Previous clinical study using HT in combination with oleuropein reported no observed effect on body weight in overweight men. On the other hand, mitochondrial stress and dysfunction as a result of reduction of ATP formation induced lipogenesis and therefore adipose tissue hypertrophy and hyperplasia. *In vitro* studies showed that 25-100 μM HT increased oxygen consumption and ATP generation, which are needed for mitochondrial biogenesis and therefore reduces hyperplasia and hypertrophy. Another *in vitro* and *in vitro* study using zebra fish model demonstrated the potential of HT to down regulate adipogenesis through the down regulation of expression of adipogenesis-related genes, TG levels and the PPARγ signalling pathway, which is involved in the regulation of adipogenesis and activates the transcription of a large number of genes required in the control of adipocyte differentiation and lipid accumulation. Taken together, these data suggest that HT might reduce the size of adipocytes and be beneficial for reducing the risk of obesity.	2017)
Osteoporosis	Bone modeling and remodeling processes depend on hormonal, nutritional and mechanical factors. Previous studies reported a protective effect of Mediterranean diet on bone health (formation and maintenance). In addition, *in vitro* and *in vivo* studies using ovariectomized rats (model of postmenopausal osteoporosis) showed that HT stimulated the deposition of calcium, decreased lipid	(Puel *et al.*, 2008; Hagiwara *et al.*, 2011; García-Martínez *et al.*, 2014, 2016)

	peroxidation and oxidative stress (by reducing H_2O_2) in addition to the prevention of the decline in total femoral, diaphyseal and metaphyseal bone mineral density. Another *in vitro* study using an osteosarcoma cell line reported a significant induction in osteoblast proliferation levels.

7.6 The limitations and future perspectives of this study

7.6.1 *In vitro* assays

Atherosclerosis is a complex disease involving multiple cell types and involves the interactions of a number of molecular mechanisms and cellular processes (Lusis, 2000; Tabas *et al*., 2015; Prashar *et al.*, 2017). One common approach involved in studying the impact of single gene product assumed to play a role in atherosclerosis based on its known biology involves modification of this gene through genetic engineering (e.g. knock out or knock in). This is followed by analysis of their targets *in vitro* using cells as in this study or *in vivo* in order to assess disease development and to discover new therapeutic targets (Scheidt *et al.*, 2017). Numerous such studies have identified a number of novel targets associated with atherosclerosis (Stylianou *et al.*, 2012).

The *in vitro* part of this study was performed using BMDM from wild-type control, ERK1$^{-/-}$ and STAT1 S727A mice with or without HT stimulation (Chapters 3-4). Data presented provided key insight into the role of these genetic modifications on a number of aspects contributing to macrophage foam cell formation, monocyte migration, pro-inflammatory gene expression and ROS production. The studies also suggested potential functional redundancy (e.g. with STAT1 Tyr701 phosphorylation, ERK2) or important roles of other factors such as different members of the MAPK signalling pathway. Therefore, other approaches should be considered to fully understand the role of these genes (e.g. cells deficient in both ERK-1 and -2, STAT1 or modification at both tyrosine 701 and serine 727 phosphorylation sites).

Because of time limitations and issues with animal breading, some experiments were not performed and could potentially be carried out in the future to expand on the findings identified so far and to provide further understanding on the role of the ERK1:STAT1 serine 727 phosphorylation axis on inflammatory processes and athero-protective mechanisms of HT actions. These include:

- IFN-γ induced expression of key pro-inflammatory genes and proteins. Following on from this, the effect of genetic modifications could be investigated on other aspects of IFN-γ signalling such as:
  - The effect on macrophage polarisation to M1, M2 and other phenotypes;
  - The effect on inflammasome activation;
  - The effect of HT treatment on cholesterol efflux.

In addition to macrophages, a number of other cell types play an important role in atherosclerosis pathology; for example, ECs and SMCs. EC dysfunction is a key early event in the initiation of atherosclerosis while SMC migration and proliferation is characteristic of advanced plaques (McLaren *et al.*, 2011; Ashlin *et al.*, 2012). Future work could include the effect of the genetic modifications and HT treatment on key events related to atherosclerosis in these two cell types from wild type and genetically modified mice. This would allow for a better understanding of the role of ERK1: STAT1 S727 phosphorylation axis on atherosclerosis pathology.

7.6.2 *In vivo* assays

Studies in Chapter 5 were designed to generate initial data to evaluate the potential of HT treatment for 3 weeks using wild type mice fed a HFD before moving on to 12 weeks, long-term feeding study using $LDLR^{-/-}$ mice, which are capable of developing atherosclerotic plaques unlike wild type mice (Chapter 6). Because of time limitations, some key experiments (e.g. Plaque size and cellular content) could not be performed. Nevertheless, tissues were collected for future studies and could be processed in the future to expand on the current findings and to provide further understanding of HT actions. These could include:

- The effect of HT on plaque morphology and stabilization, which could be investigated by plaque morphometry and immunohistochemistry techniques. This

could include determining plaque size and lipid content (haemotoxylin and eosin, and oil red O staining, respectively), cell content by staining for markers for macrophages, SMCs and T-cells, foam cell quantification and collagen staining, together with cytokine levels and gene expression;

- Inclusion of additional animals (e.g. female mice) to fully evaluate the effect of HT on HSC populations and on lineage positive cell populations.

Additional studies could include:

- Potential of HT in regression of existing plaques. This would involve feeding LDLr$^{-/-}$ mice a HFD for 12 weeks before switching to a HFD or chow diet for 4 weeks containing vehicle or HT. Baseline changes should be taken at 12 weeks. This would determine whether HT is capable of inducing plaque regression and restore blood vessel function in individuals with advanced atherosclerosis;
- Applying HT treatment to atherosclerotic mice for a short time period while receiving a standard chow diet before switching to a HFD. A delay in the development of atherosclerotic plaques would represent a preventative effect of HT;
- Studies above could use different concentrations of HT to delineate whether dose response actions of HT occur;
- Combining HT with traditional pharmaceutical therapies as an additional way to achieve health targets. For this reason, studies should also treat atherosclerotic mice with HT in combination with statins, which would represent the majority of patients who would use nutraceutical therapies as add-on. Therefore, it is essential to assess the effects of HT as an additional add-on therapy to statins to ensure there are no harmful effects and whether further reductions in atherosclerosis development can be achieved;
- To fully determine the efficacy of HT treatment for atherosclerosis, long-term human trials need to be conducted in participants who are or are not receiving statins over an extensive treatment time period. Only after randomised clinical trials, can the effectiveness of HT treatment be fully determined. Therefore, it is essential to determine no harmful effects occur from sustained HT treatment.

7.7 Conclusions

In vitro investigations have indicated a role of the ERK1: STAT1 S727 phosphorylation axis on several key atherosclerosis-associated processes in BMDM from wild type, ERK1$^{-/-}$ and STAT1 S727A mice, including regulation of macrophage migration, pro-inflammatory gene expression, cellular proliferation, phagocytosis and modified LDL uptake. All of these processes are involved in foam cell formation, which is a key step in the formation of atherosclerotic plaques. These findings inform on the importance of the ERK1: STAT1 serine 727 phosphorylation axis and suggest that they may represent promising therapeutic targets against atherosclerosis.

The use of *in vitro* model systems also showed that HT was also capable of exerting some athero-protective effects through the regulation of the ERK1: STAT1 S727 phosphorylation axis. These athero-protective effects were also observed in short term *in vivo* experiments using wild type mice and long term study using LDLR$^{-/-}$ mice, both fed a HFD. Future studies are required to explore the effect of long term HT treatment on atherosclerosis development and as an add-on therapy with statins. Overall, the studies show that HT is potentially an effective and safe anti-inflammatory therapy capable of providing cardiovascular protective effects and therefore represents promising emerging therapy for atherosclerosis.

Chapter 8

8.1 Supplementary data

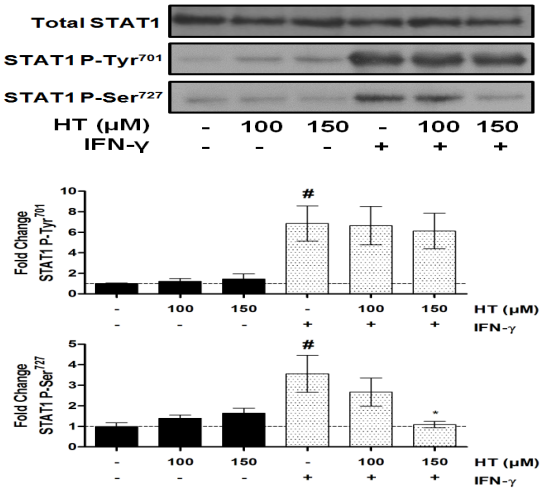

Supplementary Figure S-1 HT attenuates the IFN-γ-induced STAT1 serine 727 phosphorylation in human macrophages.

The cells were incubated for 30minutes (optimal STAT1 activation time) with or without 250U/ml IFN-γ in the presence of vehicle (-) or the indicated concentration of HT. Equal amount of cellular proteins were subjected to SDS-PAGE and Western blot analysis using antisera that recognise total STAT1, phospho-STAT1 tyrosine 701 and phospho-STAT1 serine 727. The signals were analysed by densitometry and the levels of each phospho-STAT1 protein were normalised to total STAT1. The value in vehicle has been arbitrarily assigned as 1. Statistical analysis was carried out using One-way ANOVA with Tukey's post-hoc test (#, $P<0.05$ compared to absence of IFN-γ and presence of vehicle; *, $P<0.05$ compared to presence of IFN-γ and vehicle). Data (mean ± SEM) are from three independent experiments. (Data provided by dr. Thomas Davies).

References

Abrescia, P. and Golino, P. (2005) Free radicals and antioxidants in cardiovascular diseases, *Expert Review of Cardiovascular Therapy*., 3(1), pp. 159–171.

Achmon, Y. and Fishman, A. (2015) The antioxidant hydroxytyrosol: Biotechnological production challenges and opportunities, *Applied Microbiology and Biotechnology*, 99(3), pp. 1119–1130.

Acín, S., Navarro, M. A., Arbonés-Mainar, J. M., Guillén, N., Sarría, A. J., Carnicer, R., et al. (2006) Hydroxytyrosol administration enhances atherosclerotic lesion development in Apo E deficient mice, *The Journal of Biochemistry*, 140(3), pp. 383–391.

Agostoni, C., Bresson, J., Fairweather-Tait, S., Golly, A., Korhonen, H., Lagiou, P., et al. (2011) Scientific Opinion on the substantiation of health claims related to polyphenols in olive and protection of LDL particles from oxidative damage (ID 1333, 1638, 1639, 1696, 2865), maintenance of normal blood HDL cholesterol concentrations (ID 1639), mainte, *EFSA Journal*, 9(4), p. 2033.

Ait-Oufella, H., Taleb, S., Mallat, Z. and Tedgui, A. (2011) Recent advances on the role of cytokines in atherosclerosis, *Arteriosclerosis, Thrombosis, and Vascular Biology*, 31(5), pp. 969–979.

Alarcón de la Lastra, C. and Villegas, I. (2005) Resveratrol as an anti-inflammatory and anti-aging agent: Mechanisms and clinical implications, *Molecular Nutrition & Food Research*, 49(5), pp. 405–430.

Altmann, W., Davis, R., Zhu, L., Yao, X., Hoos, M., Tetzloff, G., et al. (2004) Niemann-Pick C1 like 1 protein is critical for intestinal cholesterol absorption, *Science*, 303(5661), pp. 1201-1204.

Álvaro, H., Sara, C., Marta, F., Úrsula, C., Isaac, S., Rosa, M., et al. (2014) Olive oil polyphenols enhance high-density lipoprotein function in humans, *Arteriosclerosis, Thrombosis, and Vascular Biology*, 34(9), pp. 2115–2119.

Ambriz-Pérez, L., Leyva-López, N., Gutierrez-Grijalva, P. and Heredia, B. (2016) Phenolic compounds: Natural alternative in inflammation treatment, *Cogent Food & Agriculture*. 2(1), pp. 1131412.

Ángel, B., Liming, P., Richard, L., Tarr, P., Tangirala, K., Weinstein, M., et al. (2006) Impaired development of atherosclerosis in hyperlipidemic LDLR$^{-/-}$ and ApoE$^{-/-}$ mice transplanted with ABCG1$^{-/-}$ bone marrow, *Arteriosclerosis, Thrombosis, and Vascular Biology*, 26(10), pp. 2301–2307.

Angelo, S., Manna, C., Migliardi, V., Mazzoni, O., Morrica, P., Capasso, G., et al. (2001) Pharmacokinetics and metabolism of hydroxytyrosol, a natural antioxidant from olive oil, *Drug Metabolism and Disposition*, 29(11), pp. 1492 -1498.

Annunziata, M., Luisa, S., Assunta, M., Marika, M., Egeria, S., Carlo, S., et al. (2003) Olive oil and red wine antioxidant polyphenols inhibit endothelial activation, *Arteriosclerosis, Thrombosis, and Vascular Biology*, 23(4), pp. 622–629.

Arend, P., Malyak, M., Guthridge, J. and Gabay, C. (1998) Interleukin-1 receptor antagonist: Role in biology, *Annual Review of Immunology*, 16(1), pp. 27–55.

Ashlin, G., Buckley, M. and Ramji, D. (2012) Macrophages, lipid metabolism and gene expression in atherogenesis: A therapeutic target of the future?, *Clinical Lipidology*. 7(1), pp. 37–48.

Auñon-Calles, D., Canut, L. and Visioli, F. (2013) Toxicological evaluation of pure hydroxytyrosol, *Food and Chemical Toxicology*, 55(5), pp. 498–504.

Aydar, A., Öncü Öner, T. and Ücok, F. (2017) Effects of hydroxytyrosol on human health. *EC Naturition,* 11(4), pp. 147- 157.

Bäck, M. and Hansson, K. (2015) Anti-inflammatory therapies for atherosclerosis, *Nature Reviews Cardiology*, 12(4), pp. 199-211.

Bai, C., Yan, X., Takenaka, M., Sekiya, K. and Nagata, T. (1998) Determination of synthetic hydroxytyrosol in rat plasma by GC-MS, *Journal of Agricultural and Food Chemistry*, 46(10), pp. 3998–4001.

Baigent, C., Landray, J., Reith, C., Emberson, J., Wheeler, C., Tomson, C., et al. (2011) The effects of lowering LDL cholesterol with simvastatin plus ezetimibe in patients with chronic kidney disease (Study of Heart and Renal Protection): A randomised placebo-controlled trial, *Lancet*, 377(9784), pp. 2181–2192.

Baigent, C., Blackwell, L., Emberson, J., Holland, L., Reith, C., Bhala, N., et al. (2010) Efficacy and safety of more intensive lowering of LDL cholesterol: a meta-analysis of data from 170,000 participants in 26 randomised trials, *Lancet,* 376(9753), pp. 1670–1681.

Banach, M., Nikolic, D., Rizzo, M. and Toth, P. (2016) IMPROVE-IT: What have we learned?, *Current Opinion in Cardiology*, 31(4), pp. 426-433.

Barish, D., Atkins, R., Downes, M., Olson, P., Chong, W., Nelson, M., et al. (2008) PPARδ regulates multiple proinflammatory pathways to suppress atherosclerosis, *Proceedings of the National Academy of Sciences*, 105(11), pp. 4271-4276.

Barp, J., Araújo, R., Fernandes, G., Rigatto, V., Llesuy, S., Belló-Klein, A. and Singal, P. (2002) Myocardial antioxidant and oxidative stress changes due to sex hormones, *Brazilian Journal of Medical and Biological Research*, 35(9), pp. 1075–1081.

Barter, P. (2005) The role of HDL-cholesterol in preventing atherosclerotic disease, *European Heart Journal Supplements*, 7(suppl F), pp. F4–F8.

Baylis, A., Gomez, D., Mallat, Z., Pasterkamp, G. and Owens, K. (2017) The CANTOS trial: One important step for clinical cardiology but a giant leap for vascular biology, *Arteriosclerosis, Thrombosis, and Vascular Biology*, 37(11), pp. 174–177.

Bays, H. and Stein, A. (2003) Pharmacotherapy for dyslipidaemia – current therapies and future agents, *Expert Opinion on Pharmacotherapy*, 4(11), pp. 1901–1938.

Ben, J., Zhu, X., Zhang, H. and Chen, Q. (2015) Class A1 scavenger receptors in cardiovascular diseases, *British Journal Of Pharmacology*, 172(23), pp. 5523–5530.

Berg, AH. and Scherer, PE. (2005) Adipose Tissue, Inflammation, and Cardiovascular Disease, *Circulation Research*, 96(9), pp. 939–949.

Berrougui, H., Ikhlef, S. and Khalil, A. (2015) Extra virgin olive oil polyphenols promote cholesterol efflux and improve HDL functionality, 2015(10), *Evidence-Based Complementary and Alternative Medicine*, pp. 1-9.

Betters, L. and Yu, L. (2010) NPC1L1 and cholesterol transport, *FEBS letters*, 584(13), pp. 2740–2747.

Binder, J., Hartvigsen, K., Chang, K., Miller, M., Broide, D., Palinski, W., et al. (2004) IL-5 links adaptive and natural immunity specific for epitopes of oxidized LDL and protects from atherosclerosis, *The Journal of Clinical Investigation*, 114(3), pp. 427–437.

Bisgaard, S., Mogensen, K., Rosendahl, A., Cucak, H., Nielsen, B., Rasmussen, E. and Pedersen, X. (2016) Bone marrow-derived and peritoneal macrophages have different inflammatory response to oxLDL and M1/M2 marker expression – implications for atherosclerosis research, *Scientific Reports*, 6, pp. 35234.

Bloom, E., Cafiero, E., Jané-Llopis, E., Abrahams-Gessel, S., Reddy Bloom, L., Fathima, S., et al. (2012) The global economic burden of noncommunicable diseases, *A report by the World Economic Forum and the Harvard School of Public Health* 2012(9), pp. 1–46.

de Bock, M., Derraik, G., Brennan, M., Biggs, B., Morgan, E., Hodgkinson, C., et al. (2013) Olive (Olea europaea L.) leaf polyphenols improve insulin sensitivity in middle-aged overweight men: A randomised, placebo-controlled, crossover trial, *PLoS One*, 8(3), PP. e57622.

Boisvert, W. (2004) Modulation of atherogenesis by chemokines, *Trends in Cardiovascular Medicine*, 14(4), pp. 161–165.

Bonita, R., Magnusson, R., Bovet, P., Zhao, D., Malta, C., Geneau, R., et al. (2013) Country actions to meet UN commitments on non-communicable diseases: A stepwise approach, *The Lancet*, 381(9866), pp. 575–584.

Boskou, D. (2009) Olive Oil Minor Constituents and Health, 1st edn, *CRC press*, pp. 1-231.

Boss, A., Bishop, K., Marlow, G., Barnett, M. and Ferguson, L. (2016) Evidence to support the anti-cancer effect of olive leaf extract and future directions, *Nutrients,* 19(8), pp.513-535.

Bot, I., Ortiz Zacarías, V, de Witte, A., de Vries, H., van Santbrink, J., van der Velden, D., et al. (2017) A novel CCR2 antagonist inhibits atherogenesis in APOE deficient mice by achieving high receptor occupancy, *Scientific Reports*, 7(1), pp. 52.

Bourdillon, C., Poston, N., Covacho, C., Chignier, E., Bricca, G. and McGregor, L. (2000) ICAM-1 deficiency reduces atherosclerotic lesions in double-knockout mice (ApoE($^{-/-}$)/ICAM-1($^{-/-}$)) fed a fat or a chow diet., *Arteriosclerosis, Thrombosis, and Vascular Biology*, 20(12), pp. 2630–2635.

Bovicelli, P. (2010) Radical-scavenging polyphenols: New strategies for their synthesis, *Journal of Pharmacy and Pharmacology*, 59(12), pp. 1703–1710.

Boxel-Dezaire, H. and Stark, R. (2007) Cell type-specific signaling in response to interferon-γ, *Interferon*, 316, pp. 119–154.

Bradley, R. (2007) TNF-mediated inflammatory disease, *The Journal of Pathology*, 214(2), pp. 149–160.

Brown, S. and Goldstein, L. (1986) A receptor-mediated pathway for cholesterol homeostasis., *Science*, 232(4746), pp. 34–47.

Brzosko, S., Curtis, A., Murzilli, S., de gaetano, giovanni, Donati, M. and Iacoviello, L. (2002) Effect of extra virgin olive oil on experimental thrombosis and primary hemostasis in rats, *Nutrition, Metabolism, and Cardiovascular Diseases*, 12(6), pp. 337-342.

Buckland, G. and González, A. (2010) Trends in olive oil production, supply and consumption in mediterranean countries from 1961 to the present day, *San Diego: Academic Press*, Chapter 72, pp. 689–698.

Buckley, M. and Ramji, D. (2015) The influence of dysfunctional signaling and lipid homeostasis in mediating the inflammatory responses during atherosclerosis, Biochimica et Biophysica Acta - Molecular Basis of Disease, 1852(7), pp. 1498–1510.

Bulotta, S., Celano, M., Lepore, M., Montalcini, T., Pujia, A. and Russo, D. (2014) Beneficial effects of the olive oil phenolic components oleuropein and hydroxytyrosol: Focus on protection against cardiovascular and metabolic diseases, *Journal of Translational Medicine*, 12(1), pp. 219-228.

Caligiuri, G., Rudling, M., Ollivier, V., Jacob, M., Michel, J., Hansson, K. and Nicoletti, A. (2003) Interleukin-10 deficiency increases atherosclerosis, thrombosis, and low-density lipoproteins in apolipoprotein E knockout mice, *Molecular Medicine* 9(1–2), pp. 10–17.

Camaré, C., Pucelle, M., Nègre-Salvayre, A. and Salvayre, R. (2017) Angiogenesis in the atherosclerotic plaque, *Redox Biology*, 12(8), pp. 18–34.

Camargo, A., Ruano, J., Fernandez, M., Parnell, D., Jimenez, A., Santos-Gonzalez, M., et al. (2010) Gene expression changes in mononuclear cells in patients with metabolic syndrome after acute intake of phenol-rich virgin olive oil, *BioMed Central Genomics*., 11(4), pp. 253-264.

Cannon, P., Blazing, M., Giugliano, R., McCagg, A., White, J., Theroux, P., et al. (2015) Ezetimibe added to statin therapy after acute coronary syndromes, *New England Journal of Medicine*, 372(25), pp. 2387–2397.

Cao, K., Xu, J., Zou, X., Li, Y., Chen, C., Zheng, A., et al. (2014) Hydroxytyrosol prevents diet-induced metabolic syndrome and attenuates mitochondrial abnormalities in obese mice, *Free Radical Biology and Medicin*, 67, pp. 396-407.

Catapano, A., Farnier, M., Foody, J., Toth, P., Tomassini, J., Brudi, P. and Tershakovec, A. (2014) Combination therapy in dyslipidemia: Where are we now?, *Atherosclerosis*, 237(1), pp. 319–335.

Celermajer, D., Chow, C., Marijon, E., Anstey, N. and Woo, K. (2012) Cardiovascular disease in the developing world, *Journal of the American College of Cardiology*, 60(14), pp. 1207–1216.

Cerit, L. (2017) Fibrinogen and atherosclerosis, *Arquivos Brasileiros de Cardiologia*, 108(2), pp. 189–190.

Chamberlain, J., Francis, S., Brookes, Z., Shaw, G., Graham, D., Alp, N. J., et al. (2009) Interleukin-1 regulates multiple atherogenic mechanisms in response to fat feeding, *PloS One*, 4(4), pp. 5073–5073.

Chanput, W., Mes, J. and Wichers, H. (2014) THP-1 cell line: An in vitro cell model for immune modulation approach, *International Immunopharmacology*, 23(1), pp. 37–45.

Charo, I. and Taubman, M. (2004) Chemokines in the pathogenesis of vascular disease, *Circulation Research*, 95(9), pp. 858–866.

Charoenprasert, S. and Mitchell, A. (2012) Factors influencing phenolic compounds in table olives (Olea europaea), *Journal of Agricultural and Food Chemistry*, 60(29), pp. 7081–7095.

Chen, C., Chow, M., Huang, W., Lin, Y. and Chang, Y. (2004) Flavonoids inhibit tumor necrosis factor-alpha-induced up-regulation of intercellular adhesion molecule-1 (ICAM-1) in respiratory epithelial cells through activator protein-1 and nuclear factor-kappa B: Structure-activity relationships, *Molecular Pharmacology*, 66(3), pp. 683-693.

Chen, L., Cheng, D., Chu, J., Zhang, T., Dong, Z., Lou, H. (2018) A novel method to image macropinocytosis in vivo, *Frontiers in Neuroscience*, 12, pp. 324-332.

Chen, P., Qin, L., Li, G., Tellides, G. and Simons, M. (2016) Smooth muscle FGF/TGFβ cross talk regulates atherosclerosis progression, *EMBO Molecular Medicine*, 8(7), pp. 712–728.

Cheng, Y., Sheen, J., Hu, W. and Hung, Y. (2017) Polyphenols and oxidative stress in atherosclerosis-related ischemic heart disease and stroke, *Oxidative Medicine and Cellular Longevity*, 2017(5), pp. 1-16.

Cheng, Y., Qu, Z., Fu, X., Jiang, Q. and Fei, J. (2017) Hydroxytyrosol contributes to cell proliferation and inhibits apoptosis in pulsed electromagnetic fields treated human umbilical vein endothelial cells in vitro, *Molecular medicine reports*, 16(6), pp. 8826–8832.

Chew, M., Zhou, J., Daugherty, A., Eriksson, T., Ellermann-Eriksen, S., Hansen, P. R. and Falk, E. (2003) Thalidomide inhibits early atherogenesis in apoE-deficient mice, *APMIS,* 109(1), p. 113—116.

Chiara Maiuri, M., de stefano, D., Di Meglio, P., Irace, C., Savarese, M., Sacchi, R. et al. (2005) Hydroxytyrosol, a phenolic compound from virgin olive oil, prevents macrophage activation, *Naunyn-Schmiedeberg's Archives of Pharmacology*, 371(6), pp.457-465.

Christian, M., Sharper, V., Hoberman, A., Seng, J., Fu, L., Covell, D. et al. (2004) The toxicity profile of hydrolyzed aqueous olive pulp extract, *Drug and Chemical Toxicology*, 27(4), pp. 309–330.

Chuang, C. and McIntosh, M. (2011) Potential mechanisms by which polyphenol-rich grapes prevent obesity-mediated inflammation and metabolic diseases, *Annual Review of Nutrition*, 31(1), pp. 155–176.

Chung, E., Kim, S. and Ma, X. (2006) Regulation of cytokine production during phagocytosis of apoptotic cells, *Cell Research*. 16(2), pp. 154-161.

Chyu, K. and Shah, P. (2011) Emerging therapies for atherosclerosis prevention and management, *Cardiology Clinics*, 29(1), pp. 123–135.

Cicerale, S., Lucas, L. and Keast, R. (2010) Biological activities of phenolic compounds present in virgin olive oil, *International Journal of Molecular Sciences*, 11(2), pp. 458–479.

Collins, R., Velji, R., Guevara, N., Hicks, M., Chan, L. and Beaudet, A. (2000) P-Selectin or intercellular adhesion molecule (ICAM)-1 deficiency substantially protects against atherosclerosis in apolipoprotein E-deficient mice, *The Journal of Experimental Medicine*, 191(1), pp. 189–194.

Costa, G., Francisco, V., Lopes, M. and Batista, M. (2012) Intracellular signaling pathways modulated by phenolic compounds: application for new anti-inflammatory drugs discovery, *Current Medicinal Chemistry*, 19(18), pp. 2876–2900.

Crispe, I. (2009) The liver as a lymphoid organ, *Annual Review of Immunology*, 27(1), pp. 147–163.

Soler-Rivas, C., Espín, J. and Wichers H. (2000) Oleuropein and related compounds, *Journal of the Science of Food and Agriculture*, 80(7), pp. 1013–1023.

Curtiss, L. (2000) ApoE in Atherosclerosis, *Arterioscler Thromb Vascular Biology*, 20(8), pp. 1852–1853.

D'Addato, S., Scandiani, L., Mombelli, G., Focanti, F., Pelacchi, F., Salvatori, E., et al. (2017) Effect of a food supplement containing berberine, monacolin K, hydroxytyrosol and coenzyme Q(10) on lipid levels: A randomized, double-blind, placebo controlled study, *Drug Design, Development and Therapy*, 11, pp. 1585–1592.

Das, UN. (2008) Essential fatty acids and their metabolites could function as endogenous HMG-CoA reductase and ACE enzyme inhibitors, anti-arrhythmic, anti-hypertensive, anti-atherosclerotic, anti-inflammatory, cytoprotective, and cardioprotective molecules, *Lipids in Health and Disease*, 7(1), pp. 15-37.

Dave, V. and Kaul, D. (2010) Coronary heart disease: Significance of liver X receptor α genomics, *World journal of cardiology*, 2(6), pp. 140–149.

Davenport, P. and Tipping, P. (2003) The role of interleukin-4 and interleukin-12 in the progression of atherosclerosis in apolipoprotein E-deficient mice, *The American Journal of Pathology*, 163(3), pp. 1117–1125.

Demyanets, S., Huber, K. and Wojta, J. (2012) Vascular effects of glycoprotein130 ligands — Part II: Biomarkers and therapeutic targets, *Vascular Pharmacology*, 57(1), pp. 29–40.

Devlin, C., Kuriakose, G., Hirsch, E. and Tabas, I. (2002) Genetic alterations of IL-1 receptor antagonist in mice affect plasma cholesterol level and foam cell lesion size, *Proceedings of the National Academy of Sciences*, 99(9), pp. 6280 -6285.

De Winther, M., van Dijk, K., Havekes, L. and Hofker, M. (2000) Macrophage scavenger receptor class A: A multifunctional receptor in atherosclerosis, *Arteriosclerosis, Thrombosis, and Vascular Biology* , 20(2), pp. 290–297.

Dietrich, T., Hucko, T., Schneemann, C., Neumann, M., Menrad, A., Willuda, J., et al. (2012) Local delivery of IL-2 reduces atherosclerosis via expansion of regulatory T cells, *Atherosclerosis*, 220(2), pp. 329–336.

Dinarello, C. (1996) Biologic basis for interleukin-1 in disease, *Blood*, 87(6), pp. 2095 - 2147.

Dinarello, C. (2010) Anti-inflammatory agents: Present and future, *Cell*, 140(6), pp. 935–950.

Doevendans, P., Jukema, W., Spiering, W., Defesche, J. and Kastelein, J. (2001) Molecular genetics and gene expression in atherosclerosis, *International Journal of Cardiology*, 80(2), pp. 161–172.

Dotsenko, O. (2010) Stem/Progenitor cells, atherosclerosis and cardiovascular regeneration, *The Open Cardiovascular Medicine Journal*, 4, pp. 97–104.

Dreosti, I. (2016) Antioxidant polyphenols in tea, cocoa, and wine, *Nutrition*, 16(7), pp. 692–694.

Drira, R., Chen, S. and Sakamoto, K. (2011) Oleuropein and hydroxytyrosol inhibit adipocyte differentiation in 3 T3-L1 cells, *Life Sciences*, 89(19), pp. 708–716.

Dutta, P., Courties, G., Wei, Y., Leuschner, F., Gorbatov, R., Robbins, C. S., et al. (2012) Myocardial infarction accelerates atherosclerosis, *Nature*, 487(7404), pp. 325-329.

Duval, C., Chinetti, G., Trottein, F., Fruchart, J. and Staels, B. (2002) The role of PPARs in atherosclerosis, *Trends in Molecular Medicine*, 8(9), pp. 422–430.

Echeverría, F., Ortiz, M., Valenzuela, R. and Videla, A. (2017) Hydroxytyrosol and cytoprotection: A projection for clinical interventions, *International Journal of Molecular Sciences* , 18(5), pp. 930-944.

van Eck, M., Bos, I., Kaminski, W., Orsó, E., Rothe, G., Twisk, J., Böttcher, A., et al. (2002) Leukocyte ABCA1 controls susceptibility to atherosclerosis and macrophage recruitment into tissues, *Proceedings of the National Academy of Sciences of the United States of America*, 99(9), pp. 6298–6303.

Ehrenborg, E. and Skogsberg, J. (2013) Peroxisome proliferator-activated receptor delta and cardiovascular disease, *Atherosclerosis*, 231(1), pp. 95–106.

Ehrt, S., Schnappinger, D., Bekiranov, S., Drenkow, J., Shi, S., Gingeras, T., et al. (2001) Reprogramming of the macrophage transcriptome in response to interferon-γ and *mycobacterium tuberculosis* : Signaling roles of nitric oxide synthase-2 and phagocyte oxidase, *The Journal of Experimental Medicine*. 194(8), pp. 1123–1140.

Eisen, M., Spellman, P., Brown, P. and Botstein, D. (1998) Cluster analysis and display of genome-wide expression patterns, *Proceedings of the National Academy of Sciences of the United States of America*. 95(25), pp. 14863–14868.

Elena, G. and Klaus, L. (2007) Vascular adhesion molecules in atherosclerosis, *Arteriosclerosis, Thrombosis, and Vascular Biology*, 27(11), pp. 2292–2301.

Emerit, J., Edeas, M. and Bricaire, F. (2004) Neurodegenerative diseases and oxidative stress, *Biomedicine & Pharmacotherapy*, 58(1), pp. 39–46.

Engler, M. (1993) Comparative study of diets enriched with evening primrose, black currant, borage or fungal oils on blood pressure and pressor responses in spontaneously hypertensive rats, *Prostaglandins, Leukotrienes and Essential Fatty Acids*, 49(4), pp. 809–814.

Erbel, C., Achenbach, J., Akhavanpoor, M., Dengler, T. J., Lasitschka, F., Gleissner, C., et al. (2011) PARP inhibition in atherosclerosis and its effects on dendritic cells, T cells and auto-antibody levels, *European Journal of Medical Research*, 16(8), pp. 367–374.

Escolà-Gil, J., Lee-Rueckert, M., Santos, D., Cedó, L., Blanco-Vaca, F. and Julve, J. (2015) Quantification of in vitro macrophage cholesterol efflux and in vivo macrophage-specific reverse cholesterol transport, *Methods in Mouse Atherosclerosis*, 1339, pp. 211–233.

Esti, M., Cinquanta, L. and La Notte, E. (1998) Phenolic compounds in different olive varieties, *Journal of Agricultural and Food Chemistry*, 46(1), pp. 32–35.

Everett, B., Pradhan, A., Solomon, D., Paynter, N., Macfadyen, J., Zaharris, et al. (2013) Rationale and design of the cardiovascular inflammation reduction trial: A test of the inflammatory hypothesis of atherothrombosis, *American Heart Journal*, 166(2), pp. 199–207.

Fabiani, R. (2016) Anti-cancer properties of olive oil secoiridoid phenols: A systematic review of in vivo studies, *Food & Function*. 7(10), pp. 4145–4159.

Fabiani, R., De Bartolomeo, A., Rosignoli, P., Servili, M., Montedoro, G. and Morozzi, G. (2002) Cancer chemoprevention by hydroxytyrosol isolated from virgin olive oil through G1 cell cycle arrest and apoptosis, *European Journal of Cancer Prevention*, 11(4), pp. 351-358.

Fairweather, D. (2015) Sex differences in inflammation during atherosclerosis, *Cardiology*. 8(3), pp. 49–59.

Falcone Ferreyra, M., Rius, S. and Casati, P. (2012) Flavonoids: Biosynthesis, biological functions, and biotechnological applications, *Frontiers in Plant Science* , 2012(3), pp. 222-237.

Feoktistova, M., Geserick, P. and Leverkus, M. (2016) Crystal violet assay for determining viability of cultured cells, *Cold Spring Harbor Protocols* , 2016(4),1101-1112.

Fernández del Río, L., Gutiérrez-Casado, E., Varela-López, A. and Villalba, J. (2016) Olive oil and the hallmarks of aging, *Molecules*, 21(2), pp. 163-193.

Ferrara, L., Raimondi, A., d'Episcopo, L., Guida, L. and Marotta, T. (2000) Olive oil and reduced need for antihypertensive medications, *Archives of Internal Medicine*, 160(6), pp. 837–842.

Fichtlscherer, S., Schmidt-Lucke, C., Bojunga, S., Rössig, L., Heeschen, C., Dimmeler, S. and Zeiher, A. (2006) Differential effects of short-term lipid lowering with ezetimibe and statins on endothelial function in patients with CAD: Clinical evidence for "pleiotropic" functions of statin therapy, *European Heart Journal*, 27(10), pp. 1182–1190.

Fishman, A. (2015) The antioxidant hydroxytyrosol: Biotechnological production challenges and opportunities, *Applied Microbiology and Biotechnology*, 99(3), pp. 1119–1130.

Fitó, M., Cladellas, M., de la Torre, R., Martí, J., Muñoz, D., Schröder, H., et al. (2007) Anti-inflammatory effect of virgin olive oil in stable coronary disease patients: a randomized, crossover, controlled trial, *European Journal Of Clinical Nutrition*, 62(4), pp. 570-574.

Förstermann, U. (2008) Oxidative stress in vascular disease: Causes, defense mechanisms and potential therapies, *Nature Clinical Practice Cardiovascular Medicine*, 5(6), pp. 338-349.

Fortes, C., García-Vilas, J., Quesada, A. and Medina, M. (2012) Evaluation of the anti-angiogenic potential of hydroxytyrosol and tyrosol, two bio-active phenolic compounds of extra virgin olive oil, in endothelial cell cultures, *Food Chemistry*, 134(1), pp. 134–140.

Frank, P. and Lisanti, M. (2008) ICAM-1: Role in inflammation and in the regulation of vascular permeability, *American Journal of Physiology. Heart and Circulatory Physiology*, 295(3), pp. 926–927.

Freigang, S., Ampenberger, F., Weiss, A., Kanneganti, T., Iwakura, Y., Hersberger, M. and Kopf, M. (2013) Fatty acid–induced mitochondrial uncoupling elicits inflammasome-independent IL-1α and sterile vascular inflammation in atherosclerosis, *Nature Immunology*. 14(10), pp. 1045-1053.

Frolova, E., Sopko, N., Blech, L., Popovic, Z., Li, J., Vasanji, A., Drumm, C., et al. (2012) Thrombospondin-4 regulates fibrosis and remodeling of the myocardium in response to pressure overload, *Official Publication of the Federation of American Societies for Experimental Biology*, 26(6), pp. 2363–2373.

Frostegård, J. (2013) Immunity, atherosclerosis and cardiovascular disease, *BMC Medicine*, 11(1), pp. 117-130.

Funk, J., Feingold, K., Moser, A. and Grunfeld, C. (1993) Lipopolysaccharide stimulation of RAW 264.7 macrophages induces lipid accumulation and foam cell formation, *Atherosclerosis*, 98(1), pp. 67–82.

Funke, H. and Assmann, G. (1999) Strategies for the assessment of genetic coronary artery disease risk, *Current Opinion in Lipidology*, 10(3), pp.285-291.

van Galen, K., Tuinenburg, A., Smeets, E. and Schutgens, R. (2012) Von Willebrand factor deficiency and atherosclerosis, *Blood Reviews*, 26(5), pp. 189–196.

García-Martínez, O., De Luna-Bertos, E., Ramos-Torrecillas, J., Ruiz, C., Milia, E., Lorenzo, M. L., et al. (2016) Phenolic compounds in extra virgin olive oil stimulate human osteoblastic cell proliferation, *Plos One*, 11(3), pp. 150045–150045.

García-Martínez, O., Rivas, A., Ramos-Torrecillas, J., De Luna-Bertos, E. and Ruiz, C. (2014) The effect of olive oil on osteoporosis prevention, *International Journal of Food Sciences and Nutrition*, 65(7), pp. 834–840.

Georgia vogiatzi, Tousoulis, C. (2009) The role of oxidative stress in atherosclerosis, *Hellenic Journal of Cardiology*, 50(5), pp. 402–409.

Getz, G. and Reardon, C. (2012) Animal models of atherosclerosis, *Arteriosclerosis, Thrombosis, and Vascular Biology*, 32(5), pp. 1104 -1115.

Gharavi, N., Alva, J., Mouillesseaux, K., Lai, C., Yeh, M., Yeung, W., et al. (2007) Role of the JAK/STAT pathway in the regulation of interleukin-8 transcription by oxidized phospholipids in vitro and in atherosclerosis in vivo, *Journal of Biological Chemistry* , 282(43), pp. 31460–31468.

Gilbert, J., Lekstrom-Himes, J., Donaldson, D., Lee, Y., Hu, M., Xu, J., Wyant, T. and Davidson, M. (2011) Effect of CC chemokine receptor 2 CCR2 blockade on serum C-reactive protein in individuals at atherosclerotic risk and with a single nucleotide polymorphism of the monocyte chemoattractant protein-1 promoter region, *American Journal of Cardiology*, 107(6), pp. 906–911.

Ginhoux, F. and Jung, S. (2014) Monocytes and macrophages: developmental pathways and tissue homeostasis, *Nature Reviews Immunology*, 14(6), pp. 392-404.

Ginzinger, D. (2002) Gene quantification using real-time quantitative PCR: An emerging technology hits the mainstream, *Experimental Hematology*, 30(6), pp. 503–512.

Giordano, E., Dávalos, A. and Visioli, F. (2014) Chronic hydroxytyrosol feeding modulates glutathione-mediated oxido-reduction pathways in adipose tissue: A nutrigenomic study, *Nutrition, Metabolism and Cardiovascular Diseases*, 24(10), pp. 1144–1150.

Gofman, J., Lindgren, F., Elliott, H., Mantz, W., Hewitt, J., Strisower, B., Herring, V. and Lyon, T. (1950) The Role of lipids and lipoproteins in atherosclerosis, *Science*, 111(2877), pp. 166 -186.

Golledge, J., Clancy, P., Maguire, J., Lincz, L. and Koblar, S. (2011) The role of tenascin C in cardiovascular disease, *Cardiovascular Research*, 92(1), pp. 19–28.

González, M., Martín-Bautista, E., Carrero, J., Fonollá, J., Baró, L., Bartolomé, M., et al. (2006) One-month administration of hydroxytyrosol, a phenolic antioxidant present in olive oil, to hyperlipemic rabbits improves blood lipid profile, antioxidant status and reduces atherosclerosis development, *Atherosclerosis*, 188(1), pp. 35–42.

Gonzalez, M., Zarzuelo, A., Gamez, M., Utrilla, M., Jimenez, J. and Osuna, I. (1993) Hypoglycemic activity of olive leaf, *Planta medica*. 58(6), pp.513-515.

Gordon, T., Kannel, WB., Castelli, WP., and Dawber, TR. (1981) Lipoproteins, cardiovascular disease, and death: The Framingham Study, *Archives of Internal Medicine*, 141(9), pp. 1128–1131.

Gosling, J., Slaymaker, S., Gu, L., Tseng, S., Zlot, C., Young, S., Rollins, B. and Charo, I. (1999) MCP-1 deficiency reduces susceptibility to atherosclerosis in mice that overexpress human apolipoprotein B, *The Journal of Clinical Investigation*, 103(6), pp. 773–778.

Grainger, D., Reckless, J. and McKilligin, E. (2004) Apolipoprotein E modulates clearance of apoptotic bodies in vitro and in vivo, resulting in a systemic proinflammatory state in apolipoprotein E-deficient mice, *The Journal of Immunology*, 173(10), pp. 6366 -6375.

Granados-Principal, S., Quiles, J., Ramirez-Tortosa, C., Sánchez-Rovira, P. and Ramirez-Tortosa, M. (2010) Hydroxytyrosol: From laboratory investigations to future clinical trials, *Nutrition reviews*, 68(4), pp. 191-206.

Greenow, K., Pearce, N. and Ramji, D. (2005) The key role of apolipoprotein E in atherosclerosis, *Journal of Molecular Medicine*, 83(5), pp. 329–342.

Gu, L., Okada, Y., Clinton, S., Gerard, C., Sukhova, G., Libby, P. and Rollins, B. (1998) Absence of monocyte chemoattractant protein-1 reduces atherosclerosis in low density lipoprotein receptor–deficient mice, *Molecular Cell*, 2(2), pp. 275–281.

Guadalupe, O., Luis, M., Purificacion, H., Beñat, M., Virginia, L, Oscar, L., et al. (2009) Suppressors of cytokine signaling modulate JAK/STAT-mediated cell responses during atherosclerosis, *Arteriosclerosis, Thrombosis, and Vascular Biology*, 29(4), pp. 525–531.

Guichard, C., Pedruzzi, E., Fay, M., Marie, J., Braut-Boucher, F., Daniel, F., et al. (2006) Dihydroxyphenylethanol induces apoptosis by activating serine/threonine protein phosphatase PP2A and promotes the endoplasmic reticulum stress response in human colon carcinoma cells, *Carcinogenesis*, 27(9), pp. 1812–1827.

Gustafsson, Å. and Gottlieb, R. (2007) Bcl-2 family members and apoptosis, taken to heart, *American Journal of Physiology-Cell Physiology*, 292(1), pp. 45–51.

Hagiwara, K., Goto, T., Araki, M., Miyazaki, H. and Hagiwara, H. (2011) Olive polyphenol hydroxytyrosol prevents bone loss, *European Journal of Pharmacology*, 662(1), pp. 78–84.

Halliwell, B. (1994) Free radicals, antioxidants, and human disease: Curiosity, cause, or consequence?, *The Lancet*, 344(8924), pp. 721–724.

Hamden, K., Allouche, N., Damak, M. and Elfeki, A. (2009) Hypoglycemic and antioxidant effects of phenolic extracts and purified hydroxytyrosol from olive mill waste in vitro and in rats, *Chemico Biological Interact*, 180(3), pp. 421-432.

Hartman, J. and Frishman, W. (2014) Inflammation and atherosclerosis: A review of the role of interleukin-6 in the development of atherosclerosis and the potential for targeted drug therapy, *Cardiology in Review*, 22(3), pp.147-151.

Harvey, E. and Ramji, D. (2005) Interferon-γ and atherosclerosis: Pro- or anti-atherogenic?, *Cardiovascular Research*, 67(1), pp. 11–20.

Hauer, A. , Uyttenhove, C., de Vos, P., Stroobant, V., Renauld, J., van Berkel, T., van Snick, J. and Kuiper, J. (2005) Blockade of interleukin-12 function by protein vaccination attenuates atherosclerosis, *Circulation*, 112(7), pp. 1054–1062.

Heek, M., Farley, C., Compton, D., Hoos, L. and Davis, H. (2001) Ezetimibe selectively inhibits intestinal cholesterol absorption in rodents in the presence and absence of exocrine pancreatic function, *British Journal of Pharmacology*, 134(2), pp. 409–417.

Hewlett, L, Prescott, A. and Watts, C. (1994) The coated pit and macropinocytic pathways serve distinct endosome populations, *The Journal of Cell Biology*, 124(5), pp. 689-703.

Hmimed, S., Belarbi, M. and Visioli, F. (2016) Hydroxytyrosol augments the redox status of high fat diet-fed rats, *PharmaNutrition*, 4(4), pp. 139–142.

Hsiao, A., Wong, M., Kanouse, D., Collins, R., Liu, H., Andersen, R., et al. (2003) Complementary and alternative medicine use and substitution for conventional therapy by HIV-infected patients, *Journal of Acquired Immune Deficiency Syndromes*, 33(2), pp.157-165.

Hu, Y., Dietrich, H., Metzler, B., Wick, G. and Xu, Q. (2000) Hyperexpression and activation of extracellular signal–regulated kinases (ERK1/2) in atherosclerotic lesions of cholesterol-fed rabbits, *Atherosclerosis, Thrombosis and Vascular Biology,* 20(1), pp. 18–27.

Huber, S., Sakkinen, P., David, C., Newell, M. and Tracy, R. (2001) T helper-cell phenotype regulates atherosclerosis in mice under conditions of mild hypercholesterolemia, *Circulation*, 103(21), pp. 2610—2616.

Huijgen, R., Boekholdt, S., Arsenault, B., Bao, W., Davaine, J., Tabet, F., et al. (2012) Retracted: Plasma PCSK9 levels and clinical outcomes in the TNT (Treating to new targets) trial, *Journal of the American College of Cardiology*, 59(20), pp. 1778 -1784.

Insull, W. (2009) The pathology of atherosclerosis: plaque development and plaque responses to medical treatment, *The American Journal of Medicine*, 122(1), pp. 3–14.

Iqbal, J. and Hussain, M. (2009) Intestinal lipid absorption, *American Journal of Physiology, Endocrinology and Metabolism*, 296(6), pp. 1183–1194.

Iwona, C., Atilla, Y., Michael, K., Dieter, R., Brigstock David, R., et al. (2005) Connective tissue growth factor is overexpressed in complicated atherosclerotic plaques and induces mononuclear cell chemotaxis in vitro, *Arteriosclerosis, Thrombosis, and Vascular Biology*, 25(5), pp. 1008–1013.

Jablonski, K., Amici, S., Webb, L., Ruiz-Rosado, J, Popovich, P., Partida-Sanchez, S. and Guerau-De-arellano, M. (2015) Novel markers to delineate murine M1 and M2 macrophages, *PLoS ONE*, 10(12), pp. 1-25.

Jacob, G., Yehuda, S., Boris, G., Arnon, A., Aviv, S. and Dror, H. (2000) Requisite role for interleukin-4 in the acceleration of fatty streaks induced by heat shock protein 65 or mycobacterium tuberculosis, *Circulation Research*, 86(12), pp. 1203–1210.

Jemai, H., El Feki, A. and Sayadi, S. (2009) Antidiabetic and antioxidant effects of hydroxytyrosol and oleuropein from olive leaves in alloxan-diabetic rats, *Journal of Agriculture and Food Chemistry*, 57(19), pp. 8798-8804.

Jemai, H., Fki, I., Bouaziz, M., Bouallagui, Z., El Feki, A., Isoda, H. and Sayadi, S. (2008) Lipid-lowering and antioxidant effects of hydroxytyrosol and its triacetylated derivative recovered from olive tree leaves in cholesterol-fed rats, *Journal of Agriculture and Food Chemistry*, 56(8), pp. 2630-2636.

Jian, G., Van Eck, M., Twisk, J.,Maeda, N., Benson, G., Groot, PH. and Van Berkel, TJ. (2003) Transplantation of monocyte CC-chemokine receptor 2–deficient bone marrow into ApoE3–leiden mice inhibits atherogenesis, *Arteriosclerosis, Thrombosis, and Vascular Biology*, 23(3), pp. 447–453.

Johnson, J. L. and Newby, A. (2009) Macrophage heterogeneity in atherosclerotic plaques, *Current Opinion in Lipidology*, 20(5), pp. 370–378.

Kamari, Y., Shaish, A., Shemesh, S., Vax, E., Grosskopf, I., Dotan, S., White, M., et al. (2011) Reduced atherosclerosis and inflammatory cytokines in apolipoprotein-E-deficient mice lacking bone marrow-derived interleukin-1α, *Biochemical and Biophysical Research Communications*, 405(2), pp. 197–203.

Kander, M., Cui, Y. and Liu, Z. (2017) Gender difference in oxidative stress: A new look at the mechanisms for cardiovascular diseases, *Journal of Cellular and Molecular Medicine*, 21(5), pp. 1024–1032.

Khurana, S., Venkataraman, K., Hollingsworth, A., Piche, M. and Tai, C. (2013) Polyphenols: Benefits to the cardiovascular system in health and in aging, *Nutrients,* 5(10), pp.3779-3827.

Killeen, M., Linder, M., Pontoniere, P. and Crea, R. (2014) NF-κβ signaling and chronic inflammatory diseases: Exploring the potential of natural products to drive new therapeutic opportunities, *Drug Discovery Today*, 19(4), pp. 373–378.

King, K. Y. and Goodell, M. (2011) Inflammatory modulation of HSCs: Viewing the HSC as a foundation for the immune response, *Immunology*, 11(10), pp. 685–692.

Kishore, R. and Verma, S. (2012) Roles of STATs signaling in cardiovascular diseases, *JAK-STAT*, 1(2), pp. 118–124.

Kitagawa, K., Matsumoto, M., Sasaki, T., Hashimoto, H., Kuwabara, K., Ohtsuki, T. and Hori, M. (2002) Involvement of ICAM-1 in the progression of atherosclerosis in APOE-knockout mice, *Atherosclerosis*, 160(2), pp. 305–310.

Kleemann, R., Verschuren, L., van Erk, M., Nikolsky, Y., Cnubben, N., Verheij, E., et al. (2007) Atherosclerosis and liver inflammation induced by increased dietary cholesterol intake: A combined transcriptomics and metabolomics analysis, *Genome Biology*, 8(9), pp. 200–216.

Kleemann, R., Zadelaar, S. and Kooistra, T. (2008) Cytokines and atherosclerosis: A comprehensive review of studies in mice, *Cardiovascular Research*, 79(3), pp. 360–376.

Klucken, J., Büchler, C., Orsó, E., Kaminski, W., Porsch-Ozcürümez, M., Liebisch, G., et al. (2000) ABCG1 (ABC8), the human homolog of the Drosophila white gene, is a regulator of macrophage cholesterol and phospholipid transport., *Proceedings of the National Academy of Sciences of the United States of America*, 97(2), pp. 817–822.

Kojima, Y., Weissman, I. and Leeper, N. (2017) The Role of efferocytosis in atherosclerosis, *Circulation*, 135(5), pp. 476–489.

Kouro, T. and Takatsu, K. (2009) IL-5- and eosinophil-mediated inflammation: from discovery to therapy, *International Immunology*, 21(12), pp. 1303–1309.

Kozera, B. and Rapacz, M. (2013) Reference genes in real-time PCR, *Journal of Applied Genetics*, 54(4), pp. 391–406.

Kraemer, R. (2000) Regulation of cell migration in atherosclerosis, *Current Atherosclerosis Reports*, 2(5), pp. 445–452.

Kramer, F., Just, S. and Zeller, T. (2018) New perspectives: systems medicine in cardiovascular disease, *BioMed Central*, *Systems Biology*, 12(1), pp. 57-70.

Kromhout, D., Keys, A., Aravanis, C., Buzina, R., Fidanza, F., Giampaoli, S., et al. (1989) Food consumption patterns in the 1960s in seven countries, *The American Journal of Clinical Nutrition*, 49(5), pp. 889–894.

Kruth, H., Huang, W., Ishii, I. and Zhang, W. (2002) Macrophage foam cell formation with native low density lipoprotein, *Journal of Biological Chemistry* , 277(37), pp. 34573–34580.

Kruth, H., Jones, N., Huang, W., Zhao, B., Ishii, I., Chang, J., et al. (2005) Macropinocytosis is the endocytic pathway that mediates macrophage foam cell formation with native low density lipoprotein, *Journal of Biological Chemistry* , 280(3), pp. 2352–2360.

Kruth, H. S. (2011) Receptor-independent fluid-phase pinocytosis mechanisms for induction of foam cell formation with native LDL particles, *Current opinion in lipidology*, 22(5), pp. 386–393.

Kubo, N., McCurdy, S. and Boisvert, W. (2015) Defective fas expression on bone marrow derived cells alters atherosclerotic plaque morphology in hyperlipidemic mice, *Discoveries*, 3(1), pp. 37-57.

Kuehnast, S., van der Hoorn, J., Pieterman, E., van den Hoek, A., Sasiela, W., Gusarova, V., et al. (2014) Alirocumab inhibits atherosclerosis, improves the plaque

morphology, and enhances the effects of a statin, *Journal of Lipid Research,* 55(10), pp. 2103-2115.

Kunjathoor, V., Febbraio, M., Podrez, E., Moore, K., Andersson, L., Koehn, S., et al. (2002) Scavenger receptors class A-I/II and CD36 are the principal receptors responsible for the uptake of modified low density lipoprotein leading to lipid loading in macrophages, *Journal of Biological Chemistry* , 277(51), pp. 49982–49988.

de la Torre-Robles, A., Rivas, A., Lorenzo-Tovar, M., Monteagudo, C., Mariscal-Arcas, M. and Olea-Serrano, F. (2014) Estimation of the intake of phenol compounds from virgin olive oil of a population from southern Spain, *Food Additives & Contaminants: Part A*. 31(9), pp. 1460–1469.

Laguna, J. and Alegret, M. (2012) Regulation of gene expression in atherosclerosis: insights from microarray studies in monocytes/macrophages, *Pharmacogenomics,* 13(4), pp. 477-495.

Lamy, S., Ouanouki, A., Béliveau, R. and Desrosiers, R. (2014) Olive oil compounds inhibit vascular endothelial growth factor receptor-2 phosphorylation, *Experimental Cell Research*, 322(1), pp. 89–98.

Lee-Huang, S., Huang, P. L., Zhang, D., Lee, J. W., Bao, J., Sun, Y., et al. (2007) Discovery of small-molecule HIV-1 fusion and integrase inhibitors oleuropein and hydroxytyrosol: Part I. fusion inhibition, *Biochemical and Biophysical Research Communications*, 354(4), pp. 872–878.

Lee-Huang, S., Zhang, L., Lin Huang, P., Chang, Y. and Huang, P. (2003) Anti-HIV activity of olive leaf extract (OLE) and modulation of host cell gene expression by HIV-1 infection and OLE treatment, *Biochemical and Biophysical Research Communications*, 307(4), pp. 1029–1037.

Lee, C., North, K., Bray, M., Couper, D., Heiss, G. and Zeldin, D. (2008) Cyclooxygenase polymorphisms and risk of cardiovascular events: The Atherosclerosis risk in communities (ARIC) study, *Clinical Pharmacology and Therapeutics*, 83(1), pp. 52–60.

Lee, D., Li, H., Lim, H., Lee, H., Jeon, R. and Ryu, J. (2012) Anti-Inflammatory activity of sulfur-containing compounds from garlic, *Journal of Medicinal Food*. 15(11), pp. 992–999.

Lee, Y. and Hirani, A. (2006) Role of interleukin-4 in atherosclerosis, *Archives of Pharmacal Research*. 29(1), pp. 1–15.

Lee, Y., Kim, P., Lee, W. and Hirani, A. (2010) Interleukin-4, oxidative stress, vascular inflammation and atherosclerosis, *Biomolecules & therapeutics*, 18(2), pp. 135–144.

Lemieux, I., Lamarche, B., Couillard, C., Pascot, A., Cantin, B., Bergeron, J., et al. (2001) Total cholesterol/HDL cholesterol ratio vs LDL cholesterol/HDL cholesterol ratio as indices of ischemic heart disease risk in men: The Quebec cardiovascular study, *Archives of Internal Medicine*, 161(22), pp. 2685–2692.

Levy, E., Ouadda, A., Spahis, S., Sane, A., Garofalo, C., Grenier, et al. (2013) 'PCSK9 plays a significant role in cholesterol homeostasis and lipid transport in intestinal epithelial cells', *Atherosclerosis*, 227(2), pp. 297–306.

Lewis, W. (1931) Pinocyosis, *John Hopkins Hosp Bull*, 49, pp. 17–27.

Ley, K. and Huo, Y. (2001) VCAM-1 is critical in atherosclerosis, *The Journal of Clinical Investigation*, 107(10), pp. 1209–1210.

Ley, K., Miller, Y. and Hedrick, C. (2011) Monocyte and macrophage dynamics during atherogenesis, *Arteriosclerosis, Thrombosis, and Vascular Biology* , 31(7), pp. 1506–1516.

Ley, K., Miller, Y. and Hedrick, C. (2011) Monocyte and Macrophage Dynamics During Atherogenesis, *Arteriosclerosis, Thrombosis, and Vascular Biology*, 31(7), pp. 1506–1516.

Li, L., Blumenthal, D., Terry, C., He, Y., Carlson, M., and Cheung, A. K. (2011) PDGF-induced proliferation in human arterial and venous smooth muscle cells: Molecular basis for differential effects of PDGF isoforms, *Journal of Cellular Biochemistry*, 112(1), pp. 289–298.

Li, N., McLaren, J., Michael, D., Clement, M., Fielding, C. a and Ramji, D. (2010) ERK is integral to the IFN-γ-mediated activation of STAT1, the expression of key genes implicated in atherosclerosis, and the uptake of modified lipoproteins by human macrophages, *Journal of immunology*, 185(5), pp. 3041–3048.

Li, N., Salter, R. and Ramji, D. (2011) Molecular mechanisms underlying the inhibition of IFN-γ-induced, STAT1-mediated gene transcription in human macrophages by simvastatin and agonists of PPARs and LXRs, *Journal of Cellular Biochemistry*. 112(2), pp. 675–683.

Libby, P. (2012) Inflammation in Atherosclerosis, *Arteriosclerosis, Thrombosis, and Vascular Biology*, 32(9), pp. 2045–2051.

Libby, P., Bornfeldt, K. and Tall, A. (2016) Atherosclerosis, *Circulation Research*, 118(4), pp. 531–534.

Lim, J. and Gleeson, P. (2011) Macropinocytosis: an endocytic pathway for internalising large gulps, Journal of *Immunology and Cell Biology*, 89(8), pp. 836–843.

Lim, W., Timmins, J. M., Seimon, T., Sadler, A., Kolodgie, F., Virmani, R. and Tabas, I. (2008) Signal transducer and activator of transcription-1 is critical for apoptosis in macrophages subjected to endoplasmic reticulum stress in vitro and in advanced atherosclerotic lesions in vivo, *Circulation*, 117(7), pp. 940–951.

Lin, X., Xiao, L., Tang, Z., Jiang, Z. and Liu, M. (2018) Role of PCSK9 in lipid metabolism and atherosclerosis, *Biomedicine & Pharmacotherapy*, 104, pp. 36–44.

Liu, M, Tang, Z., Li, G., Qu, S., Zhang, Y., Ren, Z., Liu, L. and Jiang, Z. (2013) Janus-like role of fibroblast growth factor 2 in arteriosclerotic coronary artery disease: Atherogenesis and angiogenesis, *Atherosclerosis*, 229(1), pp. 10–17.

Liu, N., Lossinsky, A., Popik, W., Li, X., Gujuluva, C., Kriederman, B., Roberts, J., Pushkarsky, T., et al. (2002) Human immunodeficiency virus type 1 enters brain microvascular endothelia by macropinocytosis dependent on lipid rafts and the mitogen-activated protein kinase signaling pathway, *Journal of Virology*, 76(13), pp. 6689–6700.

Livak, K. J. and Schmittgen, T. (2001) Analysis of relative gene expression data using real-time quantitative PCR and the 2−ΔΔCT Method, *Methods*. Academic Press, 25(4), pp. 402–408.

Lockyer, S., Rowland, I., Spencer, J., Yaqoob, P. and Stonehouse, W. (2017) Impact of phenolic-rich olive leaf extract on blood pressure, plasma lipids and inflammatory markers: A randomised controlled trial, *European journal of Nutrition*, 56(4), pp. 1421–1432.

Logue, J., AL-Ghibiwi, H., Alamri, A. and Preiss, D. (2015) Systematic review of studies exploring reasons for statin non-adherence and of randomised controlled trials of interventions to improve adherence, *Atherosclerosis*, 241(1), pp. 32-72.

López-Villodres, J., Abdel-Karim, M., De La Cruz, J., Rodríguez-Pérez, M., Reyes, J., Guzmán-Moscoso, R., et al. (2016) Effects of hydroxytyrosol on cardiovascular biomarkers in experimental diabetes mellitus, *The Journal of Nutritional Biochemistry*, 37, pp. 94–100.

Louis, S. and Zahradka, P. (2010) Vascular smooth muscle cell motility: From migration to invasion, *Experimental & Clinical Cardiology*, 15(4), pp. 75–85.

Lum, H. and Roebuck, K. (2001) Oxidant stress and endothelial cell dysfunction, *American Journal of Physiology-Cell Physiology*, 280(4), pp. 719–741.

Luque-Sierra, A., Alvarez-Amor, L., Kleemann, R., Martín, F. and Varela, L. (2018) Extra-virgin olive oil with natural phenolic content exerts an anti-inflammatory effect in adipose tissue and attenuates the severity of atherosclerotic lesions in LDLR$^{-/-}$ leiden mice, *Molecular Nutrition & Food Research*, 62(13), pp. 1-11.

Lusis, A. (2000) Atherosclerosis, *Nature*, 407(6801), pp. 233–241.

Lutfi, E., Babin, P., Gutiérrez, J., Capilla, E. and Navarro, I. (2017) Caffeic acid and hydroxytyrosol have anti-obesogenic properties in zebrafish and rainbow trout models, *PloS One*, 12(6), pp. 178833–178833.

Madjid, M., Awan, I., Willerson, J. and Casscells, S. (2004) Leukocyte count and coronary heart disease: Implications for risk assessment, *Journal of the American College of Cardiology*, 44(10), pp. 1945–1956.

Madjid, M., Casscells, S. and Willerson, J. (2007) Biomarkers of inflammation as surrogate markers in detection of vulnerable plaques and vulnerable patients, *Cardiovascular Medicine*, pp. 641–651.

Madjid, M. and Fatemi, O. (2013) Components of the complete blood count as risk predictors for coronary heart disease: in-depth review and update, *Texas Heart Institute Journal*, 40(1), pp. 17–29.

Mallat, Z. (2014) Macrophages, *Arteriosclerosis, Thrombosis, and Vascular Biology*, 34(12), pp. 2509–2519.

Mangas-cruz, M., Fernández-moyano, A., Albi, T., Guinda, A., Relimpio, F., Lanzón, A., et al. (2001) Effects of minor constituents (non-glyceride compounds) of virgin olive oil on plasma lipid concentrations in male Wistar rats, *Clinical Nutrition*, 20(3), pp. 211–215.

Manna, C., Galletti, P., Maisto, G., Cucciolla, V., D'Angelo, S. and Zappia, V. (2000) Transport mechanism and metabolism of olive oil hydroxytyrosol in Caco-2 cells, *FEBS Letters*, 470(3), pp. 341–344.

Manning-Tobin, J., Moore, K., Seimon, T., Bell, S., Sharuk, M., Alvarez-Leite, J., et al. (2009) Loss of SR-A and CD36 activity reduces atherosclerotic lesion complexity without abrogating foam cell formation in hyperlipidemic mice, *Arteriosclerosis, Thrombosis, and Vascular biology*, 29(1), pp. 19–26.

Manz, M., Traver, D., Miyamoto, T., Weissman, I. and Akashi, K. (2001) Dendritic cell potentials of early lymphoid and myeloid progenitors, *Blood*, 97(11), pp. 3333-3341.

Martinez, F., Helming, L. and Gordon, S. (2009) Alternative activation of macrophages: an immunologic functional perspective, *Annual Review of Immunology*, 27(1), pp. 451–483.

Masanori, A., Elena, R., Seigo, S., Yoshihiro, F., Yutaka, F., Masashi, S. and Peter, L. (2001) An HMG-CoA reductase inhibitor, cerivastatin, suppresses growth of macrophages expressing matrix metalloproteinases and tissue factor in vivo and in vitro, *Circulation*, 103(2), pp. 276–283.

McLaren, J. E., Michael, D., Ashlin, T. and Ramji, D. (2011) Cytokines, macrophage lipid metabolism and foam cells: Implications for cardiovascular disease therapy, *Progress in Lipid Research*, 50(4), pp. 331–347.

McLaren, J. and Ramji, D. (2009) Interferon gamma: a master regulator of atherosclerosis., *Cytokine & Growth Factor Reviews*, 20(2), pp. 125–135.

Mead, J. and Ramji, D. (2002) The pivotal role of lipoprotein lipase in atherosclerosis, *Cardiovascular Research*, 55(2), pp. 261–269.

Mendis, S., Puska, P. and Norrving, B. (2011) Global atlas on cardiovascular disease prevention and control, Geneva, World *Health Organization in collaboration with the World Heart Federation and the World Stroke Organization,* 2011, pp. 155.

Merhi-Soussi, F., Kwak, B., Magne, D., Chadjichristos, C., Berti, M., Pelli, G., et al. (2005) Interleukin-1 plays a major role in vascular inflammation and atherosclerosis in male apolipoprotein E-knockout mice, *Cardiovascular Research*, 66(3), pp. 583–593.

Michael, D., Ashlin, T., Davies, C, Gallagher, H., Stoneman, T., Buckley, M. and Ramji, D. (2013) Differential regulation of macropinocytosis in macrophages by cytokines: Implications for foam cell formation and atherosclerosis, *Cytokine*, 64(1), pp. 357–361.

Millán, J., Pintó, X., Muñoz, A., Zúñiga, M., Rubiés-Prat, J., Pallardo, L. F., Masana, L., Mangas, A., Hernández-Mijares, A., González-Santos, P., Ascaso, J. and Pedro-Botet, J. (2009) Lipoprotein ratios: Physiological significance and clinical usefulness in cardiovascular prevention, *Vascular Health and Risk Management*, 5, pp. 757–765.

Miller, A., Xu, D., Asquith, D., Denby, L., Li, Y., Sattar, N., Baker, A., McInnes, I. and Liew, F. (2008) IL-33 Reduces the Development of Atherosclerosis, *The Journal of Experimental Medicine*, 205(2), pp. 339-346.

Miserez, A., Muller, P., Barella, L., Barella, S., Staehelin, H., Leitersdorf, E., Kark, J. and Friedlander, Y. (2002) Sterol-regulatory element-binding protein (SREBP)-2 contributes to polygenic hypercholesterolaemia, *Atherosclerosis*, 164(1), pp. 15–26.

Mollie, R., Nan, W., Seongah, H., Laurent, Y., Carrie, W. and R., Tall. A. (2006) Decreased atherosclerosis in low-density lipoprotein receptor knockout mice transplanted with ABCG1$^{-/-}$ bone marrow, *Arteriosclerosis, Thrombosis, and Vascular Biology*, 26(10), pp. 2308–2315.

Montecucco, F., Braunersreuther, V., Viviani, G., Lenglet, S. and Mach, F. (2012) Update on the pathophysiological role of intracellular signaling pathways in atherosclerotic plaques and ischemic myocardium, *Current Signal Transduction Therapy*, 7(2), pp. 104–110.

Moore, K. and Freeman, M. (2006a) Scavenger receptors in atherosclerosis: Beyond lipid uptake, *Arteriosclerosis, Thrombosis, and Vascular Biology*, 26(8), pp. 1702–1711.

Moore, K. J., Sheedy, F. J. and Fisher, E. a (2013) Macrophages in atherosclerosis: a dynamic balance, *Nature reviews. Immunology*, 13(10), pp. 709–21.

Moore, K. J. and Tabas, I. (2011) The cellular biology of macrophages in atherosclerosis, *Cell*, 145(3), pp. 341–355.

Morrell, C. (2008) Reactive oxygen species: Finding the right balance, *Circulation Research*, 103(6), pp. 571–572.

Moss, J. and Ramji, D., (2015) Interferon-γ: Promising therapeutic target in atherosclerosis, *World Journal of Experimental Medicine*, 5(3), pp. 154-159.

Moss, J., Davies, T., Garaiova, I., Plummer, S., Michael, D.. and Ramji, D. (2016) A unique combination of nutritionally active ingredients can prevent several key processes associated with atherosclerosis in vitro, *PLOS ONE*, 11(3), pp. e0151057.

Moss, J. and Ramji, D. (2016) Nutraceutical therapies for atherosclerosis, *Nature Review Cardiology*. 13(9), pp. 513–532.

Muslin, A. (2008) MAPK signalling in cardiovascular health and disease: Molecular mechanisms and therapeutic targets, *Clinical Science*, 115(7), pp. 203–18.

Myhre, O., Sterri, S., Bogen, I. and Fonnum, F. (2004) Erk1/2 phosphorylation and reactive oxygen species formation via nitric oxide and Akt-1/Raf-1 crosstalk in cultured rat cerebellar granule cells exposed to the organic solvent 1,2,4-trimethylcyclohexane, *Toxicological Sciences*, 80(2), pp. 296–303.

Nadkarni, S., Bouma, B., de Boer, J. and Tearney, G. (2009) Evaluation of collagen in atherosclerotic plaques: The use of two coherent laser-based imaging methods, *Lasers in Medical Science*, 24(3), pp. 439–445.

Nageh, M., Sandberg, E., Marotti, K., Lin, A., Melchior, E., Bullard, D. and Beaudet, A. (1997) Deficiency of inflammatory cell adhesion molecules protects against atherosclerosis in mice, *Arteriosclerosis, Thrombosis, and Vascular Biology*, 17(8), pp. 1517–1520.

Navarese, E., Buffon, A., Andreotti, F., Kozinski, M., Welton, N., Fabiszak, T., et al. (2013) Meta-analysis of impact of different types and doses of statins on new-onset diabetes mellitus, *American Journal of Cardiology*, 111(8), pp. 1123–1130.

Nishinakamura, R., Nakayama, N., Hirabayashi, Y., Inoue, T., Aud, D., Mcneil, T., et al. (1995) Mice deficient for the IL-3/GM-CSF/IL-5 βc receptor exhibit lung pathology and impaired immune response, while βIL3 receptor-deficient mice are normal, *Immunity*, 2(3), pp. 211–222.

Nus, M., Martínez-Poveda, B., MacGrogan, D., Chevre, R., D'Amato, G., Sbroggio, M., et al. (2016) Endothelial Jag1-RBPJ signalling promotes inflammatory leucocyte recruitment and atherosclerosis, *Cardiovascular Research*, 112(2), pp. 568–580.

O'Farrelly, C. and Crispe, I. (1999) Prometheus through the looking glass: reflections on the hepatic immune system, *Immunology Today*, 20(9), pp. 394–398.

O'Dowd, Y., Driss, F., Dang, P., Elbim, C., Gougerot-Pocidalo, M., Pasquier, C. and El-Benna, J. (2004) Antioxidant effect of hydroxytyrosol, a polyphenol from olive oil: scavenging of hydrogen peroxide but not superoxide anion produced by human neutrophils, *Biochemical Pharmacology*, 68(10), pp. 2003–2008.

Ohashi, R., Mu, H., Wang, X., Yao, Q. and Chen, C. (2005) Reverse cholesterol transport and cholesterol efflux in atherosclerosis, *International journal of medicin*, 98(12), pp. 845-856.

Oliveira, H., Cosso, R., Alberici, L., Maciel, E., Salerno, A., Dorighello, G., Velho, J.., de Faria, E. and Vercesi, A. (2004) Oxidative stress in atherosclerosis-prone mouse is due to low antioxidant capacity of mitochondria, Federation of American Societies for Experimental Biology, 19(2), pp. 278–280.

Olsen, B. (1995) The roles of collagen genes in skeletal development and morphogenesis, *Experientia*, 51(3), pp. 194–195.

Oram, J. (2003) HDL Apolipoproteins and ABCA1, *Arteriosclerosis, Thrombosis, and Vascular Biology*, 23(5), p. 720 LP-727.

Oram, J. and Heinecke, J. (2005) ATP-binding cassette transporter A1: A cell cholesterol exporter that protects against cardiovascular disease, *Physiological Reviews*, 85(4), pp. 1343–1372.

Oram, J. and Vaughan, A. (2006) ATP-binding cassette cholesterol transporters and cardiovascular disease, *Circulation Research* , 99(10), pp. 1031–1043.

Oulion, S., Bertrand, S. and Escriva, H. (2012) Evolution of the FGF Gene Family, *International Journal of Evolutionary Biology*, 20(11), pp.563-569.

Owen, R. ., Haubner, R., Mier, W., Giacosa, A., Hull, W., Spiegelhalder, B. and Bartsch, H. (2003) Isolation, structure elucidation and antioxidant potential of the major phenolic and flavonoid compounds in brined olive drupes, *Food and Chemical Toxicology*, 41(5), pp. 703–717.

Owen, R., Mier, W., Giacosa, A., Hull, W., Spiegelhalder, B. and Bartsch, H. (2000) Phenolic compounds and squalene in olive oils: the concentration and antioxidant potential of total phenols, simple phenols, secoiridoids, lignansand squalene, *Food and Chemical Toxicology*, 38(8), pp. 647–659.

Pacurari, M., Kafoury, R., Tchounwou, P. and Ndebele, K. (2014) The Renin-angiotensin-aldosterone system in vascular inflammation and remodeling, *International Journal of Inflammation*, 24(6), pp.983-991.

Parmar, K., Larman, H., Dai, G., Zhang, Y., Wang, E., Moorthy, S., Kratz, J., et al. (2006) Integration of flow-dependent endothelial phenotypes by Kruppel-like factor 2, *The Journal of Clinical Investigation*. 116(1), pp. 49–58.

Patel, S., Thiagarajan, R., Willerson, J. and Yeh, E. (1998) Inhibition of α4 integrin and ICAM-1 markedly attenuate macrophage homing to atherosclerotic plaques in ApoE-deficient mice, *Circulation*, 97(1), pp. 75–81.

Peng, J., Luo, F., Ruan, G., Peng, R. and Li, X. (2017) Hypertriglyceridemia and atherosclerosis, *Lipids in Health and Disease* 16(1), pp. 233-245.

Pennings, M., Meurs, I., Ye, D., Out, R., Hoekstra, M., Van Berkel, T. and Eck, M. Van (2006) Regulation of cholesterol homeostasis in macrophages and consequences for atherosclerotic lesion development, *FEBS Letters*, 580(23), pp. 5588–5596.

Peters, V., Joesting, J. and Freund, G. (2013) IL-1 receptor 2 (IL-1R2) and its role in immune regulation, *Brain, Behavior, and Immunity*, 32(8), pp. 1–8.

Peyrol, J., Riva, C. and Amiot, M. J. (2017) Hydroxytyrosol in the Prevention of the Metabolic Syndrome and Related Disorders, *Nutrients*., 9(3), pp. 306-424.

Pham-Huy, L., He, H. and Pham-Huy, C. (2008) Free Radicals, Antioxidants in Disease and Health, *International Journal of Biomedical Science* 4(2), pp. 89–96.

Phan, B., Dayspring, T. and Toth, P. (2012) Ezetimibe therapy: mechanism of action and clinical update, *Vascular Health and Risk Management*, 8, pp. 415–427.

Phillips, C. and Perry, I. (2013) Does Inflammation Determine Metabolic Health Status in Obese and Nonobese Adults?, *The Journal of Clinical Endocrinology & Metabolism*, 98(10), pp. 1610–1619.

Phillips, M. (2014) Molecular mechanisms of cellular cholesterol efflux, *The Journal of Biological Chemistry*, 289(35), pp. 24020–24029.

Pierre, G., Alexia, S., Cédric, F., Victorine, D., Barbara, G., Bertrand, C., François, T., Francis, B. and Jean-François, A. (2007) Transforming growth factor activity is a key determinant for the effect of estradiol on fatty streak deposit in hypercholesterolemic mice, *Arteriosclerosis, Thrombosis, and Vascular Biology*. 27(10), pp. 2214–2221.

Pinderski Oslund Laura, J., Hedrick Catherine, C., Olvera, T., Hagenbaugh, A., Territo, M., Berliner Judith, A. and Fyfe Alistair, I. (1999) Interleukin-10 blocks atherosclerotic events in vitro and in vivo, *Arteriosclerosis, Thrombosis, and Vascular Biology*, 19(12), pp. 2847–2853.

Plotnikov, A., Zehorai, E., Procaccia, S. and Seger, R. (2011) The MAPK cascades: Signaling components, nuclear roles and mechanisms of nuclear translocation, *Biochimica et Biophysica Acta- Molecular Cell Research*, 1813(9), pp. 1619–1633.

Prasad, K. and Kalra, J. (1993) Oxygen free radicals and hypercholesterolemic atherosclerosis: Effect of vitamin E, *American Heart Journal*, 125(4), pp. 958–973.

Prashar, Y., Ritu, Bais, S. and Gill, N. S. (2017) Emerging role of various signaling pathways in the pathogenesis and therapeutics of atherosclerosis, *Reviews in Vascular Medicine*, 10–11, pp. 1–12.

Puel, C., Mardon, J., Agalias, A., Davicco, M., Lebecque, P., Mazur, A., Horcajada, M., Skaltsounis, A.,. and Coxam, V. (2008) Major phenolic compounds in olive oil modulate bone loss in an ovariectomy/inflammation experimental model, *Journal of Agricultural and Food Chemistry*, 56(20), pp. 9417–9422.

Rabar, S., Harker, M., O'Flynn, N. and Wierzbicki, A. (2014) Lipid modification and cardiovascular risk assessment for the primary and secondary prevention of cardiovascular disease: Summary of updated NICE guidance, *British Medical Journal*, 349, pp. 4356-4413.

Racoosin, E. and Swanson, J. (1989) Macrophage colony-stimulating factor (rM-CSF) stimulates pinocytosis in bone marrow-derived macrophages, *The Journal of Experimental Medicine*, 170(5), pp. 1635 -1648.

Rafieian-Kopaei, M., Setorki, M., Doudi, M., Baradaran, A. and Nasri, H. (2014) Atherosclerosis: Process, indicators, risk factors and new hopes, *International Journal of Preventive Medicine*, 5(8), pp. 927–946.

Rakesh, K. and Agrawal, D. (2005) Controlling cytokine signaling by constitutive inhibitors, *Biochemical Pharmacology*, 70(5), pp. 649–657.

Ramana, C., Gil, M., Schreiber, R. and Stark, G. (2002) Stat1-dependent and -independent pathways in IFN-γ-dependent signaling, *Trends in Immunology*, 23(2), pp. 96–101.

Ramji, D. and Davies, T. (2015) Cytokines in atherosclerosis: Key players in all stages of disease and promising therapeutic targets, *Cytokine & Growth Factor Reviews*, 26(6), pp. 673-685.

Ramkumar, S., Raghunath, A. and Raghunath, S. (2016) Statin Therapy: Review of safety and potential side effects', *Acta Cardiologica Sinica*. Taiwan Society of Cardiology, 32(6), pp. 631–639.

Rana, J., Boekholdt, S., Ridker, P., Jukema, J., Luben, R., Bingham, S., et al. (2007) Differential leucocyte count and the risk of future coronary artery disease in healthy men and women: the EPIC-Norfolk prospective population study, *Journal of Internal Medicine*, 262(6), pp. 678–689.

Reape, T. and Groot, P. (1999) Chemokines and atherosclerosis, *Atherosclerosis*, 147(2), pp. 213–225.

Reboredo-Rodríguez, P., Varela-López, A., Forbes-Hernández, T., Gasparrini, M., Afrin, S., Cianciosi, D., Zhang, J., Manna, P. (2018) Phenolic compounds isolated from olive oil as nutraceutical tools for the prevention and management of cancer and cardiovascular diseases, *International Journal of Molecular Sciences*, 19(8), pp. 2305-2326.

Recinos, A., LeJeune, W., Sun, H., Lee, C., Tieu, B., Lu, M., et al. (2007) Angiotensin II induces IL-6 expression and the Jak-STAT3 pathway in aortic adventitia of LDL receptor-deficient mice, *Atherosclerosis*, 194(1), pp. 125–133.

Reddy, S., Hsiao, K., Abernethy, V., Fan, H., Longacre, A., Lieberthal, W., et al. (2002) Phagocytosis of apoptotic cells by macrophages induces novel signaling events leading to cytokine-independent survival and inhibition of proliferation: Activation of Akt and inhibition of extracellular signal-regulated kinases 1 and 2', *The Journal of Immunology*, 169(2), pp. 702 LP-713.

Regitz-Zagrosek, V. (2006) Therapeutic implications of the gender-specific aspects of cardiovascular disease, *Nature Reviews Drug Discovery*, 5(5), pp. 425-435.

Reiss, A., Awadallah, N., Malhotra, S., Montesinos, M., Chan, E., Javitt, N. and Cronstein, B. (2001) Immune complexes and IFN-γ decrease cholesterol 27-hydroxylase in human arterial endothelium and macrophages, *Journal of Lipid Research* , 42(11), pp. 1913–1922.

Reiss, A., Siegart, N. and De Leon, J. (2017) Interleukin-6 in atherosclerosis: Atherogenic or atheroprotective?, *Clinical Lipidology*, 12(1), pp. 14–23.

Ren, J., Zhang, S., Kovacs, A., Wang, Y. and Muslin, A. J. (2005) Role of p38; MAPK in cardiac apoptosis and remodeling after myocardial infarction, *Journal of Molecular and Cellular Cardiology*, 38(4), pp. 617–623.

Richard, N., Arnold, S., Hoeller, U., Kilpert, C., Wertz, K. and Schwager, J. (2011a) Hydroxytyrosol is the major anti-inflammatory compound in aqueous olive extracts and impairs cytokine and chemokine production in macrophages, *Planta Medica*, 77(17),pp.1890-1897.

Ricote, M. and Glass, C. (2007) PPARs and molecular mechanisms of transrepression, *Biochimica et Biophysica Acta*, 1771(8), pp. 926–935.

Ridker, P., Everett, B., Thuren, T., MacFadyen, J., Chang, W., Ballantyne, C., Fonseca, F., et al. (2017) Antiinflammatory therapy with canakinumab for atherosclerotic disease, *New England Journal of Medicine*, 377(12), pp. 1119–1131.

Ridker, P., Thuren, T., Zalewski, A. and Libby, P. (2011) Interleukin-1β inhibition and the prevention of recurrent cardiovascular events: Rationale and design of the canakinumab anti-inflammatory thrombosis outcomes study (CANTOS)', *American Heart Journal*, 162(4), pp. 597–605.

Ridley, A., Schwartz, M., Burridge, K., Firtel, R., Ginsberg, M., Borisy, G., et al. (2003) Cell Migration: Integrating signals from front to back, *Science*, 302(5651), pp. 1704 - 1709.

Risk factors- *World Heart Federation-FACT SHEET* (2017). A vailable online at: https://www.world-heart-federation.org/resources/risk-factors/.

Rivera, J., Lozano, M., Navarro-Núñez, L. and Vicente, V. (2009) Platelet receptors and signaling in the dynamics of thrombus formation, *Haematologica*, 94(5), pp. 700–711.

Robbins, C., Chudnovskiy, A., Rauch, P., Figueiredo, J., Iwamoto, Y., Gorbatov, R., et al. (2012) Extramedullary hematopoiesis generates Ly-6Chigh monocytes that infiltrate atherosclerotic lesions, *Circulation*, 125(2), pp. 364–374.

Robinson, M., Harmon, C. and O'Farrelly, C. (2016) Liver immunology and its role in inflammation and homeostasis, *Cellular & Molecular Immunology*, 13(3), pp. 267–276.

Roger, V., Go, A., Lloyd-Jones, D., Adams, R., Berry, J., Brown, T., Carnethon, M. et al. (2011) Heart disease and stroke statistics-2011 update: A report from the American Heart Association, *Circulation*, 123(4), pp. 18–209.

Romero, C., Brenes, M., Yousfi, K., García, P., García, A. and Garrido, A. (2004) Effect of cultivar and processing method on the contents of polyphenols in table olives, *Journal of Agricultural and Food Chemistry*, 52(3), pp. 479–484.

Romero, M., Toral, M., Gómez-Guzmán, M., Jiménez, R., Galindo, P., Sánchez, M., et al. (2016) Antihypertensive effects of oleuropein-enriched olive leaf extract in spontaneously hypertensive rats, *Food & Function*, 7(1), pp. 584–593.

Rosignoli, P., Fuccelli, R., Fabiani, R., Servili, M. and Morozzi, G. (2013) Effect of olive oil phenols on the production of inflammatory mediators in freshly isolated human monocytes, *The Journal of Nutritional Biochemistry*, 24(8), pp. 1513–1519.

Rőszer, T., Menéndez-Gutiérrez, M. P., Cedenilla, M. and Ricote, M. (2013) Retinoid X receptors in macrophage biology, *Trends in Endocrinology & Metabolism*, 24(9), pp. 460–468.

Roth, G., Johnson, C., Abajobir, A., Abd-Allah, F., Abera, S., Abyu, G., *et al.* (2017) Global, regional, and national burden of cardiovascular diseases for 10 causes, 1990 to 2015, *Journal of the American College of Cardiology*, 70(1), pp. 1–25.

Russo, M., Hoofnagle, J., Gu, J., Fontana, R., Barnhart, H., Kleiner, D., et al. (2014) Spectrum of statin hepatotoxicity: experience of the drug-induced liver injury network, *Hepatology,* 60(2), pp. 679–686.

Samet, I. (2014) Effect of olive leaf components on the proliferation and viability of hematopoietic stem cells, *Asian Journal of Biomedical and Pharmaceutical Sciences*, 4(39), pp.2014-2017.

Santangelo, C., Vari, R., Scazzocchio, B., Benedetto, R., Filesi, C. and Masella, R. (2007) Polyphenols, intracellular signalling and inflammation, *Ann Ist Super Sanita,* 43(4), pp. 394–405.

Santhakumar, A. B., Battino, M. and Alvarez-Suarez, J. (2018) Dietary polyphenols: Structures, bioavailability and its protective effects against atherosclerosis, Food and Chemical Toxicology, 113,pp. 49-65.

Scheidt, V., Zhao, Y., Kurt, Z., Pan, C., Zeng, L., Yang, X., et al. (2017) Applications and limitations of mouse models for understanding human atherosclerosis, *Cell Metabolism*, 25(2), pp. 248–261.

Schreyer, S., Peschon, J. and LeBoeuf, R. (1996) Accelerated atherosclerosis in mice lacking tumor necrosis factor receptor p55', *Journal of Biological Chemistry*, 271(42), pp. 26174–26178.

Schrijvers, D., De Meyer, G., Herman, A. and Martinet, W. (2007) Phagocytosis in atherosclerosis: Molecular mechanisms and implications for plaque progression and stability, *Cardiovascular Research*, 73(3), pp. 470–480.

Seeland, U. and Regitz-Zagrosek, V. (2012) Sex and gender differences in cardiovascular drug therapy, *Handbook of Experemental Pharmaology,* 214(2012), pp. 211–236.

Sheehy, A., Mokelke, E., Lloyd, P., Sturek, J. and Sturek, M. (2006) Reduced expression of leukemia inhibitory factor correlates with coronary atherosclerosis in the metabolic syndrome, Federation of American Societies for Experimental Biology,

20(4), pp. A698–A698.

Shen, Y., Song, S., Keum, N. and Park, T. (2014) Olive leaf extract attenuates obesity in high-fat diet-fed mice by modulating the expression of molecules involved in adipogenesis and thermogenesis, *Evidence-Based Complementary and Alternative Medicine,* 2014 (1), pp. 1-12.

Shu, Q., Lennemann, N., Sarkar, S., Sadovsky, Y. and Coyne, C. (2015) ADAP2 is an interferon stimulated gene that restricts rna virus entry, *PLoS Pathogens*, 11(9), pp. 1005150–1005150.

Silbiger, V., Luchessi, A., Hirata, R.., Lima-Neto, L., Cavichioli, D., Carracedo, A., et al. (2013) Novel genes detected by transcriptional profiling from whole-blood cells in patients with early onset of acute coronary syndrome, *Clinica Chimica ACTA*, 421(5), pp. 184–190.

Singer, K., DelProposto, J., Lee Morris, D., Zamarron, B., Mergian, T., Maley, N., et al. (2014) Diet-induced obesity promotes myelopoiesis in hematopoietic stem cells, *Molecular Metabolism*, 3(6), pp. 664–675.

Smith, J. (2010) Apolipoprotein A-I and its mimetics for the treatment of atherosclerosis, *Current Opinion in Investigational Drugs*, 11(9), pp. 989–996.

Soehnlein, O., Drechsler, M., Döring, Y., Lievens, D., Hartwig, H., Kemmerich, K., et al. (2013) Distinct functions of chemokine receptor axes in the atherogenic mobilization and recruitment of classical monocytes, *EMBO Molecular Medicine*, 5(3), pp. 471–481.

Soobrattee, M., Neergheen, V., Luximon-Ramma, A., Aruoma, O. and Bahorun, T. (2005) Phenolics as potential antioxidant therapeutic agents: Mechanism and actions, *Mutation Research/Fundamental and Molecular Mechanisms of Mutagenesis*, 579(1), pp. 200–213.

Sookoian, S., Gianotti, T., Rosselli, M., Burgueño, A., Castaño, G. and Pirola, C. (2011) Liver transcriptional profile of atherosclerosis-related genes in human nonalcoholic fatty liver disease, *Atherosclerosis*, 218(2), pp. 378–385.

Sosnowska, B., Penson, P. and Banach, M. (2017) The role of nutraceuticals in the prevention of cardiovascular disease, *Cardiovascular diagnosis and therapy*, 7(1), pp. S21–S31.

Stoka, K., Maedeker, J., Bennett, L., Bhayani, S., Gardner, W., Procknow, J., et al. (2018) Effects of increased arterial stiffness on atherosclerotic plaque amounts, *Journal of Biomechanical Engineering*, 140(5), pp. 51007–51010.

Storniolo, C., Roselló-Catafau, J., Pintó, X., Mitjavila, M. and Moreno, J. (2014) Polyphenol fraction of extra virgin olive oil protects against endothelial dysfunction induced by high glucose and free fatty acids through modulation of nitric oxide and endothelin-1, *Redox biology*, 2(2014), pp. 971–977.

Stylianou, I., Bauer, R., Reilly, M. and Rader, D. (2012) Genetic basis of atherosclerosis: Insights from mice and humans, *Circulation Research*, 110(2), pp.337-355.

Subramanian, M., Thorp, E. and Tabas, I. (2015) Identification of a non-growth factor role for GM-CSF in advanced atherosclerosis: Promotion of macrophage apoptosis and plaque necrosis through IL-23 signaling, *Circulation research*, 116(2), pp. 13–24.

Agrawal, S., Febbraio, M., Podrez, E., Cathcart, M., Stark, G., Chisolm, G.,(2007) Signal transducer and activator of transcription 1 is required for optimal foam cell formation and atherosclerotic lesion development, *Circulation*, 115(23), pp. 2939–2947.

Sun, H., Krauss, R., Chang, J. and Teng, B. (2018) PCSK9 deficiency reduces atherosclerosis, apolipoprotein B secretion, and endothelial dysfunction, *Journal of Lipid Research* , 59(2), pp. 207–223.

Suzuki, H., Kurihara, Y., Takeya, M., Kamada, N., Kataoka, M., Jishage, K., (1997) A role for macrophage scavenger receptors in atherosclerosis and susceptibility to infection, *Nature*, 386(6622), pp. 292–296.

Swanson, J. and Watts, C. (1995) Macropinocytosis, *Trends in Cell Biology*, 5(11), pp. 424–428.

Tabas, I. (2005) Consequences and therapeutic implications of macrophage apoptosis in atherosclerosis: the importance of lesion stage and phagocytic efficiency, *Arteriosclerosis, Thrombosis, and Vascular Biology*, 25(11), pp. 2255–2264.

Tabas, I. (2009) Macrophage death and defective inflammation resolution in atherosclerosis, *Nature Reviews Immunology*. 10(1), pp. 3646.

Tabas, I., García-Cardeña, G. and Owens, G. (2015) Recent insights into the cellular biology of atherosclerosis, *The Journal of Cell Biology*, 209(1), pp. 13 -22.

Takai, S., Jin, D., Kawashima, H., Kimura, M., Shiraishi-Tateishi, A., Tanaka, T., (2009) Anti-atherosclerotic effects of dihomo and gamma-linolenic acid in ApoE-deficient mice, *Journal of Atherosclerosis and Thrombosis*, 16(4), pp. 480–489.

Takatsu, K. (2011) Interleukin-5 and IL-5 receptor in health and diseases, *Proceedings of the Japan Academy. Series B, Physical and Biological Sciences*, 87(8), pp. 463–485.

Talayero, B. and Sacks, F. (2011) The role of triglycerides in atherosclerosis, *Current Cardiology Reports*, 13(6), pp. 544–552.

Tang, Z., Peng, J., Ren, Z., Yang, J., Li, T., Wang, Z., et al. (2017) New role of PCSK9 in atherosclerotic inflammation promotion involving the TLR4/NF-κB pathway, *Atherosclerosis*, 262, pp. 113–122.

Tavori, H., Fan, D., Blakemore, J., Yancey, P., Ding, L., Linton, M. and Fazio, S. (2013) Serum proprotein convertase subtilisin/kexin type 9 and cell surface low-density lipoprotein receptor: Evidence for a reciprocal regulation, *Circulation*, 127(24), pp. 2403–2413.

Taylor, F., Ward, K., Moore, T., Burke, M., Davey Smith, G., Casas, J.. and Ebrahim, S. (2011) Statins for the primary prevention of cardiovascular disease, *The Cochrane Database of Systematic Reviews*, 31(1), pp. 4816-4828.

Tedgui, A. and Mallat, Z. (2006) Cytokines in Atherosclerosis: Pathogenic and Regulatory Pathways, *Physiological Reviews*, 86(2), pp. 515–581.

Tennant, M. and McGeachie, J. (2018) Platelet-derived growth factor and its role in atherogenesis: a brief review, *Australian and New Zealand Journal of Surgery*, 61(7), pp. 482–488.

Terzuoli, E., Giachetti, A., Ziche, M. and Donnini, S. (2016) Hydroxytyrosol, a product from olive oil, reduces colon cancer growth by enhancing epidermal growth factor receptor degradation, *Molecular Nutrition & Food Research*, 60(3), pp. 519–529.

Thorp, E., Li, Y., Bao, L., Yao, P., Kuriakose, G., Rong, J., Fisher, E. and Tabas, I. (2009) Brief report: Increased apoptosis in advanced atherosclerotic lesions of Apoe-/- mice lacking macrophage Bcl-2, *Arteriosclerosis, Thrombosis, and Vascular Biology*. 29(2), pp. 169–172.

Von der Thüsen, J., Kuiper, J., Van Berkel, T. and Biessen, E. (2003) Interleukins in Atherosclerosis: Molecular pathways and therapeutic potential, *Pharmacological Reviews*, 55(1), pp. 133 -166.

Toma, I. and McCaffrey, T. (2012) Transforming growth factor-β and atherosclerosis: Interwoven atherogenic and atheroprotective aspects, *Cell and Tissue Research*, 347(1), pp. 155–175.

Tregouet, D., Barbaux, S., Poirier, O., Blankenberg, S., Bickel, C., Escolano, S., et al. (2003) SELPLG gene polymorphisms in relation to plasma SELPLG levels and coronary artery disease, *Annals of Human Genetics*, 67(6), pp. 504–511.

Trinchieri, G. (2003) Interleukin-12 and the regulation of innate resistance and adaptive immunity, *Nature Reviews Immunology*, 3(2), pp. 133-146.

Tsujita, K., Sugiyama, S., Sumida, H., Shimomura, H., Yamashita, T., Yamanaga, K., et al. (2015) Impact of dual lipid-lowering strategy with ezetimibe and atorvastatin on coronary plaque regression in patients with percutaneous coronary intervention: The multicenter randomized controlled PRECISE-IVUS trial, *Journal of the American College of Cardiology*, 66(5), pp. 495–507.

Tuck, K., Freeman, M., Hayball, P., Stretch, G., and Stupans, I. (2001) The in vivo fate of hydroxytyrosol and tyrosol, antioxidant phenolic constituents of olive oil, after intravenous and oral dosing of labeled compounds to rats, *The Journal of Nutrition*, 131(7), pp. 1993–1996.

Tuck, K. and Hayball, P. (2002) Major phenolic compounds in olive oil: Metabolism and health effects, *The Journal of Nutritional Biochemistry*, 13(11), pp. 636–644.

Turner, C., Badu-Nkansah, K., Crowley, D., van der Flier, A. and Hynes, R. (2015) α5 and αv integrins cooperate to regulate vascular smooth muscle and neural crest functions in vivo, *Development*, 142(4), pp. 797-808.

Upadhya, S., Mooteri, S., Peckham, N. and Pai, R. (2004) Atherogenic effect of interleukin-2 and antiatherogenic effect of interleukin-2 antibody in Apo-E-deficient mice, *Angiology*, 55(3), pp. 289–294.

Vacek, T., Rehman, S., Neamtu, D., Yu, S., Givimani, S. and Tyagi, S. (2015) Matrix metalloproteinases in atherosclerosis: Role of nitric oxide, hydrogen sulfide, homocysteine, and polymorphisms, *Vascular Health and Risk Management*, 11, pp. 173–183.

Valledor, A., Sánchez-Tilló, E., Arpa, L., Park, J., Caelles, C., Lloberas, J. and Celada, A. (2008) Selective roles of MAPKs during the macrophage response to IFN-γ, *The Journal of Immunology* , 180(7), pp. 4523–4529.

Vaughan, C., Gotto, A. and Basson, C. (2000) The evolving role of statins in the management of atherosclerosis, *Journal of the American College of Cardiology*, 35(1), pp. 1–10.

Venza, M., Visalli, M., Beninati, C., De Gaetano, G., Teti, D. and Venza, I. (2015) Cellular mechanisms of oxidative stress and action in melanoma, *Oxidative Medicine and Cellular Longevity*, 2015, pp.481782-481793.

Vilaplana-Pérez, C., Auñón, D., García-Flores, L. and Gil-Izquierdo, A. (2014) Hydroxytyrosol and potential uses in cardiovascular diseases, cancer, and AIDS, *Frontiers in Nutrition*, 1, pp. 18-29.

Vinante, F. and Rigo, A. (2013) Heparin-binding epidermal growth factor-like growth factor/diphtheria toxin receptor in normal and neoplastic hematopoiesis, *Toxins*, 5(6), pp. 1180–1201.

Visioli, F., Bellomo, G. and Galli, C. (1998a) Free radical-scavenging properties of olive oil polyphenols, *Biochemical and Biophysical Research Communications*, 247(1), pp. 60–64.

Visioli, F., Bellomo, G., Montedoro, G. and Galli, C. (1995) Low density lipoprotein oxidation is inhibited in vitro by olive oil constituents, *Atherosclerosis*, 117(1), pp. 25–32.

Visioli, F., Galli, C., Bornet, F., Mattei, A., Patelli, R., Galli, G. and Caruso, D. (2000) Olive oil phenolics are dose-dependently absorbed in humans, *FEBS Letters*, 468(2–3), pp. 159–160.

Visioli, F., Galli, C., Grande, S., Colonnelli, K., Patelli, C., Galli, G. and Caruso, D. (2003) Hydroxytyrosol excretion differs between rats and humans and depends on the vehicle of administration, *The Journal of Nutrition*, 133(8), pp. 2612–2615.

Visioli, F., Wolfram, R., Richard, D., Abdullah, M. and Crea, R. (2009) Olive phenolics increase glutathione levels in healthy volunteers, *Journal of Agricultural and Food Chemistry*, 57(5), pp. 1793–1796.

Vissers, M., Zock, P., and Katan, M. (2004) Bioavailability and antioxidant effects of olive oil phenols in humans: a review', *European Journal Of Clinical Nutrition*. Nature Publishing Group, 58, p. 955.

Vissers, M., Zock, P., Roodenburg, A., Leenen, R. and Katan, M. (2002) Olive oil phenols are absorbed in humans, *The Journal of Nutrition*, 132(3), pp. 409–417.

Vogel, C. and Marcotte, E. (2012) Insights into the regulation of protein abundance from proteomic and transcriptomic analyses, *Nature reviews. Genetics*, 13(4), pp. 227–232.

van der Vusse, G., Glatz, J., Stam, H., and Reneman, R. (1992) Fatty acid homeostasis in the normoxic and ischemic heart, *Physiological Reviews*. 72(4), pp. 881–940.

Wain, J., Kirby, J. and Ali, S. (2002) Leucocyte chemotaxis: Examination of mitogen-activated protein kinase and phosphoinositide 3-kinase activation by monocyte chemoattractant proteins-1, -2, -3 and -4, *Clinical and Experimental Immunology*, 127(3), pp. 436–444.

Wall, R., Ross, R., Fitzgerald, G. and Stanton, C. (2010) Fatty acids from fish: The anti-inflammatory potential of long-chain omega-3 fatty acids, *Nutrition Reviews*, 68(5), pp. 280–289.

Wang, N., Liang, H. and Zen, K. (2014) Molecular mechanisms that influence the macrophage M1–M2 polarization balance, *Frontiers in Immunology*, 5, pp. 614-623.

Wang, Y., Xiong, X., Chen, Z., Liu, K., Yang, J., Wen, Q., Wu, F., et al. (2015) Expansion of myeloid-derived suppressor cells in patients with acute coronary syndrome, *Cellular Physiology and Biochemistry*, 35(1), pp. 292–304.

Warnke, I., Goralczyk, R., Fuhrer, E. and Schwager, J. (2011) Dietary constituents reduce lipid accumulation in murine C3H10 T1/2 adipocytes: A novel fluorescent method to quantify fat droplets, *Nutrition & Metabolism*. 8(1), pp. 30-43.

Weischenfeldt, J. and Porse, B. (2008) Bone marrow-derived macrophages (BMM): Isolation and applications, *Cold Spring Harbor Protocols* , 3(12), pp.5080-5087.

Wen, Y. and Leake, D. (2007) Low density lipoprotein undergoes oxidation within lysosomes in cells, *Circulation Research*, 100(9), pp. 1337–1343.

Westerterp, M., Murphy, A., Wang, M., Pagler, T., Vengrenyuk, Y., Kappus, M., Gorman, D. J., et al. (2013) Deficiency of ATP-binding cassette transporters A1 and G1 in macrophages increases inflammation and accelerates atherosclerosis in mice, *Circulation Research*, 112(11), pp. 1456–1465.

Wheeler-Jones, C. (2005) Cell signalling in the cardiovascular system: an overview , *Heart*, 91(10), pp. 1366–1374.

Whitman, S., Ravisankar, P., Elam, H. and Daugherty, A. (2000) Exogenous interferon-γ enhances atherosclerosis in apolipoprotein $E^{-/-}$ mice, *The American Journal of Pathology*, 157(6), pp. 1819–1824.

Whitman, S., Ravisankar, P. and Daugherty, A. (2002) IFN- γ Deficiency exerts gender-specific effects on atherogenesis in apolipoprotein E $^{-/-}$ mice, *Journal of Interferon & Cytokine Research,* 22(6), pp.661-670.

WHO (2011) *Cardiovascular diseases (CVDs)* (Online). Avalible at: https://www.who.int/cardiovascular_diseases/en/

Williams, K. J. and Tabas, I. (1995) The response-to-retention hypothesis of early atherogenesis, *Arteriosclerosis, Thrombosis, and Vascular Biology*, 15(5), pp. 551–561.

Winter, C., Silvestre-Roig, C., Ortega-Gomez, A., Lemnitzer, P., Poelman, H., Schumski, A., Winter, J., et al. (2018) Chrono-pharmacological targeting of the CCL2-CCR2 axis ameliorates atherosclerosis, *Cell Metabolism*, 28(1), pp. 175–182.

Wolf, D., Stachon, P., Bode, C. and Zirlik, A. (2014) Inflammatory mechanisms in atherosclerosis, *Hamostaseologie*, 34(1), pp. 63–71.

Wolf, S. and Lawson, C. (2012) ICAM-1 : Contribution to vascular inflammation and early atherosclerosis, *Coronary Artery Disease – New Insights and Novel Approaches*, edited by Squeri A, InTech, 2012, pp. 65–90.

Wolfram, J. and Donahue, J. (2013) Gene therapy to treat cardiovascular disease, *Journal of the American Heart Association*, 2(4), pp. 119–130.

Wormald, S. and Hilton, D. (2004) Inhibitors of cytokine signal transduction, *Journal of Biological Chemistry* , 279(2), pp. 821–824.

Wortzel, I. and Seger, R. (2011) The ERK cascade: distinct functions within various subcellular organelles, *Genes and Cancer*, 2(3), pp. 195–209.

Wu, C., Tang, Z., Jiang, L., Li, X.-F., Jiang, Z., and Liu, L. (2011) PCSK9 siRNA inhibits HUVEC apoptosis induced by ox-LDL via Bcl/Bax-caspase9-caspase3 pathway, *Molecular and Cellular Biochemistry*, 359(1-2), pp. 347-358.

Wu, C., Zhao, Y., Chen, R., Liu, D., Liu, M., Proksch, P., Guo, P. and Lin, W. (2016) Phenolic metabolites from mangrove-associated *Penicillium pinophilum* fungus with lipid-lowering effects, The Royal Society of Chemistry, 6(26), pp. 21969–21978.

Wuttge, D., Zhou, X., Sheikine, Y., Wågsäter, D., Stemme, V., Hedin, U., Stemme, S., et al. (2004) CXCL16/SR-PSOX is an interferon-γ–regulated chemokine and scavenger receptor expressed in atherosclerotic lesions, *Arteriosclerosis, Thrombosis, and Vascular Biology* , 24(4), pp. 750–755.

Xagorari, A., Roussos, C. and Papapetropoulos, A. (2002) Inhibition of LPS-stimulated pathways in macrophages by the flavonoid luteolin, *British Journal of Pharmacology*, 136(7), pp. 1058–1064.

Xu, Q. (2006) The impact of progenitor cells in atherosclerosis, *Nature Clinical Practice Cardiovascular Medicine*. 3(2), pp. 94-101.

Yang, D., Liu, X. and Xiang, M. (2011) The correlation between lipids ratio and degree of coronary artery stenosis, *High Blood Pressure & Cardiovascular Prevention : The Official Journal of the Italian Society of Hypertension*, 18(2), pp. 53—56.

Yang, J., Zhang, L., Yu, C., Yang, X.-F. and Wang, H. (2014) Monocyte and macrophage differentiation: Circulation inflammatory monocyte as biomarker for inflammatory diseases, *Biomarker Research*, 2(1), pp. 1-9.

Yao, W., Li, K. and Liao, K. (2009) Macropinocytosis contributes to the macrophage foam cell formation in RAW264.7 cells, *ACTA Biochimica et Biophysica Sinica* , 41(9), pp. 773–780.

Yoon, J. and Baek, S. (2005) Molecular targets of dietary polyphenols with anti-inflammatory properties, *Yonsei Medical Journal*, 46(5), pp. 585–596.

Yoshimura, A., Naka, T. and Kubo, M. (2007) SOCS proteins, cytokine signalling and immune regulation, *Nature Reviews Immunology*, 7(6), p. 454-465.

Yoshinaka, Y., Shibata, H., Kobayashi, H., Kuriyama, H., Shibuya, K., Tanabe, S., et al. (2010) A selective ACAT-1 inhibitor, K-604, stimulates collagen production in cultured smooth muscle cells and alters plaque phenotype in apolipoprotein E-knockout mice, *Atherosclerosis*, 213(1), pp. 85–91.

Young, I. and Woodside, J. (2001) Antioxidants in health and disease, *Journal of Clinical Pathology*, 54(3), pp. 176-186.

Yu, L., Bharadwaj, S., Brown, J., Ma, Y., Du, W., Davis, M., Michaely, P., et al. (2006) Cholesterol-regulated translocation of NPC1L1 to the cell surface facilitates free cholesterol uptake, *Journal of Biological Chemistry*, 281(10), pp. 6616–6624.

Yu, L., Hammer, R., Li-Hawkins, J., Von Bergmann, K., Lutjohann, D., Cohen, J. and Hobbs, H. (2002) Disruption of ABCG5 and ABCG8 in mice reveals their crucial role in biliary cholesterol secretion, *Proceedings of the National Academy of Sciences of the United States of America*, 99(25), pp. 16237–16242.

Yu, X., Fu, Y., Zhang, D., Yin, K. and Tang, C. (2013) Foam cells in atherosclerosis, *Clinica Chimica ACTA*, 424, pp. 245–252.

Zeinali, N., Hashemi, M., Mirmohammadsadeghi, M., Mirmohammadsadeghi, H., Eskandari, N. and Sabzghabaee, A. (2015) Association of angiotensin-converting enzyme genotype, insertion/deletion polymorphism and saphenous vein graft atherosclerosis in iranian patients, *Brazilian Journal of Cardiovascular Surgery*, 30(5), pp. 557–561.

Zernecke, A. and Weber, C. (2010) Chemokines in the vascular inflammatory response of atherosclerosis, *Cardiovascular Research*, 86(2), pp. 192–201.

Zhang, D., Fang, P., Jiang, X., Nelson, J., Moore, J. K., Kruger, W. D., Berretta, R. et al. (2012) Severe hyperhomocysteinemia promotes bone marrow-derived and resident inflammatory monocyte differentiation and atherosclerosis in LDLr/CBS-deficient mice, *Circulation Research*, 111(1), pp. 37–49.

Zhang, X., Cao, J., Jiang, L. and Zhong, L. (2009) Suppressive effects of hydroxytyrosol on oxidative stress and nuclear factor-kappa B activation in THP-1 cells, *Biological and Pharmaceutical Bulletin*, 32(4), pp. 578–582.

Zhang, X., Cao, J. and Zhong, L. (2009) Hydroxytyrosol inhibits pro-inflammatory cytokines, iNOS, and COX-2 expression in human monocytic cells, *Naunyn-Schmiedeberg's Archives of Pharmacology*, 379(6), pp. 581-586.

Zhang, Y., Chen, Y., Liu, Z. and Lai, R. (2018) ERK is a negative feedback regulator for IFN-γ/STAT1 signaling by promoting STAT1 ubiquitination, *BMC cancer*, 18(1), pp. 613-623.

Zhao, B., Ma, Y., Xu, Z., Wang, J., Wang, F., Wang, D., Pan, S., et al. (2014) Hydroxytyrosol, a natural molecule from olive oil, suppresses the growth of human hepatocellular carcinoma cells via inactivating AKT and nuclear factor-kappa B pathways, *Cancer Letters*, 347(1), pp. 79–87.

Zhou, B., Pan, Y., Yu, Q. and Zhai, Z. (2013) Fibrinogen facilitates atherosclerotic formation in Sprague-Dawley rats: A rodent model of atherosclerosis, *Experimental and Therapeutic Medicine*, 5(3), pp. 730–734.

Zhou, Q. and Liao, J. K. (2009) Statins and cardiovascular diseases: from cholesterol lowering to pleiotropy, *Current Pharmaceutical Design*, 15(5), pp. 467–478.

Zhou, X., Yin, Z., Guo, X., Hajjar, D. P. and Han, J. (2010) Inhibition of ERK1/2 and activation of liver x receptor synergistically induce macrophage ABCA1 expression and cholesterol efflux, *The Journal of Biological Chemistry*, 285(9), pp. 6316–6326.

Zhu, P., Sun, W., Zhang, C., Song, Z. and Lin, S. (2016) The role of neuropeptide Y in the pathophysiology of atherosclerotic cardiovascular disease, *International Journal of Cardiology*, 220, pp. 235–241.

Zubair, H., Bhardwaj, A., Ahmad, A., Srivastava, S., Khan, M., Patel, G., Singh, S. and Singh, A. (2017) Hydroxytyrosol induces apoptosis and cell cycle arrest and suppresses multiple oncogenic signaling pathways in prostate cancer cells, *Nutrition and Cancer*, 69(6), pp. 932–942.